Development of Fibre-Optic Based Techniques for Measurement of Aqueous Chemical Species

by

Zoheir Mouaziz

A thesis submitted to City University for the Degree of Doctor of Philosophy in Electrical and Electronic Engineering

City University

Measurement and Instrumentation Centre

Department of Electrical, Electronic and Information Engineering

Northampton Square, London EC1V 0HB

November 1993

List of Headings

List of Tables and Figures

Tables

Figures

Chapter 1

Chapter 2

Chapter 6

Appendices

Acknowledgements

I wish to express my thanks and gratitudes to Professor K.T.V. Grattan for his supervision and financial support during the course of this work.

I am deeply indebted to Professor R. Briggs for his support and motivation during this work and also for providing his valuable time to discuss problems of all sorts and also for his patience in reviewing this manuscript. In addition, I would like to acknowledge his continuous and tireless efforts in getting the industrial support for this project.

I wish to acknowledge the support of the Algerian Ministry of Higher Education for allowing me to study for this degree through a grant. I also acknowledge the financial support of WRC and Severn Trent for the work done on Chlorine.

I grateful to Dr A. Augousti for his suggestion and fruitful discussion as well as reviewing the manuscript. I also want to thank Mr Z. Olyabeck for his suggestions during the writing of this thesis.

I would like to thank the secretarial and technical staff for their help especially R. Staines, R. Valsler, D. Jackson and B.D.Harper.

Finally I would like to pay a special tribute to my parents, sisters and brothers who have supported me in many ways throughout the course of my studies and to whom this thesis is dedicated.

Declaration

I grant powers of discretion to the University Librarian to allow this thesis to be copied in whole or in part without further reference to the author. This permission covers only single copies made for study purposes, subject to normal conditions of acknowledgements.

Abstract

The feasibility and design of a fibre-optic based system for measurement of the concentration of molecular species dissolved in aqueous solutions has been researched. The use of optical fibres as an alternative approach to the use of conventional optical procedures has been demonstrated to have significant advantages in terms of cost and flexibility in design as well as sensitivity and reliability in the measurement.

In the particular embodiments investigated, absorption of light in the visible and the ultraviolet part of the electromagnetic spectrum has been used to quantify both the hydronium ion (H_3O^+) and hypochlorite ion (OCl^-) concentration in a range of natural waters and effluents. This was carried out by monitoring the variation of the light intensity at the sensing wavelength caused by the interaction of light with the molecules.

Two different approaches were utilised, the first of which was based on the measurement of the absorption of light by a dye indicator whose concentration is chemically affected by the the species and this was used to monitor the concentration of the hydronium ion (indirect method). In the second approach, the variation of the light intensity caused by the absorption of the chemical species itself was monitored (direct method). The latter method was applied to monitor the concentration of chlorine in the form of hypochlorite ion in various types of water sources.

Theoretical analysis of the indirect method was carried out and a simulation of the response of the sensor was provided with emphasis on the computation of the pH value in the biomedical range. The implementation of the sensor was based on the use of low cost optoelectronics and enhanced signal processing schemes. In this application, the reference signal, used to compensate for chemical and electrical interference, was obtained in two fundamentally different ways. In the one implementation of the pH sensor, an external light source was used while in another, the fluorescence of a ruby crystal was used to generate the reference signal. The latter scheme has the distinct advantage of using the same light source for sensing and referencing. Performance of the sensor was analysed in terms of noise and sensitivity.

In the direct method, the monitoring of the chlorine as hypochlorite ion was carried out by measurement of light absorption in the ultraviolet part of the spectrum. Spectral characteristics were compiled to provide a basis for the design and implementation of an on-line residual chlorine monitor according to the water industry standards. Detailed evaluation of the sensor performance was carried out and analysis of the engineering problems and their solutions have been presented together with the performance of the sensor in long term operation.

In the case of pH, an accuracy of ±0.05 pH units was achieved and for the residual chlorine monitor ±100µg/l chlorine concentration was obtained with a reproducibility in the order of ±3%.

List of symbols

γ_i	Coefficient of activity.
ψ	Proportionality constant between light sources.
ε	Coefficient of extinction.
δ	Difference between pH anpK.
Δ	Error symbol.
ν	Wave number.
λ	Wavelength in nm.
ω	Angular frequency.
Ω	Resistance units.
β	Reflected and incident angle at the core cladding interface
γ	Angle of the refracted beam
θ	Angle of the launche beam
A	Absorption.
a_i	Activity of the specified ion
au	Absorption units
C	Concentration of chemical species.
C	Capacitor.
Cd	Capacitance of the PIN diode.
Ca	Capacitance of the amplifier.
°C	Temperature in degrees celcius.
dB	Decibell.
E_1, E_o	First and ground energy level respectively in chapter 2 also "redox" potential in chapter 3and 4 .
E	Nernstian potential
f	Frequency in Hertz.
f	Faraday constant
FOS	Fibre Optic Sensor
[HInd]	Concentration of the undissociated part of the dye.
[Ind]	Concentration of the dissociated part of the chemical dye.
k	Boltzmal constant.
K	Equilibrium constant of indicator.
LED	Light emitting diode.
l, L	Path length.
L_f	Fresnel losses.
ln	Logarithm to base e (Naperian).
Log	Logarithm to base 10.
m	Constant of the pH meter.
n	Index of refraction of a material also number of moles in chapter 3
NA	Numerical apperture of the fibre.
n_o	Index of refraction of air.
P	Incident light power.
P_o	Initial light power.
pH	Logarithm of the concentration of hydronium ion.
pK_{ind}	Logarithm of the equilibrium constant of the dye.
$p_{\lambda s}$	Signal light power as a function of wavelength.
$p_{\lambda r}$	Reflected light power as function of wavelength.

P_s	Signal light power.
P_{total}	Total light power.
Q	Quality factor for electrical filters.
R	Resistor.
R	Gas constant
S	Stray light proportion.
T	Temperature in Kelvin.
[T]	Total concentration of the dye.
V	V number of the fibre.

Chapter 1

Introduction and Background

1.1 Introduction

The measurement of the composition of bulk matter whether in aqueous, solid or gaseous form has always been of paramount importance in scientific and industrial fields. The importance of this information resides in the knowledge of the different chemical parameters forming this matter and their concentrations. This is used in carrying out the complete breakdown analysis of a particular compound. The structure of the latter may then be quantitatively and (or) qualitatively described. Various industries require such analyses. For instance, the food and pharmaceutical industries utilise such analytical techniques to monitor the quality and level of possible toxicity in their end products. In the biomedical field, knowledge of the concentration of many substances such as carbon dioxide, oxygen and pH value in blood or urine is essential especially during surgical operations as well as in the determination of effects on humans through component analysis. Another field of application is the Water Industry. Due to the importance of good quality of water for the survival of living organisms, particularly the human race, the water industry has to comply with the defined standards and hence, monitors the level of chemicals used for cleaning and purifying drinking water before it reaches the consumer. More recently, the European Community has generated a new set of standards concerning the acceptable level of concentration of pollutants such as nitrate ion (NO_3^-), ammonia (NH_3) and total organic carbon (TOC)[1]. These can be used to predetermine the level of pollution in source waters and in effluents from sewage treatment plants. Additionally, the analysis obtained from the qualitative measurements forms a basis for the development of new materials as in the case of the semiconductor industry where selectively doped materials would result in a major enhancement of their electrical properties. The analytical techniques are not only performed to assess the chemical composition of materials but also to understand the process and mechanism involved in a particular chemical reaction. Information related to the production and the control of a particular species and the

chemical reactions involved is then obtained. For example, kinetic information related to the reaction of monochloramine in the presence of excess chlorine in aqueous solution is monitored by measuring the decrease of monochloramine concentration in the ultraviolet part of the spectrum [2].

Different methods for the measurement of the concentration of the species have been developed alongside instrumentation refined by technological advances. These were generated by a more demanding need for a scientific framework on which analytical techniques were based. It was Lavoisier who first highlighted the importance of using the mechanical balance as a tool for the analysis of the results of experiments such as in the measurement of the concentration of silver in the silver-silver chloride reaction. In this particular instance, the unknown parameter is measured through the use of precipitation and weighing. Sophisticated research in sciences such as biology, chemistry and physics provided a background for the development of reliable, accurate and powerful instrumentation for the quantitative analysis of species in the parts per billion range. This instrumentation was also developed to render the tasks facing people from various backgrounds and fields easier to carry out.

The existing analytical methods rely on the transducing effect generated when a parameter is subjected to a physical, chemical or electrical disturbance or a combination of these. Each parameter possesses particular properties which in turn identifies it and thus makes it distinguishable among others. Consequently, instruments based on the properties of the species were developed to suit particular applications. Most of these instruments were used in laboratory analysis and therefore, needed knowledgeable technical personnel to handle the different steps and hence the overall cost was increased further. Additionally, delays in the measurement could result in introduction of errors caused by sample content variation from the collection time to the time of analysis. These errors were, in most cases, not accounted for and hence the results obtained did not provide a true measurement of the parameters under investigation and affected the reproducibility of the instrument itself, although it was correctly measuring the level of the parameter present in the sample. As a result, the desire for better, automated, sensitive and robust instrumentation became a necessity.

Most of the on-line instrumentation was dominated by electrochemical techniques because they were easy to implement, not very expensive and sensitive[3]. However, certain problems were considered as major drawbacks. First, the need for a reference potential

from within the cell, which was unaffected by the presence of other ions present in the solution. Second, they were not very selective and this is probably their weakest point. Finally, the potential that develops across the liquid junction was affected by the sample[4]. Optical spectroscopic techniques were thus used to overcome these problems. However, they also presented problems of their own. For instance, due to the logarithmic relationship between the light intensity and the concentration of the chemical parameter, a variable error was generated (in the case of absorption techniques), and their high cost, fragility and their inability to be automated were major restrictions on their development. This, however has the potential for significant changes with the development of the laser and the reduction in the transmission losses of the optical fibres below 1dB/km. The advent of the laser in the early sixties provided a driving force for further developments and research. Communication, which was dominated at that time by wire transmission, was the first industry to take advantage by moving to the optical medium. This boosted technological advances in the fabrication processes of optical glass fibres and the associated optoelectronics and opened up the potential for implementation of many analytical methods and also lowered the price of many components [5].

Chemical sensors for the measurement of the concentration of single parameters were developed further using optical fibres and hence analytical spectroscopy became viable for use in industrial and medical fields [6][7][8]. Bulky and expensive laser emitters were used in most of the sensors to provide the exciting wavelength. Few of these took advantage of the simple and very cheap optoelectronic components such as light emitting diodes and photodetectors. With the latter enhanced electronic signal processing was needed in order to obtain better signal to noise ratios and consequently better sensitivities. On the other hand, the chemistry involved, especially for colorimetric techniques, was developed to immobilise the dye onto large polymer structures to be used in the reusable and reversible miniaturised sensors, as opposed to simply a probe.

The market demand for optical fibre based chemical sensors has been reported to increase annually [9]. This opened the way for more investment in research in this field. It came as a result of the potential advantages gained by the inert glass fibre in terms of flexibility, safety aspects, portability, almost real time measurement, reduced cost of the instrument as well as operation, miniaturisation and immunity to electromagnetic interference. It was reported that savings of up to $500,000 per site were achieved for the remote monitoring of groundwater contamination when using optical fibre based technology [10]. Moreover,

the ability to measure the concentration of certain species remotely was seen as a major advantage as in the case of the measurement of fissile parameters used in the nuclear industry, which otherwise would have presented a major health hazard [11]. The use of fibres in explosive environments was also regarded as potentially suitable although some doubts regarding this aspect were expressed [12]. It was found that there exists a relation between the size of the object and the power of the beam before ignition occurs at a threshold value of 80mW which is well below the carrying capacity of the fibre and possible to be generated with laser diodes. However, no conclusive evidence was provided when the power involved was below 80mW for a surface area of the object of 0.25mm. This energy range is well above the level required for most chemical sensors applications and in this work, 'safe' levels of radiations have been used.

Thus, more work in the development and improvement of the techniques applied to the automation of the measurement of chemical parameters to be used in control processes was seen to be required. Optical fibre technology offered substantial advantages and spectroscopic analytical methods in the ultraviolet-visible and infrared part of the spectrum were also well suited for the design of the quantitative measuring instruments which can solve many of the problems of existing instruments.

In this work, the author has studied the use of absorption of electromagnetic radiation in the ultraviolet (UV) and visible part of the spectrum as a refined quantitative technique which lies at the heart of the design of optical fibre based instruments. These were intended for the measurement of various parameters dissolved in aqueous solutions.
Two parameters deemed to be very important to monitor have been used as examples for which the design of optical fibre systems was carried out and the prototypes were constructed [13].

The first parameter studied is the hydronium ion H_3O^+, and a measure of the concentration of this species was related to the absorption of colorimetric dyes with which it reacted in the biological range i.e. 6 to 8 pH units. The measurement of the pH value in this range is very important since many living organisms cannot tolerate their pH to be out of this range.

The second chemical parameter chosen was chlorine because of its important properties and widespread use. It has been the major chemical disinfectant used in most water treatment plants since the discovery of its bleaching properties in the late 18th century.

The use of optical fibre in such instrumentation is a novel and attractive approach to the implementation of the free space optical absorption technique that was deployed and developed as early as the 1930's. This technique is known to be accurate, and reliable. Nonetheless, it is less sensitive when compared to other techniques such as fluorescence[14]. However, one of the main advantages resides in the fact that absorption occurs with a wider range of species than does fluorescence. Hence, there is an increasing number of applications where this technique can be implemented. Further, it does not present a major investment as in the case of other techniques e.g. chromatographic techniques. Once the feasibility of such devices is proven and they are found to be reliable and reproducible, the full power of optical fibres with their main advantages will be used to devise multiplexed monitors where the measurement of the concentration of a large number of parameters can be achieved. In addition, the low cost of the final design is an added advantage especially when multiplexing techniques are used to monitor multiple parameters using the same hardware.

1.2 Aims and Objectives

The current research aims at investigating the potentials lying behind the use of optical methods, mainly absorption techniques, as the fundamental transducing effect on which the design of fibre optic chemical sensors are based. This is intended for the on-line measurement of chemical concentration of species dissolved in aqueous solution. The concentration of the chemical species is related to the variation of the light intensity of a particular sensing wavelength through the Beer-Lambert law. The existing instrumentation based on optical spectroscopy has been directed towards laboratory use only. From the research carried out in the water industry, it was clearly shown that the state of the current instrumentation was not adequate to cope with the increasing demands either from the legislation or from the consumer[15]. Indeed, there is a lack of instruments for the monitoring of species that are widely used such as chlorine in the case of disinfection of drinking water, or to monitor pollutants such as ammonia and nitrate. Hence the need for the water industry to acquire instruments that are not only robust and accurate but also reliable for long term use, is becoming apparent.

Different methods and techniques are analysed for this purpose. Absorption of light in the visible and ultraviolet part of the spectrum when used with fibre optic techniques have been shown to have the potential for solving the current problems of the water industry in

particular and other fields in general. These problems which are principally caused by the inefficiency of the transducing effect and the harsh environment in which the instrument is used can be overcome by using optical spectroscopic techniques. One of the aims of this work is to provide a solution to the problems associated with existing instrumentation and to enable the design and production of cost effective sensing systems.

In this work, it is proposed to investigate the practical implementation of the absorption of light to relate to the concentration of chemical species using optical fibre systems and this is summarised as follows:

- Analysis of the basic physical phenomenon underlying the process of light absorption by the molecules and establishing a quantitative relationship.
- This investigation is carried out by analysing two methods: indirect and direct measurements.
- Investigation of colorimetric techniques as an indirect measurement of the concentration of the chemical species and their advantages as well as their limitations for a fibre optic implementation.
- Designing a fibre optic based colorimetric instrument to measure the pH using phenol red dye indicator.
- The analysis of a direct method will be carried out on crucial and widely used chemical species e.g. chlorine, and its optical characteristics in the ultraviolet part of the spectrum.
- Design and implementation of an on-line fibre optic based residual chlorine monitor which can also be used for the measurement of combined chlorine.
- A comparative discussion on indirect and direct methods in conjunction with fibre optic in order to design and build sensors for use in a variety of industrial fields

The work which is subsequently described has been divided into two parts:

In the first part of this work, colorimetric techniques were modified to suit optical fibre use and consisted in monitoring the change of colour of organic dyes, mainly the use of phenol red for the quantitative measurement of the concentration of the proton H_3O^+ which is expressed in terms of pH units.

In this approach e.g. the colorimetric method, two different schemes were deployed in order to provide the optical reference signal. In the first option, the reference signal was generated externally using different Light Emitting Diodes (LEDs) which emit light in a

free dye-absorption band. Secondly, a fundamentally different approach was used in order to generate the reference signal. A unique wavelength was selected to provide a measure of the absorption of the dye and at the same time it was used to excite a ruby crystal. The latter emitted light at a different wavelength i.e. a longer wavelength, by way of fluorescence.

In the second part of the work, measurements were made in the ultraviolet part of the spectrum to monitor directly the change in absorption brought about by changes in the concentration of the residual chlorine present in processed and non processed waters. This method has a clear advantage over other optical techniques in which a carcinogenic indicator N,N-Diethyl-p-phenylenediamine (DPD) is used to monitor the level of residual chlorine present by measuring the absorption of visible light at a wavelength of 515nm. Cost and health hazard were the major shortcomings when this method was used in an on-line monitoring system for the measurement of chlorine, although it is recognised as a standard laboratory procedure by the water industry.

A less effective method was conceived by Aoki[16] in which chlorine was allowed to diffuse through a PTFE membrane into an alkaline sample and then monitoring of ultraviolet light intensity provided a measure of the hypochlorite ion level present in the water. Although this method covered a larger range of chlorine concentration (e.g. 0 to 700mg/l), it remained for laboratory use only. Moreover, this method was dramatically affected by temperature which induced membrane diffusion rate variation and hence resulted in a significant error in the measurement.

The approach taken in the second part of this work has a distinct advantage over the method described above and has avoided most of the problems encountered there. In this approach, the use of a membrane has been discarded and the measurement of the concentration of chlorine carried out by directly monitoring the light intensity in the ultraviolet part of the spectrum (i.e. light at 290nm). The variation in the light intensity at the particular sensing wavelength reflected a measure of the concentration of chlorine present in the sample. The spectral analysis of chlorine in various water sources i.e. swimming pool, tap and pond water, was used to investigate the optical characteristics of chlorine. The results of this research were used to compile a feasibility study for the Water Research Centre (WRC) for the design of an on-line Residual Chlorine Monitor (RCM)[17].

The reference signal, in this part of the work, was provided by the same wavelength used

to sense the absorption of chlorine. In contrast to the work carried out in the first part of the project, the reference signal was obtained by chemically removing the species itself through a chemical reaction. This resulted in the conversion of chlorine into chloride ion (Cl^-) which does not absorb at the sensing wavelength. A fully automated system in which a fibre optic link was used, was designed and constructed according to the water industry specifications and provided all the required control commands, signal processing and display of the analytical data. Furthermore, a field trial was carried out in order to assess the problems encountered during a long term operation of the instrument and the results of this evaluation provided valuable information for a future implementation.

1.3. Structure of the Thesis

A brief introduction is given in chapter one in which a review of the analytical methods is presented. This is carried out with an emphasis on the drawbacks of the existing techniques, especially the electrochemical one, and the reasons why optical methods, with the use of optical fibres, can have a promising future. The different schemes used in most optical fibre based chemical sensors are presented and the results of a brief market research study are also produced.

The relevant theoretical background on the phenomena of molecular absorption and its relation to the qualitative and quantitative identification of parameters is presented in chapter 2. A detailed study of the light propagation in the fibre and the mechanism of light losses within the fibre as well as at its boundaries is undertaken. This also provides a background from where optimisation of light coupling and interfacing with other optical components is rendered more efficient.

In chapter 3, a theoretical analysis is provided on the use of organic dyes for the quantitative measurement of pH in titrimetric environments. Interaction between light in the visible range and dyes in general, and phenol red in particular, is discussed with the implication that it had for a fibre optic system. A feasibility study on the use of such indicators within an optical fibre system is performed.

An implementation of the two approaches used in this part of the work is described in chapter 4. The electronic design of the sensor is explained and a full description of the methods and components used is given. An analysis of the results is provided and error considerations are discussed. Two methods fundamentally different for providing a

reference signal are implemented and the results compared. A final conclusion is reached and a comparative analysis of the two methods is given.

In chapter 5, a feasibility study of the use of UV light for the monitoring of residual chlorine in real time is depicted. The effects of temperature, water sources and pH are analysed. Additionally, a study of different referencing methods is performed.

The implementation of the fibre optic techniques for the design of a residual chlorine monitor for an on-line measurement based on the feasibility study is described in chapter 6. The optical, mechanical, electrical and electronic configurations are proposed with a full description of the auto-sampling, reagent mixing, detection and signal processing, arithmetic and display section. A laboratory-made calibration of the instrument with the analysis of the results is given at the end of the chapter together with the results of a field trial.

Finally, a general conclusion relating to the use of optical fibres in conjunction with ultraviolet and visible absorption spectroscopy is summarised in chapter 7. The implementation of different referencing schemes with their advantages and drawbacks is also given and the future trend of the work is discussed.

1.4 Review of Analytical methods

Most of the methods for the determination of the concentration of chemical parameters dissolved in aqueous solutions on which analytical techniques are based can be grouped in four major categories, as shown in Table.1.1, although other methods exist. This,

Instrumental Methods			
Spectroscopy	Electrochemical	Chromatography	Miscellaneous
Absorption and emission spectroscopy	Conductometry	Gas chromatography	Thermal analysis
Fluorimetry	Potentiometry	Liquid chromatography	Mass spectroscopy
Polarimetry	Voltammetry		Kinetic techniques
Refractometry	Electrogravimetry		Photoacoustic techniques
Raman effect	Coulometry		Hybrid
Electron spin resonance			
Nuclear magnetic resonance			

Table 1. 1 Classification of analytical techniques for the chemical instrumentation domain.

however, is not the only classification that can be found in the literature. The diversity of the grouping is due to the importance of the principle of the method, its usefulness ,and its widespread use.

1.4.1 Electrochemical Methods

These methods are based on the electrical properties of the species present in aqueous solutions and the information obtained, related to the concentration of the species, can be expressed as a function of the voltage that develops between dissimilar electrodes, as in the potentiometric method, or as a function of the current that flows across these electrodes when a voltage is applied between them (amperometric methods). Furthermore, the impedance of the sample can also be used to determine the concentration of the species.

In the ***Potentiometric*** (ion selective electrode) method, the measurement of the variation of the electrode potential is monitored. This is related to the activity coefficient of the species in the sample, by a logarithmic relationship, using the Nernst equation. The activity of the species represents the concentration of the species when the concentration of the latter is low. Usually, there are two types of indicator electrodes; bare metallic and membrane covered metal electrodes. In the case of metallic electrodes, there is a need for two; an active and a reference electrode. The latter is the one which is not affected by the contents of the solution while the first electrode is sensitive to the activity of the ion of interest. This method although fast, non destructive and easy to automate, has two major disadvantages. Firstly, because of the logarithmic relation between the potential and the ion activity, the technique is less accurate [3]. Secondly, unless the thermodynamic equilibrium constants are required, an error which is not in most cases negligible is introduced by assigning the value of the activity to concentrations as shown in Equation 1.1.

$$E = E^{o} - (RT/nf) \ln[C_i] - (RT/nf) \ln(\gamma_i) \qquad [1.1]$$

$$a_i = \gamma_i C_i$$

where γ_i is the coefficient of proportionality, a_i is the activity of the parameter, C_i is the concentration of the ion, E_o is the potential of the "redox" couple and E is the Nernstian potential. In this case n, R, T and f represent the number of moles, the gas constant, the temperature and faraday constant respectively. The value of the coefficient can vary from 1 in very dilute samples to 0.3 in less dilute samples and it is reported that if the ionic

strength of the test solution is 0.16 and the activity of the ion is taken for its concentration, the magnitude of the error that results is as high as 25% [4]. Additionally, the potential that develops at the sample-reference junction (liquid junction) is affected by the presence of interfering ions. Usually, the error is accounted for during the calibration of the instrument but does not necessarily solve the problem unless the activities of the interfering ions are known, which in itself is a limiting factor. This problem can be clearly seen in the case of the pH electrode when used in environments which varies greatly from the calibration conditions as in the case of the measurement of the blood pH.

In the ***electrolysis*** method, the correlation between the current passing through the liquid and the voltage appearing at the electrode surface is used for the quantitative identification of parameters, as in the case of the ***voltametric*** method, also commonly known as ***polarography*** (when the indicator electrode is the dropping mercury electrode). The voltage present at the indicator electrode and the current passing through the sample are used to give an indication about concentration of the type of species dissolved in the sample. Other methods are based on electrolytic separation followed by weighing of the substance under analysis and is known as ***electrogravimetry***. ***Coulometry*** involves the measurement of charge transfer through the electrolytic cell which is responsible for the transformation of a mass of substance in an electrochemical reaction. This method is very selective and accurate especially with the development of electronics.

Conductometric methods are based on the measurement of the change in the conductivity of the electrolyte. When a chemical reaction occurs, the ions which are responsible for the conduction process are used and their concentration decreases, affecting the passage of current through the sample. This method is used in dilute samples such as weak acids or bases i.e. measurement of dissociation of weak electrolytes but is avoided when oxidation-reduction reactions take place.

1.4.2 Chromatography

Chromatography in all its forms i.e. liquid-liquid, gas-liquid is used in order to qualitatively analyse a chemical component by measuring its basic elements. The principle used in this technique is the selective adsorption of individual species which occurs in a column (e.g. ion exchange resin). These elements are then desorbed sequentially using the liquid or gaseous phase and are detected by either light absorption or mass spectrometric techniques and their peak which is represented as a function of retention time indicates the time it

takes the parameter to appear at the detector side after the start of the wash. Time in this method is a measure of the separation of different molecules based on their molecular weight. Peak heights are a measure of the concentration of the particular species. This techniques necessitates trained technical personnel to carry it out and is expensive to exploit. It also requires the use of standards for calibration of peak heights.

1.4.3 Optical and Spectroscopic Methods

Spectroscopic analysis involves the interaction of an electromagnetic wave with matter. This interaction is seen through the exchange of energy between the two systems i.e. molecules or atoms and the surrounding media and can occur in different forms. Quantitative information related to the species is then obtained through the analysis of the returned energy as in the case of light absorption and emission.

1.4.3.1 Absorption and Emission of Radiation

The principle behind the absorption and (or) emission of radiation lies in the interaction of the electromagnetic wave with matter. Rules, established by quantum mechanics which predict that molecules and atoms interact with the wave by exchanging fixed amounts of energy, are used to quantitatively identify the species. When the substance absorbs energy, it becomes excited and moves to a higher energy state. However, it cannot stay in this excited state and falls back to ground level energy by emitting this extra energy to the surrounding media through a radiative or non-radiative process. The former process occurs when light is emitted through fluorescence or phosphorescence at a longer wavelength. An identification of the species is then obtained and related to its concentration by using the Beer-Lambert law in the case of absorption or by measuring either the decay time or the quantity of the light emitted in the case of fluorescence which is then related to the concentration of the parameter under test. The latter effect is more sensitive than the absorption process. However, there are fewer species that fluoresce and hence absorption is likely to cover a much wider range of elements.

Depending on the wavelength of the interacting wave, different types of molecules and structures can be determined using either absorption or emission or both. In the ultraviolet and visible range, outer layer electrons are involved while in the infrared part of the spectrum only lower interaction energy is involved i.e. vibrational or rotational energies.

1.4.3.2 Emission and Absorption Flame Spectroscopy

Flame spectroscopy is a technique based on the identification of parameters by looking at the transmission variation of a hollow cathode lamp emitting at a wavelength which coincides with the absorption of the parameter under test. The latter is excited by thermal evaporation and the transmission characteristics of the light are monitored. For each parameter a special lamp with distinctive optical properties is used. This is known as absorption flame spectroscopy. In the case of emission flame spectroscopy, the same principle applies, however, the fluorescence of the species is monitored rather than its absorption. Hence, this method does not necessitate the use of a light source.

Flame spectroscopy is directed towards laboratory measurement and is stable, accurate but difficult to automate and expensive to maintain especially in an on-line system.

1.4.4 Electron Spin Resonance

Electron Spin Resonance (ESR) is a valuable technique for the analysis of chemical species having unpaired electrons and consists of immersing the sample in a strong magnetic field while varying the frequency of the microwave field. Resonance occurs when the energy of the microwave is equal to the splitting of the energy levels of the molecule.

1.4.5 Nuclear Magnetic Resonance Spectroscopy

Nuclear Magnetic Resonance Spectroscopy (NMRS) relies on the interaction between a weak field whose alignment is perpendicular to a second strong magnetic field and the nucleus of the unknown species. The absorption of the weaker field caused by the transition of the nuclei from one energy level to another one allows for the determination of the constituents of the nucleus of the sought element. However, initially, this technique was less sensitive than others and it was found difficult to maintain a common operating procedure. In addition the instrumentation needed was very expensive [18].

1.4.6 Raman Spectroscopy

The Raman effect results in the appearance of two additional spectral lines, known as Stokes and anti-Stokes lines displaced in wavelength terms from the exciting wavelength when the molecules are irradiated by an intense electromagnetic field such as the one generated by a laser beam. Normal Rayleigh scattering results in light at the same wavelength as the exciting one, and is a dominant process, often causing interference with

the observation of the Raman lines .

1.4.7 Miscellaneous methods

These rely on different physical and electrical properties of the species. In the case of ***mass spectrometry*** the qualitative and quantitative information about organic and non organic species is carried out by transforming the species into its gaseous form and then sorting these according to their mass-charge ratio. The method is found to be more sensitive than any other analytical method and is used to identify and quantify known and unknown parameters.

1.5 Fibre Optic Systems

Most of the optical fibre based chemical sensors stem from an extension of the implementation of free space spectroscopy. The use of the fibre provides a degree of flexibility regarding the arrangement of the different optical components especially the position of the optical cell where the interaction between the light and the measurand occurs. These systems can be classified in various ways in the literature [19]. A simple approach is taken here where their classification is grouped into two main groups depending on whether the fibre interacts actively (intrinsic) with the sample or is used as a passive waveguide (extrinsic).

1.5.1 Intrinsic Sensors

Intrinsic sensors rely on chemically or physically-induced changes in the characteristics of the lightwave travelling through the fibre making the latter an active component in the detection process. This can be achieved through the changes of the core, cladding or the jacket of the fibre. A fibre optic based hydrogen gas sensor was demonstrated using interferometric techniques to measure the effective changes of the path length which resulted from the changes of the fibre core dimensions. A thin layer of palladium was deposited on a stripped length of the fibre and was found to react to hydrogen by reversibly and linearly expanding, hence changing the fibre dimensions. Sensitivities of 0.01ppm were achieved [20]. This device is shown diagramatically in Fig.1.1

Refractometry and evanescent wave methods are also used in a large number of fibre optic chemical sensors [21][22]. The method relies on the measurement of losses of light guided through the fibre which are induced by a change in the index of refraction of the medium

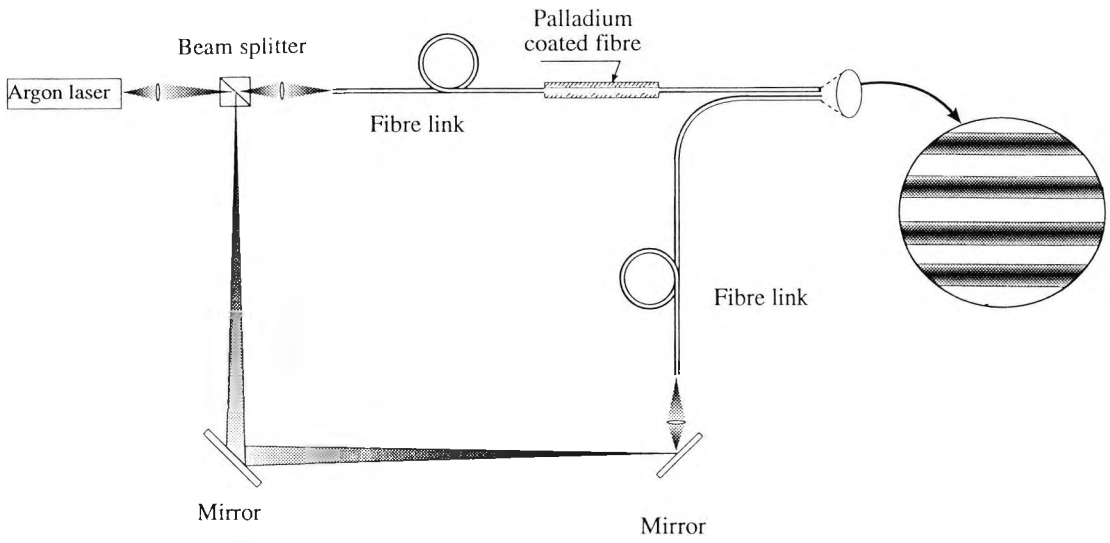

Fig. 1.1 Set-up of the fibre optic hydrogen sensor

surrounding the fibre. In the former method, the light, transmitted through the core of the fibre by way of multiple reflection of light rays, varies when the refractive index changes, i.e. more light rays are reflected resulting from the fact that when the refractive index of the cladding decreases, the critical angle value increases. In the case of the evanescent wave method, the light that travels mainly through the cladding is affected by the change of index of refraction of the cladding section, resulting in absorption of the light.

One of the fibre optic methods which has not found any aspect of application in the chemical field, and was found to be reliable in the monitoring of power supply lines, consists of the monitoring of the variation of the degree of polarisation of light travelling through a monomode optical fibre [23]. In the latter application, the electromagnetic field generated by the power lines modified the properties of the light travelling in the core of the unmodified fibre i.e. changed the degree of polarisation of one particular mode travelling inside the core. There has been no mention of the use of electromagnetic transducing effects used for intrinsic chemical sensing in the literature.

1.5.2 Extrinsic Sensors

In this type of sensor, the optical fibre cable is a passive component and is used only as a convenient way of transporting the desired wavelength, or range of wavelengths from a light source to the optical cell where the transducing effect takes place. The desired information i.e. concentration, which is then encoded in the lightwave in various forms i.e. intensity change [24], fluorescence [25] or chemiluminescence [26], is guided to a detector for further spectroscopic analysis using the same or a different fibre. In the case of

chemiluminescence, no light source is required since the light is generated by a chemical reaction which could be an advantage.

The various techniques used for the detection and the measurement of the concentration of chemical parameters dissolved in water are carried out by either a direct or indirect monitoring of the light reaching the detector. In a direct measurement, the parameter under investigation reacts with the light at a specific wavelength. The intensity of the latter is then monitored and related to the concentration as in the case of the measurement of the radioactive nature of uranium by means of fluorescence in the ultraviolet part of the spectrum [11] or as in the case of the measurement of residual chlorine monitor by using absorption techniques in the ultraviolet part of the spectrum [27][28]. In the indirect mode the parameter is substituted by another element which has enhanced optical characteristics. The latter is then used to interact with light providing a measure of the concentration of the former parameter as is the case in colorimetric techniques or as in the case of the measurement of ammonia. As the latter does not absorb in the UV part of the spectrum, monochloramine, which results from the reaction of chlorine with ammonia, absorbs at 244nm and is used to provide a measure of the concentration of ammonia. Alternatively, a dye is used in other systems to interact with the parameter of interest and changes its colour when the concentration of the parameter changes, as is the case for pH measurement [29]. Usually the coefficients of extinction for these dyes are very large i.e. a large absorption value (e.g. phenol red ~10^{+4}au./M.cm) [30]. As a result, better sensitivities are reached and hence low performance components may be used.

1.6 Sensor Configurations

These sensors exist in three major configurations. As Fig. 1.2 shows, the transmission type is mainly used in 'flow through' sampling situations, although, in some situations, it is not a very flexible set-up and the size of the probe head not very practical. However, it is the most common system utilised. Furthermore, it is easy to implement and has been used as a non-invasive method for the measurement of the arterial oxygen saturation of the blood [31], and in most absorption based monitors. This system provides a minimum of light losses through the probe head. A number of fibres are used to guide the light from the light source to the probe head and back to the detector [32].

The second type is a reflection based probe system. The light guided by a fibre is projected onto a reflecting surface which could be used simply for reflection or can contain a material

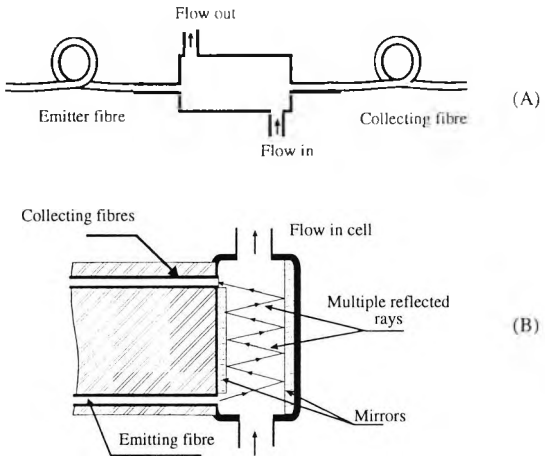

Fig. 1.2 schematic diagram of transmission type probe head set-ups:
(A) straight through, (B) by multiple reflections

which reacts to the measurand by changing its reflecting properties [33]. A fibre positioned alongside to the emitting fibre collects the reflected light which is then guided back to a detector. If the reflected light is weak, a fibre bundle surrounding the fibre can be employed to collect the reflected light as is shown in Fig.1.3. In this particular case the fibre or fibre bundle could be positioned alongside or at right angles to the emitting fibre as in the case of its use for turbidity measurement.

The third type is shown in Fig.1.4 and is of a reflection type where the same fibre which is used to guide the light from the light source to the probe head is also used to collect the reflected light from the probe. The separation of the collected light from that emitted is

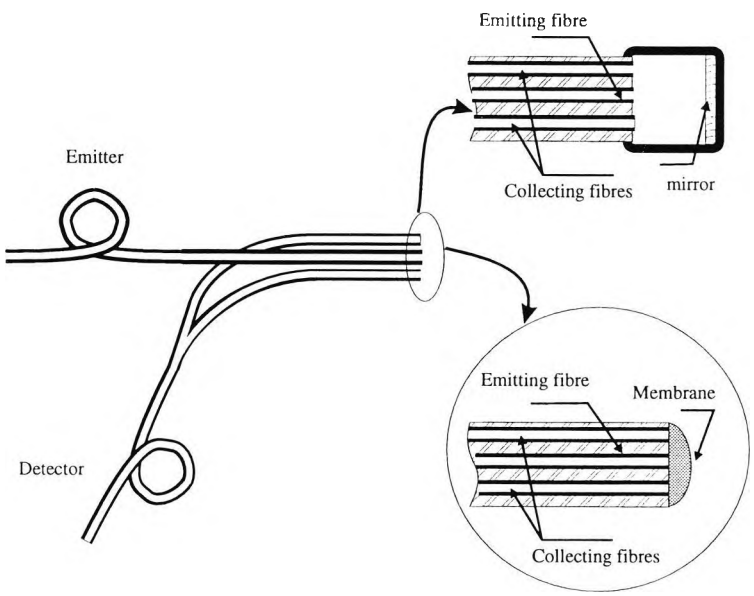

Fig. 1.3 Schematic diagram of a reflected light probe set-up

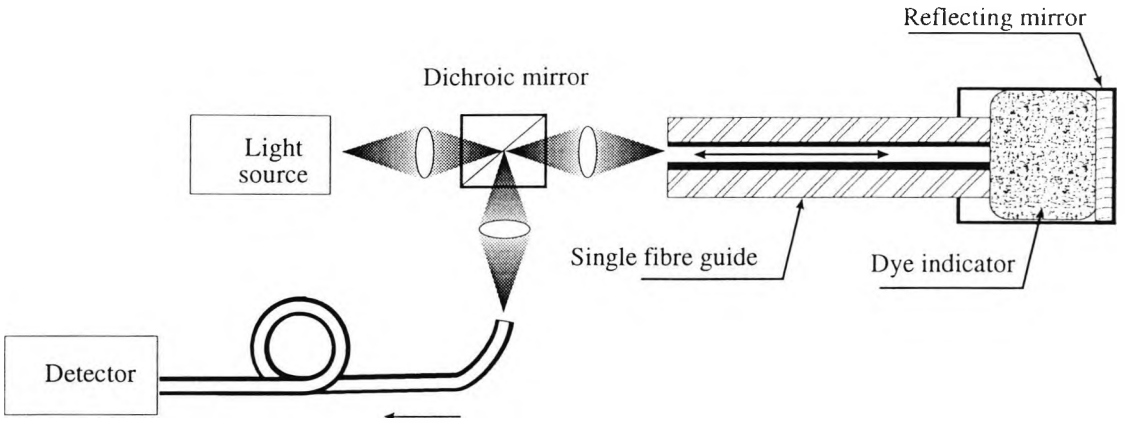

Fig. 1.4 Absorption based sensor using a single fibre set-up

carried out by using a dichroic mirror which reflects the returning beam while it allows the entering beam to pass through. Simple optics are used to project this light on to the detector. Another fibre could be used for this purpose. This type of set-up is usually used where access to the sample is limited[34]. However, it requires the use of powerful light sources e.g. laser or xenon lamp etc., to maintain an acceptable signal level.

1.7 Optical Schemes in Fibre Optic Instrumentation

The different transducing effect used in fibre optic chemical and biosensors can be classified according to their widespread use and importance [35]:

1.7.1 Absorption

This effect, which consists of monitoring the intensity of the transmitted light through a liquid sample, is very popular due to its simplicity and sensitivity especially for extended path lengths and has been implemented in many sensors. Measurement of pH using colorimetric techniques has been the first practical field of exploitation [36][37][38].

The measurement of pH was also used to monitor the level of carbon dioxide (CO_2) dissolved in water since the latter has the effect of decreasing the pH value of the sample in which it is present with increasing concentration of CO_2 [39]. Additionally, pH measurement has been related to the concentration of ammonium ion that diffuses through a PTFE membrane to affect the pH of the internal solution[40].

When the measurement is relative, since the concentration is determined by computing the

ratio of the received intensities before and after removing the species of interest, the magnitude of the light intensity is only important in order to keep the signal to noise ratio (SNR) above a threshold value. This has the advantage of reducing the photo-decomposition effect on dyes or chemical parameters that are sensitive to light. Absorption techniques have been used in this work and will be discussed extensively in Chapter Two.

1.7.2 Fluorescence

The absorbed energy in some species is emitted by a radiative process which consists of emitting light at a longer wavelength. This frequency of the emitted light is shifted toward a lower frequency since the returned energy is always smaller than the absorbed energy. A general implementation of a fibre optic sensor using this scheme is shown in Fig.1.5. Fluorescence has been used in pH measurement using a fluorescent dye called fluoresceinamine [41] and probably the best well known is the fluorescence quenching of oxygen [42]. This method which is also used in biosensors [43] and enzymatic based sensors [44], has the advantage of being more sensitive than other methods, is less affected by interference and does not require the use of a reference channel when the measurement is based on the decay time. However, when the light intensity is monitored, other species

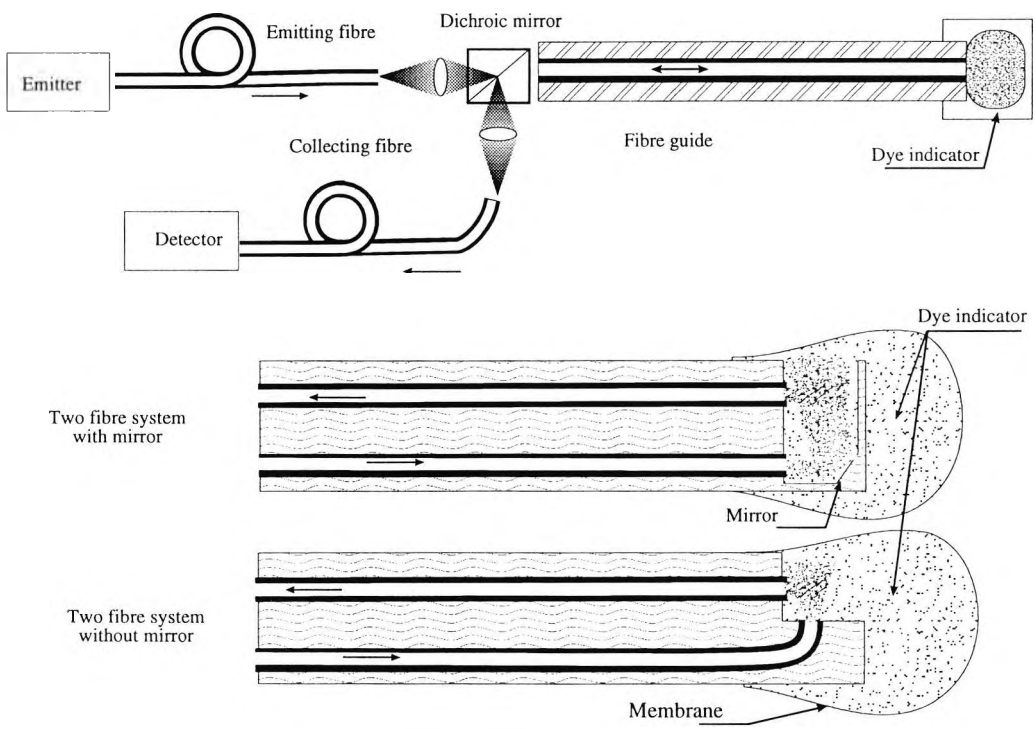

Fig. 1.5 Various sensor set-ups based on the fluorescence phenomenon

in the sample can interfere either by absorbing or scattering the emitted light. Different techniques are used in order to measure the lifetime of the decay, which is related to the concentration of the parameter. Another method also used, consists of measuring the quenching effect that some chemical species have on the fluorescent light. This effect was used in the oxygen fibre optic sensor [45].

1.7.3 InfraRed (IR) Spectroscopy

Infrared spectroscopy is used to monitor the absorption of light in the infrared region by molecules caused by vibrational transitions. It is used mainly to measure species that have C-H, O-H and N-H bonds. The very low numerical values of the extinction coefficients require the use of long path lengths to achieve good sensitivities. Infrared instrumentation requires special fibre technology especially in the 2.5 to 20μm range. Also, some bonds such as C=C, C≡C, S-S are invisible in IR detection however they were reported to exhibit strong Raman bands [30]. This technique can be complementary to NIR or IR techniques.

1.7.4 Raman Method

The Raman method relies on the inelastic scattering of light from a laser beam which is caused by changes in polarisability of the molecule during a vibration process. The information acquired is related to the properties of a large variety of organic compounds and hence is not limited, as is fluorescence. A major advantage of Raman instrumentation is that it does not need specialised component technology. Glass fibre and visible-to-near infrared light sources can be used hence taking advantage of existing products. On the other hand, the intensity of the detected light is very weak,e.g. around 6 orders of magnitude lower when compared to fluorescence under comparable conditions. This results in the technique being prone to interference from traces of fluorescent impurities [46].

While Raman scattering is of the inelastic type and the polarisability of the molecule changes, there exists elastic types of scattering which are known as Rayleigh and Mie scattering where the polarisability of the molecules remains constant. The difference between the first one and the second is related to the size of the particles with respect to the wavelength: Rayleigh scattering occurs when the size of the particles is around the same size as the wavelength and Mie scattering can be seen when the size of the particles is larger than the wavelength as in the case of turbidity measurement.

1.7.5 Reflectometry

Reflectometry is based on the reflection of the beam of light at the surface between two media. The useful information is extracted from the diffuse light which results from the reflection of the beam that penetrates the second medium which contains the dye. Part of the light beam is absorbed by the molecules in the second medium and a mathematical relationship may be expressed between the concentration of the molecule of interest and the intensity of the diffuse light. Kubela and Munk developed this relationship which is believed to have produced good results[47]. A fibre optic system based on the variation of the light reflected from a jugular vein was successfully used to monitor heart beat rate by monitoring the variations of the reflected light intensity caused by blood flow [48].

1.7.6 Refractometry

Refractometry relies on the change in the guided light caused by a variation of the multiple reflection of the light inside the core of the fibre as a result of the change in the index of refraction of the cladding. This type of sensor has been exploited to measure the index of refraction of liquids, and also to measure pH [49]. However, a main drawback of such systems is the temperature dependence of the index of refraction but presumably, this could be compensated for by use of a dual system with one sensor in a buffered solution whose temperature is similar to the sample temperature.

1.7.7 Evanescent Wave

The light that travels through the core of a fibre by multiple reflections bounces back at each reflection at the core-cladding interface. The electric field that follows the beam has a decreasing exponential profile inside the cladding until it is negligibly small. This depth is a function of the index of refraction of the core and the cladding. Hence by making the refraction index of the cladding sensitive to a chemical species, the depth of penetration can be modified and related to the concentration of the parameter by monitoring the light intensity of the beam travelling through the core. This light could result from fluorescence or absorption by the chemical species.

When a thin layer of silver (e.g.55nm) is deposited on the core of the fibre after removing the cladding, the intensity of the evanescent field is enhanced by 2 orders of magnitude. This is attributed to the photons coupling with the electrons on the surface of the metal. This phenomenon is known as surface plasmon resonance (SPR) and is exploited in a

different manner. A light beam travels through a prism and bounces back to exit the prism on the opposite side. One side of the prism is made in contact with the chemical of interest through layers of silver and silicone oil. The measurement is related to the parameter when the exiting beam reaches a minimum of intensity while the incident beam is scanning through various angles of incidence with a resolution of 0.02°[50].

1.7.8 Miscellaneous Methods

Various methods can be implemented using a fibre optic system to monitor different chemical parameters. Opto-acoustic techniques are used in cases where the sample absorbs and re-emits the energy as heat. In a closed system, the heat is converted into pressure. When the light modulation is in the audio range the acoustic signal hence generated can be detected by a microphone. One of the advantages of such a system resides in the self-filtering of the detected signal which emanates from the interacting signal i.e. only the energy that is converted into heat produces the acoustic signal. Consequently, this method is not affected by light scattering and can be applied to various types of surfaces [51].

Interferometric techniques are also used in chemical sensing and rely on the physical changes of the fibre resulting in the variation of the path difference between the two interfering light beams or as in ellipsometry were the polarisation state of the reflected light from a thin layer surface is monitored [52].

1.8 Advantages and Drawbacks of Fibre Optic Sensors (FOS)

The use of light as a means of measurement has been pushed forward by technological enhancements in optical fibres. These can be seen as follows:

1.8.1 Advantages

- Remote measurements can be easily implemented especially for reagentless sensors i.e. species that fluoresce naturally or where the reagent is a building block of the fibre e.g. evanescent wave, reflectometric or interferometric techniques. The sensing head can be located remotely and linked to the optical and control section by a fibre optic cable system as has been demonstrated in the measurement of radioactive species [53].
- Safety aspect of the fibre link especially in environments where electrical transducing effects present a fire or explosion risk, although some research has demonstrated that the optical medium is not totally safe but even so, the fibre still represents a smaller hazard

risk than do other systems. Additionally, fibre optic systems can be steam sterilisable.

- Temperature range of working fibre optic systems is larger than many other systems.
- Miniaturisation of fibre optic systems can exceed that of electro-chemical based techniques[54] and this can make them potentially attractive for medical use [55].
- In some applications, there is no requirement for a reference signal since the measurement is directly related to the chemical species present in the sample. For instance, the measurement of the decay time does not need a reference measurement. However, this is not true when performing intensity measurement since some of the light could be absorbed or scattered by large molecules present in the sample. Also, the reference information is needed to relate the detected signal to the species when fibre positioning and bending induced losses occur.
- Electrical interferences other than the one generated by the presence of other chemicals cannot be induced in the glass fibre. Hence, a fibre optic based sensor is protected from external electrical interference.
- Multiplexing and large information transmission capacity capabilities of fibres can provide a sound base for the development of a multi-parameter monitor system.
- Basic material is non destructive and less susceptible to corrosion by most strong chemicals and temperature
- Available fibre optic systems are using optical techniques only, however there could be promising future for hybrid techniques as in opto-acoustic techniques.
- Some systems provide better performance than electrochemical systems such as in the case of residual chlorine monitoring where the DPD method represents the standard although it is very expensive to automate.
- Flexibility in the design of most Fibre Optic Sensors (FOS). Because the fibre is a flexible link between the different electrical and chemical parts, the design of these instruments is rendered easy.
- Complete electrical isolation between the electrical and the liquid part of the sensor e.g. detector, power supply, signal processing boards and pumps.

On the other hand, fibre optic systems do exhibit some severe limitations resulting from the transducing effect they rely on for the design of instruments used in the measurement of the different chemical parameters. These are:

1.8.2 Disadvantages

- Limited life of immobilised reagent in optrodes and membrane based technology. Moreover the immobilisation technique inherently reduces the sensitivity of the dye reagent [30].
- Effect of photo-bleaching especially in fluorescent based sensors.
- Response time delay exists because of the mass transfer needed to establish a mass equilibrium.
- Limited dynamic range of most reagent based sensors. This has been seen especially in colorimetric techniques where the linear relationship between the absorption and the measurand concentration is valid only in a limited range as is the case in optical pH meters based on dyes.
- Costs are still high for systems operating in the ultraviolet part of the spectrum. This results from the special material needed to fabricate the optoelectronic and optical devices. Quartz based fibres can transmit light in the ultraviolet part of the spectrum down to 200nm and Sapphire can transmit light in the 185nm region. The market need for this particular region in the spectrum is rather small. Basically, when species absorb in the ultraviolet part of the spectrum, colorimetric techniques are used whenever possible so that visible light can be utilised.
- Fibre losses and degradation of the fibre in the sub-200nm wavelength range which results from the higher level energy photons interacting with the medium. However, most manufacturers have not produced any analytical data to confirm or reject this long term effect.
- Large diameter fibres cannot be bent easily without creating micro-cracks which probably are invisible to the naked eye but which can reduce the light transmission of the fibre and hence diminish the working lifetime of the fibre.
- No standards regarding interfacing or communications are yet established in the field of sensing which could enable FOS to be more portable.
- In indirect measurements such as in the case of pH, errors generated by common ion effects and ionic strength, are not considered. Furthermore, these systems measure the concentration of the dissociated or the undissociated part of the dye and are related to the pH value rather than the activity of the H_3O^+ ion. Hence the method is only valid when dealing with dilute solutions or when the instrument is calibrated using a sample whose characteristics are similar to the one on which the measurement is carried out.

1.9 Market Aspect of FOS

As a result of many of the advantages that a fibre optic based system has over the conventional ones, the market demand for these types of sensors has steadily increased and has been compared to the growth in the semiconductor market in the early 60's as has been shown through a number of market surveys[56]. In a matter of 12 years the prediction for a market headed mainly by communication and military electronics went from $11.7 M (million) to $833 M as is reported in Table.1.2. The full power of fibre optic systems is portrayed by communication which has provided the main background for further developments in fibre optic and associated technologies. In 1990, fibre optics in communication represented almost 70% of the total market demand while, in 1978 only a 17% share of the same market. Hence, fibre optic communication did gain popularity not for itself only, but by providing the right opportunity for other fields to develop further, and make use of its powerful features as is the case in optical instrumentation. In the chemical sensing field pH sensors were the first to be investigated followed by chemical sensors based on optical properties; these were developed to be used in biomedical and medical fields and in the chemical and food industries too[8][57].

	production	**value**	**($Million)**
Application	1978	1984	1990
Business Electronics	0.4	2	7
Commercial Communication	2.1	142	581
Consumer Electronics	-	19	61
Commercial Computer System	2.1	27	75
Military Electronics	2.9	26	47
Industrial Electronics	0.3	5	16
Instrumentation	0.2	1	3
Adjustment	3.7	23	43
Total	11.7	245	833

Table 1.2 Market trends in fibre optic systems [9]

Chapter 2

Theoretical Analysis of Absorption as a Transduction Mechanism for Use in Fibre Optic Devices

Abstract

The interaction of electromagnetic waves with matter occurs through a process of absorption and emission. The overall energy of a system made of atoms or group of atoms and the environment is kept constant, hence, exchange and conversion of energy from one form into an other is occuring continually. This is used in order to determine quantitatively the concentration of chemical parameters dissolved in aqueous solutions. The relationship between the species under investigation and the energy of the wave is mathematically determined using the Beer-Lambert Law which when used under appropriate conditions, linearly relates the losses in energy of the light beam travelling through the sample to the concentration of the chemical parameter. The visible and ultraviolet region of the spectrum are used to investigate both the theoretical and practical feasibility of a measuring instrument based on the optical properties of the chemical parameter. This is aided by the advantages of fibre optic cables as a light carrying medium from the sensor head and the many interfaces to the instrument. An analysis of the various sources of error introduced by the absorption law and the hardware is also given.

2.1 Interaction Between Matter and Electromagnetic Waves

Light in its electromagnetic form interacts with matter through a mechanism of energy exchange which takes place between the wave and the atoms or molecules from which matter is made. This occurs through a process of absorption of radiation which results in exciting the molecules into a higher energy state. Consequently, the molecule becomes unstable and cannot remain in this state indefinitely and thus, it regains its lowest energy state which is the more stable state i.e. the ground state, by emitting the total amount of energy acquired, back to the environment. This can happen through a radiative process, a non-radiative process or a combination of the two. However, not all molecules can undergo such transitions since they have to obey certain laws of quantum mechanics. According to Bohr, a molecule or atom can only absorb radiation whose energy corresponds to the difference between two permissible energy levels existing within the molecule as stated by Eq.2.1

$$h\nu = E_1 - E_o \qquad [2.1]$$

where h is Planck's constant, ν is the frequency of the electromagnetic wave and E_1 and E_o represent the corresponding energy levels. The existence of these energy levels is a direct consequence of solving the Schrodinger equation which describes the atoms and molecules in terms of wave functions, and with each wave function an energy level is associated. The latter represents the orbital in which the electron has the highest probability of existence. Each electron in an atom moves around the nucleus in a particular orbital having a predetermined energy value. However, when the atom absorbs an amount of energy, it can only be excited to a permissible energy level by the transition of the electron into the corresponding orbital. This transition usually is concerned with the electron rather than the atom because of the Franck-Condon principle[58]. The nucleus of an atom is heavier* than the electron orbiting around it and as a result the inertia of the former delays the transition of the nucleus into a higher energy level since the time corresponding to a radiation absorption is in the order of 10^{-15}s[59]. Consequently, the nucleus of an atom remains static during the absorption process. Thus only the electron transits to the higher energy level.

* *The mass of a proton whose number equals the number of electrons in an electrically neutral atom is 1830 times larger than the mass of one electron.*

The energy level involved in this mechanism varies depending on the energy content of the wave and the type of interaction between the wave and the molecule. As a consequence of the theory of quantum mechanics, the energy of the wave i.e. a photon when in the visible part of the electromagnetic spectrum, cannot be split and therefore results in a selective interaction between certain types of molecules and the electromagnetic wave. These interactions can be classified as follows[60]:

- Translational energy
- Rotational energy
- Vibrational energy
- Electronic energy

2.1.1 Translational Energy

This deals with the movement of the centre of gravity of a molecule. Because light can not interact with the molecule to change its kinetic energy, the translational energy is not used in spectroscopy.

2.1.2 Rotational Energy

The rotational energy range lies between $4x10^{-4}$ to 0.4 $kJ.mol^{-1}$. Only molecules with a permanent electric dipole show a rotational absorption or emission behaviour e.g. Raman spectra. It can occur in a large wavelength bandwidth from the microwave to the far infrared part of the spectrum. However, it can occur in the near infrared, visible and ultraviolet as well but would not be the main molecular energy source.

For a linear molecule, the only rotations are with respect to the Y and Z axis (X being the axis linking the centre of the two molecules and the three axes meet at the centre of gravity of the molecule). There is no rotation about the X axis since it does not involve any energy exchange. In a non linear molecule the movement about the three axes occurs and hence there are three rotational energy levels, e.g. the water molecule H_2O.

2.1.3 Vibrational Energy

This type of interaction involves a higher energy level when compared with rotational energy. Its range lies between 0.4 and 40 $kJ.mol^{-1}$ and corresponds to a wavelength bandwidth of mainly infrared energy. It can also occur in the visible and ultraviolet region

of the electromagnetic spectrum as a second order effect.

The vibrational energy in a molecule depends on its type. Additionally, the number of modes present is a function of the number of atoms that form the molecule.

In a linear molecule the number of modes is 3n-5, n being the number of atoms (e.g. 4 in the case of CO_2), while it is 3n-6 in a non linear molecule (e.g. 3 for the water molecule). The linear molecule has more vibrational modes than a non linear molecule. These modes can be normal if they are directional vibrations or degenerate if the bond forms an angle with the axis. In every vibrational energy level, a rotational level exists since the energy involved in a rotation is smaller.

2.1.4 Electronic Energy

In this category, the energy level involved is high because the interaction involves the absorption of the radiation which results in the movement of the electron orbiting in the last filled orbital into the next available orbital according to the rules of quantum mechanics. The range of energy involved lies between 40 and $4x10^3$ $kJ.mol^{-1}$ and occurs only in the visible and ultraviolet part of the spectrum. Additionally, rotational and vibrational energy levels exist within each electronic energy level. It is through these types of energy levels that the energy is returned to the environment.

2.2 Mechanisms of Interaction

When light impinges on matter, part of the energy contained in the electromagnetic wave is acquired by the molecule in an absorption process. The state of the molecule changes since it possesses a higher level of energy. The molecule, however, cannot remain indefinitely in this state and a process of energy exchange between the excited molecule and the environment takes place. It consists of returning the additional energy in different steps and various forms. The molecule loses part of the additional energy by moving down the energy scale on to a vibrational level. Sometimes an internal conversion occurs and the molecule loses the remaining energy either as heat (vibrational energy) or as light emission if the energy gap corresponds to the emitted photon energy, as shown in Fig.2.1.[61]

2.2.1 Absorption

Absorption results from the transfer of energy mainly from an electromagnetic radiation

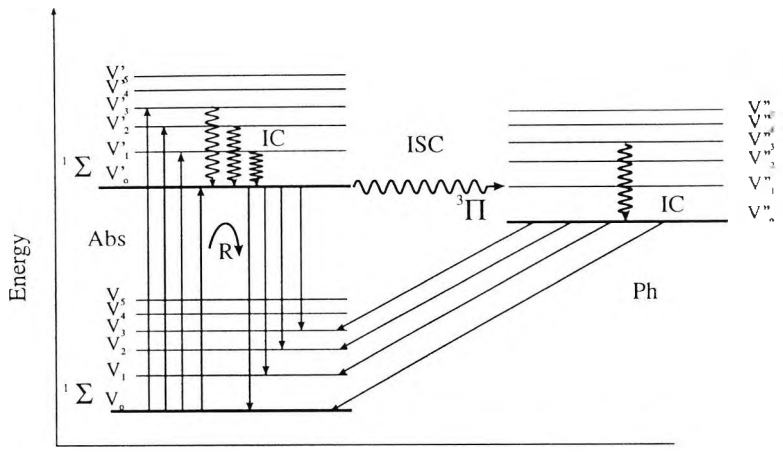

Fig. 2.1 General description of the energy level of a molecule
Abs: absorption; IC: internal conversion; ISC: inter system crossing;
Ph: phosphorescence; R: resonance, S:singlet state; P: triplet state.[61]

to another system e.g. molecules or atoms, according to the laws of quantum mechanics which predict that for this process to take place, the energy content of the electromagnetic wave must fall within an existing energy level of the molecule. Hence, not all molecules can absorb the same radiation since the permitted energy levels are defined by the structure of the molecule, the chemical bonds linking the atoms from which the molecule is made and the number of electrons in each atom. This particular effect allows the use of absorption as a very selective technique in order to determine qualitatively the type of molecule and bonds existing in a given sample. The principle of energy conservation predicts that energy cannot be created or destroyed. It can only be converted from one form into another. Therefore, when a molecule acquires energy by the very rapid process of absorption e.g. 10^{-15} s, the total energy of the molecule is increased and it becomes excited, thus, the molecule becomes unstable. This can result in the breaking of the bonds within the molecules. The disposition of the electrons of atoms in the existing orbitals according to the Pauli principle forces the formation of bonding links first . Other selection rules which govern the the absorption of radiation by molecules forbid the promoted electron to change the spin and in the case of vibrational transition $\Delta v = \pm 1$[62]. However, the molecules cannot remain in this excited state and lose their rotational and vibrational energy in levels that exist within each electronic transition.

2.2.2 Vibrational Relaxation

Once the electron jumps into a higher energy level the whole molecule becomes unstable and loses this additional energy though a combination of internal conversion processes where the vibrational energy depends on the internal vibrational levels existing within the

permitted energy level of the molecule. This vibrational relaxation tends to make the molecule vibrate and results in increasing the temperature of the medium and is known as radiationless de-excitation of the molecule.

2.2.3 Fluorescence

Fluorescence is the result of a radiative de-excitation process which takes place after the electron has lost part of its energy by internal conversion. It then decays to the ground level by emitting radiation whose frequency is proportional to the gap between the energy level from where the electron decayed. This energy is smaller than the energy absorbed and hence the emitted photon has a longer wavelength. This process which is accomplished during a relatively short time 10^{-8} to 10^{-6}s, is affected by temperature since the population of the energy level from where the decay occurs decreases with increasing temperatures. This variation can be linear only over a small temperature range.

2.2.4 Phosphorescence

Phosphorescence relies on a different principle. It has been reported that it can occur in systems having a triplet state from which the electron decays in order to emit light. The time required for this process to take place can extend from 10^{-4} to 10^{+2} s. The longer time scale of the phosphorescence is attributed to the slow leakage between singlet and triplet states. These usually have similar energy levels, but this process would rarely occur since it falls in a spin forbidden transition situation.

2.3 Peak Broadening

The absorption peak profile in the visible and ultraviolet part of the spectrum is rather large. Although the absorption in this part of the spectrum is of a discrete nature, it cannot be resolved with available instrumentation as is done by Fourrier Transform Spectroscopy in the infrared region of the spectrum. Thus, only the envelope can be detected. Moreover, the superposition of vibrational and rotational absorption leads to an enlargement of the absorption profile. The origin of this enlargement is related to the Heisenberg Uncertainty Principle where the energy level is blurred. This is also known as lifetime broadening. This can be seen through the absorption spectrum of the same element at different temperatures as is shown in Fig.2.2. An additional cause of peak broadening is the Doppler shift effect which results from the fact that molecules in solution and especially those in gaseous form are not static and move with high velocities. Thus, a measuring system would detect the

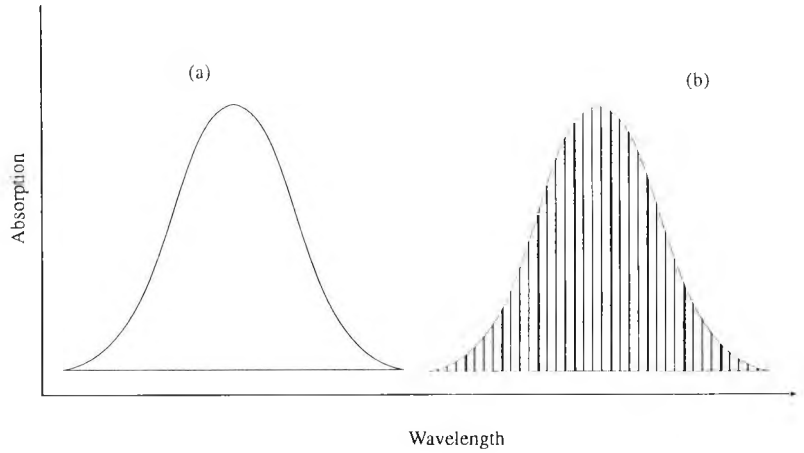

Fig. 2.2 Effect of temperature on the appearance of the fine structure of the absorption spectrum beside the absorption generated by the electronic transition.
a) at room temperature
b) at very low temperature

light emitted by these molecules as being different since the velocity of each molecule is different. Consequently, although these molecules are emitting light at the same wavelength, the latter is detected as being of different wavelengths. This effect is temperature dependent and the broadening enlarges with increasing temperatures[59].

2.4 Beer-Lambert Law

The relation between the light intensity of a radiation of a particular wavelength and the number of molecules that absorb this radiation is given by the Beer-Lambert law. It was found that the ratio of the transmitted to the emitted light intensities varied logarithmically with the concentration of the molecules responsible for the absorption. It was also found that the same ratio of the transmitted to the incident light was logarithmically proportional to the path length (L) through which the light travelled. Hence, the combined relationships were used to formulate the Beer-Lambert law as is shown in Eq.2.2 through Eq.2.5.

$$\int_{p} dp = -\int_{x} kpdl \qquad [2.2]$$

$$\ln p/p_o = -kL \qquad [2.3]$$

where P and Po represent the transmitted and incident light power. The constant k of proportionality becomes k_1 when changing the Napieren logarithm to a decimal logarithm i.e. $k_1 = \ln k / \ln 10$. Similarly the same equation results when the path length is replaced by the concentration of the absorbing molecule and b_1 corresponds to the proportionality

constant expressed as the decimal logarithm of b.

$$\ln p/p_o = -bC \qquad [2.4]$$

When Eqs.2.3 and 2.4 are combined the resultant equation expresses the relation between the concentration of the molecules under examination and the change of the ratio of the initial to received transmitted lights as shown in Eq.2.5

$$\text{Log } P/P_o = -\varepsilon_\lambda L C \qquad [2.5]$$

$$A = \text{Log } P_o/P \qquad [2.6]$$

where C denotes the concentration of the analyte, A is the absorbance and ε_λ represents the extinction coefficient which is a function of the wavelength. In Eq.2.5, the factor of the length can be used to enhance the sensitivity of the measurement especially in the case of species with low molar extinction coefficients as in the case of hypochlorite ion. On the contrary, the length is reduced to a minimum with parameters such as nitrate ion and most coloured dyes because the numerical value of their extinction coefficient is of the order of 10^{+4}au/(mole.cm). (au: absorption unit).

2.4.1 Coefficient of Extinction

A quantum analysis made by Graybeal[63] associates the number of molecules interacting with the radiation in terms of the statistical number of molecules in a given volume that are likely to absorb energy and populate a certain energy level*. Hence, when a scan through the wavelength range is carried out and the concentration of the sample is kept constant, the variation of the transmission (or absorption) of the light through the sample at a fixed path length is mainly due to the coefficient of extinction. Therefore, this coefficient which is a function of the wavelength, is used in order to determine the concentration of molecules present in the sample. The most appropriate wavelength to use can be calculated from the first derivative of the extinction coefficient as a function of wavelength when the analytical expression of the extinction coefficient is known.

* *For example, this is used to determine the population of the excited level in a given crystal before lasing can occur.*

2.4.2 Deviation From Beer-Lambert Law

There are a number of situations where the Beer-Lambert law cannot be applied to represent a true relationship between the concentration of the analyte and the ratio of the transmitted light and therefore a correcting factor must be introduced in order to adjust for the resulting errors. These are generated by the following situations:

2.4.2.1 Stray Radiation

The stray radiation is the result of radiation other than the one selected by devices such as a monochromator. This is combined with the absorbing wavelength and is detected when both the stray and the absorbing light fall on the detector which can not differentiate between the two. The effect of such interfering light can be seen through the Beer-Lambert law which relies on the ratio of the initial to the transmitted lights to determine the relative concentration of the species as is shown in Eq. 2.7.

$$A = Log \frac{p_o + p_s}{p + p_s} \qquad [2.7]$$

where P_o and P are the incident and the transmitted light intensities respectively and P_s is the stray light intensity. When the ratio of the detected light comprising the analytical wavelength and the stray light is computed, the resulting absorbance does not represent the variation of the transmission of the absorbing wavelength only but that of the combined light intensity. This effect is pronounced when the concentration of the variable is high or when the absorbance is high i.e. in the limit of P reaching 0.

$$\text{When } p \rightarrow 0 \text{ consequently } A \rightarrow A_o = Log\left(\frac{p_o}{p_s} + 1\right) \qquad [2.8]$$

It can be seen as a consequence of the stray light intensity, the logarithm of the ratio is limited at higher values of absorption resulting from either the high extinction coefficient of the species or very concentrated sample.

In a more general analysis[64], when a total amount of light $P_{total} = P + P_s$ falls on the sample, a portion β (at the analytical wavelength) reacts with the sample as well as a portion (α) of the stray light. Hence, the detected transmission is represented as T as in Eq. 2.9.

$$T = \frac{\beta p_o + \alpha p_s}{p_o + p_s} \qquad [2.9]$$

with $S = \frac{p_s}{p_o + p_s}$ being the fractional stray light, hence the transmitted light intensity is shown Eq.2.10

$$T_{total} = \beta + S(\alpha - \beta) \qquad [2.10]$$

This gives rise to three particular situations which are:

$\alpha > \beta$ This case causes a negative deviation where the amount of transmitted light is larger than the real value since most of the stray light is not affected by the sample. This leads to the situation where the absorbance of the sample, at the analytical wavelength, is smaller than the real one and this results in an increase of the error as is shown in Fig.2.3. This effect is more pronouced at higher concentration values and thus, the measurement becomes less sensitive.

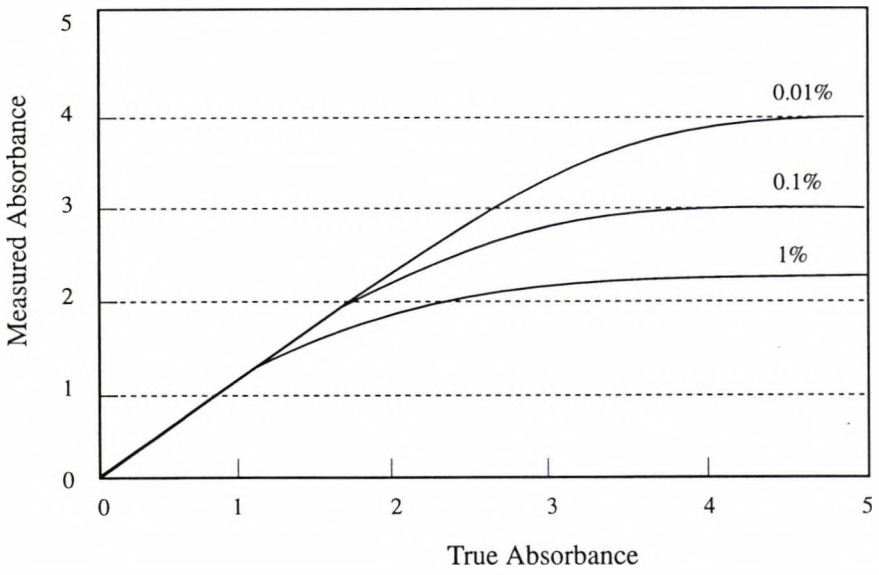

Fig. 2.3 Figure showing the deviation of the response as a function of the light intensity when using the Beer-Lambert law for several values of the stray light intensity

$\alpha < \beta$ When most of the stray light is absorbed by the sample while the analytical wavelength remains almost unaffected, a positive deviation from the true absorbance is created. This is rare but can be seen as in the case of benzene where the minimal absorption occurring between the different absorption peaks is higher than the one predicted.

$\underline{\alpha = \beta}$ When the same amount of stray light and light at the analytical wavelength are absorbed by the sample the resulting error is minimal since the difference is nil ($\alpha - \beta = 0$). This, however, means that the sample has a flat response in the range of the spectrum; this is only seen in special materials e.g. "All Pass" filter used to check the accuracy of the instrument without being affected by the stray light.

Additionally, the stray radiation can limit the maximum absorbance of the instrument to a low value and becomes independent of the signal to noise ratio of the detector. For instance, with a 1% stray light radiation the maximum absorbance is limited to 2 units of absorption as can be seen by using Eq.2.8 and replacing P_s by $0.01P_o$:

$$A = \log\left(\frac{p_o}{p_s} + 1\right) \text{ and thus } A_{\max} = Log\left(\frac{1}{0.01} + 1\right) \approx 2$$

This results demonstrates the importance of the stray light effect which can, in some cases, limit the performance of a sensitive and expensive detector having an excellent signal to noise ratio. Best detector performance can be achieved by carefully designing optical chambers and filters to reduce the effect of light reflections.

2.4.2.2 Non Monochromaticity

The Beer-Lambert law specifically states that the relationship is valid for monochromatic light. However, such narrow wavelength sources can be difficult and costly to obtain and, however small the bandwidth is, it would always have a certain range. Usually the resulting error is acceptable when line emission lamps are used. This error results from the fact that in most detectors it is the radiant power of the component wavelengths that are additive while the Beer-Lambert law requires their logarithms to be additive. The measuring system would be considered to follow the Beer-Lambert law if the absorptivity remains constant over the bandwidth of the emitting light source or the bandpass of the filter. In the ultraviolet part of the spectrum, the mercury discharge lamp, which has a strong mercury line at 254nm, can be considered as a monochromatic light source since the absorption profile of chemicals are in general very broad in the same region.

2.4.2.3 Scattering Effect

This effect is mainly seen when large colloidal suspended particles are present in the sample especially when using the ultraviolet part of the spectrum. The numerical value of the coefficient of extinction decreases linearly with the sample concentration.

The total incident light consists of an absorption term and a scattering term as shown in Eq.2.11

$$dP = -kPcdl + Pn^2v^2dl \qquad [2.11]$$

where n represents the number of the scattering particles and the v the volume which is supposed to remain constant while k is a constant and P is the light power.

2.4.2.4 Fluorescence Effect

When a material absorbs and fluoresces at the same time, the detected light which results from the combination of the transmitted light and the fluorescent light, represents a value which does not correspond to the absorbed light. As a result a lower concentration value is obtained. Moreover, the fluorescent light could be absorbed by the species or the interfering parameter. The solution to this problem resides in filtering the optical signal using grating devices or high transmission optical filters with a narrow band width. The latter should be small enough to remove the fluorescent light.

2.4.2.5 Refractive Index

The refractive index of the solution affects the absorption of the sample in a proportional manner. The resulting effect is seen through the extinction coefficient which increases with increasing values of index of refraction[65]. In general, a sample concentration of 10^{-3} molar represents the upper limit at which the index of refraction of the sample remains substantially constant and does not change sufficiently to cause large errors. For example, in the case of an eosin sample, the error generated with a concentration of $7x10^{-2}$ mole.l^{-1} was found to be 1.8%[66]. The relation between the index of refraction and the coefficient of extinction is shown in Eq.2.12

$$A = A_{true}\frac{n}{(n^2+2)^2} \qquad [2.12]$$

where n is the refractive index of the aqueous sample and A its absorptivity. Measurement of the sample at high concentration values is still possible by using calibration curves. However, care must be taken when dealing with a larger range of concentrations.

2.4.2.6 Changes in the Chemical Equilibrium

Changes caused by the dissociation, association or polymerisation of the absorbing parameters affect the value of the coefficient of extinction and at the same time the relationship between the radiant light power and the concentration of the particular species. For example, this can be seen through the dilution process of the dichromate ion. In this particular case, the dichromate ion which absorbs light in the visible range of the spectrum (i.e. 450nm) is affected when the solution is diluted since the chemical reaction shifts towards the left of Eq.2.13.

$$2CrO_4^{2-} + 2\,H^+ \longleftrightarrow 2HCrO_4^- \longleftrightarrow Cr_2O_7^{2-} + H_2O \qquad [2.13]$$

To avoid the shift of the equilibrium, all the chromium ions should be converted to (CrO_4^{2-}) by making the solution in 0.05M potassium hydroxide.

In the case of chlorine, as can be seen in chapter 5, the chemical reaction of chlorine with water is pH dependent and therefore can be a source of error when absorption measurements are made in the ultraviolet part of the spectrum. Thus , if the pH is not maintained constant during the measurement an additional error can be generated.

2.4.3 Instrumental Deviations

These deviations are caused mainly by the use of unstable light sources, especially discharge lamps such as the one used to generate the ultraviolet light, or temperature sensitive laser diodes, where the wavelength can shift as a function of temperature, and additionally noise exists in the light emission modules and detector stages. Other effects, can be overcome by carefully choosing appropriate devices in the design of the measuring instrument. Some of the deviations can be compensated for in the calibration of the instrument and hence can be included in the instrument parameters.

2.5 Error Analysis

Because of the logarithmic relationship between the concentration of the chemical parameter and the variation of the transmitted light through the sample, the error generated by this relationship is not constant. It varies as a function of the light transmission (or absorption) value. The relation between the relative error and the transmitted light intensity is obtained by rearranging the Beer-Lambert law and calculating the first derivative as a function of light power as can be seen in Eq.2.14 where the relative error of the

concentration is defined as follows:

$$C = \frac{1}{\varepsilon L} Log\,(\frac{P_o}{P}) \qquad [2.14]$$

by differentiating Eq.2.14 with the variable P it becomes:

$$\frac{dC}{C} = \frac{1}{\varepsilon LC}\frac{d}{dp}(Log\,\frac{P_o}{P}) = \frac{-0.434}{A}(\frac{dP}{P}) \qquad [2.15]$$

Hence, the relative error in the concentration using the Beer-Lambert law is a function of the absorbance. In order to determine the optimum value of the absorbance where the relative error on the concentration is minimum a derivative of Eq.2.15 as a function of power produces the value at which minimum error is expected and this is shown in Eq.2.16.

$$\frac{d}{dP}(\frac{dC}{C}) = \frac{dP}{(2.30P_o)}(P\,Log\,\frac{P_o}{P})^{-2}(Log\,\frac{P_o}{P} - 0.434) \qquad [2.16]$$

A solution is then obtained by solving $\frac{d}{dP}(\frac{dC}{C}) = 0$ and it represents the minimum error in the concentration by using the Beer-Lambert law, and can occur at the absorbance value of A= 0.434 which corresponds to a transmission value of T = 0.368. Consequently, the error for this particular value of absorbance can be computed from Eq.2.15 and is found to be equal to:

$$\frac{\Delta C}{C} = -\frac{0.434}{A}(\frac{\Delta P}{P}) \qquad [2.17]$$

Thus, an absolute error in the measurement of the transmission of light of 3% is reported as an error of 8% in the concentration of the chemical species.

A plot of the error in the concentration as a function of absorbance is shown in Fig.2.4 and a flat curve can be seen between two approximate values of 0.3 and 0.6 units of absorption. Thus when a measurement is made while the absorbance is in this range the resulting error is minimal. It can be seen that when the variation of the light is very small, the error increases. This happens in two different cases. The first one occurs when the a value of the signal comparable to the resolution of the detector is reached, thus the signal variation is drowned in the noise. The second case occurs when the variation of the signal is very large

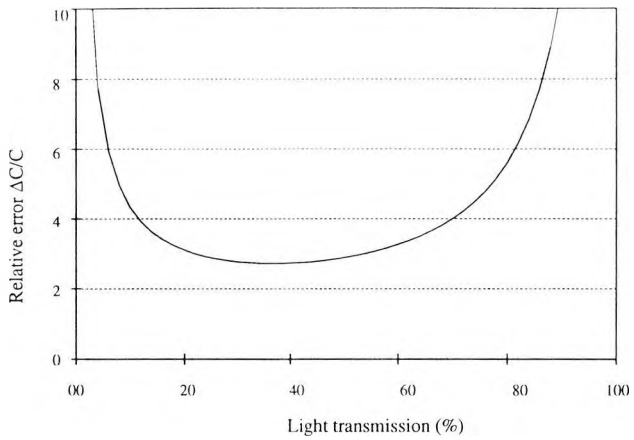

Fig. 2.4 Plot of the variation of the relative error on the concentration as a function of light transmission

and the light reaching the detector is small, hence comparable to the noise level. These cases occur when the transmission is below 10% and over 80%.

2.6 Fibre optic cables

Optical fibres are a particular type of dielectric waveguide which allow the propagation of the electromagnetic waves in the frequency range (e.g.10^{+12} to 10^{+15}Hz). The energy trapped in the core of the fibre is guided by a mechanism of multiple internal reflections at the core-cladding boundary along the length of the fibre. The core is made in general of silica for the low loss fibres used in the visible and infrared part of the spectrum and quartz or Sapphire when used in the ultraviolet part of the spectrum. Recently, advances in fibre fabrication techniques have reduced the losses and hence increased the maximum distance between repeaters used in communication over long distances. In addition Erbium doped glass which has the property of absorbing part of the light it carries, fluoresces at the same wavelength as the one carrying the information. As a consequence, the pulses weakened by the absorption and other losses are amplified, thus resulting in a decrease in the number of repeaters in the network [67].

A typical optical fibre is made of a cylindrical core having an index of refraction n_1 and surrounded by a cladding layer made of a similar material but having a slightly lower index of refraction n_2 so that $n_1 > n_2$. The two concentric cylinders are protected by a plastic jacket which gives the fibre its mechanical strength. Moreover, it protects the fibre from environmental effects including those caused by corrosive contaminants. A general profile of the fibre is shown in Fig.2.5

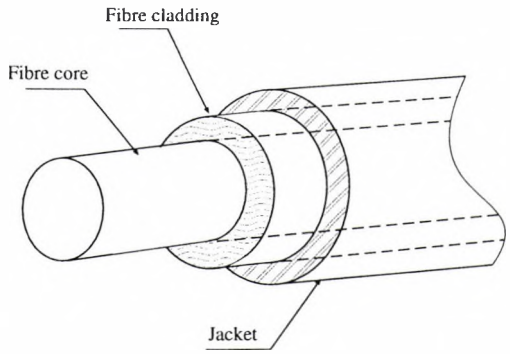

Fig. 2.5 Profile of a fibre optic cable

According to Snell's law, refraction of a light beam at the interface of two surfaces of different refractive indices occurs only when Eq.2.19 is satisfied:

$$n_1 \text{ Sin } \beta = n_2 \text{ Sin } \gamma \qquad [2.19]$$

where β is the incidence angle and γ is the angle between the refracted beam and the vector which is normal to the surface of the interface and these are shown in Fig.2.6. For a fixed values of n_1 and n_2 there exists a particular value of the incident angle, known as the critical angle, for which the emerging light beam is not refracted. Instead, it is reflected and propagates inside the fibre core. As a result of this effect, only the light beams incident to the interface (core-cladding) with an angle (β) larger than the critical angle, are reflected back into the core of the fibre and propagate along the fibre through the multiple internal reflection mechanism. When a light source is coupled to a fibre, because of the lower index of refraction of air, beams with an angle (θ) larger angle than the critical angle, travel through the fibre only for the first few reflections. However, they radiate and either propagate through the cladding for a short distance and get attenuated or leave the cladding through the jacket.

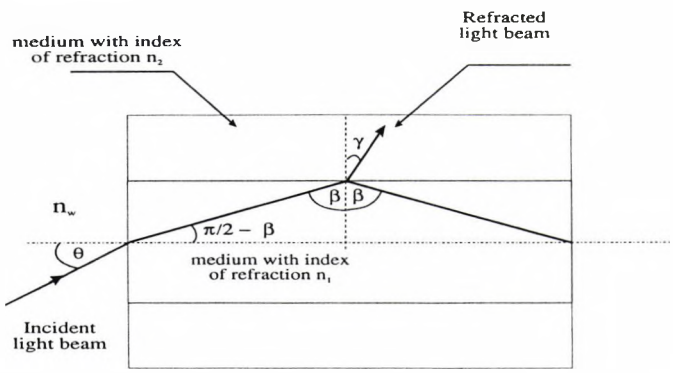

Fig. 2.6 Refraction of light at the interface of media having different refractive indices n_1, n_2 and n_w.

In order to fuly describe the propagation of the electromagnetic wave inside the fibre it is necessary to use the electromagnetic theory which introduces the the notion of modes. These are the solutions of the Maxwell equations which are represented by Bessel functions*. The number of the modes that can propagate in the core of the fibre is determined as a function of the wavelength, the index of refraction and the fibre dimensions.

Due to the nature of the propagation of the light inside the glass fibre, the ability to carry a large number of frequencies of the modulated wave is affected by a number of physical effects which limit the bandwidth of the fibre. For instance, when a light pulse is guided through a length of fibre, its profile changes and takes a bell shaped appearance on exiting the fibre. This is caused partially by the arrival of the different wavelengths which form the optical components of the signal at different times. This effect is known as the intramodal dispersion. In addition, material dispersion causes the pulse to become distorted and the time required to allow the side bands of the pulse to settle below a threshold value is increased, hence decreasing the carrying capacity of the fibre. The other origin of pulse broadening is caused by the intermodal dispersion which results from the fact that the velocity of the modes travelling through the fibre varies with the mode of the light. Consequently, some modes from which the pulse is made have different delays and the pulse is not reconstructed properly as a function of time on arrival at the end of the fibre. In optical communication the bandwidth factor is of a prime importance since the speed of the communication and the number of channels that can be used are determined by the material dispersion properties of the fibre. An other factor which is important to consider is the light attenuation of the fibre. This parameter affects the minimal distance before the optical signal is amplified i.e. the number of repeaters that have to be used in a network. However, these considerations can be different when the fibre is used in optical instrumentation and sensors where more flexible requirements on both the fibre and optical components are allowed. In chemical optical sensors, amplitude modulation and monitoring is normally a widely used technique for the measurement of various species. The capacity and bandwidth of the fibre is not a major restricting factor since in most applications, the speed of the propagation of a signal is far faster than transducing effect that takes place. Only in few applications such as the one concerned with refractive index

* *Bessel functions are the solutions of Maxwell differential equations in cylindrical coordinates.*

measurement requires the transporting medium i.e. fibre, to protect the polarisation information.

To overcome the problem of the pulse broadening, different types of fibre can be used in order to increase the bandwidth of the fibre, or the amount of light intensity guided through, depending on the situation.

2.6.1 Gradient Index Fibres

These types of fibres are used mainly in applications where there is a requirement for large bandwidths and a high optical signal power travelling through the fibre. The dimensions of the core in this particular type of fibre are in the order of few 100μm and can be as large as few 1000 μm. The profile of the index of refraction follows a gradual radial decrease from the centre of the core as is shown in Fig.2.7(b) which also gives an indication of the way the light beam travels inside the fibre. This profile of the index of refraction allows for a very low intermodal dispersion with the possibility of launching more powerful light beams into the fibre because of the large core diameter. The low intermodal dispersion is a result of the fact that the beams guided in the layer close to the cladding can travel at higher speed than the beams travelling near the core of the fibre. However, the latter travel along a shorter distance and hence the shape of the pulse is maintained and consequently,

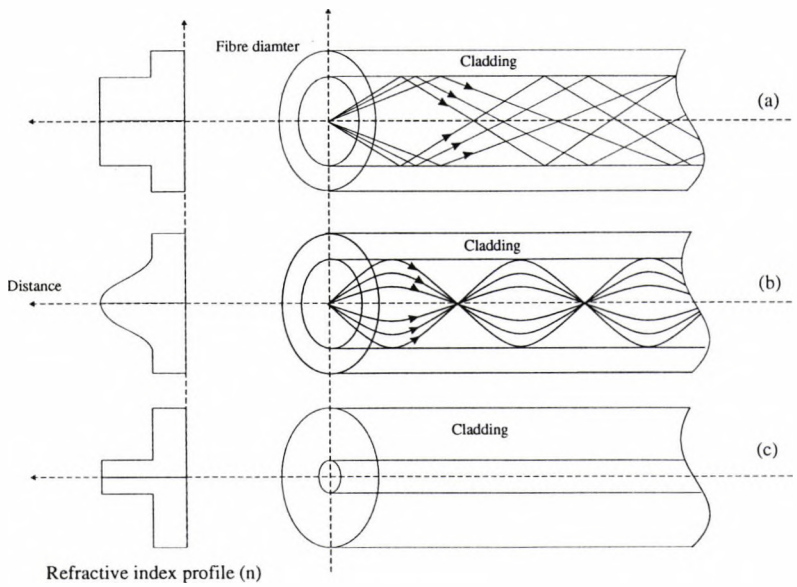

Fig. 2.7 Comparative figure showing the propagation of light through different types of optical fibres their respective refractive index profile:
(a) Step-index fibre multimode fibre
(b) Graded-index multimode fibre
(c) Step-index single mode fibre.

the intermodal dispersion is limited. On the other hand, due to the nature of the index of refraction of the fibre, the fabrication process for these fibres is likely to be more difficult.

2.6.2. Step-Index Fibres

The profile of the index of refraction of the step-index fibre is constant over the entire diameter of the core of the fibre. The propagation of the light beams inside the core of the fibre occurs in a straight line as is shown in Fig.2.7(a) and (c). In this type of fibre, the dimension of the core is very important since this determines the type and number of light modes which can propagate along the fibre. There are two main types of fibres; multimode and single mode fibres.

2.6.2.1 Multimode Fibres

For large diameter core fibres e.g. 50 to 1000μm, (known as multimode fibres), the different light beams that enter the glass guide travel at the same speed for different distances inside the fibre. This results in the delayed arrival of some of the modes. As a consequence, the intermodal dispersion is increased. Although these fibres are not used in communications because they are a major source of bandwidth limitations, they are very useful in applications were light power is more important than intermodal dispersion and speed[68]. This is the case where light from an ultraviolet lamp or visible indicator type LEDs is used to provide an optical light source. As a result of the spreading of the light beam generated in these type of lamps i.e. diverging beams, it is more difficult to launch the light into the fibre unless the core diameter is enlarged. This is the case for amplitude modulation techniques where intensity is the main measured variable. This type of fibre is mostly used in instrumentation and sensor applications where the speed of modulation of optical signals is very low (i.e. 0 to 100kHz) which is the case in the work described in this thesis.

2.6.2.2 Single Mode Fibres

When the dimensions of the core of a similar type of fibre are reduced to the order of 5 to 10μm, better bandwidth capacity is achieved through the propagation of a single mode, and this fibre is known as single mode fibre[69]. As a result, the intermodal dispersion is eliminated because there is no delay between the modes travelling since there is only one mode propagating along the fibre. The modal dispersion is then mainly caused by the material dispersion which cannot be avoided since it is inherent in the material used in the

fabrication process. This type of fibre is used in most communication networks since it can achieve a very high bandwidth capacity and where speeds of gigabits/second have been implemented in practice[70]. Interferometry is another field where single mode fibres are the only fibre that can be used because theses fibres can protect the phase and polarisation information of the light, especially in sensors such as current, pressure and temperature sensors[71]. However, launching light from general purpose light sources can be a tedious problem because of the small dimensions of the fibres. On the other hand, laser light sources (e.g. laser diodes), can be easily coupled to the fibre since the divergence of the light beam emitted from the laser source is maintained within the acceptance angle of the fibre.

2.6.3 Characteristic Parameters of Fibres

Optical fibres are characterised by a number of parameters mainly numerical aperture and V number.

The numerical aperture of a given fibre is a measure of the maximum acceptance angle so that the entering beam can be guided by way of multiple internal reflections along its length. It is independent of the dimensions of the fibre but is only a function of the refractive indices of the core and cladding and the medium from which the beam is launched e.g. in most case it is air where n = 1. However, in the case of the light source and the fibre both being immersed in the liquid, the numerical aperture value changes according to the refractive index of the liquid, and, usually decreases since the refractive indices of liquids is larger than that of air. This also results in a decrease in the divergence of the beam of light at the exit end of the fibre. In order to obtain an accurate calculation of this parameter, the numerical aperture is calculated from Eq.2.19 by changing the value of the index of refraction of air by the corresponding value for the liquid.

As a result of applying Snell's law $n_w \sin(\theta) = n_1 \sin(\alpha)$ and $n_1 \sin(\beta) = n_2 \sin(\gamma)$. The condition of the critical angle results in $\gamma = \pi/2$. Hence, the numerical aperture (NA) is expressed as a function of the largest launch angle (θ) as follows:

$$NA = \arcsin\theta = \frac{1}{n_w}\sqrt{n_1^2 - n_2^2} \qquad [2.19]$$

where θ, β, γ are as shown in Fig.2.8 and n_w, n_1, n_2 are the refractive indices of the water sample, core and cladding of the fibre respectively.

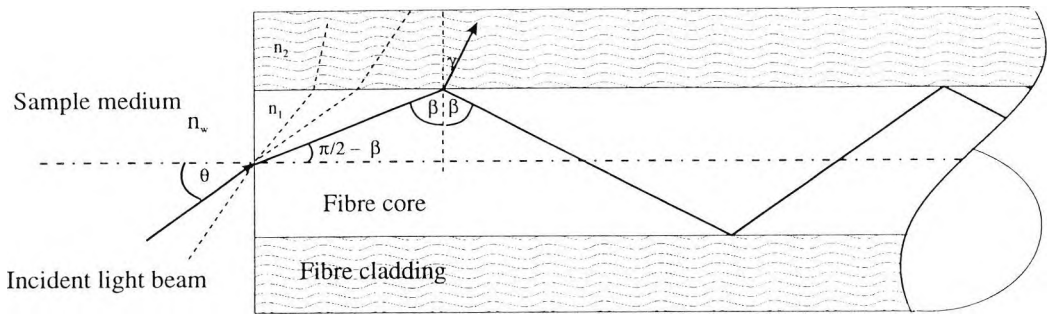

Fig. 2.8 Figure showing the angle of acceptance of a fibre using a ray propagation theory.

This can also be expressed as a function of the numerical aperture with respect to air and is given by the following:

$$NA = NA_{air} / n_w \qquad [2.20]$$

For instance, in the case of the silica fibre used in this work, the Numerical Aperture (NA) as defined by the manufacturer at the air-glass interface is 0.4. Consequently, the maximum acceptance angle for an air-glass interface is approximately 23°. However this value decreases when the fibre is immersed in water whose index of refraction is around 1.3 where NA = 0.3 giving a maximum acceptance angle as 18°(the index of refraction of most species can vary from 1.4 to 1.6 hence giving a relative NA as low as 0.28 and $\theta_{max} = 16°$ or NA = 0.25 , $\theta_{max} = 14°$ respectively)[72]. This effect has the advantage of reducing the spread of the beam leaving the fibre when used in water and hence allows for a stronger optical signal to be guided or collected by the returning fibre.

V number is a fibre parameter which gives an indication about the number of modes that can propagate along the fibre. It represents the low cut off frequency for which no mode can propagate in the core of the fibre. Some other modes whose frequencies are below the cut off frequency can still propagate in the core for a short distance and then exit the core of the fibre to be guided in the cladding before leaving the fibre completely. However, these modes are not important since they do not contribute to the total amount of light that reaches the end of the fibre. This parameter (V) is also a function of the numerical aperture and is inversely proportional to the wavelength i.e. $V = \frac{2\pi}{\lambda} r\,(NA)$ where λ is the wavelength, r the radius of the core and NA the numerical aperture of the fibre .

2.6.4 Loss Mechanisms Within Fibres

The attenuation of light travelling inside a silica fibre can be attributed to three major sources which have been conveniently summarised in the literature [73]:

- Absorption
- Scattering
- Mechanical

2.6.4.1 Absorption

Absorption results from the interaction of the light as an electromagnetic wave with the constituents of the glass fibre, with the associated impurities and defects, and can be classified into three types.

a) ***Intrinsic***: In this case the losses are attributed to the stimulation of electron transitions in the glass structure caused by higher energy excitations that occur in the ultraviolet part of the spectrum. This results in an exponential decay which increases with decreasing wavelengths. A second phenomenon occurring in the infrared region is due to the molecular vibrations which result in fundamental and overtone absorption bands such as Si-O (9.2μm) or Ge-O (11.0μm).

b) ***Extrinsic***:This type of absorption is caused by impurities deposited in the core and cladding material during the fabrication process. Their concentration can be in the low part per billion range (PPB). Nevertheless, they can cause attenuation throughout the UV and visible range as high as 2 $dB.km^{-1}$. For example, Fe^{3+} absorption occurs at 400nm with an attenuation of $0.15dB.km^{-1}$, Cu^{2+}, (685nm and $0.1dB.km^{-1}$) and Fe^{2+}, (1100nm,0.68 $dB.km^{-1}$). Another source of attenuation is related to the hydroxyl ion (OH^-) which can be as water vapour dissolved in the glass. As opposed to the other impurities, (OH^-) effects occur in the near infrared and infrared, and are thus far removed from the spectral range where UV and visible light are utilised.

c) ***Defects***: These defects are usually generated by material vacancies within the crystalline structure of the glass. They can also be induced thermally or by means of radiation.

2.6.4.2 Scattering

a) ***Rayleigh***: The most common scattering effect which causes attenuation of light in the fibre is Rayleigh scattering. This is found to proportional to the inverse of the

wavelength to the power four ($1/\lambda^4$). As a result, the shorter the wavelength the more important the losses become. Although this does not cause major problems in the communication field it could give rise to some power transmission problems in the ultraviolet part of the spectrum. These attenuations can be estimated to be approximately 512dB.km^{-1} at a wavelength of 200nm and only 8dB.km^{-1}at a wavelength of 560nm for a similar fibre. The effect of Rayleigh scattering has been calculated to represent only 50% of the losses of the particular fibre used in this work. This result was obtained by calculating the theoretical value of the Rayleigh scattering attenuation and comparing it with the transmission profile data of the fibre provided by the manufacturer.

b) ***Bulk and Wavelength Imperfections***: The physical irregularities generated during the fabrication process especially at the core cladding interface provide a means of reducing the transmission by total internal reflection since the latter is no longer sustained because of the resultant variations in the angle of incidence of the light on the interface. Scattering due to bubbles and cracks in the core of the fibre can also contribute to the loss of the light, especially when the dimensions of the irregularities are comparable to the wavelength. This effect is known as Mie scattering.

c) ***Raman and Brillouin Scattering***: This type of scattering is a non linear effect as opposed to the two types of scattering described earlier. Brillouin scattering affects the modulation of light through thermal molecular vibration within the fibre. The photon involved in the process generates a phonon of an acoustic frequency and also a scattered photon. This effect take place only above a certain threshold value for the optical power. A similar effect known as Raman scattering also takes place however, it a phonon in the optical frquency is generated during this process. The power threshold for Raman scattering is three orders of magnitude that of Brillouin scattering. These two effects can be avoided by choosing a sufficiently low level of light power.

2.6.4.3 Mechanical

a) ***Fibre Bending:*** According to ray theory, the multiple internal reflection principle can only be sustained if the reflected light beam falls within the acceptance angle along the fibre as shown in Fig.2.9 (a). When the fibre is bent, the angle of incidence changes and the beam can propagate through the cladding. This effect, as can be seen in Eq. 2.21, is a function of the critical curvature radius i.e. where the losses are large. It is also a function of wavelength and results in different loss values for different wavelengths, especially if the gap difference between the wavelengths is large. In a sensor system

using two different wavelengths, one as the sensing wavelength and the other as the reference wavelength, a non systematic error is introduced during the measurement process when the guiding fibre is bent, especially for systems where each fibre is used to guide one particular wavelength.

$$R_c \approx \frac{3n_1^2\ \lambda}{4\pi\ (n_1^2 - n_2^2)^{3/2}} \qquad [2.21]$$

where n_1 and n_2 are the refractive indices of core and cladding, R_c is the curvature radius and λ is the wavelength.

b) ***Coupling***: A change in the refractive index in the connecting part of the fibres is usually the source of the losses at the fibre-fibre interface. The most common is the gap between fibres. As can be seen in Fig.2.9(b), there is always a gap between the two fibres however well polished and flat the fibre ends are. Hence, there is a band gap made of air which has a different refractive index to that of the glass and hence will result in a loss of light power. Other effects such as fibre misalignment tend also to produce a loss of light power since the total area of the cores of the fibres are not in line, hence part of the energy is transmitted into the cladding of the second fibre. This effect although very

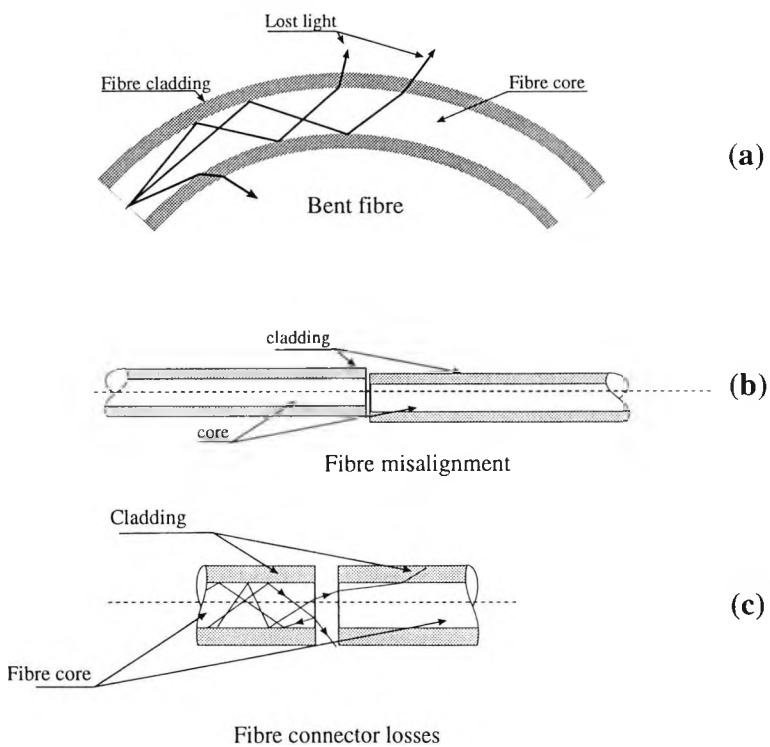

Fig. 2.9 Descriptive drawing of the main types of fibre losses:
(a) Fibre losses caused by fibre bending
(b) Losses resulting from fibre misalignement
(c) Fresnel losses at the fibre-fibre conection

important for small diameter fibre e.g. 10 to 100μm is usually insignificant in large diameter fibre e.g. 500 to 1000μm diameter since the control of the positioning of the fibres is easier.

A second source of energy loss within fibres is due to Fresnel effects as depicted in Fig.2.9(c). These losses are inherent in the process of light guidance in a fibre. Similar to the reflection of light inside a fibre, the air (or water sample), and fibre interface behave in the same way as the core cladding interface. Because the index of refraction of air is smaller than that of the fibre core, the light is partially reflected back into the fibre. This effect is used in optical time domain reflectometers (OTDR) as a mean of locating splices and fibre breaks. Fresnel losses are calculated from Eq.2.22.

$$L_{Fresnel} = -10 \log_{10} \left(1 - \left\{ \frac{n_1 - n}{n_1 + n} \right\}^2 \right) \qquad [2.22]$$

where n_1 and n are the refractive indices of fibre core and medium (usually air or index matching gel) respectively. The losses are smaller when the interface is made of water and glass since the difference in their respective refractive indices is small.

2.6.5 Fibre Reliability

Much emphasis has been placed on fibre reliability and long term effects depend upon on three major factors. These are related to fibre strength, changes in attenuation due to radiation and finally the effect of hydrogen on the increase in the OH^- absorption profile.

a) The fibre strength is related to the appearance of micro cracks caused by fibre bending and fibre stress. These are believed to be generated by chemically or mechanically induced flaws, usually at the surface of the fibre, and result in a local failure. Coating fibres with different polymers and hermetic materials to prevent moisture damage to the fibre surface has been proposed as a feasible solution to these problems[74].

b) The effect of strong ionising radiation on the attenuation profile of the fibre has been found to be an important factor in the design of instruments using fibre links. The radiation can affect the chemical bonds in the glass matrix. These are then disrupted giving rise to absorption in the visible and infrared part of the spectrum. This structural damage is seen to affect multicomponent fibres (e.g. silica doped with GeO_2) more than fibres made out of pure silica[75]. This structural damage is found to be caused by the removal of the oxygen atom from the glass matrix, thus generating defect sites.

c) Finally, the increase of attenuation in the fibre is related to the hydrogen induced losses. This is the result of the reaction of hydrogen, dissolved in the glass, with the rest of the matrix. Although the phenomenon which causes this absorption is understood, the mechanism of reaction of non-dissolved hydrogen with the glass lattice is still not clear[76]. It has been observed also that these OH^- absorption losses occur in the red and infrared part of the spectrum which is not very relevant to the work described in this thesis.

Unfortunately, there has been no discussion in the literature about the transmission degradation caused by high energy radiation such as the light emitted in the ultraviolet region of the spectrum. Also the information obtained from manufacturers was not conclusive in respect to possible damage to pure quartz fibres when used in very harsh conditions over long periods of time i.e. UV radiation.

2.7 Optical Emission and Detection Systems

In optical instrumentation two important stages form the basis of the measurement, once the transducing principle has been chosen. These consist of the light source and the light detection systems. In addition to the correct choice of these devices, the influence of the noise level in the detected optical signal must be considered.

2.7.1 Light Sources

Two different types of light sources, namely light emitting diodes and low pressure discharge lamps have been used in the design and the implementation of fibre optic chemical sensors and are discussed subsequently. These were chosen because of the light power/cost ratio and the fact that they were small and hence would not present a major problem in the minimisation of the overall dimensions of the instrument. Additionally, they can be electronically modulated so that the effect of noise and ambient perturbations can be filtered out electronically.

2.7.1.1 Light Emitting Diode (LED)

In the case of the LED, light is generated through a process of electroluminescence which occurs when a voltage is applied to the electrodes of a semiconductor junction diode. Recombination of electron-hole pairs which are formed due to the passage of an electric current in the diode results in light emission whose peak wavelength is a function of the

energy levels within the semiconductor structure itself. When different dopants are used, different energy levels are created which in turn are used to generate light at a specific wavelength. The nature of the dopant is not the only factor responsible for the emission of a specific wavelength, its concentration can change the peak wavelength as in the case of the green and yellow LEDs (GaP semiconductor) which use the same dopant e.g. nitrogen. The only difference between the two LEDs resides in the fact that the concentration of nitrogen in the case of the yellow LED is higher than in the case of the green LED[77].

LEDs are considered to have Lambertian light emission where the power distribution follows a cosine function i.e. $p = p_o \cos \theta$ where θ is the angle between the light beam and the normal to the surface of the LED. Hence the light beams appear to be more parallel around $\theta = 0$ when the plastic housing has a domed profile.

The characteristics of the peak wavelength and the width of the emission are both sensitive to temperature, especially over the large temperature range as shown in Fig.2.10. Although there is a shift of the peak wavelength towards higher wavelengths and also width broadening, this effect is not important since absorption in the UV-visible part of the Electromagnetic Spectrum (EM) is broad and the range of temperature is significantly smaller. Additionally, these LEDs can be easily electronically driven which reduces the complexity of the drive circuitry.

Alternatively, laser diodes can be used. Their light intensity emission is higher and their

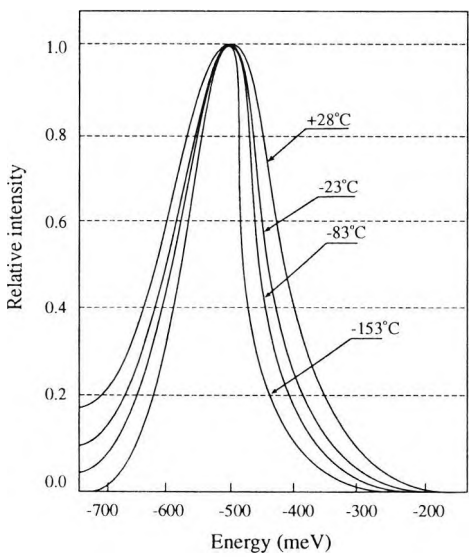

Fig. 2.10 Broadening due to temperature (-153 to +25°C) occuring in the emission of GaP LED with an acceptor concentration of 10^{+18} cm^{-3}. The horizontal scale represents the emission peak energy minus E_g.[77]

spectral output is purer than the output of LEDs. The beam divergence is so small that most of the light is launched into the fibre provided that the dimension of the core of the fibre is larger than the beam dimension. However, their spectral output is very sensitive to temperature changes and they behave linearly only over a limited current range. Moreover, few laser diodes can produce the wavelength required to be utilised with the visible part of the spectrum.

LEDs are not available for generating light in the UV part of the spectrum since no suitable material has been found that can be used in order to generate the required bandgap and furthermore they would be even more inefficient than blue LEDs.

2.7.1.2 Mercury Discharge Lamp

The low pressure e.g. 10^{-2} Torr, discharge lamp works on the principle of the breakdown of a high voltage across the electrodes. This happens once the gas has been ionised through a process of multiple collision which results from the intense local electrical field. Usually mercury is used because it is a unique metal which is volatile and is chemically inert to the envelope and electrodes. Additionally, it has a lower ionisation energy level and can have enough vapour pressure at low temperatures hence it emits resonance lines. Consequently, it is widely used in general fluorescent lighting. This type of UV light source can be dc or ac powered. In the latter case, a negative relationship exists between the driving current and the applied voltage. Hence a limiting current device is fitted in the power supply to control the "run away" effect of the current. Although the power supply for such a device is complex, ac power provides a low electrical consumption, low heating of both the lamp and the power supply and the modulation can be used to protect the optical signal from ambient lighting and optical and electrical interferences. The requirements from a power supply to maintain a stable output are the provision of 500 to 1000V and a current of 20 to 30 mA. The modulating frequency can range from 1 to 100kHz.

The spectral properties of this particular type of UV light source consist in the provision of an intense line occurring at 253.7nm in contrast to continuous light emission obtained from the deuterium lamp. This line has been reported to result from 60% of the input energy[78]. Another line is emitted at 185nm but is usually absorbed by the glass envelope. Other lines occurring at different wavelengths are a result of the same process but have emission peaks of less intensity. The emitted lines correspond to the permitted energy levels of mercury. Additionally there are some lines which are mainly generated by the

type of material used as electrodes.

Major problems associated with the discharge lamp are amplitude instability and a short working life especially when compared to LEDs and laser diodes. Maximum working periods of 10,000 hours are common when used on a continuous basis. However an additional drawback of the discharge lamp consists in the variation of the intensity of the light during the warming of the lamp. Stability is reached only after the lamp reaches a certain working temperature. The time required for the lamp to reach this stability can vary from 1/4 hour to 3/4 hour on average. Initially, the mercury is cold and the impedance of the lamp is low. Consequently, the lamp requires intense current which leads to increasing ionisation of the atoms. Stability is reached when mercury is completely ionised and the temperature of the lamp is then stabilised. This problem can be overcome by heating the lamp and thermostatically maintaining it at a constant temperature.

2.7.2 Light Detectors

There are three types of light detector that can be used in fibre optic related instrumentation: Junction photodiodes (phototransistors), avalanche diodes and photomultipliers.

2.7.2.1 Junction Diode

The junction photodiode is basically a diode whose junction is covered by a glass window only in order to allow light to penetrate the device and interact with the carriers in the depletion region to produce free electrons. When the electron absorbs the light energy, it jumps from the valence band into the conduction band. As a result, a hole is liberated and a pair (electron-hole) is generated. These are attracted to opposite sides of the junction by the electrical field thus generating a flow of current. This current is proportional to the intensity of the incident light to the diode e.g. photodiode. Devices such as current converters transform this signal into a different form without loss of information. The most common material used is silicon which has a varying sensitivity to light as a function of wavelength. The peak of sensitivity is reached in the 900nm region. However, it is used in the visible with good results and when the glass window is replaced by a quartz window, the same device can be used to detect ultraviolet energy to a maximum wavelength of 250nm although with a much reduced sensitivity e.g. 1.5 to 2 compared to 6 at 900nm. Different materials having enhanced optical properties such as germanium (Ge) and indium gallium arsenide (InGaAs) are used in the design of photodetectors. These are mainly used for the detection of infrared and far infrared wavelengths. Hence they are not suitable for

ultraviolet and visible light detection[79].

A major factor which affects the response of the photodiode is the dark current which represents the current flowing without illumination. This effect can be superposed onto the main detected signal and reduces the signal to noise ratio. Large values are obtained with germanium e.g.100nA, but are low in the case of silicon (e.g. 1nA). Additionally the dark current is sensitive to temperature and can reach values as large as 1μA at 40°C for germanium. These photodiodes have a response in the order of 10^{-9}s. Performance is enhanced when an intrinsic layer is sandwiched between the p and n regions creating a longer depletion region where most of the photons are absorbed to produce an electron-hole pair and this is known as a positive-intrinsic-negative (PIN) device. As a result of this layer, longer wavelengths can be detected and the sensitivity of the diode is increased.

When speed is not a major requirement e.g. below the μs range, a phototransistor which relies on the same physical effect, can be used to measure the light. The collector-base junction is used as the photon converting part and the generated carrier is amplified in the same device. A Darlington structure can also be used to amplify the current to the required level.

2.7.2.2 Avalanche Photodiodes

Avalanche photodiodes are similar devices to the photodiodes with improved carrier amplification which occurs by impact ionisation. This is the result of an intense electric field created by the high reverse bias voltage (e.g. 100 to 400V). Amplification as high as 10^{+4} can be achieved in defect-free material. This is very useful especially in conditions where the detected light is very weak as is the case in certain types of instrumentation. However, both the random nature of the gain mechanism and its sensitivity to temperature tend to increase the noise level. Additionally, the high gain which is reverse bias voltage dependent is not constant over the optical spectrum since it is a function of the wavelength. Finally, this device is targeted towards communication type wavelengths and hence their cost tends to be high when developed for use in the visible and ultraviolet part of the spectrum for instrumentation use.

2.7.2.3 Photomultiplier

A different type of detector could be used but is usually avoided because of its fragility and power supply requirements. This device is the photomultiplier. It uses a different

mechanism in order to detect and amplify the signal. When light falls on a thin layer of conducting material such as Cesium, an electron is extracted from the metal. The latter is accelerated through an electric field generated by a difference of voltage of the order of 100V applied to a successive number of dynodes. On impact on the collecting dynode, more electrons are extracted which in turn are accelerated through by the high voltage existing between these dynodes. The gain in the detection process is so high that this device is sensitive to light power in the 10^{-12}W range. It has a flat response especially in the ultraviolet part of the spectrum and is widely used. This device is very sensitive to the fluctuation of the bias voltage since the gain is a function of the high voltage value and hence requires a very stable power supply. Recently, robust and miniaturised devices have become available, particularly in Japan[80] (Hamamatsu Corp.), and in future research could prove to be valuable.

2.7.3 Noise Considerations

The effect of noise in the measurement of the optical signal is the major limiting factor in the final accuracy and hence the optimal sensitivity of the sensor. The noise generated in a photodetector device without any internal gain (PN junction or PIN PD) can be attributed to Shot noise. Two major sources of this type of noise are the dark current which represents the reverse leakage current without illumination and the analogue quantum noise which is the consequence of the recombination time of the carriers which occurs over a fluctuating time. This results from the fact that some carriers can recombine within the average recombination distance and some require a longer time to do so. In the photodiode with internal gain, the fluctuation of the gain is also included in the calculation of the total noise in the detector. Although thermal noise is attributed to the passive component i.e a resistor, it is sometimes a dominant figure of the detector-amplifier system performance.

The noise generated by a detector on its own, does not provide a real estimation of the overall noise performance of the system. Not only is the performance of the combination of the detector-amplifier required but so is the bandwidth-gain relationship, and it is case dependent[81]. In a simple analysis[82] three amplifiers- low and high impedance front end and the transimpedance amplifiers are discussed and the noise performance analysed (Appendix 1). In the case of the low impedance front end amplifier, the noise level is relatively high and the sensitivity is low since these parameters are proportional to the resistor value (the resistor being the device used to convert the current into voltage). When the resistor value is increased the noise level is reduced and the sensitivity is enhanced

however the bandwidth is reduced e.g. $B_{max} \approx 10$ kHz. This limitation is caused by the capacitance of the photodiode whose value lies in the 1 to 2pF range. This is inherent in the design of the photodiode and, in combination with the resistor, acts as a low pass filter. On the other hand, a transimpedance amplifier offers a larger bandwidth and better sensitivity, however, it cannot equal the noise performance of the high impedance front end amplifier. The transimpedance amplifier provides good stability and improves the effect of load on the photodiode because of the very high input impedance of the operational amplifier[83]. A Noise Equivalent Power (NEP) is usually used to give a figure of merit of the noise performance of the detector and is the value of the power needed at the input so that an electrical signal is present at the output of the device which equals the noise value when no light is applied. Numerically it is the ratio of the noise current to the responsivity of the photodiode as in Eq.2.23.

$$NEP = \frac{noise\ current\ (^{A}/_{Hz^{1/2}})}{Responsivity\ (^{A}/_{W})} \quad (^{W}/_{Hz^{1/2}}) \qquad [2.23]$$

The smaller the value of the NEP the better the detector is, however this is proportional to the inverse of the root square of the bandwidth. Hence, the larger the bandwidth the larger the noise level[84].

2.8 Conclusion

The interaction of light with matter results in the characterisation of the type of material forming matter. This property is then used in the analysis of matter by means of absorption of the radiation travelling through the analytical sample. Although the Beer-Lambert law, which is used to relate the concentration of the absorbing species to the detected light intensity, is affected by some instrumental and real factors such as monochromaticity, stray radiation and changes in the index of refraction, and the resulting error can be a function of the light power, it is nonetheless an appropriate and simple method which can provide adequate accuracy and stability within a limited range for the measurement of chemical species. The use of optical fibres as part of the optical set-up can only provide more flexibility. It has been shown in this chapter that there is not one set of rules to use in order to devise and built a measuring instrument but the development is rather case dependent so that the choice of the light source and detector system and also an appreciation of the noise performance of the system which will be described appropriately in Chapter 4 and

Chapter 6 is vital in the final design. Additionally, a characterisation of the optimum type of fibre and their performance as well as the related optoelectronic assessment indicate the usefulness of fibres and related electronics in the design of chemical sensors based on the absorption of light.

Chapter 3

pH Measurement with Dyes for Titrimetric Applications in the Biological Range

Abstract

An analysis of the colorimetric techniques for use with optical fibres is presented in this chapter and a system analysis is carried out to provide the basis of the design of an optical fibre based pH meter. This relies on the absorption of a phenol red dye in order to relate the pH of the sample to the concentration of a particular form of the dye which is sensitive to the change in pH value. Furthermore, this is used to predict the response of the sensor and the major factors on which the design is based so that optimum performance can be achieved. This is emphasised through the identification of the intrinsic and extrinsic sources of error and lead to a relationship between the error in the measurement and the error in the pH value.

3.1 Introduction

The measurement of pH is of vital importance in the chemical and biomedical fields. The knowledge of the pH value can help to establish optimum conditions for the control of chemical reactions as is the case for the reaction of chlorine with ammonia where optimum reaction time is achieved when the pH value is approximately around 8. Measurement of pH in the medical and biomedical fields is also an important factor, especially when setting the optimum living conditions in cell growth experiments and also in diagnosing some illnesses. For instance the pH of blood lies, under normal conditions, around a value of 7.4 and can vary from venous to arterial by 0.02 pH units[85]. In this particular case, freedom from toxicity and reduced probe head size are some of the major requirements of the pH sensor. Accuracy is also demanded in medical diagnosis, as is stability.

The pH of a liquid sample is a measure of the activity of the hydronium ion H_3O^+ usually defined as in Eq 3.1.

$$pH = - Log (H_3O^+) \qquad [3.1]$$

where (H_3O^+) represents the activity of the hydronium ion. The activity of the ion gives an indication of the ability of the ion to influence an equilibrium in a chemical reaction. Consequently, in dilute samples the activity is approximated to the concentration of the ion. However, when the sample concentration is high i.e. higher than 0.1molar[86] , the number of ions that can influence a reaction decreases although the concentration of that ion remains the same. Hence the difference between concentration and activity enlarges. The activity of the ion is related to its concentration by the activity coefficient which can vary with the ionic strength of the sample. The activity can then be related as follows:

$$(H_3O^+) = \gamma_{H_3O^+} C_{H_3O^+} \qquad [3.2]$$

where γ_{H+} is the activity coefficient of the ion and C_{H^+} its concentration.

The work carried out in this thesis was performed on the basis that $\gamma_{H+} = 1$ i.e. dilute samples. This assumption is further discussed in the concluding part of this chapter.

Different methods are available to carry out the measurement of pH under various environmental conditions. The most widely used methods are based on electrochemical or optical phenomena. In the case of electrochemical methods, potentiometric techniques are

deployed to monitor the activity of the hydrogen ion based on the Nerst equation which relates the activity of the ion to the numerical value of the pH, as in Eq.3.1. The resultant voltage that develops across two electrodes, one of which is a reference electrode, provides a voltage output which represents a measurement of the pH, as is depicted in Fig.3.1. In potentiometric measurements, this electrode could be a liquid junction whose voltage E_j is assumed to remain constant since it is generated by the solution of reference. The voltage appearing at the electrode of a system consisting of a combination of {indicator electrode/sample//reference solution/reference electrode}, can be expressed as in Eq.3.3

$$E_{system} = E_{indicator} - E_{ref} + E_j \qquad [3.3]$$

where E_{system}, $E_{indicator}$, E_{ref} and E_j are the potentials that develop for the complete system, the indicator and reference electrodes and the liquid junction respectively.

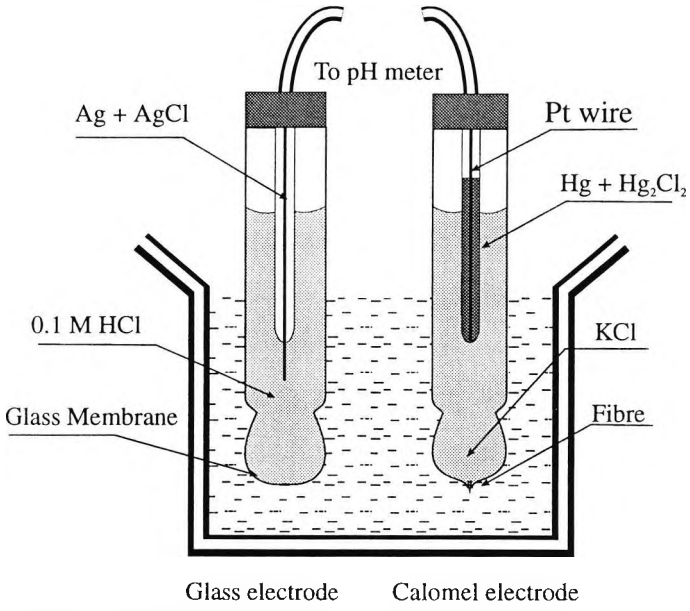

Fig. 3.1 Schematic drawing of a pH measuring device based on the potentiometric technique using the Calomel reference

To overcome the problem of liquid junction variation, salt bridges were used and different systems operating without a liquid junction were devised. For example the glass electrode pH meter has a glass membrane which is hydrogen ion-selective. A voltage develops across the glass membrane and is related to the activity of the hydrogen ion. In this case the reference electrode is a calomel or Ag/AgCl electrode.

A second effect which might reduce the field of use of such a technique is the ionic strength of the sample. The activity of the ion is a function of the ionic strength and it was found

that this relationship influences the activity of the ion, for an ionic strength larger than 3[3]. Additionally, the local electrical potential is known to affect the measurement of pH value. Moreover, the pH of solutions where a current flows cannot be measured by this technique e.g. in a liquid battery.

In the case of colorimetric techniques, the pH measurement is obtained by monitoring the change of the colour of organic dyes which are sensitive to the hydrogen ion concentration present in a given sample. conventionally, the numerical value of the pH of a substance is approximately estimated by comparing the intensity of the colour of a "universal indicator" paper on which specific dyes have been adsorbed with a calibrated reference paper. Furthermore, colorimetric techniques can be used in a variety of situations, even in liquids, where other electrical effects are taking place, as is the case for electroplating plants. This results from the fact that the transducing effect is completely optical. However, the major drawback of the colorimetric techniques resides in the fact that interaction of light with the dye results in obtaining a measure of the concentration of the dye which has reacted with the species, in this case H_3O^+. Hence, the change of colour is related to the concentration of either the dissociated or the undissociated part of the dye, depending on the case. This, in turn, is related to the concentration of the hydrogen ions present in the sample. Approximations in the relationship between the hydronium ion concentration and its activity are made so that the measurement of pH value is obtained[87]. This technique in combination with spectrometry provided a sound base for the development of a mathematical model which can be used to overcome the problem of insensitivity of the naked eye. Furthermore, with the advances of optoelectronic and fibre optic fabrication, colorimetry could be made to suit the requirement of the medical and industrial fields. The chemistry of these indicators is well established and has been extensively discussed in the literature[88]. It is not the aim of this work to develop these indicators, but it is to develop appropriate fibre optic instrumentation and its implementation.

Fibre optic pH meters were at the centre of attention of fibre optic based sensors development and work in this area has been focusing on the chemical aspect [89][90]. These early systems were bulky, and used costly and powerful optical light sources. Additionally, spectrometers were used to monitor the change in colour of the dye. In this work, the aim is concentrated on the use of simple techniques for improving the electrical and electronic aspects of the sensors. For instance, indicator type LEDs were used as light sources and modulation techniques were used to guide the combined light from such sources into the

same fibre and also the system was designed to provide a simple detection method, without having to resort to expensive and additional components such as optical filters and mechanical choppers. Furthermore, two different methods for generating the reference signal were implemented and their results compared and discussed.

3.2 Colour Indicators

Colour indicators, which consist of large organic molecules, are weak acids or bases and interact with matter through chemical reactions [91]. This results in a change in their spectral properties, as is the case with acid-base indicators. In this instance, the pH of an aqueous solution is determined by the change in the overall intensity of the dye. When the latter is in an aqueous solution, a certain percentage of it reacts with the sample and dissociates while the rest remains undissociated, as is shown in Eq.3.4

$$H_2O + HInd \longleftrightarrow H_3O^+ + Ind^- \qquad [3.4]$$

where HInd and Ind^- are the undissociated and the dissociated part of the indicator respectively. These two species i.e. HInd and Ind^-, are known as tautomers[92]* and absorb light in the visible part of the spectrum at two different wavelengths respectively, or more precisely over two different bands of wavelength, since the absorption in the visible is broad. Hence the colour of the substance is determined by the highest concentration of either the undissociated or the dissociated part of the dye. For instance, in an acid sample, phenolphthalein is colourless (pH < 8) and becomes red in an alkaline sample. The constant of equilibrium of Eq.3.4 is K_{ind} and this can be given by :

$$K_{ind} = \frac{[\,H_3O^+\,]\,[\,Ind^-\,]}{[\,Hind\,]} \qquad [3.5]$$

Hence the ratio of the dissociated to the undissociated parts of the dye is inversely proportional to the concentration of the hydronium ion, as is given by Eq.3.6

$$\frac{[\,Ind^-\,]}{[\,HInd\,]} = \frac{K_{Ind}}{[H_3O^+]} \qquad [3.6]$$

* **Tautomerism** *is the existence of a substance in equilibrium between two interconvertible forms. In this case, there are two absorption peaks whose overall intensity remains constant while the intensity of absorption of each form varies with pH*

It is established that when the ratio of the concentration of the dissociated to the undissociated part is smaller than 10, the colour exhibited by the dissociated part of the dye becomes undetectable[93]. On the other hand the colour, whose origin results from the undissociated part, becomes undetectable when the ratio of the concentration of the dissociated to the undissociated parts of the dye is larger than 10. As a result of this definition, the combination of Eqs 3.5 and 3.6 enables a determination of the practical range of pH values where the change of colour of the dye can be used to monitor the pH of the sample, i.e.

$$pH = -Log\,(K_{ind}) \pm 1 \qquad [3.7]$$

Consequently the maximum range of pH that can be monitored by the use of a single dye is ~2 pH units.

3.3 Spectral Properties of Dyes

There are different types of acid-base indicator, each of which operates over a limited pH range, as is shown in Table 3.1. The nature of the interaction between the electromagnetic wave and the indicator dyes is believed to be caused by structural changes. This subject is vast and is not discussed further, however a basic illustration is given in this section and some examples are given below. The major part of these indicators can be classified into three main groups. These are, phthalein, sulphonphthalein and azo compounds.

3.3.1 Phthalein

Phthalein indicators are of a type that exhibit various colours when in alkaline sample and

Common names	pH range	acid colour	base colour	type
Methyl red	4.2 - 6.3	red	yellow	sulphonphtalein
Phenol red	6.4 - 8.0	yellow	red	sulphonphtalein
Phenolphthalein	8.0 - 9.6	colourless	red	phthalein
Tymolphthalein	9.3 - 10.5	colourless	blue	phthalein
Methyl orange	3.1 - 4.4	red	yellow	azo
Methyl red	4.2 - 6.3	red	yellow	azo

Table 3.1 Example of dye indicators used for acid base titrations

are colourless when the pH value is decreased to yield an acid sample. These are reported to be unstable when in strongly alkaline samples and their colour tends to fade[94].

3.3.2 Sulphonphthalein

This type of indicator usually has two conjugate colours which are associated with the dissociated and undissociated parts of the dye. The overall concentration of the dye remains constant and the predominant colour is a function of the highest concentration of the two parts of the dye i.e. the dissociated and undissociated parts. For instance, the phenol red dye exhibits a red colour when it is in an alkaline medium and changes to yellow in an acid sample. The spectral analysis of this dye shows an absorbing wavelength in the green and blue areas, as shown in Fig.3.2. This type of dye is known to be very stable especially when used with low light levels.

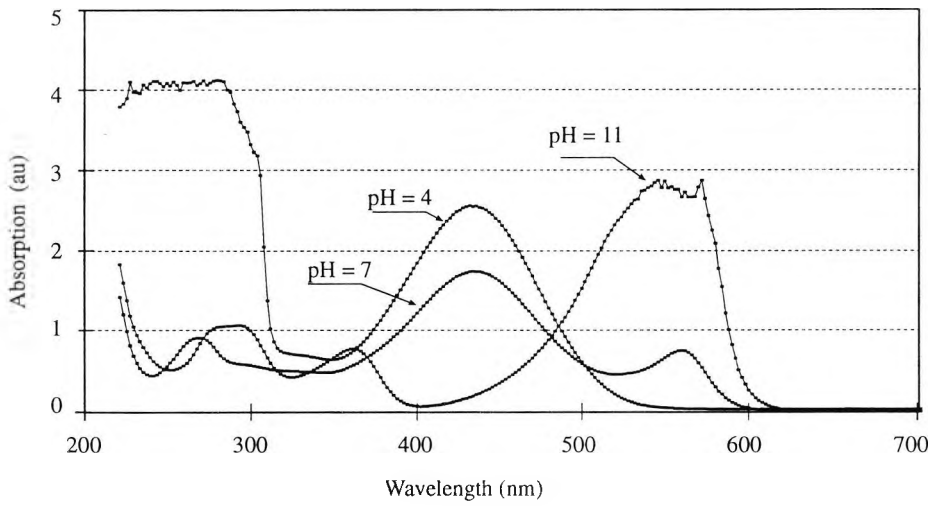

Fig. 3.2 Absorption spectra of phenol red in a sample of distilled water at three different pH values : 4, 7 and 11.

3.3.3 Azo Indicators

Azo-based dyes are often associated with a change of colour as a function of pH from the yellow to the red part of the spectrum, with increasing acidity.

3.4 Choice of the Acid-Base Indicator

In this work, there was a variety of chemical acid-base indicators that had the potential to be used for the monitoring of the pH in the biomedical and the biological range i.e. pH value between 7 and 8. The parameters that were required for a suitable dye depended on the toxicity, stability and its range of use. Phenol red suited these requirements well. It has

been used widely to determine the pH of samples in the pH range of 6 to 8 which falls in the "biological" range. Furthermore, it is known to be a non-toxic material and is also very stable. The other factor which makes it suitable for this application is the fact that one of its absorption peaks falls in the green area. This coincides with the spectral emission of an ultra-bright indicator type green light emitting diode.

The spectral profile of phenol red is shown in Fig.3.2, and it exhibits a strong absorption peak in the ultraviolet part of the spectrum. This is complemented by the two absorption peaks which appear in the green and blue region of the spectrum. In addition, the absorption in the UV can also be used to monitor the change of concentration of the undissociated part of the dye to which it is proportionally related. However due to the various difficulties that can be encountered in using the UV region for measurement, i.e. problems with the light source, high attenuation profile of optical fibres etc..., this part of the spectrum was not utilised in this work. The absorption peak in the blue region is related to the absorption of the undissociated part of the dye. The second absorption peak which occurs at a central wavelength of 560nm is shown to have a stronger absorption and hence results in a larger numerical value of the absorption coefficient e.g. 10^{+4} au/(M.cm). As depicted in Fig.3.3, these two tautomeric forms are interconvertible and hence the absorption of one peak is seen to increase when the absorption of the second peak decreases. However, there is one particular point for which the absorption of the dye remains constant and is independent of the pH of the sample. Consequently, it can be used as a reference point. As is shown in Fig.3.4, the sensitivity of the measurement when the alkaline form is used is larger than the acid form. As a result, a higher sensitivity for the pH measurement can be obtained.

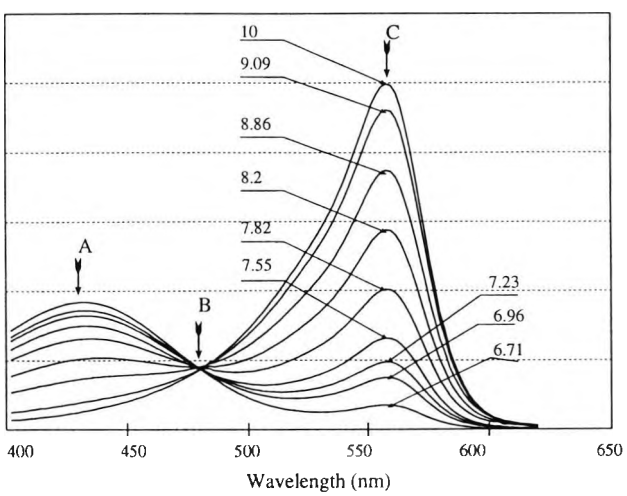

Fig. 3.3 Absorption profile of phenol red as a function of wavelength at different pH values e.g. 6.7 to 10, A and C are the wavelengths of peak absorption of each form Acid and alkaline respectively B and D are the potential reference wavelengths

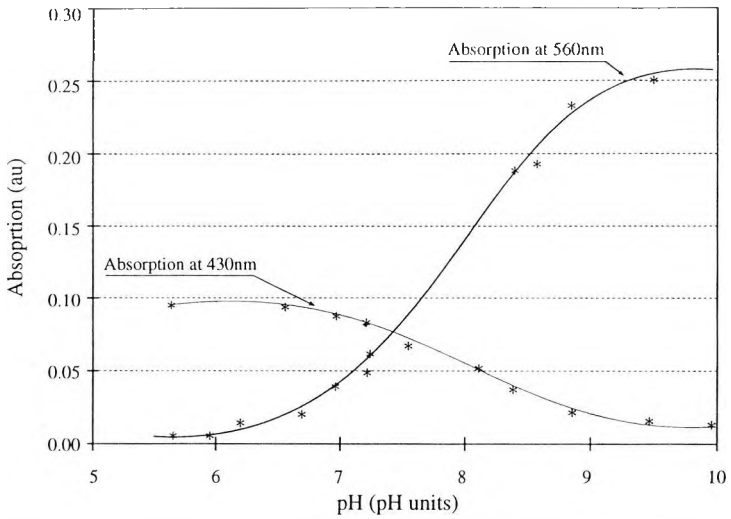

Fig. 3.4 Variation of the absorption of the phenol red with pH values at 430nm and 560nm

The ratio of the acid form to the alkaline form of the dye is approximately of the order of 2.5. Consequently, the absorption peak occurring at 560nm is more suitable for use in order to monitor the changes of concentration of the dye, since it is more sensitive to pH differences. The availability of simple and powerful light sources, and detectors that are more sensitive in this region of the spectrum and fibres with excellent transmission characteristics, all support the choice of 560nm as the operating wavelength of the measurement device. By comparison, the requirement for generating light in the blue part of the spectrum would lead to costly and bulky instrumentation and necessitate the use of optical filters.

3.5 Relationship Between Light Absorbance and pH.

The ratio of the dissociated and undissociated parts of the dye which represent the transducing function, can be linked to the light absorption at a specific wavelength through the Beer-Lambert law. The basic considerations for this relation are as follows:

a) The relationship between the light intensity absorption and the concentration of the dissociated part of the dye is written in Eq.3.8 where P, P_o, ε, L, and $[Ind^-]$ are the detected light power, the initial light power, the coefficient of extinction, the path length and the concentration of the dissociated part of the dye respectively.

$$\text{Log } P/P_o = - \varepsilon L [Ind^-] \qquad [3.8]$$

b) From the chemical reaction resulting from the mixing of the dye and the sample an equilibrium is reached and can be expressed as a function of the concentration of the

species involved.

$$K_{ind} = \frac{[\,H_3O^+\,]\,[Ind^-\,]}{[\,Hind\,]} \qquad [3.5]$$

c) The total concentration of the dye in a given experiment, [T], or in a sensor head remains constant and is the result of the sum of the dissociated and undissociated parts.

$$[T] = [Ind^-] + [HInd] \qquad [3.9]$$

Based on the above equation it can be shown the the relation between p/p_o and $[H_3O^+]$is as follows. By taking the decimal logarithm of both sides in Eq.3.5 and separating the term containing the hydronium ion concentration, Eq.3.5 becomes:

$$\text{Log } K_{ind} = \text{Log}[H_3O^+] + \text{Log } [Ind^-]/[HInd] \qquad [3.10]$$

by changing its form, Eq.3.10 may be re-written as shown in Eq.3.11.

$$pH - pK_{ind} = \text{Log } [Ind^-]/[HInd] \qquad [3.11]$$

The result of combining Eq.3.9 and Eq.3.11 introduces the term [T] defined in Eq.3.9, which reduces the number of variables and Eq.3.12 is expressed only as a function of known parameters i.e.

$$pH - pK_{ind} = -\text{Log}\{\,[T]/[Ind^-] - 1\} \qquad [3.12]$$

The anti-logarithm of Eq.3.12 results in expressing the equation in a more convenient form, as shown in Eq.3.13 below i.e.

$$10^{-(pH - pK_{Ind})} + 1 = \frac{[T]}{[Ind^-]} \qquad [3.13]$$

The direct relationship between light intensity and the concentration of the dissociated part of the dye is introduced by using Eq.3.8 and, hence, Eq.3.13 may be written as follows:

$$10^{-(pH - pK_{Ind})} + 1 = \frac{-\varepsilon L[T]}{Log\,(\frac{p}{p_o})} \qquad [3.14]$$

Hence, Eq.3.14 is modified to show the relationship between the variation of the light

intensity as a function of the concentration of the dissociated part of the dye. This relationship is described in terms of one variable only i.e. pH, while the term εL[T] is a parameter which describes the sensor head and is a constant for a given implementation. Thus εL[T]= m and pH -pK_{ind} = δ.

The final mathematical equation for the sensor is shown in Eq.3.15

$$Log(\frac{p}{p_o}) = \frac{-m}{10^{-\delta}+1} \text{ or } \frac{p}{p_o} = 10^{-m/(10^{-\delta}+1)} \qquad [3.15]$$

Due to the non-linear nature of the relationship between the relative light intensity and the variable δ, (δ = pH - pK_{ind}), the resultant curve is of an S shape and the position of the inflexion point happens to be in the middle of the S shape. In this area, i.e. approximately δ= ± 1 from either side of the point of inflexion, maximum linearity is obtained. Although this is still not enough for the curve to be linear, it can be considered as fitting a straight line whose slope is the same slope of the curve at the inflexion point within a reasonable approximation, yielding a small systematic error.

3.5.1 Choice of the Parameters

The principle parameter of the sensor to be evaluated is thus the factor m. This is carried out in order to provide a more accurate description of the required physical dimensions of the probe head and the behaviour of the sensor in various practical implementations. The choice of the value of the parameter m is dictated by two distinct situations. These are: the largest dynamic range of pH i.e. ±1 pH units, and maximum sensitivity with minimum error over the 100% transmission range.

1) Firstly, it can be seen that the point of inflexion is a function of the parameter m and it does not necessarily occur when pH = pK_{ind} for the curves computed with different values for m. The relationship between the value of the factor m and the value of pH for which the inflexion point occurs can be calculated from the second derivative of Eq.3.15 as a function of pH. The inflexion point is defined when the second derivative is nil i.e. the slope of the curve changes sign. This is shown in Eq.3.16 (see Appendix 2 for more details). Then,

$$\delta = -Log\left(\frac{-m\,ln10 + \sqrt{m^2 ln^2 10 + 4}}{2}\right) \qquad [3.16]$$

Because the pK_{ind} of phenol red is 7.92[195], and the practical range of the dye lies between 6.8 and 8.4, the optimum position of the inflexion point lies at the middle of the dynamic range of the dye e.g. pH = 7.6.

2) Secondly, the sensitivity of the measurement relies on a long path length through which the sensing light travels and hence the longer it is the more sensitive the measurement becomes. However, this is limited by two factors, the first one being the longer the path length, the smaller the signal to noise ratio, since the level of the light reaching the detector is less, and the second factor is the physical dimensions of the probe head. However, limited physical dimensions and the desire for a short path length can be compensated by using a larger dye concentration which keeps the overall dimension of the probe head within the desired volume.

The variation of the relative light transmission as a function of δ is shown in Fig.3.5 and it can be concluded that there is a range of values of the factor m for which the dynamic range of the light transmission is the largest which occurs when m> 1. Graphically, the value of m can be obtained by looking at the position of the inflexion point so that it lies at the middle of the required pH range e.g. between 7 and 8. Additionally,the error analysis showed that for values of the factor m smaller than 1.2, a large error on the measurement results when the light transmission is smaller than 10%, as is shown in Fig.3.6. Hence there is a trade off to be made so that both conditions can be satisfied i.e. minimum error and largest dynamic range.

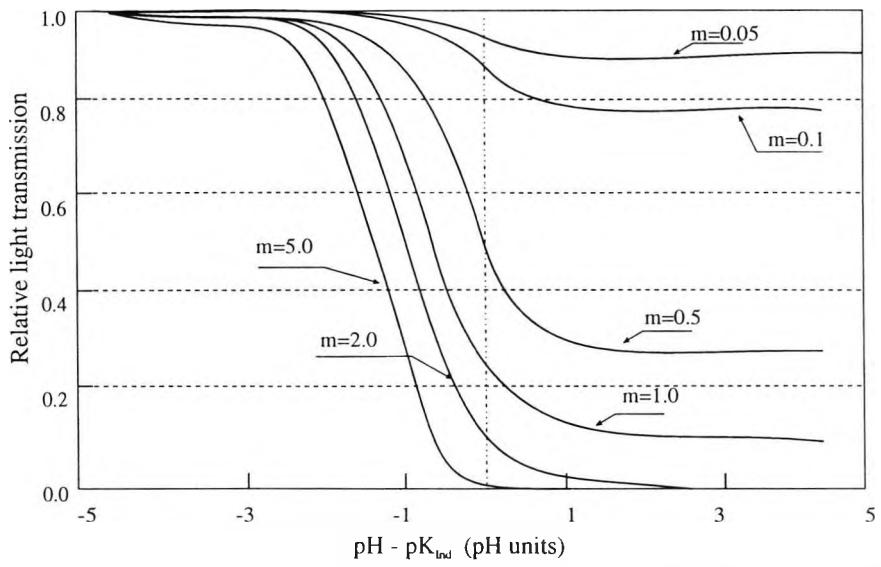

Fig. 3.5 variation of the ratio (p/p_{ref}) calculated as a function of pH-pK_{ind} with different values for m

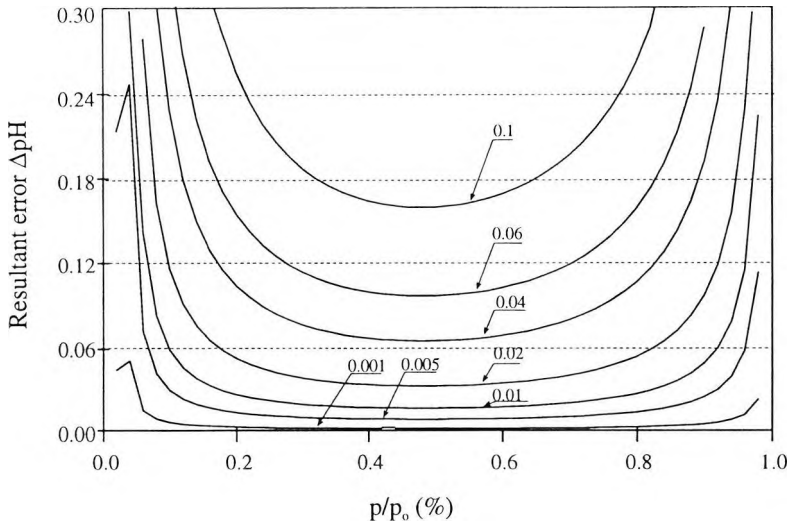

Fig. 3.6 variation of the error as a function of light transmission for different values for the relative error of the light intensity and m =1.5.

3.5.2. Referencing

Eq.3.15 requires a knowledge of the value of the initial light power emitted by the light source, P_o, in order to compensate for instrumental errors and variations in the light intensity. These are generated by disturbances other than the dye which affect the light transmission. A correcting factor is introduced into the equation which describes the sensor and is obtained by choosing an appropriate wavelength for which the factor ζ, defined as $\zeta = \frac{d\varepsilon_{\lambda_r}[Ind^-]}{d[Ind^-]}$, remains unaffected by the changes of the pH value. Only a zero value for ζ would satisfy this criterion. This situation can only be accomplished when the value of ε_λ of the indicator at that particular wavelength is nil or when the wavelength of choice is equal to the wavelength at which the absorption remains constant independently of the pH of the sample. However, because the wavelength band is so narrow at this point, only a line source or a lamp with a broad spectral output together with a very narrow band pass optical filter (e.g.2 nm) can be used, and this is not practical for most real sensor devices.

A referencing scheme can be obtained by using one of two different methods. The first one consists of using the same wavelength as the sensing one to monitor the value of the initial light intensity. For this, a reagent can be added to the sample to shift the pH to a value at which the dye does not absorb (i.e. in its acid form). Although this can be carried out in titrimetry, it is not a very practical situation for most sensors; this results in rendering the design of a simple sensor a more complex matter.

In the second method, a second wavelength is used to monitor the level of the value of the initial light emission. Such a wavelength should only be affected by changes in absorption generated by interferences other than the change of pH. This can also be used to monitor the absorption of the background and the instrumental variations. The choice of this wavelength is made by assuming that the effect of the interfering species is similar for both wavelengths i.e. the sensing and the reference wavelengths. Hence, this can only be justified when the reference wavelength is as close as possible to the sensing wavelength whilst being sufficiently removed, for the light transmission to be unaffected by the variation of the pH of the sample. In this situation, the value of the initial light power can be linearly related to the light power of the reference wavelength. This is only true in most practical situations when the wavelengths are generated from the same physical light source. Effectively, in this particular case, the problems associated with any temporary variation of the light intensity and the ageing of the light source are similar for the two wavelengths. Consequently, the ratio of the intensity of the two wavelengths can be used to eliminate this type of problem. However, this assumption is not valid when using two different light sources to generate the appropriate wavelengths, for instance, when two LEDs emitting at different wavelengths are used [96]. In these particular examples, the assumption relies on the fact that LEDs, which have been shown to have a very low rate of degradation and hence are very reliable [97], cannot differ appreciably in their spectral properties within the response time of the sensor, especially if they are used well within the manufacturer's specifications for temperature and current.

As a consequence, under these circumstances, the ratio of the light intensities of the two wavelengths can be described as a constant. i.e. $P_{\lambda s} / P_{\lambda r} = \psi$.

$$Log\frac{P}{P_o} = \frac{-\varepsilon L[T]}{10^{-\delta} + 1} \qquad [3.17]$$

Thus, the term P_o in Eq.3.11 may be replaced by $P_{ref}\,\psi$ and can be written as follows :

$$Log\,\frac{P_\lambda}{P_{ref}\,\psi} = \frac{-\varepsilon L\,[T]}{10^{-\delta} + 1} \qquad [3.18]$$

$$\frac{P_\lambda}{P_{ref}} = \psi\ 10^{\ -m/(10^{-\delta} + 1)} \qquad [3.19]$$

where $m = \varepsilon L[T]$ and $\delta = pH - pK_{ind}$ and ψ denotes the ratio between the light intensity of the sensing and reference wavelengths. These parameters represent the factors of the sensor and can be measured for a given implementation.

3.6 Error Analysis

The response of a system relying upon the absorption of light to convey information about the pH value of a sample is affected by a number of factors which can result in an error in the final measurement. The extent to which such an error has serious implications depends on the application. For example, measurement of the blood pH value lies usually in the range 7.40 to 7.60, hence errors larger than 0.1 pH units could have disastrous consequences on the diagnosis of the functioning of a biological system. Additionally, the spectral response of the dye can be altered by various factors such as the ionic strength of the sample which then results in shifting the equilibrium of the reaction of the dye with the sample, for instance, the pK value of the phenol red shifts towards lower values. However the overall spectral response remains the same. Temperature can also affect the value of the measured pH value since it is well known that the dissociation of water varies with temperature, as do most chemical species. An additional error which has been discussed in the literature recently[98], consists of the fact that it is the concentration of the hydronium ion which is measured by optical means rather than its activity. This can cause large errors in the estimation of the pH. These effects can be grouped in three main categories: chemical, analytical and electronic.

3.6.1 Chemical

Chemical errors are produced by the change of the behaviour of the dye in the presence of other molecules. These do not interfere in the absorption of the light directly, but lead to the dye changing its properties, as is the case in the ionic strength of the sample. It has been studied and is well known that the ionic strength of the sample can not only can affect the activity of some ions but can also force the equilibrium of the chemical reaction of the dye with the sample to move either towards an alkaline or an acid value. For example, in the case of phenol red, the ionic strength was reported to affect the constant of equilibrium by reducing its value with increasing ionic strength of the sample. For instance, at an ionic strength of 0, the value of pK was reported to be pK = 7.92 +0.02, and changed to pK = 7.78 + 0.02 when the ionic strength was increased to 0.25 [99]. As a result, the measurement of pH value cannot be made without prior knowledge of the ionic strength

of the sample. This can be overcome by using the right calibration curve obtained with a sample whose chemical composition is similar to the test sample.

The second effect which is related to the measurement of pH by optical techniques is the effect of the activity of the hydronium ion which is different from unity when the concentration of the sample becomes larger. This case is different from the ionic strength case, because the activity coefficient of ions present in the sample cannot be measured for thermodynamical reasons[87]. Hence, the measurement relies on certain approximations made to suit particular cases and as a result a general formula cannot be obtained for all situations.

The effect of temperature is also considered to cause changes in the behaviour of the dye as the constant of equilibrium is affected. However, this is usually relatively easy to control or to compensate.

3.6.2 Analytical

By using the Beer-Lambert law a minimal concentration error is obtained when the transmitted light intensity lies within 20 to 60 %, as has been shown in the preceding chapter. The resultant error in the measurement can then be calculated by taking the first derivative of the Eq. 3.15 as a function of the light intensity.

$$pH - pK = -Log\left(\frac{-\varepsilon L[T]}{Log\left(\frac{p}{p_o}\right)} - 1\right) \qquad [3.20]$$

As pK and εL[T] are constants, the expression for the first derivative can be rewritten after replacing the followings, εL[T] = m and $x = p/p_o$ where $dx = d(p/p_o)$ for simplification. Hence

$$dpH = \frac{m}{(ln10)^2 (Log\, x)^2} \frac{dx}{x} \frac{1}{\frac{m + Log\, x}{Log\, x}} \qquad [3.21]$$

which then becomes

$$\Delta pH = \frac{1}{(ln10)^2} \frac{m}{Log(x)\ (m + Log\, x)} \frac{\Delta x}{x} \qquad [3.22]$$

The curves that can be obtained from Eq.3.20 are functions of both parameters i.e. m and $\Delta x = \Delta(P/P_o)$. A curve similar to the curve of the relative error of the concentration as a function of light transmission is obtained when plotting the graphs representing the error in δ and hence in pH values as a function of the variation of the detected light intensity for different values of m and Δx as is shown in Fig.3.7. However, the denominator of Eq.3.20 can be nil in two different cases. This results in a large value of the absolute error. This occurs when x approaches 1 i.e. 100% light transmission or when it reaches 10^{-m}. As a result, m should be chosen so that the maximum error falls outside the range of measurement [100] e.g. light transmission smaller than 1% or 0.1%. For example, when m=1 maximum error is reached for a transmission of light of 10% and when m =2, similar error occurs at a transmission value of 1%.

Additionally some deviations from the analytical function used i.e. the Beer-Lambert law, are expected when LEDs are used since their emission profile lies over a bandwidth of ±20nm which cannot be considered as a line emission as is the case for discharge lamps. However these can be neglected since they can be considered as a systematic error and therefore are constant for a specific implementation.

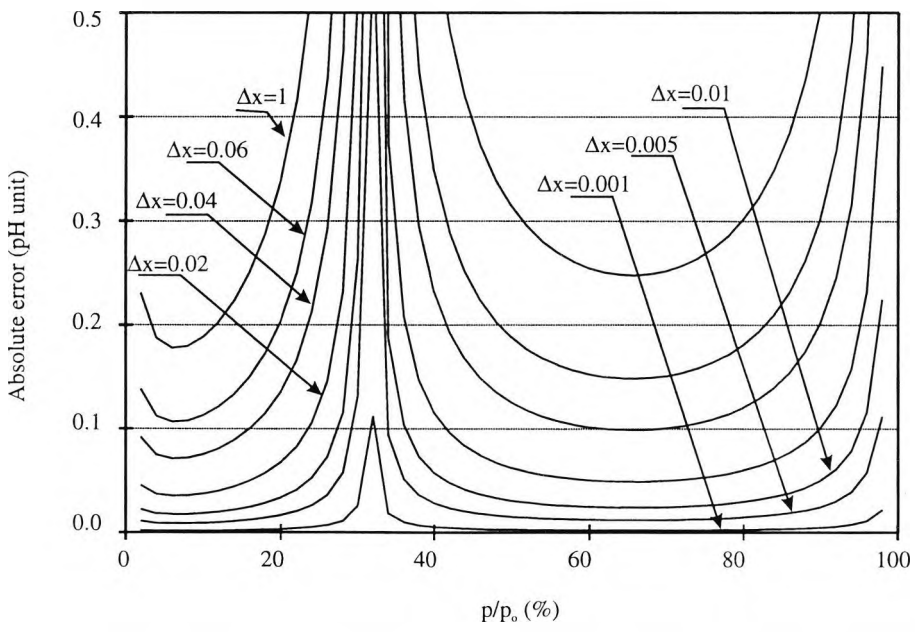

Fig. 3.7 Variation of the error on the pH value as a function of light transmission at different values of the relative error on the light intensity (m=0.5)

3.6.3 Electronics

The errors related to the electronics are mainly caused by noise generated in the detector and amplifier stages which are used to process the signal and extract the light intensity variation information. The predominant factor in the sensitivity of the measurement is the

noise associated with the light level and particularly the dynamic range of the optical signal. This, in turns, defines the dynamic Signal-to-Noise Ratio (SNR) which then dictates the resolution of the measurement of the light level and hence the limit of detection[101]. This, in combination with the error associated with the pH, can give the overall error of the measurement in terms of pH units. The sensitivity of the measurement can be enhanced by using signal processing techniques such as the reduction of the bandwidth of the electrical signal to minimise errors in the electronic system.

3.7 Conclusion

In this chapter, a theoretical description of the colorimetric measurement of pH of an aqueous solution is given. This analysis provides a basis on which a fibre optic system can be conceived even though the principle involved is non-linear. However, when the application is limited to a maximum range of 2 pH units, part of the instrument response can be approximated to a linear variation as a function of pH. Furthermore, the error analysis which relates the limitation of the detection of light absorption of the dye to the error in the measurement of pH was carried out in order to highlight particular features of the design on which emphasis should be placed, such as the constants of the sensor. This results in enhancing the performance of the sensor. The limitations of the sensor are analysed and results show that it is difficult to estimate the error of the system fully without prior knowledge of the chemical composition of the sample, since other species can modify the behaviour of the dye. It was also found that absolute errors smaller than 0.01 pH units could be obtained when the relative error in the measurement of the light intensity is smaller than 0.1%. On the basis of this analysis, a fibre optic system is designed and is described in detail in the following chapter.

Chapter 4

Design and Implementation of a Fibre Optic pH Meter

Abstract

The design of this fibre optic pH meter is based on the principle of monitoring the change of colour of an organic dye (phenol red) whose absorption of light in the visible part of the spectrum depends on the concentration of the hydronium ion (H_3O^+) present in an aqueous solution. The change of absorption of light is monitored at an optimum wavelength of 560nm which corresponded to the peak emission of an indicator type green Light Emitting Diode (LED) and was found to be linearly proportional to the variation of the pH of the sample. External interferences are monitored through a wavelength whose intensity remains unaffected by the change of absorption of the dye. This particular wavelength is generated in two different ways. In the first scheme, an InfraRed (IR) LED emitting at a central wavelength of 840nm was used not only to monitor the background absorption of the sample but also to compensate for the instrumental sources of error. In the second method, a ruby crystal was used; this fluoresces producing light in the vicinity of 690nm when excited by light in the visible spectrum i.e. 560nm. This fluorescent light falls in the region of the spectrum where the absorption of the dye is unaffected by pH changes. Hence, this method of referencing provides compensation for effects such as LED ageing and intensity fluctuations which are not compensated in the first implementation.

In both methods, the sensing signal is modulated using a square wave technique. Signal processing of the detected signals is implemented in two different ways in order to extract the information from the modulated signal.

Calibration of the instrument against an electrochemical electrode based commercial pH meter was carried out and a system characterisation and analysis of the numerous analytical and instrumental errors introduced in the two systems are appended at the end of the chapter.

4.1 Time Multiplexed Dual Wavelength Fibre Optic pH Meter

The schematic diagram of the dual wavelength with external referencing implementation is depicted in Fig. 4.1. The basis of the implementation relied on generating two wavelengths i.e. 560nm and 840nm, using two indicator type LEDs. The first LED was used to monitor the behaviour of the phenol red dye through the change of the transmitted light intensity and the second LED was used for the measurement of the background absorption and external interferences. The two optical signals i.e. from the green and infrared LEDs were time multiplexed using a square wave modulation scheme. The optical signal thus generated was guided through two short lengths of optical fibres. The light emerging from these two fibres was coupled into a single large optical fibre using an optical mixer. The optical signal was then guided to the probe head using a single path for both wavelengths. A reflecting mirror, positioned at the opposite end of the probe head facing the emitting fibre, was used to reflect the light. A bundle of fibres positioned around the emitting fibre transmitted the reflected light to the detector. Further signal processing was carried out in order to demodulate the signals corresponding to the green and infrared optical signals respectively. Separate outputs for the two signals i.e. absorption and reference signals, were provided and a subsequent ratio was then performed.

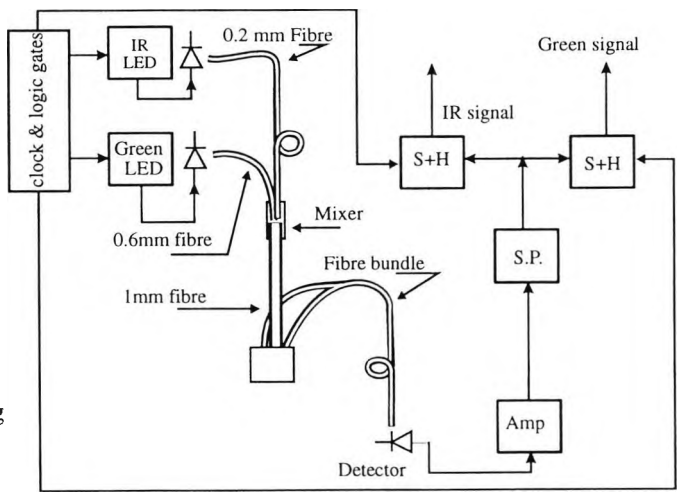

Amp: amplifier
S+H: sample & hold
SP: signal processing
IR infrared

Fig. 4.1 Set-up of the time multiplexed dual wavelength fibre optic pH meter

4.1.1 Referencing Scheme

When external effects occur, absolute measurement of the absorbed light cannot be related to the absorption of the light by the dye unless a monitoring wavelength whose light intensity remains unaffected by the change of absorption is used. Additionally, this

reference wavelength provides meaningful information about the nature of the absorption by the species present in the sample. Moreover, losses of light which were caused by diverse external effects such as light intensity fluctuation, losses due to the coupling of the fibres and the losses occurring in the fibre during the propagation of light caused mainly by fibre bending were then determined. Ideally, the wavelength of the reference light should be as close as possible to the monitoring wavelength so that most of the interfering effects would do so equally for the two wavelengths. For instance, the light transmission decreases when the fibre is mechanically bent and the resultant loss is a function of wavelength. This type of loss is caused mainly by mode conversion and light is radiated through the cladding.

In this particular implementation, phenol red absorption is unchanged for wavelengths longer than 620nm. A red LED emitting at a central wavelength of 630nm could be used. However, the broad emission characteristics of the LED e.g. ±20nm at half height, overlaps with part of the area of the absorption curve of the dye. Hence the red LED is not a suitable choice for generating a reference wavelength which otherwise necessitates the use of an optical filter to remove this overlap effect. The latter has the effect of complicating the optical set-up and introduces additional optical components. Hence an infrared LED whose central wavelength is far removed from the absorbing area e.g. emitting at 840nm, was chosen as a reference light source. The error introduced is limited and constant and could be included in the systematic error of the system*.

4.2 Initial Configuration

The fibre optic pH meter comprises an optical arrangement and an electronic section:

4.2.1 Optical Arrangement

The optical arrangement of the pH meter consists of an optical mixer, probe head, light sources, glass fibre for guiding light from the light source into the probe and a fibre bundle to collect the light from the probe and guide it to the detector.

4.2.1.1 Optical Mixer

To guide the light from the light sources to the probe head, a single, large diameter optical fibre system was preferred to a system in which the fibre was made of a bundle consisting

* *The inequality of the light losses when the fibre is bent arises from the fact that the wavelengths of absorption and reference were farther apart e.g. by 280nm*

of a number of 10 to 20 μm core diameter fibres. This was the result of choosing the single path option so that the losses from different origins do affect the optical signals in the same way and with the same intensity. Hence an optical mixer was used to position the fibres guiding the light from the two light sources with a large fibre.

The optical mixer was made from a simple SMA transmission type connector whose diameter was such that it is possible to insert two glass Plastic Clad Silica (PCS) fibres from one side and a larger one from the other side of the connector. A 200μm diameter PCS fibre and a 600μm diameter fibre of the same type were positioned alongside each other and glued inside an SMA standard connector. The overall diameter including the cladding and the jacket dimensions was approximately just over 1000μm. A second PCS fibre of a diameter of 1000μm was also glued in a fibre connector and positioned in front of the two preceding fibres. Finally, the two connectors were tightly connected to the body of the mixer as is shown in Fig. 4.2. The total area of the two fibres glued together represented the active area and was contained within the total area of the large fibre. Consequently most of the light emerging from the two fibres (200 and 600μm) was transmitted to the collecting 1000μm diameter fibre. The losses at this connection point were mainly due to Fresnel and coupling effects [102]. The former was caused by the reflection of the radiation at the glass boundary and could be calculated from Eq.4.1, and was found to be 1.9dB[103].

$$L_F = 10\,Log\,(1-r)^2 \quad \text{and} \quad r = \frac{n-n_o}{n+n_o} \qquad [4.1]$$

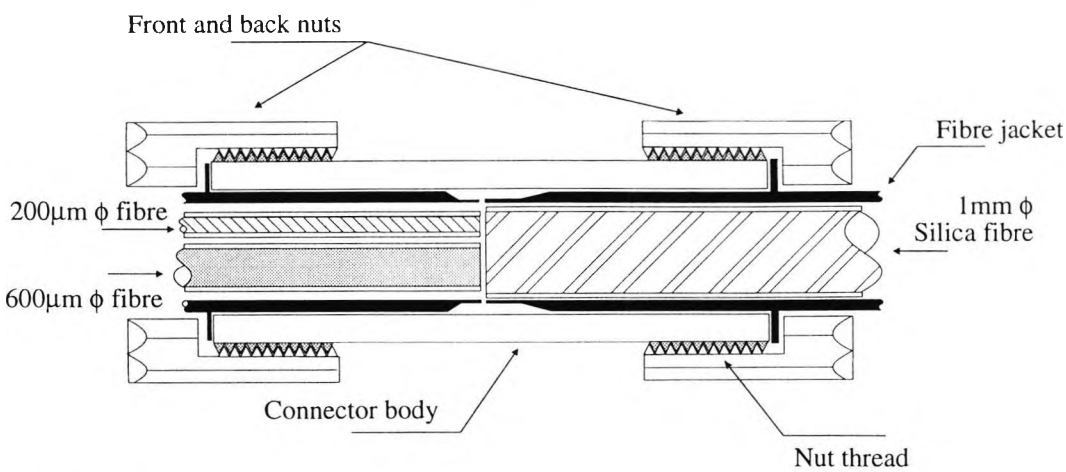

Fig. 4.2 Optical mixer and positioning of the fibres

where n and n_o are the refractive indices of the glass fibre and air respectively.

However sharply and accurately the fibres are cut and polished, there would always be a gap between the two fibres positioned in front of each other in the optical mixer. The index of refraction of the gap between the fibres which is mainly made of air is different from the index of refraction of the glass fibre. Hence, the coupling losses resulted from the mismatch of the index of refraction of the two-fibre system e.g. glass-air-glass.

4.2.1.2 Optical Fibres

The optical fibres used in this implementation were multimode glass fibres having a numerical aperture (NA) of 0.4. All the light beams having an angle greater than 24° were not guided through the fibre, instead some of them were coupled into the fibre but were lost through the cladding after the first few reflections. In this implementation, the losses due to the glass fibre were not significant since the fibre length was of the order of few meters. Glass fibres have a greater transmission percentage in the visible part of the spectrum than do plastic fibres.

The fibres collecting the light from the LEDs were of different diameters. A fibre of only 200µm diameter was needed for the purpose of guiding the infrared light from the high power IR LED while a larger diameter fibre was used to guide the sensing light from the low power green LEDs e.g. 2-3µW. The choice for the fibre dimensions was based upon two factors:

1) The optical power of the LEDs was not the same, e.g. the infrared LED was more powerful than the indicator type green LED. In addition the coupling efficiency of the infrared LED was higher than the green LED. The IR LED was designed to be used with optical fibres and was housed in an SMA type housing.

2) The fibre optic system was more flexible and the size of the probe head was reduced and its design optimised with respect to light reflection and positioning of the receiving fibres. This was achieved by using short separate fibres to guide the two wavelengths from the light sources to the single fibre. This could be fitted inside the pH meter electronic module. Hence, the single fibre and the returning fibres were the only output/input connections to the case. This way opportunities for further miniaturisation for possible use in environments where space is a major problem were available.

The length of these fibres was 100mm, this length being the distance between the case and

the optical mixer. They were glued inside a standard SMA type connector and their ends polished to provide a scratch-free surface.

The fibre used to guide the optical signal from the mixer to the probe head was approximately 1 meter long. It was glued to the SMA type connector at one end and to a machined brass connector to fit in the head probe at the other end. This was large enough to accommodate the 1mm diameter fibre and the six 600μm diameter fibres positioned around the large fibre to obtain maximum light collection as is shown in Fig.4.3. Only four of these fibres were used to guide the reflected light from a mirror positioned at 1cm from the end of the 1mm diameter fibre since there was an adequate level of reflected light.

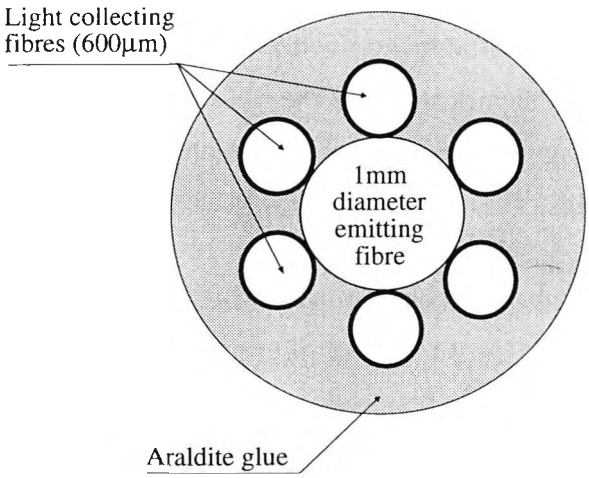

Fig. 4.3 Positioning of the emitter and receiver fibres in the probe head (bottom view)

4.2.1.3 The Probe Head Design and Construction

The probe was designed so that the fibre-probe head could be easily dipped in a sample solution. It was made from three stainless steel parts. The first part was made to connect the fibre to the probe head. This fitting was simplified for removal and cleaning when necessary. The second part consisted of a hollow cylindrical body onto which large holes were machined on its longitudinal sides so that the sample liquid could flow in and out without any restriction. The large diameter of the holes was also used to help reduce the chances of the air bubbles being trapped inside the optical probe. Air bubbles could cause large errors in the measurement by disturbing the path of the light beam. Consequently, the light intensity being reflected by the mirror and reaching the detector would not necessarily provide a true measurement of the absorption of the light by the dye. The third part of the probe head consisted of a threaded metallic end whose front surface, facing the

fibres, was well polished to produce a highly reflecting surface which was used as a mirror. Its distance from the fibres end determined the the path length of the optical cell. A facility for changing this distance was provided through a thread which was machined onto the body of the mirror. The probe head is shown schematically in Fig.4.4. The path length with such a system was twice the distance between the fibres end and the mirror. However, there was an optimum position of the mirror where maximum light intensity was reflected. This was found experimentally to be around 20mm in this implementation.

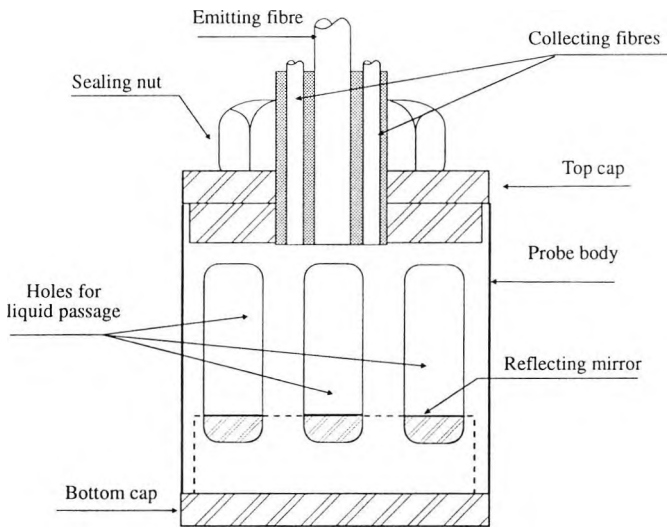

Fig. 4.4 Schematic design of the probe head for the first configuration.

4.2.1.4 Light Sources

In order to generate the appropriate wavelengths needed to monitor the change in absorption of phenol red, simple and inexpensive solid state LEDs were used. The output spectrum of the green LED which has a peak emission at 560nm matched the absorption spectrum of phenol red when it was in its alkaline form and hence was suited for this application. The bandwidth of the LED emission is ±20nm at half power. The emission spectrum of the green LED when driven at increasing dc currents changes as is shown on Fig.4.5. A small shift (2nm) of the peak of emission at 560nm was found to occur for a range of currents of 10 to 90mA. This peak shifted toward higher wavelengths and was found to be insignificant since the envelope of the emission spectrum of the LED contained in it the absorption profile of the phenol red in its alkaline form. Although the maximum dc current specified by the manufacturer was 30mA, it was found that it can be possible to drive the LED at higher current intensity provided that this occurred over a short period of time and the LED was given sufficient time to release the heat generated by the passage

of the current in the semiconductor. The general effect of temperature on the optical power output of the LED when driven at various dc currents is shown in Fig.4.6.

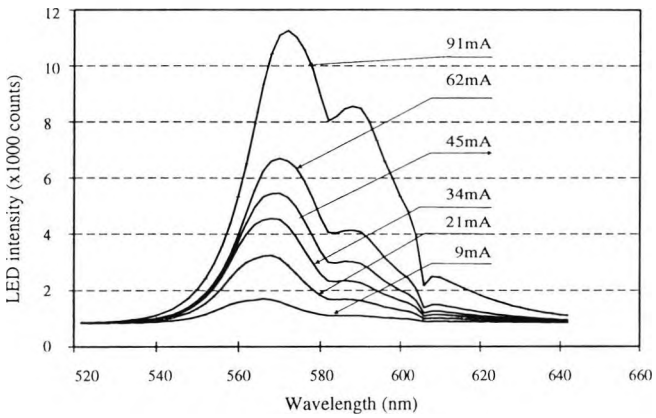

Fig. 4.5 Graph showing the spectrum of the light emitted by a green indicator type LED at various driving current intensities

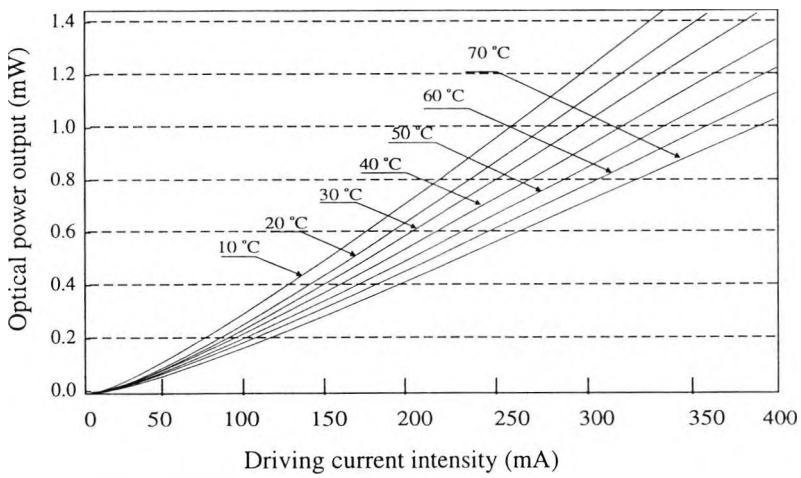

Fig. 4.6 Temperature effect on LEDs for $\lambda = 0.85\mu m$ at 20 °C for AlGaAs diode[77]

On the other hand, the infrared LED was not subjected to the same temperature conditions. As a result of the higher quantum efficiency, infrared LEDs require less current to drive them for the same optical power output than do LEDs emitting in the visible part of the spectrum. Only the intensity stability was an important factor.

These LEDs have the advantage of being easily driven and electronically modulated and hence the need for a mechanical chopper was eliminated. In this particular case it was preferred to drive both LEDs sequentially by a pulse train signal. There were two reasons for choosing this type of modulation:

1) Due to the nature of the processes occurring in the generation of light, these LEDs can be driven at a higher current without affecting their performances[82]. The limitation imposed on the driving current of an LED results from the heating of the substrate when a current passes through it. Hence, if the substrate is allowed to cool so that its temperature decreases, it can be driven at higher currents generating a more powerful optical signal since the relationship between optical power and driving current was found to be linear within a limited range.

2) The two LEDs were driven on and off sequentially. Consequently, there was no overlap of the two optical signals. An overlapping optical signal containing the two wavelengths at a ratio R_1 would not be converted into an equivalent electrical signal since the sensitivity of the detector is a function of the wavelength and was reported to be of the order of 1.72 (for λ_1=840nm and λ_2=560nm). Moreover, the state where the two LEDs were switched off for a certain time was purposely arranged so that it could be used for interference sampling i.e. dc level measurement and at the same time to allow the LED to dissipate most of the heat.

The efficiency of light coupling between an LED and glass optical fibre was reported to be up to 15% [104][105].

4.2.2 Electronic System

The block diagram of the electronic module is shown in Fig.4.7 and consisted of an emitter, receiver, amplification, demodulation and output stages.

4.2.2.1 Clock Signal

A square wave signal was used as the master clock signal and was generated using an RC network on the feedback loop of a Schmitt trigger NAND gate. The frequency drift due to the increase of the temperature of the circuit and the fluctuation of the frequency was found to be smaller than 1Hz over a period of one hour. Although this drift represented 0.03%, it was not considered to be important since the rest of the circuit was synchronised on this clock signal. The frequency of the clock was fixed at 3kHz and was set by the time constant τ given by Eq.4.2:

$$\tau = (RC)^{-1} \qquad [4.2)$$

where R is the resistor and C is the capacitor that form the RC network.

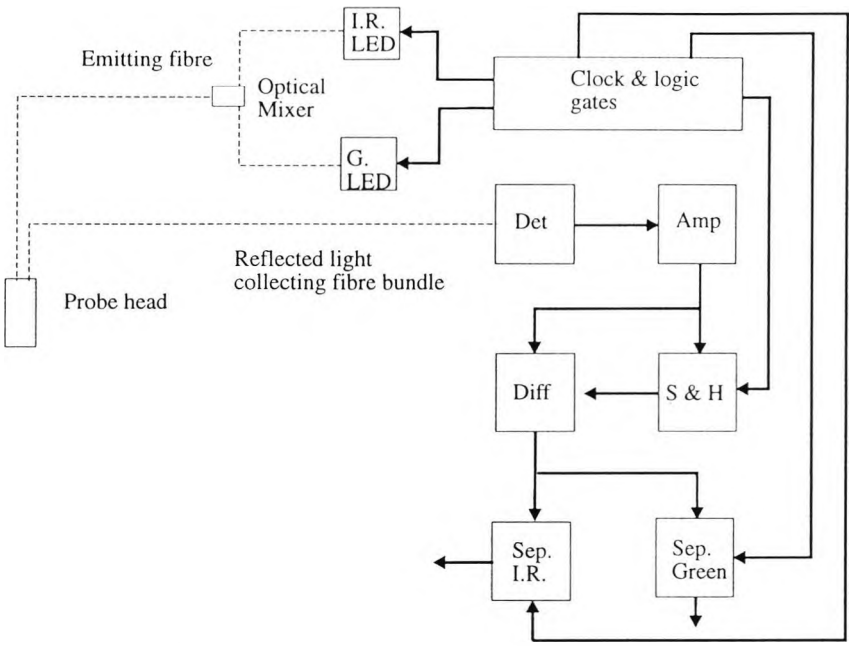

Fig. 4.7 Block diagram of the electronic circuit used in the implementation of the pH meter.

4.2.2.2 Signal Generation

Three signals were generated to perform the measurement of the pH value of a sample solution. These were:

1) A signal to drive the green LED: this was carried out by a pulsed train signal having a mark to space ratio of 1:3 and was buffered using an operational amplifier connected as a voltage follower before being applied to a transistor switch circuit which controlled the current through the green LED connected between the current limiting resistor and the collector of the transistor. The rms value of the current flowing through the LED was 60mA.

2) A signal to drive the IR LED using a similar transistor switch. However, a lower current value of 30mA was needed to drive this LED, also at mark to space ratio of 1:3.

3) Three control signals to provide the triggering pulse for controlling the timings of the sample and hold devices used to separate the signals corresponding to the green and infrared signals, and the third one which was used to sample the detected signal when both LEDs were switched off. A dc signal resulted from the output port of the sample and hold device and was approximately equal to the average value of the electrical background level.

The electronic circuit designed to generate such signals was based on the use of logic gates

(flip-flops and multivibrator) and is shown in Fig.4.8. The pulses generated for the purpose of controlling the timings of the sample and hold devices were shorter with respect to time. The detected signal contained a large number of harmonics which were not processed the same way due to the limitation in the frequency response of the various stages i.e. detector and amplifiers. Care was taken when a signal was sampled and the average value held constant until the next cycle. For this reason, the position and the length of the control pulse with respect to time did not correspond to the rise and fall of the pulse. The active time of the sampling was delayed so that sampling started after the pulse rose and the holding signal occurred before the pulse fall started. The reason for this is shown schematically in Fig.4.9, where the detected signal is presented as a function of time . This had the effect of reducing the errors introduced by the inadequate frequency response of the components, and the output of the sample and hold device represented the average voltage of the capacitor used as a memory as shown in Eq. 4.2. Polycarbonate capacitors have a very low leakage current and hence were suitable for memory applications[106] . In this case, the time required to hold the signal in the capacitor was shorter than 1.4mS and this resulted in a drop of voltage of the output signal from the sample and hold device in the order of few micro-Volts(0.002%) [107] . As the resulting error was small, the 'memorised' signal was considered to represent the intensity of the true processed signal especially when the sampling time was kept constant.

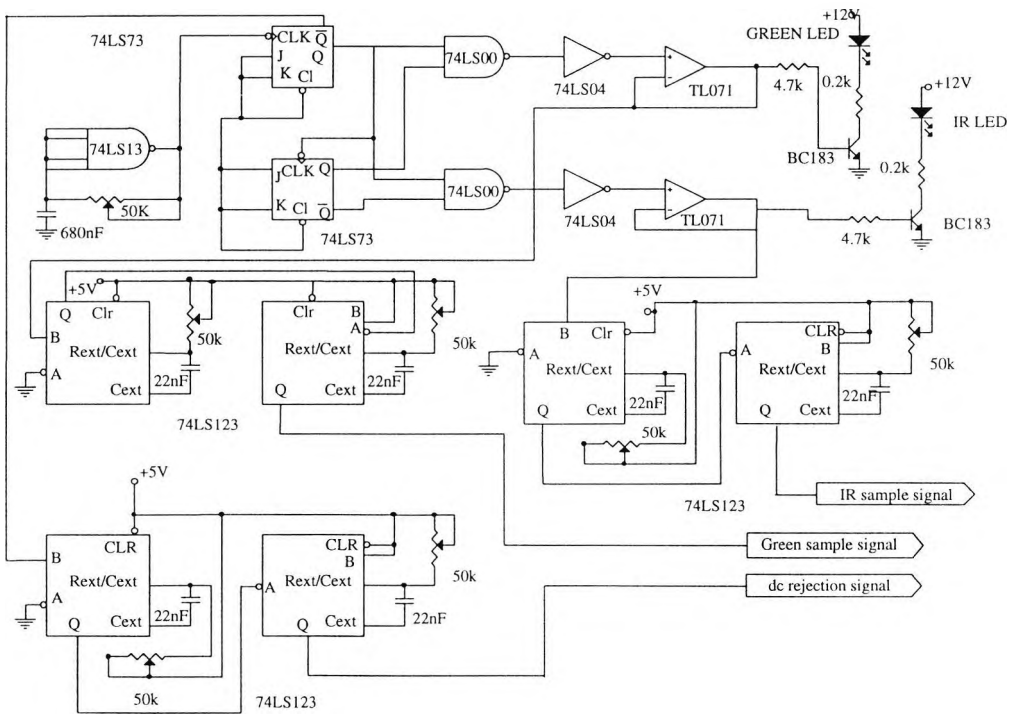

Fig. 4.8 A schematic diagram of the electronic circuit used for the emitter side of the first implementation of the pH meter.

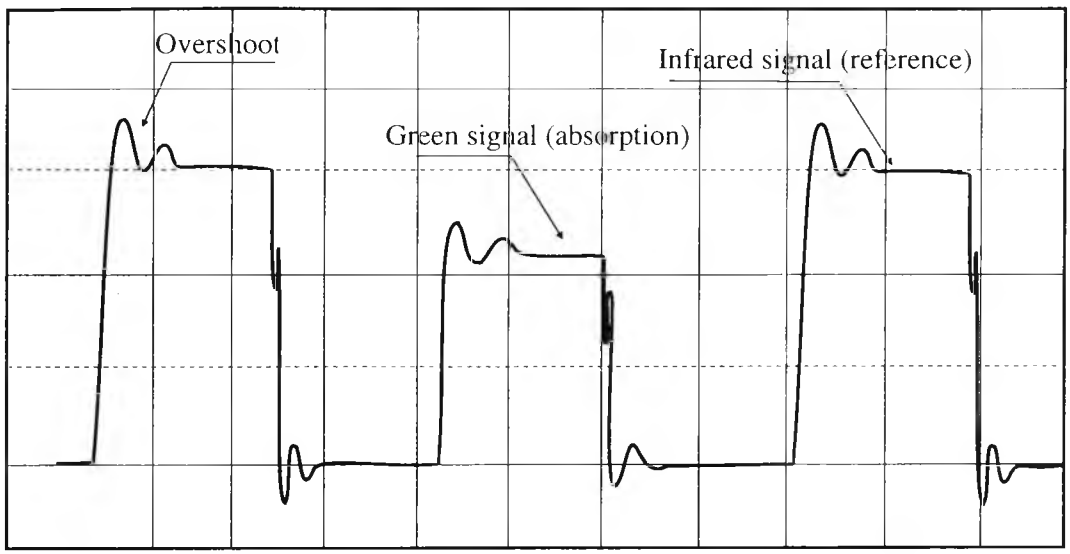

Fig. 4.9 Photograph showing the perturbation which appears as an overshoot as a result of the limited frequency response of the detector.
Scale is Vertical: 1Volt /Div, Horizontal: 200μS /div

The energy stored in the capacitor given by Eq.4.3 showed that if the value of the capacitor was properly chosen i.e. so that the time constant was large compared to the input signal, the energy stored was proportional to the average value of the signal.

$$V_{average} = \frac{1}{T}\int_{o}^{T} V_{input}\ dt \qquad [4.3]$$

4.2.3 Detection and Signal Processing Circuits

The detected optical signal containing the required information was then converted into an equivalent electrical signal prior to amplification and filtering. An output port was provided for subsequent signal measurement and the ratio of the absorption signal to the reference signal was then computed. The block diagram of the detector and signal processing stages is shown in Fig.4.10 and the electronic layout is shown in Fig.4.11

4.2.3.1 Optical Detector

The optical detector used to convert the optical signal into a proportional electrical signal consisted of a silicon photodiode. It was based on the combination of a diode and an operational amplifier, RS(308-067), configured as a transimpedance circuit built on the same substrate. This has the advantage of reducing the noise "pick-up" that usually occurs

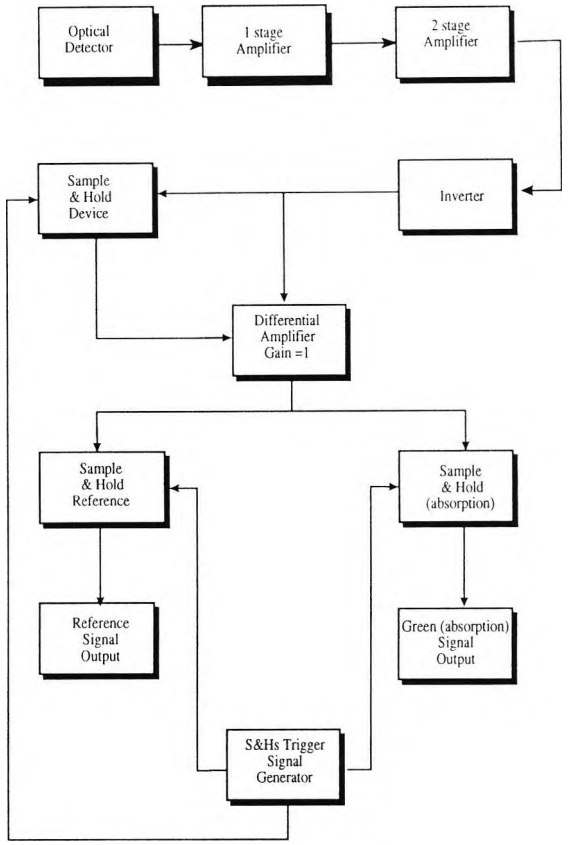

Fig. 4.10 Block diagram of the detector and signal processing scheme for the first implementation of the optical pH meter

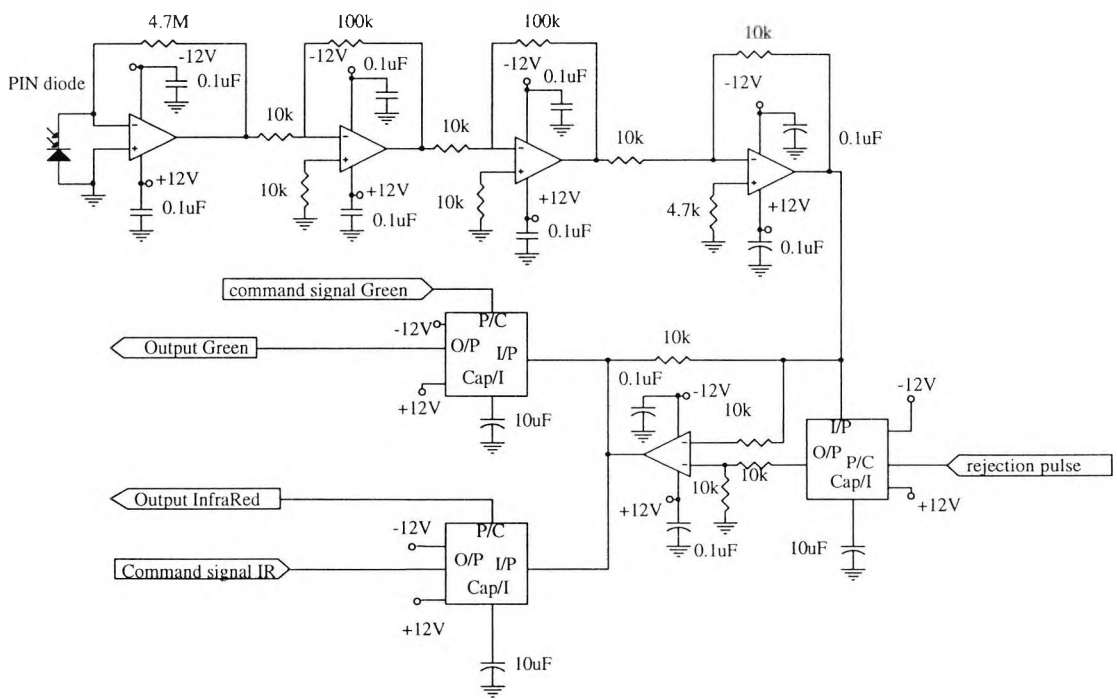

Fig. 4.11 Schematic diagram of the electronic circuit used in the receiver and signal processing section

with weak signals. The optical and frequency characteristics of the detector are shown in Fig.4.12 and Fig.4.13. A low noise amplifier connected in transimpedance mode was used to convert the electrical current generated in the photodiode into a proportional voltage signal. A resistor of a value of 4.7MΩ was used as the converting element in the circuit and was connected in the feedback loop of the amplifier. The photocurrent generated within the photodiode was essentially the current flowing through the feedback resistor since the input impedance of the operational amplifier was very high (e.g. 10MΩ), because the current flowing through the inverting input of the amplifier was considered negligible. The active area of the photodiode was 5mm^2 and the dark current output intensity average value was found to be 4nA. The intensity of the dark current was temperature dependent i.e. increasing with increased temperature. Additionally, it was of a dc nature. Hence, this effect could be minimised by either decoupling the output port of the detector using a fairly low value electrolytic capacitor, or subtracting a dc signal which was proportional to the average value of the noise signal, from the detected signal. The band width limitation of this detector e.g. 10kHz, was determined by the response of the detector to a pulse signal and overshoots appeared at the rising and falling edges of the pulse resulting from the missing or underprocessed higher harmonics of the pulse signal.

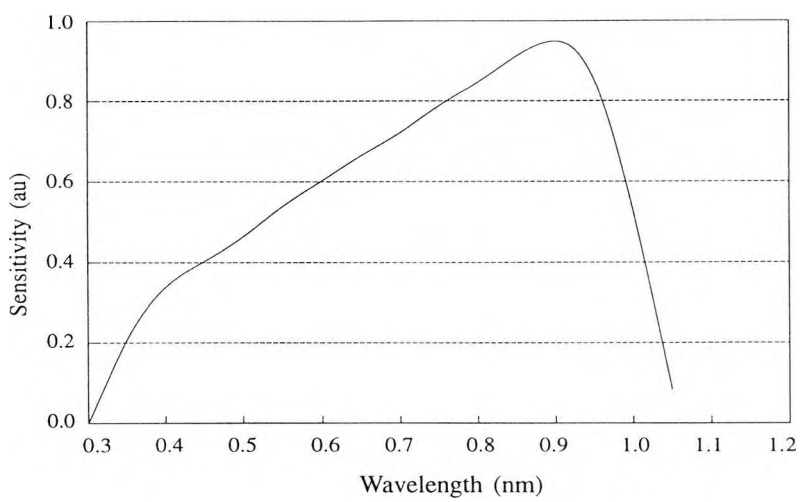

Fig. 4.12 Spectral response of the detector -amplifier module

The intensity of the output signal, from the detector-amplifier stage was about 3mV for the pulse corresponding to the green light when the sample was acid i.e. maximum light transmission. This represented an approximate value since the noise generated in the photodiode and elsewhere was mixed with signal. The detector was mounted in a standard SMA connector for ease of connection and the case was grounded. Because the can of the

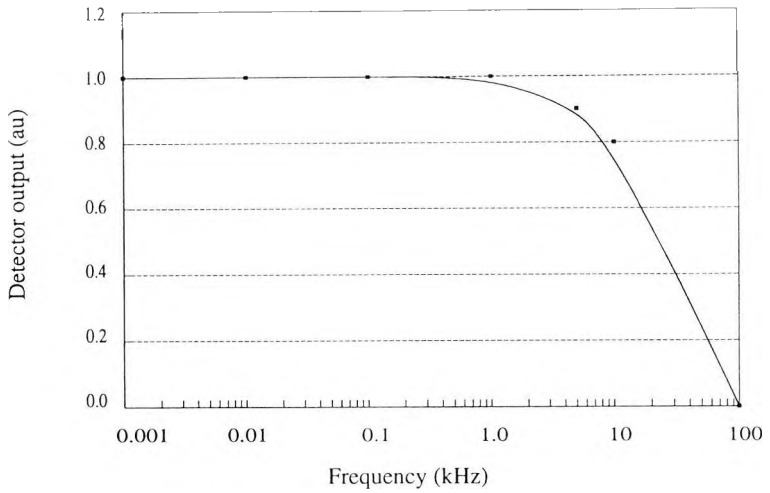

Fig. 4.13 Frequency response of the detector-amplifier module

detector was connected to the negative supply, the detector could not be grounded although this would have reduced the noise pick-up at the detector stage.

4.2.3.2 Amplifier

Operational amplifiers (TLO071) were used in an inverting amplifier mode to boost the signal from the low level amplitude to a reasonable value. The noise within the range of the signal e.g. 0 to 10kHz, was also amplified. However the limited bandwidth of the detector and the operational amplifiers was advantageously used to reduce the high frequency noise since no frequency occurring outside the frequency handling of the operational amplifiers was to be amplified, instead they were reduced. The amplifier was made from two stages because of the limited 1MHz gain-bandwidth product of the operational amplifier which defines the upper frequency as a function of the gain. The two amplifier stages were identical, each of them having a gain of 10 so that the overall gain of this stage was 100. A third amplifier having a gain of unity was used as an inverter. The noise density generated by these amplifiers was in the range of $18nV/(Hz)^{1/2}$.

4.2.3.3 Interference Rejection

The ambient light generated by daylight and the fluorescent tube lamps was seen to affect the baseline value of the detected signal hence resulting in an error in the measurement of the amplitude of the detected pulses. These optical signals were converted into electrical signals in the detector and appeared as a dc signal superimposed onto the main signal.

The main reasons which account for the presence of the dc signal were:

a) The reverse current of the photodiode (which is known as dark current), was generated by the minority carriers inside the junction of the photodiode. The amplitude of the dark current was affected mainly by temperature and the reverse bias voltage of the diode. The dark level temperature coefficient for this particular photodiode was 0.5 $mV°C^{-1}$.

b) The ambient light, i.e. daylight and dc. powered lamps, appeared as a shift of the base line of the signal. It was noticed that a certain amount of the mains light also acts as dc. signal when the intensity is low. This could result from the long reminescence time of the fluorescent light originating from mercury discharge lamps. These are coated with phosphor which is responsible for converting UV radiation into visible light. The wide use of this type of lighting and the lamps disposition can generate the effect of the dc light. However this is only true in very weak signal applications.

c) A small offset was generated in the amplifier stage. This offset voltage can be reduced by balancing the path of the signal to ground. This was achieved by equalling the value of the resistor from the non-inverting input to ground with the value of feedback resistor put in parallel with the resistor connected to the inverting input of the amplifier. However, this method did not eliminate the problem completely, since the offset of the amplifier affected the gain. For long standing measurements, very low temperature coefficient devices should be used.

A scheme to remove these offsets was deployed. It consisted of sampling the signal at the time where both LEDs were switched off using a sample and hold device triggered by pulses generated in the clock and logic gate circuitry. These were triggered to sample and then hold the signal in a polycarbonate capacitor (10μF) until the next sampling time. This time, i.e. the period between two consecutive samples was 1ms, hence the error associated with leakage was small. The output of this sample and hold device, which represented an average value of the interfering signal and was of dc nature, was then fed to the inverting input of a differential amplifier whose gain was set to one. The non-inverting input of this amplifier was connected to the main signal. Hence, environmental disturbances i.e. small variations in temperature, dark current and ambient light, were subtracted from the main signal. This scheme allowed for the measurement to be taken in broad background lighting and no special care was needed for the measurement. However it was unable to discriminate against powerful ac powered light sources.

4.2.3.4 Output Signal Separation

Each cycle contains the information relative to the green LED and infrared LED signals. These consecutive pulses needed to be separated from each other prior to the measurement of their respective intensities.

Different circuits could be used to perform the separation of the signals corresponding to the green and infrared lights. For example a set of two electronic switches could be activated, one at the time corresponding to the time where one LED is switched on and then it would be deactivated just before the falling edge of the driving pulse. This was found to be unsatisfactory because the final signal in each case would have been a pulse train signal. A further processing of these signals would have taken place so that electrical noise would have been be minimised. Instead, a more appropriate method was deployed where the output of the separation stage was enhanced in terms of signal to noise ratio. This consisted of using the filtering effect of sample and hold devices. The processed signal containing the information from the two signals was fed to the input of two sample and hold devices connected in parallel, one was triggered to sample and then hold the signal when the green LED was switched on by using a control pulse command and the second device was triggered to sample and then hold the signal at the time the IR LED was switched on with a similar control pulse. These were originally taken from the pulses driving the LEDs and were modified to occur respectively at each specific time. The duration of these pulses was shorter than the LED driving pulses, in order not to include that part of the signal where overshoot occurred. Consequently, signals corresponding to the absorption and the reference measurements were present at the output pin of these sample and hold devices continuously. Additionally, only the average value of the signal which was stored in the hold capacitor was provided, thus removing a large amount of noise [106]. The computation of the ratio of the absorption signal to the reference signal was then computed and a calibration of the measuring instrument was provided. A schematic diagram of the timing of the separation stage used to separate and filter the output signals (e.g. absorption and reference) is shown in Fig.4.14.

4.2.4 System Characterisation and Calibration

A sample was prepared from distilled water to which a few drops of phenol red were added and mixed thoroughly to become a homogeneous mixture. Because the dye was slightly alkaline the colour of the mixture was red. The concentration of the dye was calculated so that the value of m falls within the specified range e.g. 1.5 to 2 as described in Chapter 3.

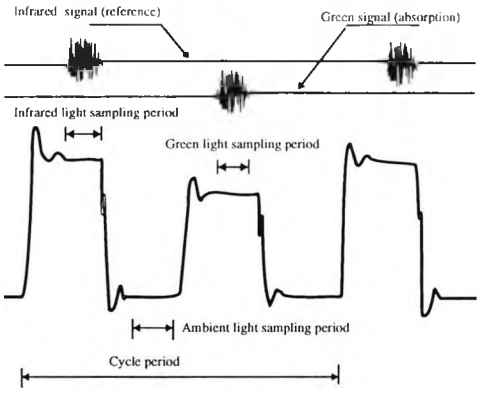

Fig. 4.14 sample signal through the separation stage using sample and hold devices with large polycarbonate hold capacitor ~ 1-10 μF.

The titration was made with hydrochloric acid (HCl). Additional volumes of HCl were mixed with the sample using a magnetic stirrer. The probe was immersed and held at the same position for the rest of the experiment in order not to introduce further errors.

When the measurement was taken, the mixing of the sample was stopped because the latter created turbulent liquid flows which contained small air bubbles and particles, and was affecting the transmission of the light beam. A few seconds were needed to allow for the sample to settle and any bubble movement to stop prior to recording the measurement. The range of pH covered was from 10 to 5 pH units. Although the dye does not linearly cover this range of pH values, it was necessary to investigate the response of the fibre optic pH meter outside the linear range of light absorption by the dye. The same solution was then mixed with increasing volumes of sodium hydroxide in order to increase the pH value and cover the same range of pH as in an acid to base titration. The volumes of acid and base were so small compared to the initial volume of the sample that the concentration of the dye remained in effect constant during the experiment. The volume of the dye phenol red was 0.5ml and was mixed thoroughly to obtain a homogeneous mixture. The ratio of the light transmitted from both green and infrared light was calculated and plotted as a function of the pH of the sample as shown in Fig.4.15. The correlation between the calculated values and the pH of the sample was carried out using a commercial potentiometric pH meter (RS 10-540) which was calibrated in two buffered solutions (pH 7 and pH 4). The range of pH values scanned during the calibration was between 5.5 to 9 pH units. Only a portion of this range could be approximated as a linear response of the instrument which occurred around the inflexion point (i.e. pH = pK).

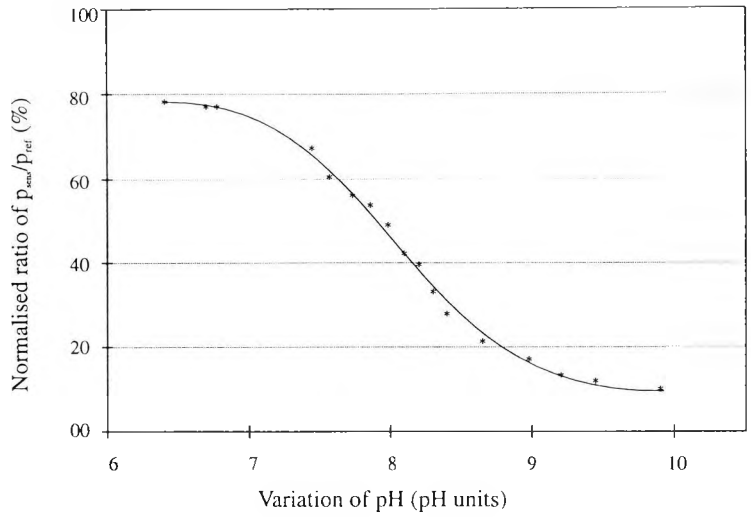

Fig. 4.15 Calibration curve of the fibre optic pH meter as a function of pH measured with a glass electrode instrument over the range of 6 to 10 pH unit values.

4.2.5 Error Considerations

As was described in chapter 3, the error in the measurement of pH using colorimetric techniques is related to the error in the measurement of the light intensity of the sensing signal. The relationship is not linear but varies with light level. Hence, a figure for noise performance can only be applied to a particular value of the measurement e.g. when the absorption of the dye is maximum for the particular sensing wavelength. Usually a signal to noise ratio is a better description of the noise performance because it is related to the level of the signal and in this case a value of 54dB was obtained for a static signal. However, for the range of pH studied the dynamic range of the signal is smaller. Consequently, the dynamic SNR is smaller and gave a more accurate value for the performance of the sensor. For example, the signal varied by 19% which corresponds to a $SNR_{dynamic}$ of 41dB. The noise level associated with the detected signal is ~10mV. The corresponding numerical value for the pH measurement is then computed and was found to be ± 0.05 pH units at its best value.

The results provided by the sensor when the pH of the sample was varied from the two extremes e.g. acid to alkaline sample, were compared with a commercial potentiometric pH meter and were found to be reproducible within the estimated error. The instrument was monitored for a period of an hour and it was found that the output varied by only ~1%. The effect of temperature on the response of the instrument was found to alter the output of the sensor by 0.04 pH K^{-1}. This was carried out by heating the sample in a temperature range of 20 to 50 °C and monitoring the variation in the value of the ratio of the green to

infrared signals.

4.3 Implementation of the Self-Referenced pH Meter

In the second configuration the principle of the measurement of pH was not changed, but the reference signal was generated in a different manner. The measurement of the light absorption by the phenol red dye at a wavelength of 560nm is related to the pH value of the sample and was established in the preceding sections. The monitoring of the fluctuations in the emission of light from the LEDs e.g. green and infrared, was not provided in the first implementation. It could have been implemented by guiding the emitted light using two small diameter fibres to a separate detector and variation in the light intensity of either of the LEDs would have been known and related to the measurement of the absorption of the phenol red dye.

In the second implementation this problem was overcome by the use of a self generated reference wavelength as in the set-up shown in Fig.4.16. The reference light was generated using the fluorescent properties of a Ruby crystal which absorbs in the ultraviolet and visible to emit a fluorescent light in an area covering most of the visible and lower infrared area. However, two distinctive strong emission lines known as R-lines appear in the red part of the spectrum i.e. 690 and 693nm. In addition, the light resulting from the fluorescence of the ruby was found to be spread over a large range. The light emitted from the green LEDs was partially absorbed by the ruby crystal (i.e. < 1%)[108] while the rest

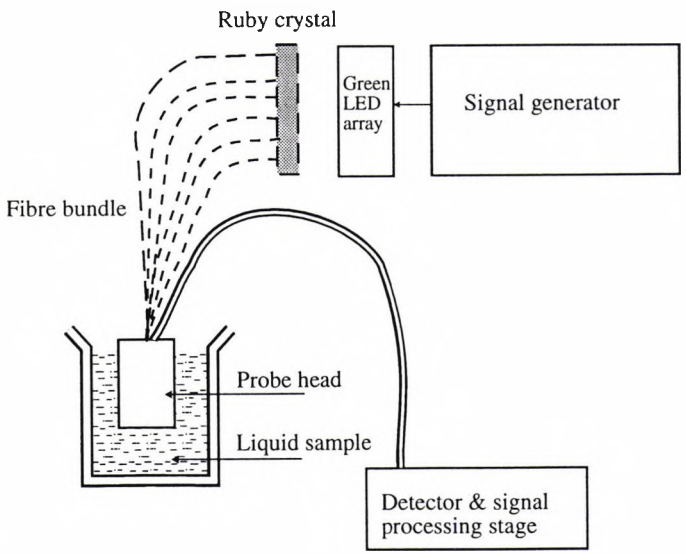

Fig. 4.16 Configuration of the self generating reference light of the optical pH meter

of the light was transmitted through. This set-up enabled the use of the same light source to generate both wavelengths i.e. absorption and reference. Consequently, problems discussed in chapter 3 and which were associated with the light source such as ageing, intensity fluctuations etc.., affect the two wavelengths with the same ratio.

A similar modulation scheme to the one deployed in the first implementation was used to drive the emitting LEDs. However, a different concept was adopted in order to extract the reference information from the sensing signal. Titration of a sample containing the phenol red dye with additional volumes of acid and base was carried out and the results were used to calibrate the instrument and provide information related to error analysis, sensitivity and stability of the instrument.

4.3.1 Ruby Crystal

Pink ruby crystal (Al_2O_3 doped with ions of Cr^{3+} at concentrations of no more than 0.05%) has been the subject of intense research especially in relation to the effect of temperature on the quantum efficiency and the properties of the fluorescent light[109 || 110]. Maiman used ruby to demonstrate and construct the first visible laser[111]. He found that the quantum efficiency of this material to be unity at a temperature of -196°C. Furthermore, Burns et al concluded that the value of the quantum efficiency did not change between -196°C to +240°C when the fluorescence over the full range of the spectrum was considered and thus as a result, the quantum efficiency remained unchanged in this temperature range[112]. It was also found that beyond a temperature of 240°C, the quantum efficiency decreased rapidly. The ruby crystal showed strong absorption peaks in the 420nm and 560nm and emitted a fluorescent light in the red region of the spectrum which consisted mainly in two sharp R-lines at 692.7 and 694.3nm[113] as shown in Fig.4.17. The monitoring of the light emission at those two wavelengths was the basis of the monitoring of temperature using a fibre optic system [56]. The intensity and the profile of the R-lines were affected by temperature, their line width increased with increasing temperature while their intensities decreased for the same variation of temperature. The quantum efficiency is unaffected by temperature changes over the range -196°C to 70°C when the quantum efficiency is measured by considering only the area under the R-lines as shown in Fig.4.18. This was found to be acceptable since the temperature of the ruby crystal is unlikely to be beyond the 50°C in the case of the optical pH meter experimental set-up. One of the strong absorptions peaks of the ruby crystal which occurred at the wavelength of 560nm,

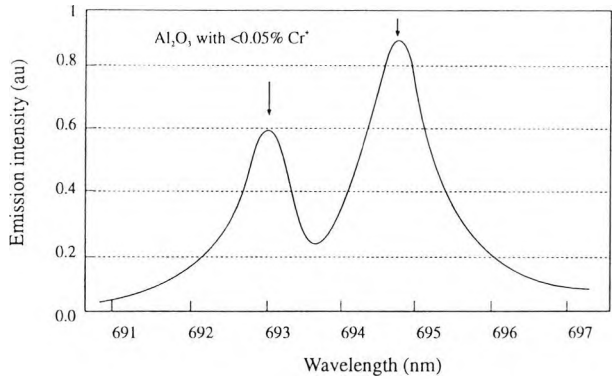

Fig. 4.17 Emission spectrum of ruby crystal in the red region showing the sharp R-lines at a temperature of 60 °C

coincided with the emission band of a green ultra-bright LED and hence the same wavelength was used to excite the ruby crystal to provide fluorescent light in the 690nm region and to sense the change in absorption of the phenol red dye. Consequently, the ruby crystal was well suited for use in this application. Furthermore, the fluorescent light occurring above the wavelength of 630nm mainly 690nm is far removed from the absorption spectrum of the phenol red dye. In addition the temperature independence over the selected spectral range provided a reliable and stable reference light source and thus was less affected by changes in the environment temperature such as the heating effect to which the crystal was subjected by the light emitted from the LEDs and the heating of the LEDs themselves.

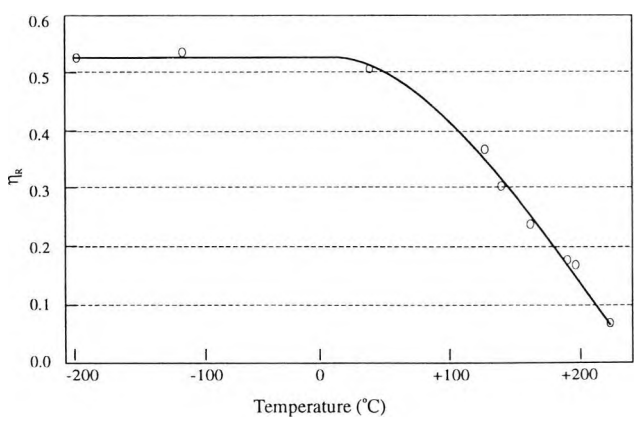

Fig. 4.18 Variation of the quantum efficiency value η_R as a function of the temperature of the crystal (this applies only to the R-lines)[112]

4.3.2 Optical Arrangement

The optical arrangement of the pH meter comprised an emitting fibre bundle, a collecting fibre, a probe head and LEDs as light sources.

4.3.2.1 Light Sources

The main light source of the system consists of a set of six (6) solid state indicator type green LEDs emitting at a wavelength of 560nm at 120mCd each. These were driven by the same pulse train signal at a current of 60mA each. The mark to space ratio is defined by the decay time of the fluorescent light emitted by the ruby crystal and is such that the LEDs remain switched off until the there was ample time for the fluorescent light to decay. Additionally, a further time was added so that it could be used for sampling the background light level. The reason for using six LEDs was to improve the signal to noise ratio of the fluorescent light signal since the fluorescent light intensity was very weak.

The shape of the ruby crystal is partially cylindrical so that most of the fluorescent light was essentially concentrated in the centre of the dome shaped ruby and it was positioned in front of each LED. This way, coupling light from the crystal into the fibre was increased. Although, the polishing of such a hard crystal is difficult and necessitates the use of a mechanical polisher for a period of one week, the ruby crystal was polished on the two sides where light enters and exits the crystal in order to minimise the losses of the low intensity fluorescent light. The crystal was glued to the head of the LED using wax. They were both put in an SMA type LED housing with a standard fibre connector as shown in Fig.4.19.

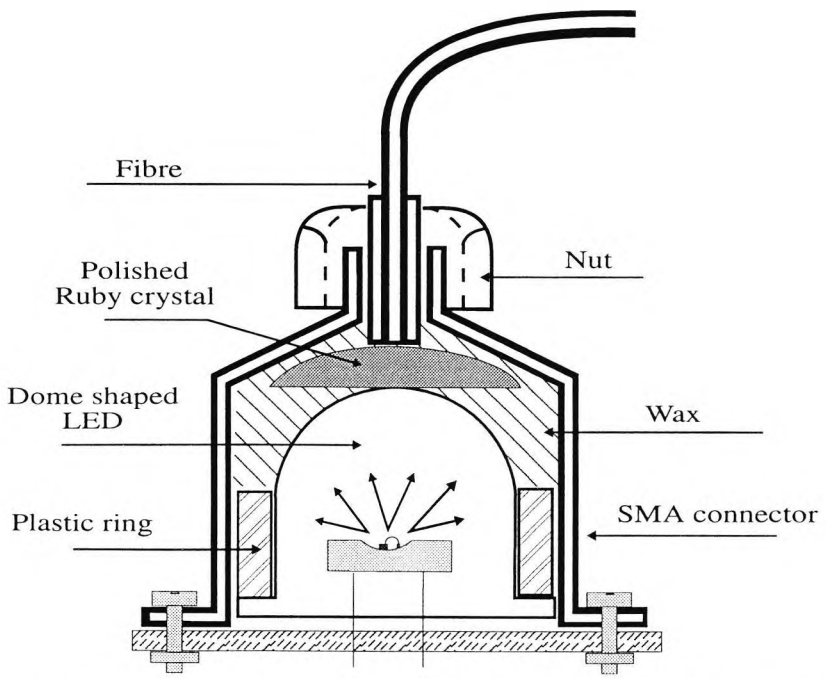

Fig. 4.19 The ruby crystal shape and the SMA housing used to house the LED, ruby and the fibre.

4.3.2.2 Emitting and Collecting Fibres

The detected fluorescent light was found to be very weak when compared to the intensity of the green light and also the signal to noise ratio of the signal corresponding to the fluorescent light was very low and hence could not be used unless the exciting light power was increased. For this purpose a bundle of plastic clad silica (PCS) fibres was used to guide the light from the light sources formed by the array of six LEDs and the ruby crystal into the probe head. Each of the six 600μm fibres of a length of 1 meter was connected to an SMA connector at one end while at the other end of the fibre bundle, they were glued alongside and around the large diameter fibre, i.e. 1mm diameter, as shown in Fig.4.20. The latter was used to carry the light reflected from the probe head to the detector. Each of these fibres guided light made of both wavelengths emerging from the ruby crystal, i.e. the fluorescent red light, and the transmitted green light.

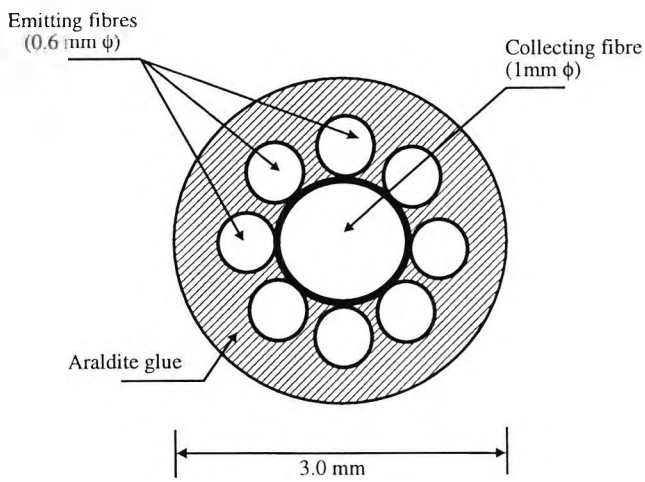

Fig. 4.20 Fibre bundle (in the probe head side) showing the disposition of the emitting and collecting fibres

4.3.2.3 Probe Head Design and Construction

The probe head for this implementation was similar to the one used for the previous implementation. However, the reflecting properties and the surface of the mirror were improved because the emitting fibres now surrounded the collecting fibre in contrast to the previous design. In this application the receiving fibre was positioned in the centre and for this reason the mirror was slightly curved inward to focus the light back onto the central fibre. The fibre connector is a cylindrical pipe, machined so that it contained the six emitting fibres and the collecting fibre. It had a thread on the external side so that it could be tightly fixed to the probe, thus reducing the effect of vibration.

The body The body was made from a stainless steel cylinder into which large holes had been drilled. They allowed for the passage of the solution outside and inside the probe head. Threads were made at each end of the cylinder so that the fibre connector and the mirror could be dismantled and mounted for cleaning purposes for example.

The mirror The mirror holder was made of brass. The reasons for such a choice were based on the 'soft' properties of this material and its ability not to react with corrosive samples e.g. alkaline and acid solutions. The face of this mirror was curved so that most of the reflected light was directed towards the central collecting fibre. The curvature of the mirror was calculated using the modified numerical aperture of the fibre since the latter is given as a function of the index of refraction of air.

The maximum angle of the beam emerging from the fibre was smaller than the beam that would emerge from the same fibre in a glass-air interface. The light beam hitting the curved surface of the mirror at any point is reflected with the same incident angle back into the collecting fibre positioned at the centre of the fibre bundle, as shown in Fig.4.21. This way more light was collected and guided to the detector. The mirror support part was threaded so that final adjustments could be done once the probe head was mounted and immersed in the sample. The path length of the beam travelling through the liquid was then fixed.

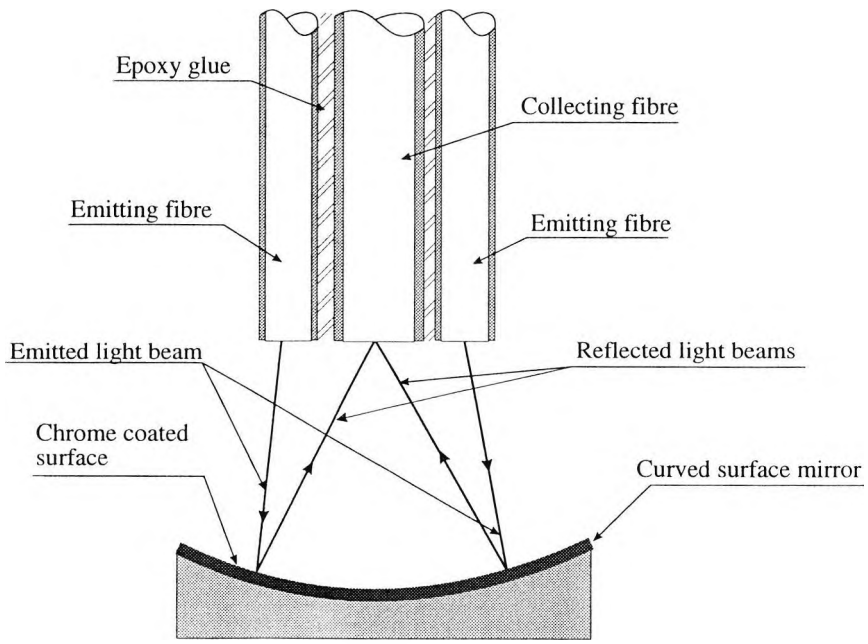

Fig. 4.21 Schematic diagram of the light beam emerging from the emitting fibres and re-entering the collecting fibre

The radius of curvature was very large and was made by polishing the surface with a worn out drill bit which was made less sharp at the edge. The shiny layer from which the surface of the mirror was made, consisted of a relatively thin chemically resistant layer of chromium deposited by an electro-deposition process. This probe head is shown in Fig.4.22.

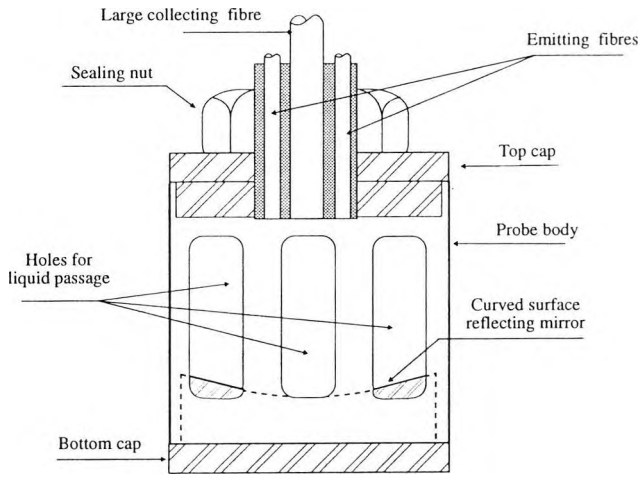

Fig. 4.22 Details of the optical probe for the self referenced pH meter with a curved mirror

4.3.3 Electronics

The block diagram of the electronic circuit comprising an emitter, detector and signal processing section is shown in Fig. 4.23.

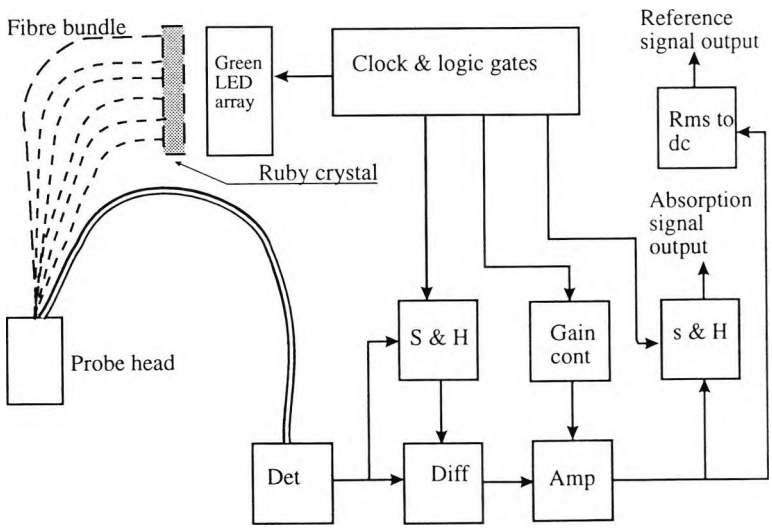

Fig. 4.23 Block diagram of the electronic section of the self generated reference signal for the pH meter.

4.3.3.1 Emitter

In this section the clock signal was generated using a monostable logic circuit (NE555) which could produce digital signals where the mark to space ratio could be controlled by choosing the appropriate values of the components i.e. capacitor and resistor values, and was set to be 1:3. The pulse and the cycle durations were calculated using Eq.4.4 and Eq.4.5

$$T_1 = (R_1 + R_2) C \qquad [4.4]$$

$$T_1 = \frac{1}{R_1 C} \qquad [4.5]$$

where R_1 and R_2 and C denote the resistors and capacitor of the circuit. The frequency of the clock was ~ 70Hz. The reason for choosing such a low frequency resulted from the following:

a) The frequency response of the combined detector-amplifier as was shown in the preceding implementation (Fig.4.13), produced a distorted signal and appeared as an overshoot at the rising and falling edges of the pulse. This system was successfully used in the first implementation since the only important part of the signal was the amplitude. In this case however, not only was the amplitude of the signal important but also the signal representing the decay of the fluorescent light (i.e. after the LEDs were switched off). There were two solutions to this problem. The first one consisted of compensating the signal by using an RC network to remove the overshoots. However, this was found to change the profile of the decaying signal and hence introduced additional errors and therefore it was discarded. The second option relied on shifting the signal bandwidth so that the frequency response of the detector was large compared with the frequency content of the signal. This was achieved by lowering the clock frequency. As a result, all the frequency components were processed in a similar manner and thus the fluorescent light intensity information was not affected.

b) The occurrence of the next pulse was delayed until the fluorescent light decayed completely to zero. Hence this imposed a restriction on the timing of the train pulse signal. A further time was added to the period corresponding to the time the LEDs were switched off to enable the sampling of the ambient light and signals generated by the electronic components such as dark current and offset voltages of the amplifiers, for subsequent filtering.

4.3.3.2 Timing Circuitry

The timing circuitry was needed to generate the triggering pulse used in the sample and hold devices, to provide a control signal for the analog switch and also to generate the driving pulse used to switch the LEDs on and off. The schematic of the emitter module is shown in Fig.4.24.

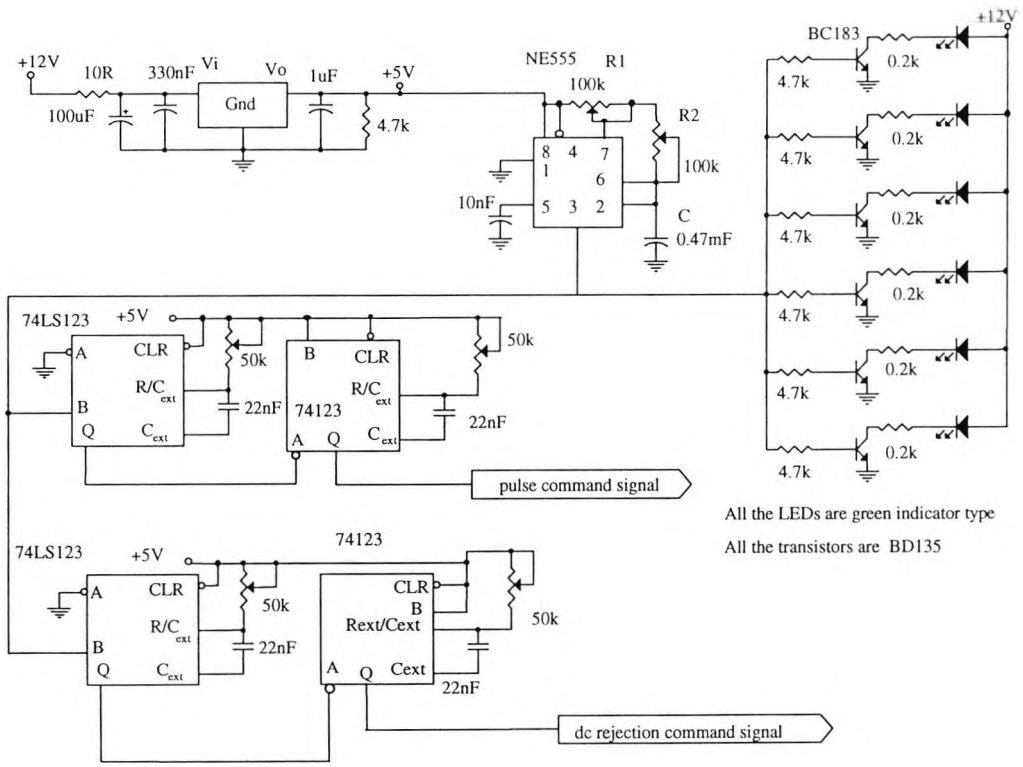

Fig. 4.24 Electronic circuit diagram of the emitter used in the second implementation of the fibre optic pH meter

4.3.3.3 Detector

The same detector as the one used in the first implementation was used in this configuration to convert the optical signal into an equivalent electrical signal. The latter consisted of a pulse shaped signal corresponding to the state of the LED being switched on, then a "tail-like" decaying signal. Additionally, the detector output consisted of the superposition of various signals from different origins such as the one generated from external influences such as temperature effects on the dark current, offset shifts and the effect of the ambient light.

4.3.3.4 dc Signal Rejection

To remove any dc electrical signal corresponding to ambient light and dark current signal generated within the photodiode, the detected signal was sampled at a time when the green

LED was switched off i.e. pulse not present, and after a time usually longer than 3e where e is the naperian antilogarithm. This was considered sufficient for the signal to have completely decayed. This dc rejection scheme was implemented by using a sample and hold device which was triggered to sample the main signal when no fluorescent or green light were present. The output signal of this unit was of a dc form and was subtracted from the main detected signal using a differential amplifier whose gain was set to unity. The control signal was generated from a dual multivibrator circuit which provided control of the duration of the pulse and the time it occurred with respect to the LEDs' driving signal.

4.3.3.5 Amplifier

It appeared from the detected signal that the ratio of intensities of the pulse to the decay signal was very high. Therefore, the feedback resistor which set the gain of the amplifier was changed during one cycle. Due to the high intensity of the green light corresponding to duration of the pulse, the gain was set at G_1 and a higher gain G_2 was set for the rest of the cycle.

Once the dc signal was filtered out, the signal was amplified. This is carried out using an operational amplifier in an inverting mode which provided enough frequency bandwidth to process the main harmonics of the signal similarly. The gain value of this type of amplifier is defined as the ratio of the feedback resistor to the input resistor. The ratio of the intensities of the pulse to the decaying fluorescent light signal was of the order of 20 to 1 and hence the gain of this amplifier was not set too high so that the amplitude information was not lost as happens when the amplifier saturates. The change of the gain value was carried out by electronically connecting a parallel resistor to the feedback resistor when the driving pulse was present. This resulted in a decrease in the overall resistance and thus reduced the value of the gain. The same connection was opened to increase the value of the resultant resistor and hence the gain was increased. Physically, the connection was made by using an analog switch controlled by the LED's drive signal. The detector and amplifier stages are shown in Fig.4.25.

4.3.3.6 Signals Separation

The signal corresponding to the absorption of the green light was sampled with a sample and hold device which was triggered by a control signal conditioned using a dual multivibrator device. The latter provided a pulse whose duration and time of occurrence with respect to the main signal was set by two separate variable resistors. Hence these two

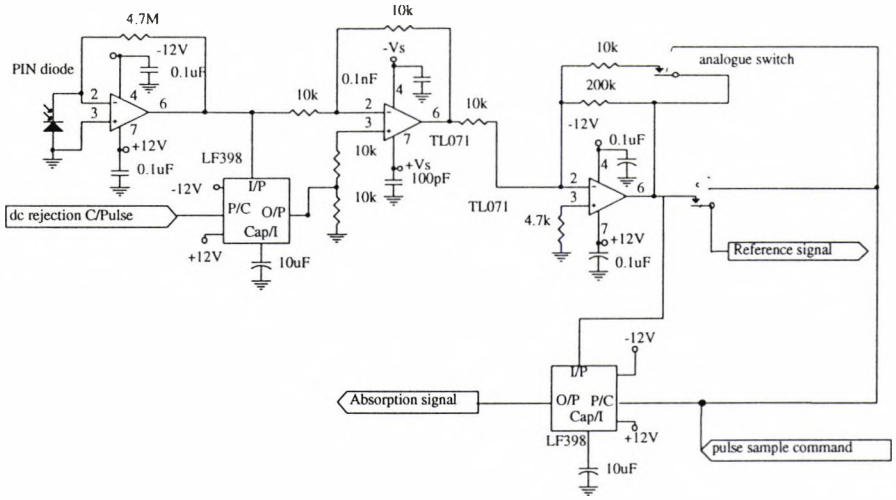

Fig. 4.25 Electronic circuit diagram representing the detector and signal processing stage.

parameters were changed to suit the application by changing the values of these resistors. The signal corresponding to the fluorescent light was directed to a separate path using an analogue switch. For this application the measurement of the rms value of the fluorescent light was not performed because the signal was noisy and needed more signal processing, preferably using digital techniques. This facility is provided in the built-in routines of a digital oscilloscope *Tektronix 7854*. As part of the numerous programmed procedures, the storage and averaging of the signal at 10, 100 or 1000 times can be obtained. It was found that averaging the signal 1000 times provided no major improvement in the signal to noise ratio. Thus there was no necessity to average the signal 1000 times and furthermore, this increased the processing time. Consequently, a 100 times averaging was used. This was achieved by triggering the oscilloscope externally using the LED drive signal which corresponded to the time when the LED was switched off. The sampled signal was digitised and stored in memory. The signal processing was then performed and the resultant form of the signal was displayed*[114]. After removing most of the noise, the rms value was computed and was related to the area under the curve defined by the two on screen pointers. This value represented the value of the reference signal generated by fluorescence. The overall process e.g. sampling, digitisation and filtering, took less than one second to perform.

* *The Tektronix 7854 oscilloscope is equipped with an on-board computer which can store the profile of a signal and compute all the different parameters. The averaging of a signal is performed through built-in routine. It consists of storing the digitised signal and then repeatedly acquiring the real time signal. A comparison of each data point with the real time data point occurring at the same time is performed and the average is computed and sorted in memory and is also displayed on screen. At any time, the stored waveform represents the algebraic mean value of the individual waveforms acquired up to that moment.*

On the other hand, the signal amplitude of the signal corresponding to the green light was obtained by measuring it from the sample and hold device output signal. A large capacitor value was used to average the sampled signal as discussed in the first implementation. The signal corresponding to the fluorescent light before and after averaging is performed is shown in Fig.4.26 and Fig.4.27.

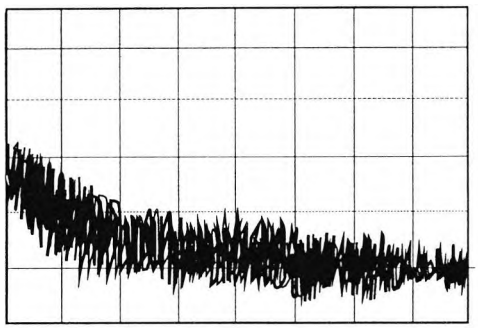

Fig. 4.26 Photograph of the decaying fluorescent signal before signal averaging is performed.

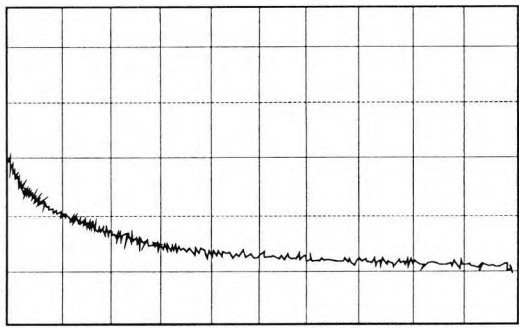

Fig. 4.27 Representation of the same signal as in Fig.4.26 after being averaged 100 times.

4.3.3.7 Timing and Control Circuitry

This circuit was the same as that used in the first implementation to control the pulse width and its occurrence time with respect to the input pulse and consisted of two multivibrators as shown in Fig.4.28. To each of the multivibrators an RC network was connected to provide the control of the pulse position and its duration.

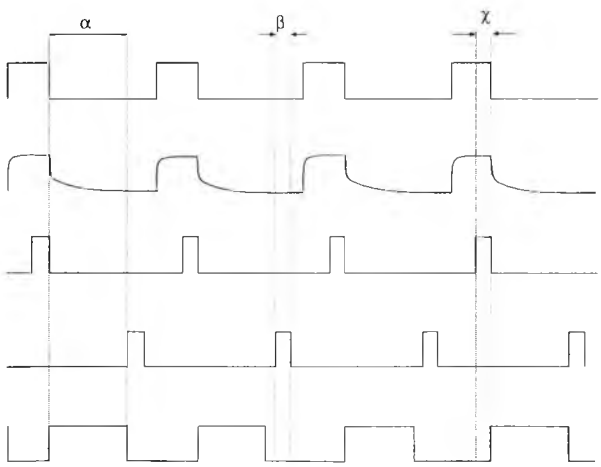

Fig. 4.28 Timing of the different pulses used for controlling the analogue switch and to trigger the sample and hold device:

A: LED drive pulse, **B**: form of the detected signal, **C**: Sampling time for the sample and hold used for the sensing signal. **D**: Timing of the pulse for the dc rejection, **E**: Signal controlling the analogue switch .
α: measurement of fluorescent light time, β: dc sampling time, χ: Absorption sampling time

4.3.4.Calibration Curve

The calibration curve for this system was obtained by mixing phenol red with a sample of distilled water and then additional volumes of hydrochloric acid were added in order to reduce the pH of the sample to a value of 5; then sodium hydroxide was mixed with the sample to increase its pH to a value of 9. The strength of the acidity and alkalinity of hydrochloric acid and sodium hydroxide was kept small during the whole process of calibration. The concentration of the phenol red was not affected by the addition of the acid or base.

The calibration curve of the optical pH meter is shown in Fig.4.29. The curve which represents the variation of the ratio of absorption to reference signals as a function of pH was found to follow the expected pattern which consists of an "s" shaped curve with a central part, i.e. around the inflexion point, that could be considered as a linear portion. This corresponded to the region of pH values between 7 and 8.5. Outside this range, the change of absorption of the light was relatively small and resulted in a larger error in the measurement. The error was at its minimum in the linear portion of the curve.

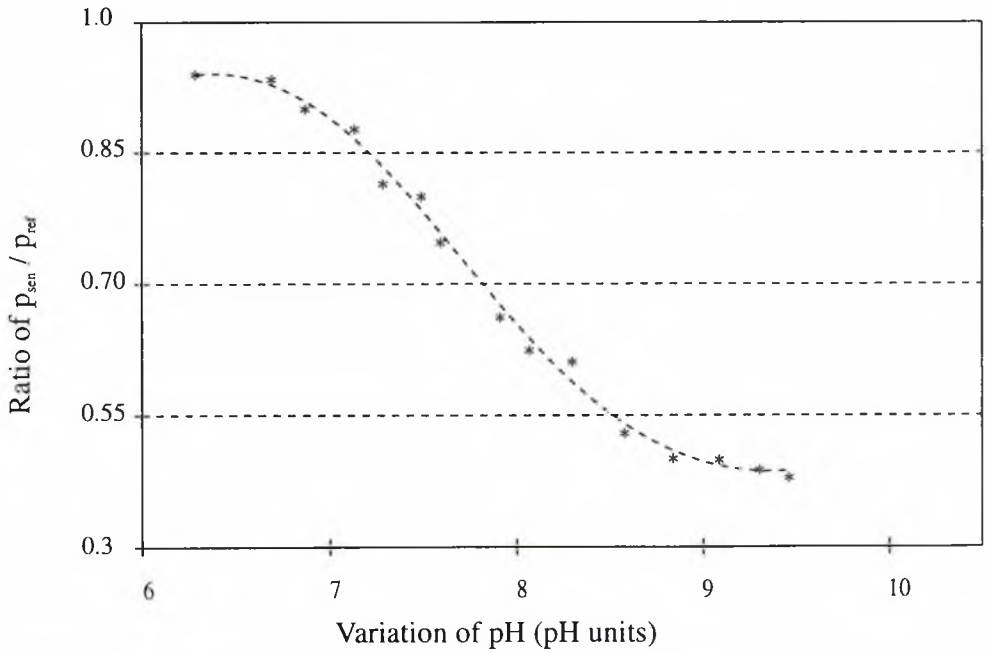

Fig. 4.29 Calibration curve of the self generating reference signal fibre optic pH meter

4.3.5 Error Considerations

In addition to the error introduced by the use of the logarithmic relationship between light and concentration of the dissociated form of the dye and the various sources of errors which

have already been discussed in detail in the first implementation e.g. section 4.2.6, an additional error resulting from the low level of the light intensity of the reference signal was considered. This is reflected in the relative error of the measurement of the light intensity which can be expressed as follows:

$$\Delta\left(\frac{p}{p_{ref}}\right) = \frac{\Delta p}{p} + \frac{\Delta p_{ref}}{p_{ref}} \qquad [4.6]$$

where p and p_{ref} are the measured light intensities of the sensing and reference wavelengths and Δp and Δp_{ref} are the absolute errors in the measurement of the sensing and reference wavelengths respectively. In this particular case, the value of the relative error on the reference signal was higher than the relative error on the sensing wavelength due to the low level of the fluorescent light whereas the sensing light intensity was high (e.g. approximately over 90% of the detected light consisted of the sensing wavelength light).

4.4 Comparison of Results and Conclusion

The design of a fibre optic pH meter based on the principle of light absorption of a chemical dye (e.g. phenol red) was investigated using two different methods for generating the reference light signal. In the first method an external light source was used to sense the variation in the absorption which is produced by interfering effects, and relate it to the absorption of the dye. In the second implementation, the fluorescent properties of a Ruby crystal were used to generate the reference wavelength whose light intensity is affected in the same manner as the sensing wavelength. The same light source was used to generate both wavelengths. The error achieved in the measurement of the pH value of the sample was governed by the error in the measurement of the light intensity at the two wavelengths. Because of the way the reference light was generated in the second implementation, the level of noise and thus error on the reference signal was higher than the noise level in the sensing signal whereas in the first implementation, the sensing and reference signal were of the same amplitude. However, the self referencing system (i.e. second implementation), provided a protection against any temporal fluctuations and any long term effects in the spectral behaviour of the light sources. This is considered to be an advantage with respect to maintenance, but it involves more signal processing. This, however, cannot be considered as a drawback because of the ready availability of digital signal processing modules which can perform most of the required signal processing. In the first system, i.e. the system using two external light sources, better results in terms of signal to noise ratio

and simplicity of the opto-electronic devices were achieved. An accuracy of ±0.05pH units was obtained for this system while ± 0.07 pH units was the accuracy of the self referenced optical pH meter e.g. second system.

Chapter 5

Feasibility Study for the Design of an On-line Residual Chlorine Monitor

Abstract

An optical method based on the absorption of light in the ultraviolet part of the spectrum for the monitoring of residual chlorine was investigated. The optical properties of chlorine dissolved in different sources of water were shown to interact with light and absorb the ultraviolet light at a wavelength of 290nm when the chlorine was in the form of hypochlorite ion which resulted from the reaction of chlorine with water in an alkaline sample. The effects of temperature and pH on the chemical reaction of chlorine with water were also described and the latter was used to condition the sample so that all the chlorine forms were converted into hypochlorite ion. This was monitored and related to the total concentration of chlorine in the sample. These results were used in order to design an on-line optical fibre based system for the measurement of chlorine in water for continuous measurement over a period of at least one month and with a response time of less than 20 seconds for a 90% step change in chlorine concentration.

Different methods for referencing against background absorption of various origins and also against electronic and optically generated errors, using both pH change and chemical removal of chlorine from the sample were described.

5.1 Historical Background

Chlorine was primarily used as a bleaching agent in the textile industry and was combined with potassium or lime to produce hypochlorite also known as Javel* water. It was in this form that it helped the disinfection of water supplies in the U.K. during the mid 18th century to control outbreaks of cholera and typhoid [115]. Subsequent research resulted in obtaining solid form of chlorine which were found to be very beneficial because there was less risk involved during transportation from the generation site to the consumer and by simple mixing with water, the reagent was usable in a short time. Few but disastrous accidents were related to have happened in the beginning of this century in the USA and Canada involving most of the time the derailment of train cars transporting liquefied chlorine, the danger being in the fact that chlorine in gaseous form could not be contained. Another form of active chlorine which was less likely to cause damages was hypochlorite although it was reported that its germicidal efficiency was less than that of chlorine as gas.

Although chlorine is a relatively good disinfectant, it nonetheless does not perform as efficiently as other agents such as ozone, bromine, iodine and ultraviolet light. However, none of these agents combine the ease of use, measurement and control as well as being free of toxic or physiological side effects and also being relatively inexpensive, as is the case with chlorine. Each of the disinfecting agents can be superior in one of the characteristics but in terms of the combination of the the characteristics, chlorine stands by far ahead of the others [116]. Nowadays, for safety reasons, chlorine as hypochlorite ion, is the most used disinfectant chemical in large numbers of water treatment sites and is easier to generate on-site. It has been widely used as a disinfectant of potable waters, sterilisation of domestic and industrial effluents and also to break down effluents containing cyanides.

5.2 Review

The large number of sites using chlorine as the main chemical in the process of disinfecting processed and drinking water resulted in the development of a range of instruments for the measurement of free and combined residual chlorine. These have proved to be unstable after some time, especially when used for continuous monitoring. Early work has

* *Javel is a small town now part of Paris, where the first experiments on chlorine were made by Berthollet in 1789.*

concentrated mainly on the use of electrochemically based analysers [117] which can be grouped into amperometric, voltametric and potentiometric types. In the amperometric analyser, a system of two electrodes is immersed in the sample one of which is a noble metal and the other is made of copper. The current which passes through the sample is expressed as a function of the concentration of the chlorine content. This method is affected by pH and temperature which can vary with time and water type. The pH of the sample depends mainly on the buffering capacity of the treated or processed water. Additionally, different species such as iodine, can interfere in the measurement although in a recent sensor a membrane was used to allow for the diffusion of hypochlorous acid only.

On the other hand optical techniques utilising colorimetric techniques were used as the basis of chlorine analysers in 1927, using a dye orthotolidine. A comparison took place between the light passing through a coloured glass and the sample. Absorption resulted in an error signal which was then used to reduce or increase the chlorine volume injected into the water in order to minimise this error signal. More recently, N,N-diethyl-p-phenylenediamine (DPD) dye was used to monitor the concentration of chlorine using the same colorimetric technique and was found to be reliable, accurate and sensitive to $\pm 25\mu g/l(Cl_2)$. Measurement was carried out using absorption techniques at a wavelength of 515nm. Although the results were accurate, this method was not deployed on on-line monitors for two reasons:

a) DPD was found to be carcinogenic and hence presented health hazards.

b) The dye was expensive and financially was unsuitable for use in continuous monitoring systems. ChemLab produced an instrument based on the absorption of light by the DPD dye. However, for this system to be competitive, reagent consumption was reduced by sampling every 15min minute amounts of water sample e.g. in the µl range. As a result, the measurement of the chlorine content was carried out after a delay due to the late arrival of the sample to the optical cell of the instrument. Consequently, positioning of this instrument with respect to the sampling point was of prime importance and this was another drawback.

Chemiluminescence has been used to measure chlorine concentrations in the Part Per Billion (PPB) range[118]. This method relied on the reaction of luminol reagent with chlorine. The light intensity was proportional to the hypochlorite ion concentration and was found to be comparable to the colorimetric technique (DPD). Because this method relied on the generation of light as a result of a chemical reaction, there was no need for a

light source and hence the optical system was very simple. Although, this method was very sensitive and unaffected by other chemical species (apart from chloramines), unfortunately it has remained in laboratory use and for practical reasons was not thought to be suitable for on-line applications.

Further work was carried out using a different reagent methyl orange[119]. The measurement relied on the diffusion of hypochlorous acid through a PolyTetra-FluoroEthylene (PTFE) membrane. This technique is affected by temperature, a problem encountered in diffusion systems, and also deposition of different species on the membrane surface which then produces a barrier effect. Reagentless techniques appeared when the same membrane was used to filter the sample and allow hypochlorous acid to diffuse through. On the opposite side of the membrane, a sample of distilled water made alkaline, collected the diffused hypochlorous acid which was then converted into hypochlorite ion. Absorption of the converted species was then monitored using a spectrophotometer[16]. A large contact area was used to allow for better sensitivity. The range of measurement using this technique was large and was reported to be 0.7 to 700mg/l, however, the response time of this system was 3 minutes for a 90% step change in chlorine concentration.

In order to reduce the response time of the measurement, a more direct approach was taken by Briggs et al, and consisted of measuring the absorption of the hypochlorite ion at a wavelength of 290nm [27]. This has been conducted through a series of optical and chemical tests carried out on chlorine and its behaviour in water. This is the method investigated in this work and the feasibility study for the use and the design of an on-line measurement system combining sampling, conditioning and measuring in a self maintained unit is described subsequently.

A comparative classification of most methods used for chlorine concentration measurement is given in Table.5.1 where the detection limit and interferences in each method are highlighted. The use of the optical properties of chlorine in the ultraviolet part of the spectrum for the quantitative measurement is fairly recent and therefore has not been assessed as fully as has been done with the DPD and the electrochemical methods. The basis of this technique relies on the direct monitoring of the absorption of chlorine in this part of the spectrum. This has the added advantage of not using any colorimetric reagent which might present a health hazard or rely on qualified technical assistance for maintenance.

5.3 Chemical Analysis of Chlorine

Chlorine is a very powerful oxidising agent. It reacts with water to produce three species,

Method	Detection limit (μg/l)	Interference
Residual chlorine electrode	50	NH_2Cl
I2 titration	40	Fe(III), Mn(II), NO_2^-
Amperometric titration	25	Cu(II), g(I), NH_2Cl,ClO_2, NCl_3, H_2Cl
O-tolidine colorimetric	10	Br_2, ClO_2, I_2, MnO_4^-, NH_2Cl
O-tolidine-arsenite colorimetric	10	Br_2, ClO_2, I_2, MnO_4^-
Ferrous DPD titration	50	MnO_4^-, Cu(II), NH_2Cl
DPD colorimetric	50	MnO_4^-, Cu(II), NH_2Cl
Ultraviolet	100	MnO_4^-,I_2

Table 5.1 Classification of the methods used for the measurement of chlorine with their limit of detection and the interference species to which they are sensitive

mainly dissolved chlorine gas Cl_2, hypochlorous acid (HOCl) and hypochlorite ion (OCl^-) according to the following reactions:

$$Cl_2 + H_2O \longleftrightarrow Cl^- + HOCl + H^+ \qquad [5.1]$$

$$HOCl \longleftrightarrow H^+ + OCl^- \qquad [5.2]$$

Since protons e.g. H^+ are produced, this reaction is affected by the pH of the sample. Consequently, the direction of the reactions 5.1 and 5.2 is dictated by the pH of the liquid solution. For example, this effect can be used to convert chlorine present in the sample into any of the three forms depending on the situation e.g. pH can be decreased to clean the cell at the same time to convert chlorine into gaseous form e.g. Cl_2. Moreover, chlorine can be found in two different forms in the same sample at the same time. For instance, at pH value of 7, 50% of the chlorine present is as hypochlorous acid while the remaining 50% is in the hypochlorite form.

5.3.1 Chlorine Speciation

When the pH value of the liquid solution is lower than 3 all the chlorine present in the sample is in gaseous form, hence, the chlorine is dissolved as Cl_2 gas in the water sample. Provided that the solubility product is not exceeded*, the gas remains in solution. With

* *The maximum solubility of chlorine in water is reported to be 7.29g*

increasing concentrations of the hydroxyl ion (OH^-) i.e. the pH value, reaction 5.1 tends to shift towards the right producing more hypochlorous acid molecules (HOCl). The stochiometric relationship between chlorine and hypochlorous acid is 2:1 where one molecule of chlorine gas produces one molecule of HOCl. However, 75g of Cl_2 produces only 62g of HOCl while the chloride ion, a by-product of the reaction, is not considered because it is inactive. The 100% conversion of the chlorine gas into hypochlorous acid is complete at a pH value of 5. Further increase of the pH of the sample drives the second reaction towards the right. Hypochlorous acid is converted to hypochlorite ion (OCl^-) with a 1:1 stochiometric ratio. At a pH value higher than 9 all the chlorine present in the sample is in the form of hypochlorite ion. Consequently the chlorine speciation is tightly controlled by the pH of the solution as is shown in Fig.5.1.

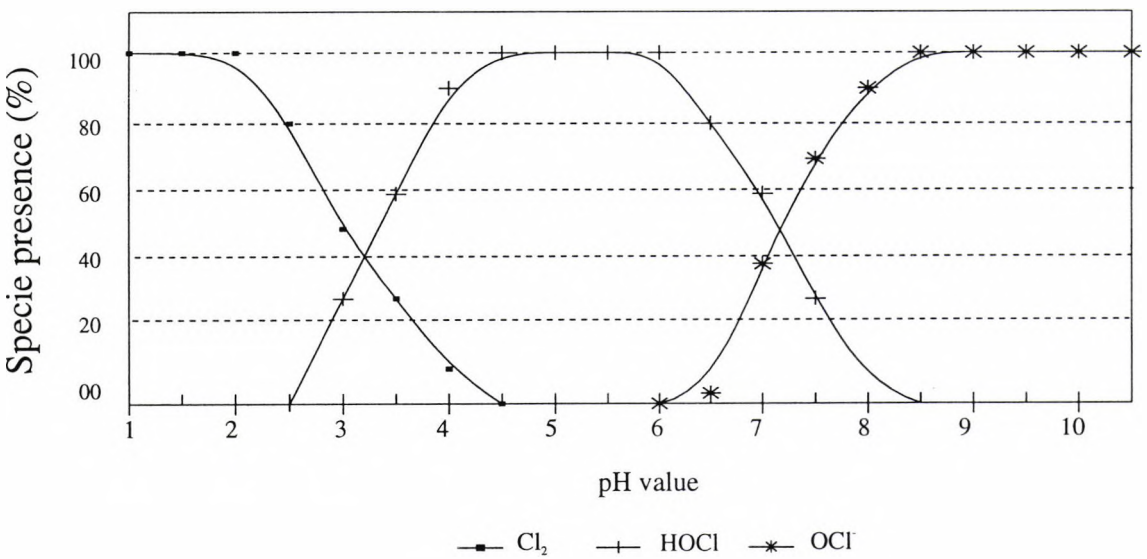

Fig. 5.1 Speciation of the chlorine present in distilled water as a function of pH

Note: The concentration of chlorine in a given sample is usually referred to in terms of the disinfecting power of Cl_2, however, the equivalence between the three forms of chlorine i.e. Cl_2, HOCl and OCl^-, is expressed according to their atomic weight. Hence, 70.9g Cl_2 is similar to 52.4g HOCl which is also similar to 51.4g OCl^-. Consequently, when the measurement is expressed as OCl^-, the value represents, in fact, half the value if the measurement was expressed as Cl_2. This is due to the fact that one atom of chlorine becomes inactive i.e. chloride ion (Cl^-), when the concentration is monitored through either HOCl or OCl^-[121]. All the measurements reported in this work have been expressed as hypochlorite ion concentration unless specifically stated otherwise.

5.3.2 External Influences

As in most chemical reactions, temperature is an important factor. Usually it affects the speed of the reaction as in the case of the reaction of chlorine with ammonia. when at an optimum pH value of 7 it takes 0.2 s for the complete reaction to occur at 25°C while five minutes are needed for the same reaction to be completed at a temperature of 0°C.

Chlorine in a sodium hypochlorite sample is greatly affected by temperature, light, pH, and the presence of metallic ions. Moreover, the degree of decomposition depends on the concentration of the solution i.e. the higher the concentration the faster the decomposition. The decomposition increases when the temperature is high and finally the presence of iron, nickel and copper increases the rate of decomposition. Ultraviolet light is known to speed the decomposition rate of chlorine further as it does with bacteria and living organisms. This was found during a study made in order to investigate the possible use of ultraviolet radiation as a mean of purification and sterilisation of drinking water avoiding the use of chlorine. The latter produces monochloramines when reacting with ammonia. Long contact times between the water to be processed and the UV light were needed to break down all the bacteria present. Furthermore, the use of UV radiation for purification could not prevent contamination of the drinking water while being transported in the water pipes. It was found that UV radiation cleaning on its own was not economically suitable. However, this process is used by some water companies as part of the water disinfection and purification processes.

The conditions for stable storage of sodium hypochlorite were found to be optimum at a strength of 10%, at a temperature of 21°C, with a concentration of iron, nickel and copper smaller than 0.5mg/l and storage in the dark. The temperature affects the conversion of one species into another. This can be seen from the data shown in Fig.5.2 where the conversion profile remains the same, the only difference being a shift along the pH axis. Any measurement carried out in the biological range i.e. pH values between 6 and 8, is prone to temperature effects and hence, temperature should be known in order to obtain accurate results. On the other hand, measurements conducted at a pH value of 5 or any pH value above 9 remain unaffected by the temperature change of the sample.

5.3.3 Photo-Decomposition of Chlorine

Chlorine is prone to dissociation under the strong radiation of ultraviolet light. Because the electromagnetic wave interacts with matter through an exchange of energy process at

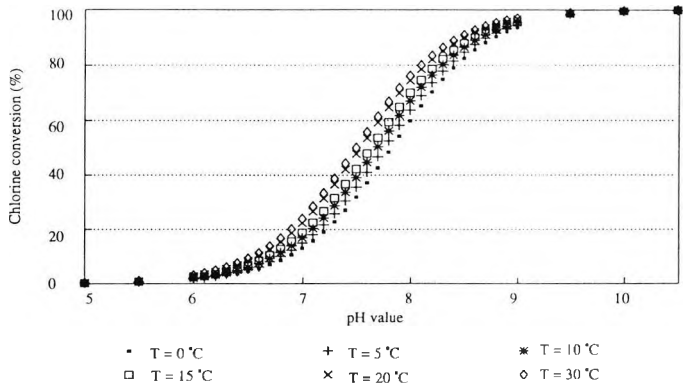

Fig. 5.2 Effect of temperature on the conversion rate of chlorine from HOCl into OCl^- form as a function of pH

high energy levels i.e. in the UV, this can lead to the dissociation of the molecule via a breaking of the bonds between the atoms concerned when the energy of the wave is higher than the energy of the bond. An analysis of the effect of UV light on the dissociation of chlorine has been performed and consisted in putting the same concentration of chlorine in a clear and coloured bottle. The result was as predicted; the chlorine contained in the clear bottle was reduced by between three and four times. Additionally, the higher the concentration the greater is the reduction in the chlorine concentration.

5.4 Optical Characteristics of Chlorine

The interaction of light with chlorine in all its forms occurs in the ultraviolet part of the spectrum only. No effects are seen in the visible or infrared regions. For each chlorine form, light absorption occurs at the peak of a broad bell shaped profile centred at a specific wavelength. Absorption of samples containing chlorine at three different pH values i.e. to produce Cl_2, HOCl and OCl^-, has been investigated by preparing a sample of distilled water to which various amounts of chlorine were added. A scan through the range of wavelengths from 200 to 350nm showed that in each of the three cases i.e. pH values, a similar absorption profile appeared. However, different peaks of absorption were found for each case and this was used to differentiate between the three species of chlorine. The peak of absorption for chlorine as Cl_2 was found to occur in the vicinity of 229nm when the pH value of the sample was 3 [16]. This appeared to be stable only for samples at low level concentrations of chlorine because at this pH value, chlorine escapes from the sample as gas. For a pH value of 5 most of the chlorine present in the sample is in the hypochlorous acid form and an absorption peak appeared at a wavelength of 233nm as is shown in Fig.5.3. When the pH of the sample was increased to the value of 9, the absorption of light occurred in the

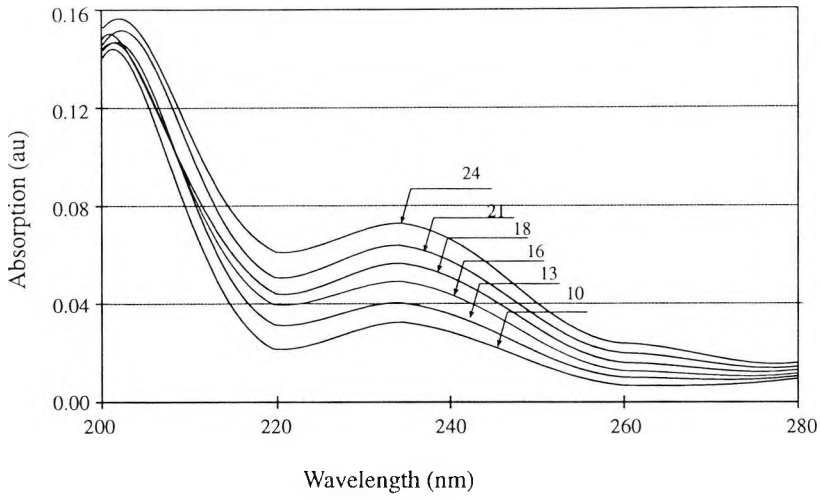

Fig. 5.3 Absorption of a water sample containing varying concentrations of chlorine (mg/l) at a pH value of 5

vicinity of 290nm and this was related to hypochlorite ion for a sample of chlorine in the range of 0 to 20 mg/l and is shown in Fig.5.4. The relationship between the light absorption and the concentration of chlorine in each case was found to be linear and as a result could be expressed mathematically as a function of a first order polynomial where the slope and the intercept represent the first derivative and the background absorption value. This is shown in the case of the hypochlorite ion in Fig.5.5 where the absorption of chlorine is represented as a linear variation of the concentration in the range of 0 to 20 mg/l.

It can be seen from Fig.5.6 that the absorptivity of each form of chlorine for the same chlorine concentration is different. It appears that the most absorbing form of chlorine occurs when chlorine is in the hypochlorite ion form. Additionally, the absorption peaks

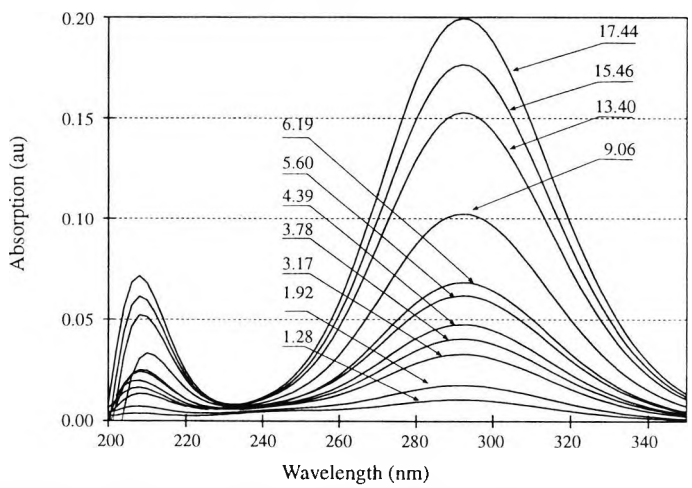

Fig. 5.4 Absorption spectra of a water sample containing varying concentrations of chlorine (mg/l) at a pH value of 10 and a pathlength of 1cm

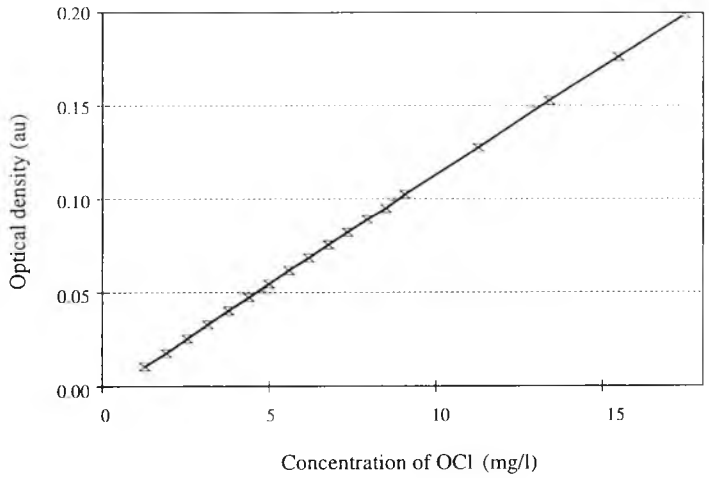

Fig. 5.5 Optical density variation as a function of chlorine concentration in the range of 0 to 20mg/l

of chlorine at pH values smaller than 9 are too close to each other e.g. the difference in wavelength is less than 4nm. The close proximity of the two absorption peaks makes the measurement of chlorine vulnerable to the effect of each peak on the other. Furthermore, the proximity of the strong absorption of nitrate ion can overlap the absorption of chlorine in this region. In this particular case the absorption of chlorine as hypochlorite ion can present some advantages since it occurs at a wavelength far removed from the absorption peak of the nitrate ion.

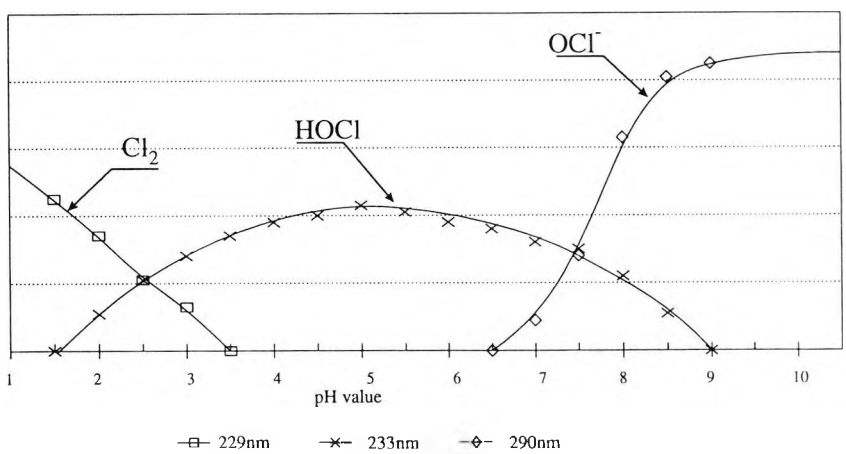

Fig. 5.6 Absorption coefficient of the three forms of chlorine as a function of pH

5.5 Optical Properties of Chlorine in Various Types of Water

Clearly, from the analysis carried out in the previous section, chlorine can be monitored using absorption techniques in the ultraviolet part of the spectrum in any of the three forms of chlorine i.e. Cl_2, HOCl or OCl^-, in samples made of distilled water. However, when

samples were made out of various types of water e.g. tap, swimming pool or pond water, interference from other species dissolved in the sample were affecting the measurement of chlorine. One of the most visible effects was caused by the strong peak of absorption of nitrate ion which occurred at 200nm. As a result, it covered the 200 to 240 nm region which made the monitoring of chlorine in the hypochlorous or gaseous form practically impossible in the region below 250nm. The only form of chlorine not affected by these interferences is the hypochlorite ion form. Consequently, analysis related to the absorption of chlorine in alkaline samples made of different water types has been carried out.

5.5.1 Tap Water

Tap water is an important type of water from which meaningful data can be obtained. Although tap water is processed water and most of the contaminants such as permanganate ion (MnO_4^-) and iodine (I_2) have been either reduced to the permissible level or completely removed, it still does contain chloramines, organic matter, various salts, and hardness. The latter is caused mainly by calcium and magnesium cations*. Hardness can cause a major problem, not in the measurement of chlorine as such, but because calcium and magnesium can precipitate at pH values higher than 10 [120]. The sample becomes opaque and light is scattered by the solid particles resulting in a large background absorption. This affects the transmission of light through the sample, hence introducing errors in the system.

A sample of tap water was first mixed with sodium hexametaphosphate $(NaPO_3)_6$ to hold in solution the cations present in the sample and prevent them from precipitating. The sample was then mixed with sodium hydroxide in order to increase the pH to a value of 10. Similar procedures to the one used for distilled water were applied and samples containing different chlorine concentrations in the range of 0 to 20mg/l were then obtained and scanned through the spectrophotometer. Their absorption spectra are shown in Fig.5.7 while the optical density plot with respect to the chlorine concentration is shown in Fig.5.8.

5.5.2 Swimming Pool Water

In this type of water, many organic elements are present in different forms and concentrations especially if the sample was collected after a heavy use of the swimming

* *A water having a hardness between 300 to 400mg/l is considered to be hard water and is found mainly in the south of England due to the nature of the layers of the soil*

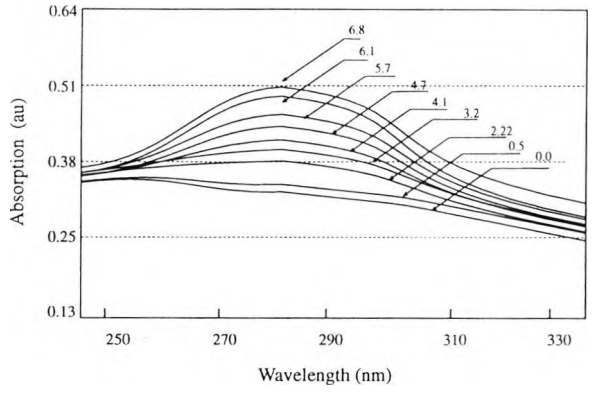

Fig. 5.7 Absorption spectra of a sample of tap water containing various concentrations of chlorine (mg/l)

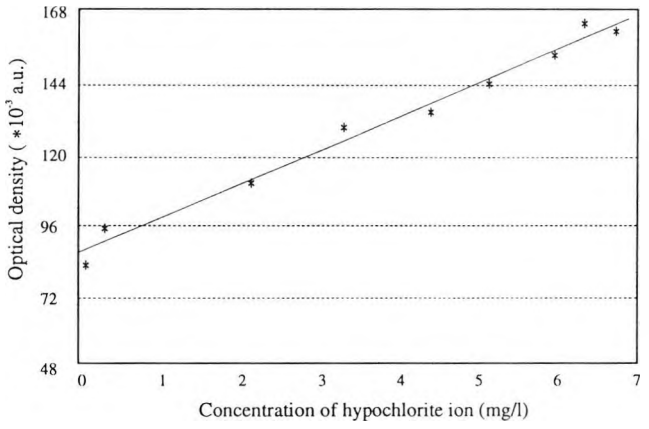

Fig. 5.8 Optical density as function of chlorine concentration in a sample of tap water

pool. Usually, it also contains chloramines since chlorine is mixed with the water for disinfection purposes. Hence, it represents a real life measurement situation. This sample was mixed with sodium hexametaphosphate (calgon) and sodium hydroxide to prevent precipitation and to increase the pH value of the water respectively. Then, appropriate volumes of chlorine were added and the sample was scanned in a 1cm path length optical cell. The profile of absorption of the sample is shown in Fig.5.9. while the linear relationship between optical density and chlorine concentration is shown in Fig.5.10.

5.5.3 Pond Water

Pond water provided a good background for water types that are not processed and which are full of organic matter generated by the algae and fish living in a closed system. After

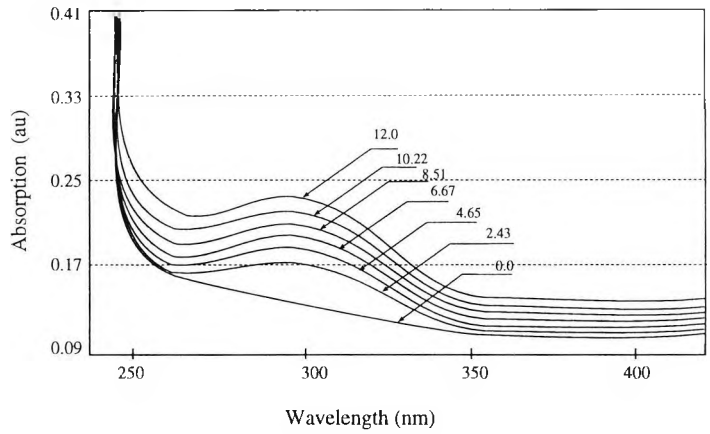

Fig. 5.9 Absorption spectra of a sample of swimming pool water mixed with various concentrations of chlorine (mg/l)

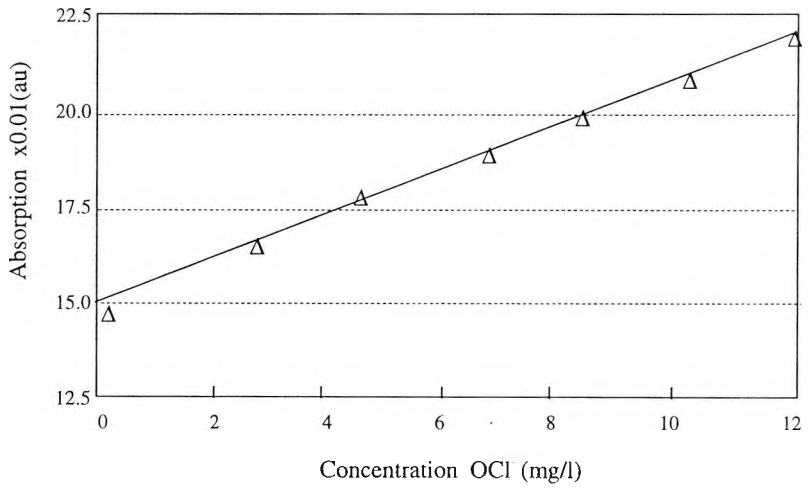

Fig .5.10 Graph showing the relationship between the optical density and chlorine concentration in the range of 0 to 12mg/l for a sample of swimming pool water

addition of reagent to increase the pH of the sample different doses of chlorine were mixed to provide the required chlorine concentrations in the range of interest e.g. 0 to 20mg/l. The sample was prepared beforehand so that the chlorine demand was satisfied. The absorption spectra of the sample are shown in Fig.5.11. The background absorption of pond water is higher than that of tap water and results from the presence of organic matter. This has an absorption profile which is high in the sub-250nm and a long 'tail'-like extension into the visible region of the spectrum. As a result of the variation of the background absorption in different types of water samples and origins, a reference measurement is necessary to compensate for errors which would otherwise be attributed to chlorine absorption.

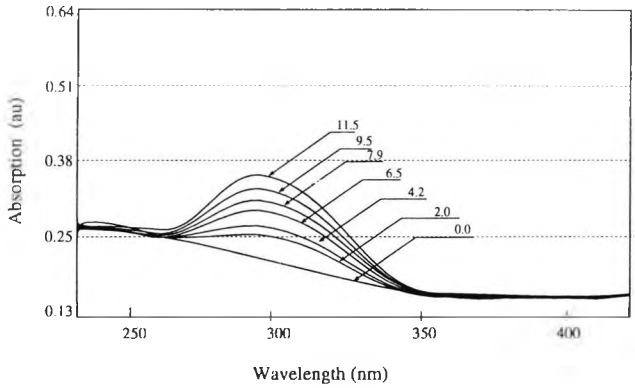

Fig 5.11 Absorption spectra of a sample of pond water containing different chlorine concentrations (mg/l)

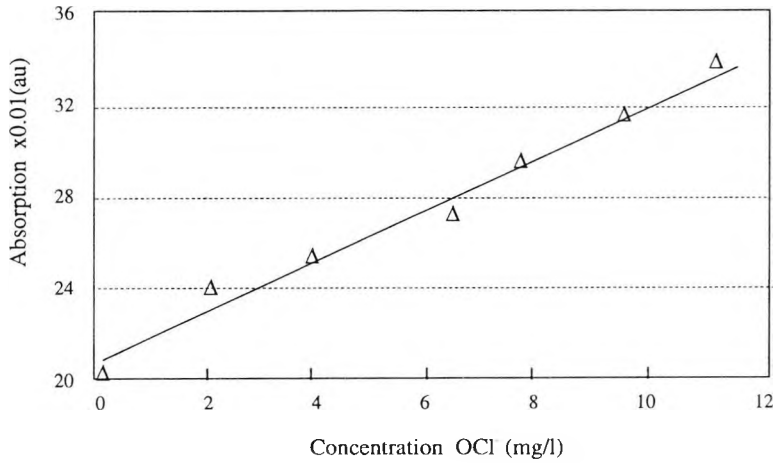

Fig 5.12 Optical desnity as a function of chlorine concentration in the range of 0 to 12 mg/l in a sample of pond water

5.6 Measurement of Total Chlorine (Residual and Combined)

Chlorine reacts with potassium iodide to liberate a molecule of iodine (I_2) and similarly with potassium bromine (Br_2) according to reactions [5.3] and [5.4].

$$2KI + HOCl \longleftrightarrow 2K^{+} + OH^{-} + I_2 + Cl^{-} \qquad [5.3]$$

$$2KBr + HOCl \longleftrightarrow 2K^{+} + OH^{-} + Br_2 + Cl^{-} \qquad [5.4]$$

The spectral analysis of iodine in the ultraviolet and visible part of the spectrum shows that a multitude of absorption peaks increasing in intensity towards the lower wavelengths can be found in the 400 to 200nm area. One of these peaks corresponds to the absorption of hypochlorite ion i.e. 290nm, hence permitting the use of the same wavelength for monitoring the absorption of both the hypochlorite and the iodine molecules giving a measure of their concentrations. It was also found that the absorption of iodine does not

occur in alkaline samples. The peak of absorption of iodine which is very intense can only appear in a sample which has already been made slightly acid e.g. pH value of 5. The remarkable sensitivity achieved with this type of detection of chlorine is shown in Fig.5.13. It has to be noticed that reaction [5.3] applies also to combined chlorine i.e. chlorine which had reacted with ammonia to produce chloramines. Hence this method cannot be used to measure the free residual chlorine content of a sample since it does not distinguish between free and combined chlorine and therefore can only be used where measurement of the total concentration of chlorine in its various forms is needed. In the case of bromine although the chemical reaction with chlorine is similar to that with iodine, the resultant bromine molecules which are released from potassium bromide have different optical properties from the ones observed with iodine. The peak of absorption of bromine occurs at a wavelength of 270nm in an acid sample. Since the peak of absorption of bromine and hypochlorite do not coincide, it would be more difficult to include the measurement of combined chlorine as part of the same optical set-up. On the other hand, this can be achieved very simply in the case of iodine. A minor step which consists of adding a reagent of acid and potassium iodide to the sample allows measurement of the total chlorine concentration in the sample without any modification to the optical or electronic set-up.

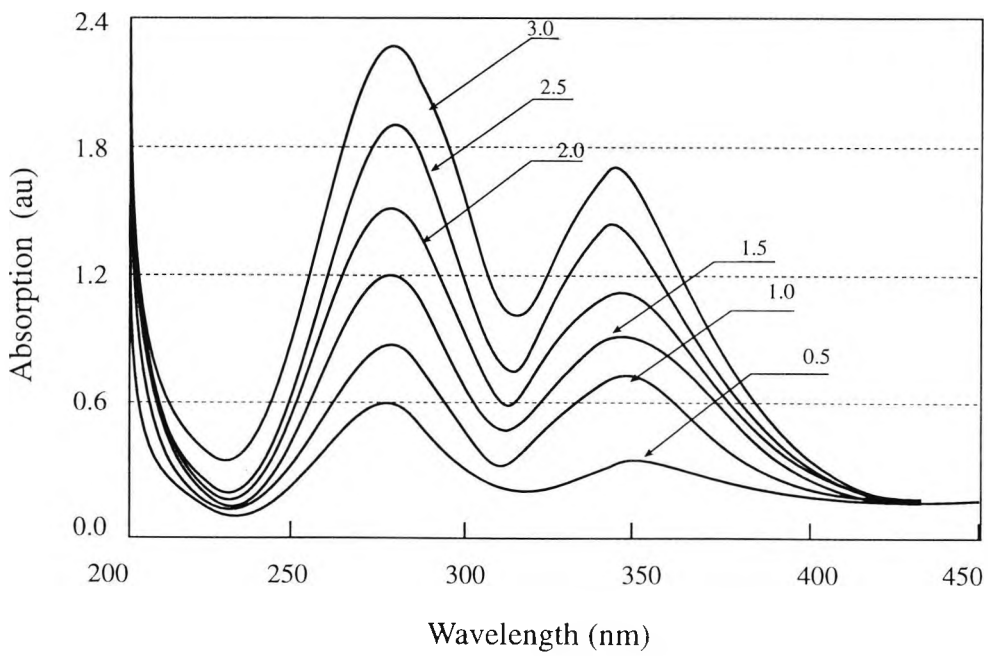

Fig. 5.13 Absorption profile of iodine liberated from potassium iodide by different concentrations of chlorine (mg/l)

5.7 Reference Information

From the study of the absorption profile of the different water types which was carried out in the previous sections, it can be concluded that the residual chlorine in these samples can be monitored as the hypochlorite ion when the pH of the sample is increased to a value of 10. For all the above experiments the type of water used was different and this was reflected in the value of the intercept of each equation hence showing that there is a shift in the background absorption for each sample. As a result, a method of providing a measure of the background absorption is needed. This way, the information concerning the chlorine concentration present in the sample is complete and remains unaffected by the sample background.

There are several ways of obtaining the information related to the background absorption value which can be either of a chemical nature or of a spectral nature summarised in the following:

5.7.1 Chemical

The chemical conversion of chlorine into a non-absorbing form is summarised in the following: conversion, chemical removal and ion exchange removal.

5.7.1.1 Chlorine Conversion

The reaction of chlorine with water was shown to be affected by the pH of the sample. Hence, by varying the pH of the solution, chlorine as hypochlorite ion can be converted into a non absorbing form (in the 290nm region) by decreasing the pH value of the sample. It was previously shown that this method of referencing was used successfully with samples made from distilled water [27]. However, this shift in the sample pH was likely to introduce shifts of the baseline of the absorption which could be caused by the variation in the absorption of different species present in the water sample due to the pH change. Hence this method of referencing was discarded.

5.7.1.2 Chemical Removal of Chlorine

There are various chemical reagents with which chlorine reacts to produce chemical species that do not absorb in the vicinity of the wavelength of 290nm, since chlorine is a very powerful oxidising agent. Chlorine is removed by reacting with Ethylene Diamine Tetra Acetic acid (EDTA). Additionally, it is practical to use because it decreases the pH of the

sample hence allowing for cleaning of the optical cell however, it is an expensive reagent. In contrast, Sodium sulphite (Na_2SO_3) reacts with chlorine to produce sodium sulphate and chloride ion as is described in Equation 5.6

$$Na_2SO_3 + NaOCl \rightarrow Na_2SO_4 + NaCl \qquad [5.6]$$

Sodium sulphate has a flat absorption in the area of interest (250nm to visible) and consequently is unlikely to change the baseline absorption. Additionally, the pH of the liquid reagent is alkaline and does not interfere in the absorption spectra.

5.7.1.3 Removal by Ion Exchange Resin

Various ion exchange resins can be used to remove chlorine from the sample by exchanging the ions. For example one particular ion exchange resin removes the hypochlorite ion from the sample by exchanging it with sodium ions. However the use of these types of resins results in the removal of other ions present in the sample which contribute to the total background absorption. Hence, the obtained absorption value, after the passage of the sample through the resin, does not represent a true measurement of the background absorption. This would lead to errors in the calculation of the residual chlorine concentration present in the water sample. Resin could not be used, although it provided a means for removing chlorine from the sample solution, it also removed the background information.

5.7.2 Spectral

This method which is reagentless presents some attractive points. These consist of monitoring a single or a range of wavelengths which are not affected by the varying absorption levels of chlorine on either side of the main peak of absorption but would still provide the reference information. Furthermore, the reference wavelength could be generated from the same light source, hence eliminating the need for monitoring the light intensity fluctuations. In this method the background absorption value at the reference wavelength is assumed to be the same as the one at the sample absorption wavelength. However, this is only valid under the condition that the background absorption is flat over the reference and sample absorption range of wavelengths.

One of the drawbacks of this technique is the requirement for a complex and usually expensive optical set-up. It can consist of a continuous spectrum light source and a filtering

system from which the required wavelength can be separated from the rest. This can be obtained by using a grating system or optical filters.

5.8 Basis for Implementation

The design of an on-line fibre optic based residual chlorine monitor relies on the construction of three separate blocks as is shown in Fig.5.14.

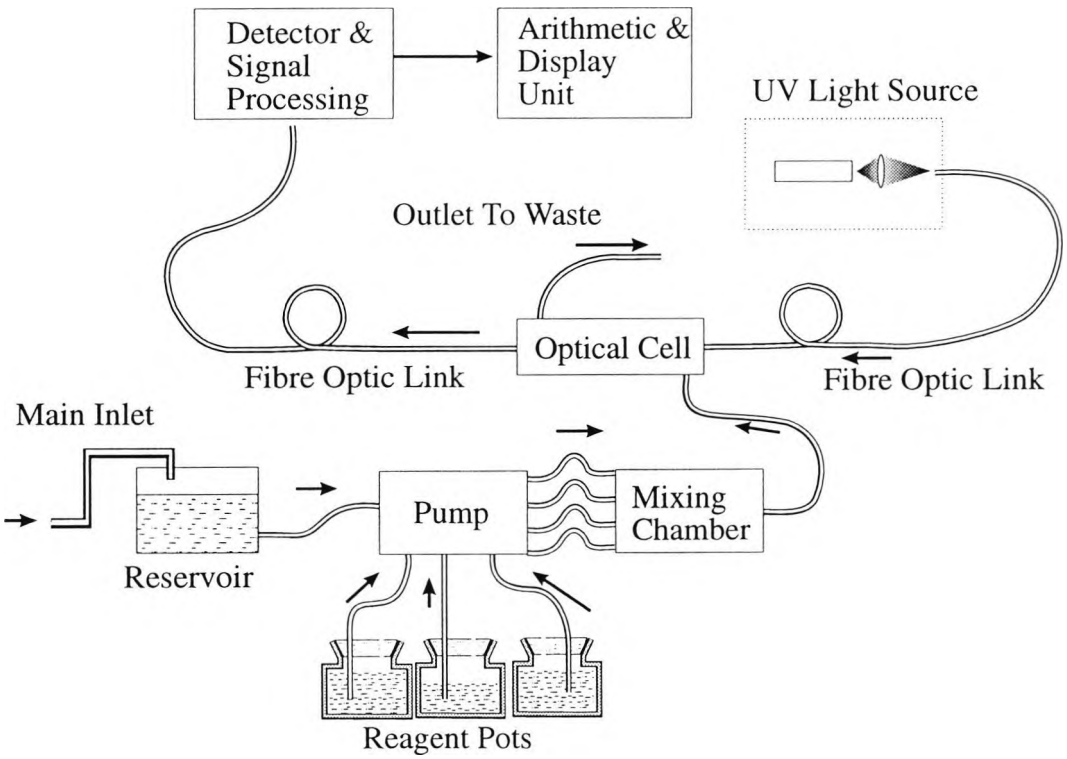

Fig. 5.14 Diagram of the proposed set-up for the design of the continuous monitoring system for the measurement of residual chlorine

5.8.1 Optical section

The first block which includes the optical arrangement would consist of the light source, optical cell and a fibre link. The latter is used to guide the light from the light source into the optical cell and a second fibre link transmits the light collected from the optical cell to the electronic detector.

For this particular application where the sensing wavelength is 290nm a simple way of generating this wavelength comprises the use of a low pressure mercury discharge lamp. This, however, is coated with a special phosphor that converts the 254nm into 290nm. This

type of lamps is readily available at a low cost. A pass band optical filter should be used in order to reject the different lines that are generated inherently with the same process otherwise, errors are introduced when using the Beer-Lambert law.

Alternatively, a continuous spectrum emission light source can be used e.g. deuterium lamp. This type of light sources has a high light emission in the ultraviolet part of the spectrum and is considered to be almost a point source which is compatible with a fibre optic system. Unfortunately, these lamps require a grating system to separate the needed wavelength from the emitted continuous spectrum or an absorption type optical filter. This can only increase the cost of such a device beside the restricted lifetime of the lamp.

Finally, the optical cell can have two configurations depending on whether the sample and the reference are obtained simultaneously or in parallel. A schematic diagram shown in Fig.5.15 depicts the set-up of the approach where the sample conditionning is carried out in a parallel and both conditionned samples are available at the same time.

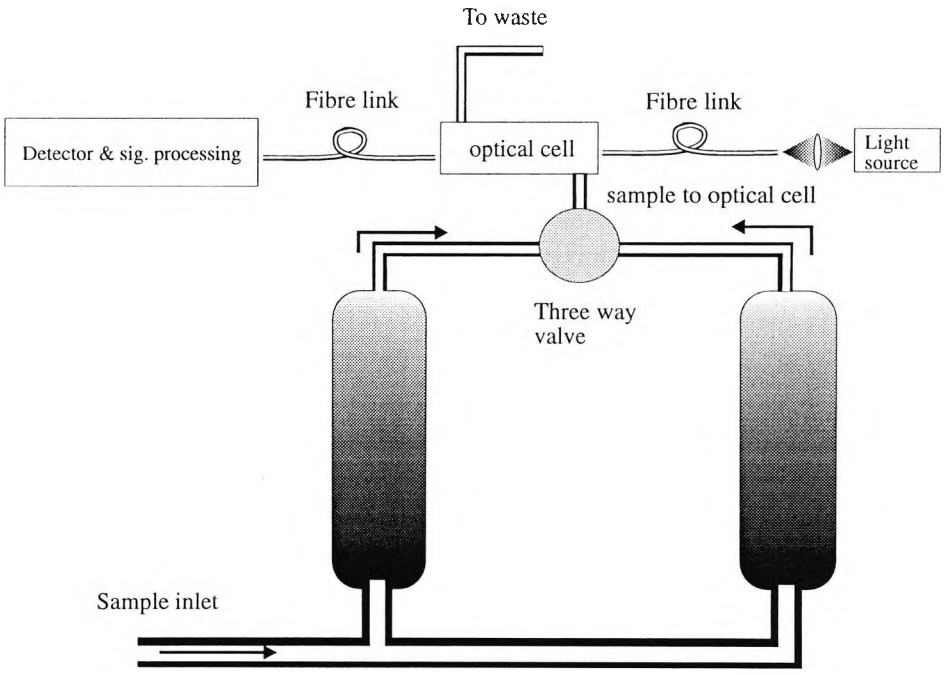

Fig. 5.15 Alternative set-up for an on-line residual chlorine monitor using parallel approach for the measurement of the absorption and the reference signals

In the first option where the sample is driven through two different paths, one providing the reference conditioning while through the second path a different conditioning is applied to the sample to monitor the absorption of chlorine. Hence, the two data are present at the same time which is convenient since it provides a shorter response time. Nonetheless, this set-up requires the duplication of most of the optical and electrical components which can

be a source of problems when the sample is affected differently through the two paths.

In contrast, the second set-up provides a single path and a single electronic set-up for the measurement of the absorption and the reference signals. This has the advantage of using fewer optical and electrical components and any effect occurring during a measurement session affects both the reference and the absorption signals. One drawback of this system, consists in the longer response time since the measurement is carried out sequentially

5.8.2 Mechanical Section

The second block is made of the mechanical pump and the valves. The pump is used to draw volumes of the sample and to pump the reagent if a liquid reagent is used. These are mixed in the static mixing chamber, thus a high flow rate is required so that the mixing is carried out efficiently. Once the sample is conditioned, it is directed towards the optical cell. The valves are used to direct the reagents into the mixing chamber when they are needed and back to their containers for the rest of the time. In the case of solid reagents, two columns can be used through which the sample is pushed. However, a longer contact time results.

5.8.3 Electronic and Electrical Section

The third part which contains the electronic and electrical components comprises the power supply module for the electronic and the ultraviolet lamp. The electronic circuit provides all the control signals which are used to activate the pump, the valves and the rest of the electrical components. The detector converts the optical signal into an electrical signal, then a signal processing stage removes the unwanted interferences. A suitable arithmetic section computes the ratio of the two signals i.e. reference and absorption signals and a display unit can be incorporated to produce a means of displaying the result of the measurement.

5.8.4 Solid Reagent

An alternative method for sample conditioning consists of putting solid reagents in the passage of the water sample. This dissolves the solid reagents which are made in the form of beads and consequently alter the pH of the sample. The implementation of such a system would have reduced the severity of maintenance problems and hence would have resulted in lowering the running costs facing the water industry. The solid reagent could be used to

increase the pH of the sample or to lower it.

The solid reagent is made of a slow release glass in the form of small spheres of an average diameter of 1 to 2mm across. Their chemical composition includes phosphate or borate glasses doped conveniently to adjust the pH value of the sample. These reagents were packed in a primary cylindrical tube in which a concentric secondary tube of a smaller diameter allows the water sample to flow through. The direction of the flow was made so that the sample enters the secondary tube through the bottom and is reflected providing equal spread of the sample over the beads. as is shown in Fig.5.16. It was then collected from the bottom side of the primary tube.

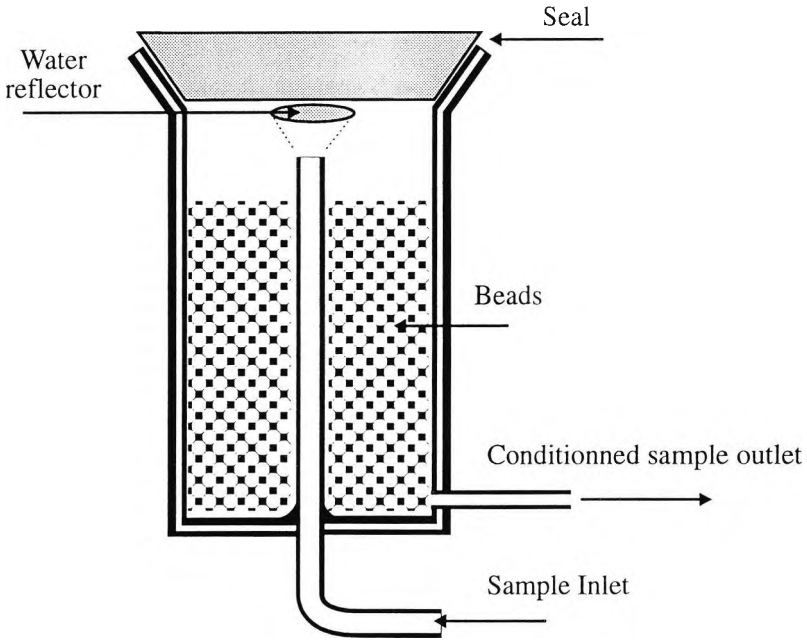

Fig. 5.16 Schematic diagram of the possible use of solid reagent for sample conditioning.

It was found that by reducing the flow of the distilled water to a few ml per minute the pH of the sample was increased to a value of 9, initially the pH value of the sample was 7. Different water samples were then used. The first volumes of each experiment showed that there was a small increase of the pH value, however this did not last long. It was found later that the calcium present in the water sample reacted with the soluble glass and created a non porous layer around the bead which acted as an isolant. This prevented further soluble glass to be in physical contact with the water sample and thus the pH value of the sample remained constant. As a result the work on the test of the beads as a mean of conditioning the sample was discarded.

5.9 Conclusion

In this chapter a detailed analysis of the interaction of light in the ultraviolet part of the spectrum with chlorine dissolved in water was made. It was shown that the hypochlorite ion which results from the reaction of chlorine with water when the latter is at a pH value 9 absorbs at a wavelength of 290nm and has a higher absorption profile when compared to hypochlorous acid or chlorine as gas. This wavelength which can be generated using a discharge lamp is well suited for the direct measurement of chlorine because it is far removed from the absorption peak of the nitrate ion which can otherwise result in large errors in the measurement. Additionally, it was shown that combined chlorine can also be measured at the same wavelength i.e. 290nm, when the sample was mixed with a solution of potassium iodide and hence can result in the use of the same optical, electrical and mechanical set-up for the measurement of both species. It was established that the energy level of the light source was low and would affect the concentration of chlorine already present in the sample. Temperature was shown not to affect the conversion of any form of chlorine into hypochlorite ion when the pH value of the sample was larger than 9. The analysis of the absorption of chlorine in various types of water was assessed in order to determine the effect of interfering species and was found to be negligible.

Different schemes for monitoring the background absorption were investigated and it was shown that chemical removal of chlorine by the sodium sulphite would provide an inexpensive and effective way of providing the reference information necessary for the correction of the effects of the interfering species. Finally, a different set-up for the design of an on-line system was discussed and various schemes of sample conditioning were investigated and their advantages and drawbacks discussed.

Chapter 6

Design of a Single Wavelength Self-referencing Residual Chlorine Monitor

Abstract

A prototype for the measurement of chlorine as hypochlorite ion OCl^- is described in this chapter. It is based on monitoring the absorption of light at the wavelength of 290nm by measuring the transmitted light intensity before and after the hypochlorite ion was removed, thus providing a reference measurement at the same wavelength as the measuring wavelength. Optical fibres were used to guide the light from the light source to the probe head and back to the detector.

The design of the Residual Chlorine Monitor (RCM) was aimed at complying with a Water Research Centre (WRC) specification regarding response time and resolution (i.e. 20s response time and a range of measurement of 0 to 1mg/l residual chlorine). In addition a 30 days maintenance-free requirement was also included in the design of the RCM.

The Residual Chlorine Monitor was provided with compensation for background absorbance and the usual sources of error (i.e. drift in the output of the lamp, variation in the fibre transmission etc.). This was achieved by measuring the absorption of the sample at the same wavelength after adding sodium sulphite to destroy OCl^-. The ratio of the absorbing and reference signals was then computed using analogue circuitry and then displayed with an incorporated digital volt meter.

A precision of 100 µg/l OCl^- has been achieved. The measurement range of this instrument can be varied from 1mg/l full scale to greater than 20mg/l full scale with appropriate changes in reagent concentrations. A stability of ±3% was reached for testing periods over 48 hours. Final conclusions and recommendations are given at the end of this chapter. A prototype, built to the water industry standards, has been completed and calibrated for use on different types of water[122].

6.1 Design Considerations of an On-Line Residual Chlorine Monitor

On-line measurement requires continuous sampling of data. The time between each measurement depends on the nature of the measurement to be made. In some applications it is necessary to measure and update the value of a particular measurand in a short period of time (i.e. 10 to 60 seconds). This is shown in the measurement of the chlorine content in drinking water at a distribution point of a water treatment plant. In other situations the rate of data sampling was slower because the process itself was slow. This could be seen in the superchlorination unit where organic ammonia is reduced to nitrogen. This reaction is slow and therefore does not require frequent measurement.

The Water Research Centre (WRC) has produced a specification for residual chlorine monitors on which the design of the on-line monitor was based following these criteria:

a) The response time of the monitor should not be longer than 20 seconds to achieve 90% of a step change and this should include the reference measurement also.

b) The monitor should be provided with a communication port for data, control and signal errors and malfunctions for interfacing with a remote control station. It could in the future be included as a part of a set of monitors for measurement of different parameters monitored by the same station.

c) The monitor should not require attention or supervision apart from replacement of components or reagents. The WRC specification in respect of this, is for a service interval of at least 30 days.

For these reasons the monitor design should include:

1) A pump to pump the sample into the optical cell and a control of the flow.

2) A set of valves to direct the reagents to the mixing chamber at the appropriate times.

3) Complete isolation of the electrical and electronic parts of the monitor from the liquid handling section. (this could be achieved by using optical fibres to guide the light to and from the cell).

4) Generation of all the control signals to operate the different parts of the monitor i.e. to pump the sample, mix it with reagents, measure and store the data, repeat the process with a different reagent, compute the ratio and then display the resulting data. In addition it should be able to detect malfunctions such as air bubbles in the system and irregular

attenuation of the measured signal such as that caused by deposition of calcium and magnesium or formation of algae on the sample cell walls thus reducing the light transmission. Fig.6.1. is a schematic representation of the front view of the residual chlorine monitor

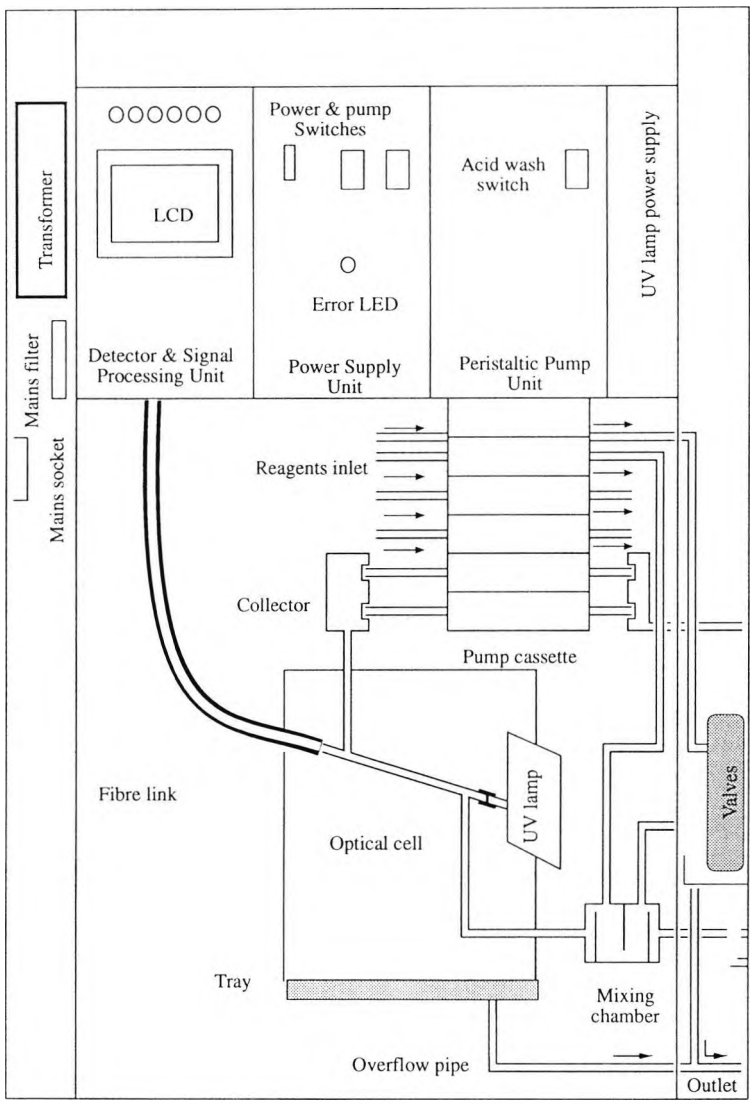

Fig. 6.1 Front representation of the Residual Chlorine Monitor (RCM) unit.

6.2 Referencing Scheme

Intensity based measurements are very sensitive to external effects. These appear as errors in the measurement system and are reflected as a change in the output signal related to the measurand. If no particular precautions are taken to reduce their effect, correcting the final measurement would be a rather difficult task.

These potential errors can be classified as random and systematic. The random nature of

an error can be seen in its uncorrelated aspect with the signal under investigation. Because of this nature, only statistical analysis can be used for minimisation of the errors.

Systematic errors are the ones that can be to a certain extent predicted. Such errors are generated in the system because of a specific effect e.g. temperature variations, drift of electronics etc. Variations in the light source intensity output can be regarded as specific and a compensation can be easily achieved. This is possible by measuring the ratio of the main signal to the reference signal provided that the variation in the signal is slow compared to the frequency of the measurements. Hence, any change of the related measurement other than that generated by measurand is then compensated for.

There were different ways of obtaining the background measurement using a single wavelength measurement and these are discussed in chapter 5. However, the solution adopted in this implementation is based on the fact that sodium sulphite does not absorb in the UV and does not change the background absorption. Additionally the cost was significantly less when compared with EDTA. This type of referencing is preferred although it requires the use of chemical reagents. An additional advantage in using this mode of referencing lies in the simplicity of the set up needed to carry out the measurement. Sodium Sulphite (Na_2SO_3), reduces the chlorine element to chloride and converts sodium sulphite into sodium sulphate. The latter is completely transparent to ultraviolet and does not affect any element that might have an absorbing spectrum in the vicinity of 290nm. Additionally the pH of the sample can be then maintained at a constant value of 10. In this way any effect of change in the pH of the sample is maintained constant during both cycles (reference and absorption). The only drawback to using sodium sulphite was that the reaction of the latter with oxygen present in the air transformed the sulphite into sulphate and thus the reduction of hypochlorite ion would not occur. However, only the surface of the reagent in contact with the air would react with oxygen.

To prevent oxygen present in the surrounding air being in contact with the reagent, an air filter consisting of a small pot filled with a highly concentrated sodium sulphite solution was used. The incoming air was directed through this solution stripping it of oxygen. Hence the volume of sodium sulphite displaced in the reagent pot would be replaced by air which did not contain any oxygen. For a period of one month the volume of reagent needed was calculated to be 12 litres. Hence the same volume of air would be filtered through a highly concentrated sodium sulphite solution. This is shown in Fig.6.2

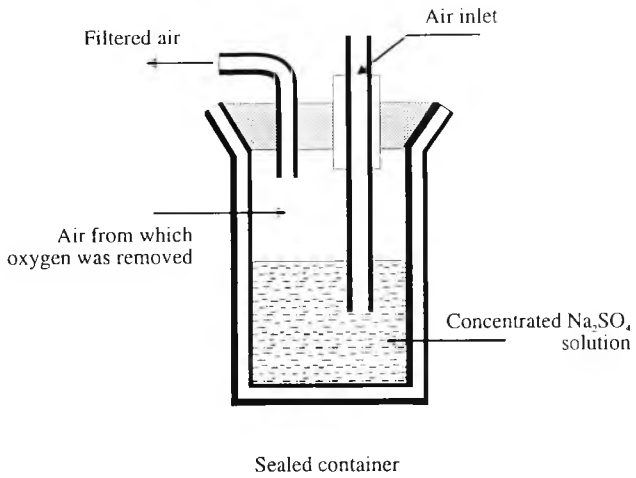

Fig. 6.2 Schematic diagram of the reagent protection system for sodium sulphite.

6.3 The description of the chlorine monitor

The chlorine monitor consists of three main systems optical, mechanical and electrical.

6.3.1 Optical System

The optical system consisted of a UV lamp and optical fibres to guide the light to and from the cell, and an optical cell. The optical cell was manufactured from Pyrex glass and fitted with inlet and outlet tubes. To help keep the system bubble-free, the cell was inclined at an angle of 30° to the horizontal.

6.3.1.1 Light Source

A single wavelength of a bandwidth of no more than ±10 nm was needed for monitoring of the absorption of chlorine at a central peak of absorption situated at a wavelength of 290nm. In addition a requirement of long life expectancy of the light source i.e. at least more than 1 year when used continuously, was a determining factor in the choice of the light source. A deuterium lamp which would have been an acceptable choice required a powerful and stable power supply (90V at 300mA). In addition the life expectancy of such a light source was given by most manufacturers as being in the order of 1000 Hours. This was found to be very short and inadequate for the purpose of monitoring the chlorine concentration on a continuous basis. Another drawback of this type of lamp consisted in the inadequacy of an electronic modulation of the light for subsequent discrimination against noise and ambient interference even though a mechanical chopper could be used.

The latter option would not have allowed efficient coupling of light through the fibre. Other types of UV light lamps were discarded for the same reasons. On the other hand, low pressure mercury lamps have a line emission spectrum but unfortunately none of these lines corresponded to the 290nm required. However, the long life expectancy (over 10000 hours), the power consumption (less than 6W) and small size of the mercury lamp suited this application particularly well. Moreover, the main line emission at 254nm was used to excite a phosphor which coated the lamp glass to generate the 290nm needed for the monitoring of the hypochlorite ion. Although most of the energy contained in the intense 254nm line was used to convert light from 254nm into the 290nm a small percentage of the original line emission was still available. The ratio of the former to the intensity of the 290nm was found to be small and was not considered to cause major problems. Beside these two wavelengths, other lines were generated as part of the mercury discharge process. Furthermore some additional lines were also generated by the metal electrodes. An optical analysis of the wavelength spectrum of the lamp output revealed however that it contained at least 12 peaks. The most energetic of these was at a wavelength of 290nm, and accounted for almost 90% of the optical power. The output of the phosphor coated lamp is shown in Fig.6.3. In addition to the 254nm and 290nm peaks, emissions at higher wavelengths were also present but their energy content was found to be small compared to that at 290nm. Even so the presence of these peaks could give rise to a significant error because the sensitivity of the UV enhanced diode detector was found to be higher in the visible and infrared than it was in the UV. Consequently a large fraction of the detected signal which consisted of unwanted optical frequencies containing no useful information was present in

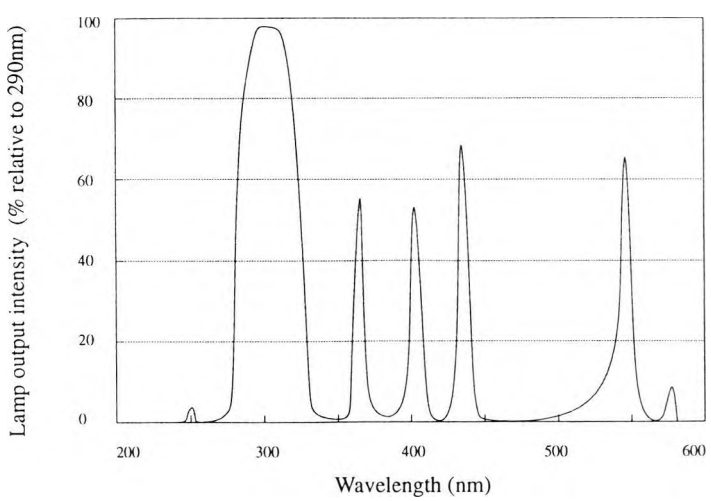

Fig. 6.3 Mercury light source output spectrum when coated with phosphor

the detected signal. Hence a narrow bandpass interference filter was used to eliminate these unwanted optical frequencies. The total power of this lamp was specified by the manufacturer to be 3mW (Jelight Company Inc.).

6.3.1.2 Power Supply for the UV Lamp

A dc to ac converter was used to supply the lamp with sinusoidal power (0.6kV at 20mA) oscillating at a frequency of 29kHz. The power supply was modulated at a frequency which was different from the mains and lighting frequencies (50 and 100Hz) making the measurand signal separable from such interferences. During tests, the unit has proved to be stable after a warm up time of 30 minutes. During this warm-up time, the frequency of the power supply varied by 0.75kHz and then remained substantially constant thereafter. However the lamp output intensity varied rapidly during the first 10 minutes but then over a period of 200 minutes it decreased slowly as is shown in Fig.6.4. The monitor was operational before total stabilisation of the light output was reached. The reason for this was that the variation of light intensity output after the first 10 minutes was so slow that between two consecutive cycles which took only 20s, the error due to this effect was considered to be negligible.

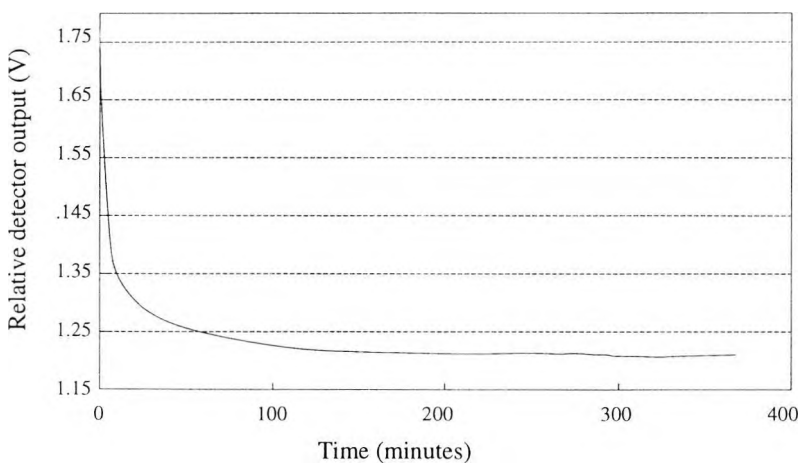

Fig. 6.4 Response of the mercury light source intensity as a function of time

6.3.1.3 Optical Cell

The optical cell was made of a cylindrical hollow Pyrex glass tube. The glass thickness was 2mm and the internal diameter of the glass tube was 3mm. The length of the optical cell i.e. the distance between the two fibre ends, was dictated by three factors:

1) An increase in the path length of the cell where the light beam travelled resulted in an increase in the absorption and hence provided a more sensitive measurement. By using the Beer-Lambert law, the increase in absorption can be seen through Eq. [6.2]

$$Log\frac{p_1}{p_o} = -\varepsilon C l_1 = -A_1 \quad \text{and} \quad Log\frac{p_2}{p_o} = -\varepsilon C l_2 = -A_2$$

$$\text{Then } A_2 = A_1 \frac{l_2}{l_1} \qquad [6.2]$$

For the same concentration C, it was found that increasing the path length by a factor of two i.e. $l_2 = 2l_1$ resulted in doubling the absorption value. Hence the longer the path length the more sensitive the measurement became.

2) The light emerging from the fibre diverges as a result of the propagation of the light through the fibre. Only the rays making an angle smaller than the one defined by the numerical aperture propagated and the rest of the beam rays were lost through the cladding. However, the angle of divergence is smaller for a glass-water interface than it is for glass-air since the index of refraction of the water is larger than the index of refraction of air. This spread of light caused the collecting fibre positioned at a distance from the emitting fibre, to receive an inferior amount of light and hence a weaker optical signal was guided through the fibre into the detector as shown in Fig.6.5.

3) The response time of the chlorine monitor for a complete measurement i.e. absorption and reference measurements, was set to 20s. Hence a 10s time was allocated to each cycle. During this time , the sample is drawn from the reservoir into the mixing chamber and then filled the optical cell. Because of the small volume of the optical cell, it

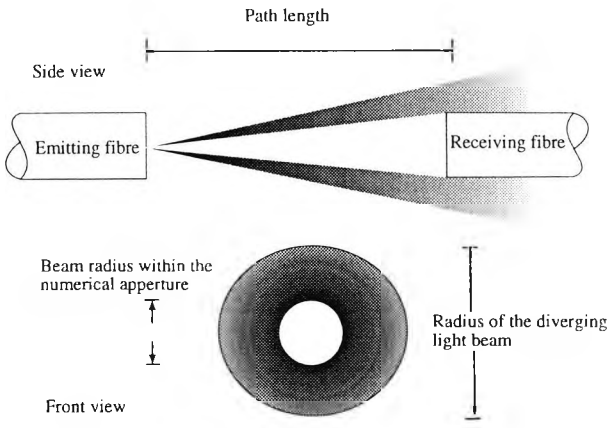

Fig. 6.5 Schematic diagram of the light divergence in the optical cell

represented only a smaller portion of the sample volume. The volume of the optical cell was calculated as a function of the path length L to be $\pi(d/2)^2 L \sim 7L$ (mm^3 for L in mm). Although the time needed to fill the optical cell was a function of the path length of the cell, it did not affect it very much. As an example, with a flow rate of 67ml/min and with a 10 cm path length only 0.7s were needed and for a 20cm path length approximately 1.4s were sufficient to fill the cell with the sample while it would take about 7 seconds to fill the path from the inlet to the mixing chamber.

Adequate light intensity reaching the detector was obtained with a path length of 150mm. A signal to noise ratio obtained with an optical cell of 150mm length was measured to be approximately 30dB. This was slightly higher when distilled water was used. The volume of the cell was then 1.05ml. With a flow rate of 67ml/min approximately one second was needed to fill the optical cell with the sample and the period of each cycle i.e. for the sample entering the instrument via the inlet connector till the moment the cell was completely filled, was measured to be 8s.

The length of the main cylinder was 200mm. The remaining 25mm on each side end were used to hold the fibre ferrules for the purpose of aligning the fibres inside the optical cell. These were concentric within the cell. On each side of the main cylinder and at 25mm from the end, sample inlet and outlet tubes made of Pyrex glass were positioned at an angle of approximately 45° with respect to the optical cell. This angle of inlet was found to reduce the effect of air bubbles trapped inside the cell at the fibre side. The flow of the sample then forced the air bubble to move along the cell as opposed to the effect of the flow on the air bubble when the angle of input was 90° as is shown in Fig.6.6.

The ferrules holding the fibres were made out of two concentric metallic tubes to provide mechanical strength mainly to reduce the vibration effect on the fibre and also to reduce the effect of air bubbles when trapped inside the cell. When the light collecting fibre protruded and an air bubble was trapped between the fibre and the cell wall, the effect of the air bubble was minimal compared to the situation where the air bubble was trapped in front of the fibre face reducing the light transmission through the fibre.

6.3.1.4 Fibre

To guide the light from the lamp into the optical cell, a Plastic Clad Silica (PCS) fibre was used. The glass material was made of pure quartz which has good transmission

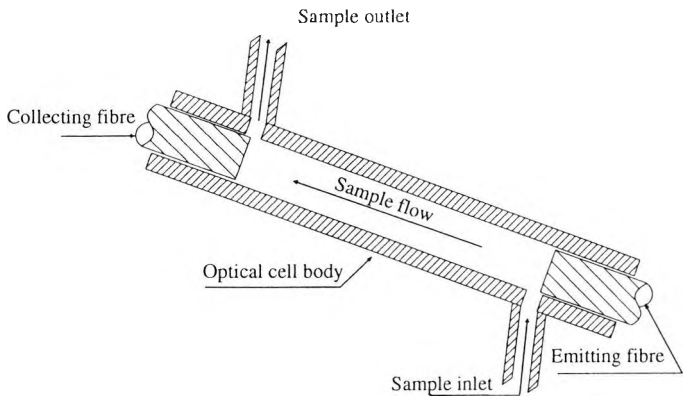

Fig. 6.6 Drawing of the optical cell with it inclined inlet and outlet.

characteristics in the UV. The losses in the fibre were approximately 10% at a wavelength of 290nm and higher than 90% at a wavelength of 200nm as is shown in Fig.6.7.

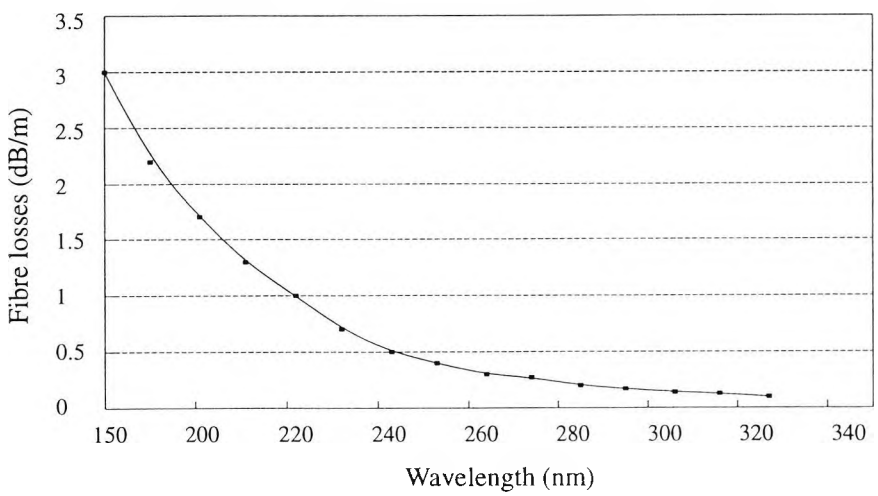

Fig. 6.7 Spectral transmission properties of the quartz fibre.

The lamp used was cylindrical in shape and was 25mm long. Therefore to couple maximum light into the fibre either a larger diameter fibre or a lens system should have been used. It was found that positioning the fibre onto the lamp glass was easier to setup while still coupling adequate light power into the fibre and did not involve a complex optical system. A 2mm diameter quartz fibre was used. Although the latter was rigid and the lamp had to be mounted near the optical cell, a fibre bundle or a liquid guide would have been more effective in keeping the system flexible and guiding enough light through the optical cell. However, this was not considered because of increased cost.

Light passing through the sample was collected at the other end by a more flexible 1mm diameter pure quartz fibre. It was possible to bend the fibre so that light could be guided to the optical detector.

The effect of ageing of the fibre especially when used with such comparatively high energy radiation i.e. ultraviolet radiation, were unknown to the manufacturer and hence no data was provided to make any conclusion in relation to the life expectancy of these fibres.

6.3.1.5 Fibre Connectors

The fibre connector which has the function of connecting the fibre to the optical cell was made of stainless steel. The latter was inert and was not corroded by samples of very alkaline waters and with waters containing high levels of chlorine. It was found that during prolonged working periods some rust developed on the metal. This resulted from the fact that the stainless steel was not pure. However, an acid wash lasting a few minutes was found to be effective in removing it.

The fibre connector which is shown in Fig.6.8 was made of two parts:

a) The first part was made of a hollow cylinder of a diameter of 2.9mm and a length of 15mm with a thread machined at one end (the exterior side). This 'ring' was then glued onto the glass cell using epoxy glue.

b) The second part of the connector was made of the same material. The inside of the tube was machined so that the first half was large enough to accommodate the fibre and its

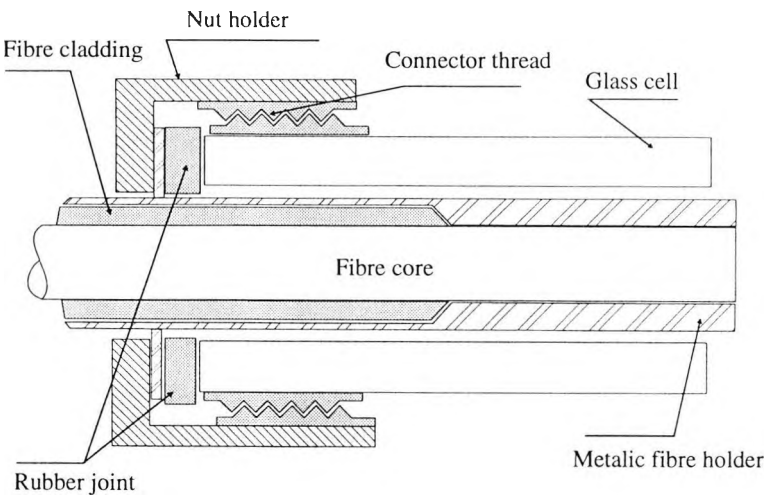

Fig. 6.8 Schematic diagram of the fibre connectors

cladding while the second half was drilled with the same diameter of the glass fibre. The cladding was removed and replaced with a thin stainless steel tube to give the protruding part of the fibre more strength. This design was found to be effective in removing air bubbles that could have become attached to the surface of the fibre tip; this was seen to happen with turbulent samples when pumped at a high flow rate. With a normal fibre end, it was found that only very few air bubbles, trapped between the glass cell wall and the connector, could not be removed by the flow of the sample. With a modified fibre connector end, the gap separating the cell wall and the connector was larger and if any air bubble was trapped, it would stay behind the fibre end, hence it would not affect the path of the light. On the external side of the connector, a stopper was machined in order to hold the first part of the connector in contact with the second part. A rubber washer was fitted between the glass and the connector to stop any water leakage.

The connector used on the side of the lamp side was similar to the first connector but was designed to hold a larger fibre core e.g. 2mm diameter. Hence only the internal dimensions were modified.

6.3.1.6 Optical Filter

In order to eliminate all the unwanted frequencies generated by the mercury lamp (i.e. 370, 420, 550, 580nm), it was necessary to use an optical filter. Although the visible part of the spectrum was not absorbed by chlorine, its presence considerably reduced the sensitivity of the measurement and produced a variable offset. This effect was exaggerated by the use of a silicon photodiode as a detector because silicon type detectors are usually six times more sensitive to light in the visible region than to light in ultraviolet part of the spectrum.

Most absorption type optical filters possess good rejection characteristics especially in relation to their pass band. However their transmission characteristics are very poor, usually not more than 20% of the incident light as is shown in Fig.6.9. On the other hand interference filters can have similar pass band characteristics with transmission values that can reach 60 to 80% [123]. The basic phenomenon used in an interference filter is to use the radiation falling on a substrate of quartz of a defined thickness onto which thin layers of specific chemicals were deposited so that interference between the different rays which originated from the same light beam occurs. At the exit side of the glass, parallel rays would have travelled different lengths inside the glass and come out parallel to the first ray to

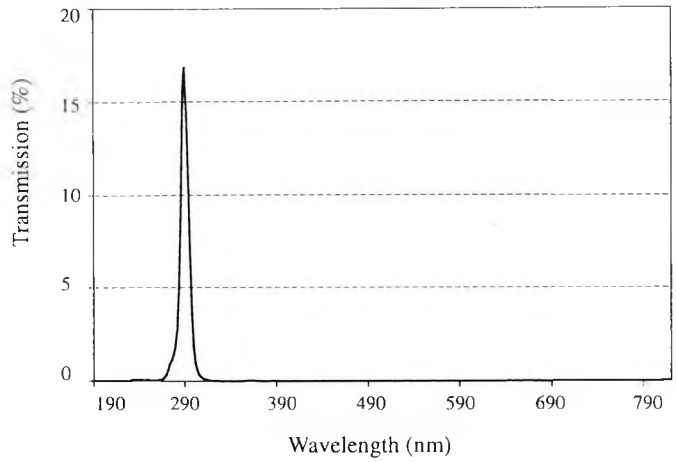

Fig. 6.9 Transmission characteristics of the absorption type optical filter centered at 290nm with a bandwidth of 20nm at half height

interfere constructively for a particular band and destructively for the rest of the stop band. The narrower the band pass is the smaller the stop band is. However because of this process, the transmission rate is very high compared to one obtained with absorption type filters. The stop band upper limit was found to be approximately twice the central wavelength i.e.580nm. The transmission characteristics of the interference filter used in this application are shown in Fig.6.10.

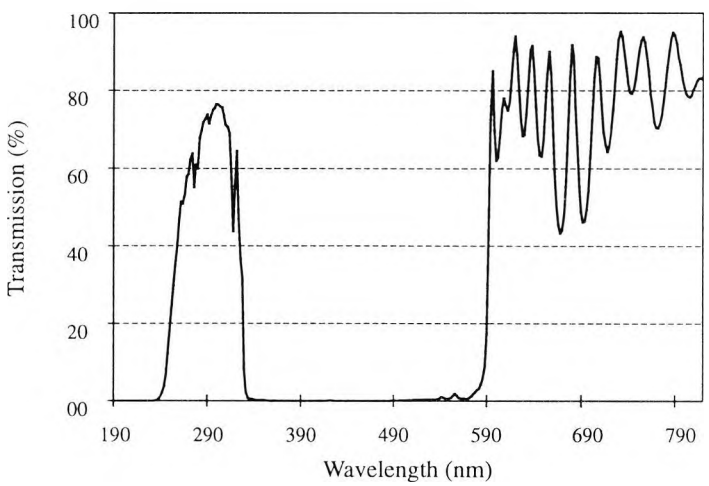

Fig. 6.10 Transmission characteristics of an interference type filter

6.3.2 The Mechanical System

The mechanical system consisted of a peristaltic pump, a mixing chamber and a set of valves. The pump was used to suck the sample from an external source into the mixing chamber and also to supply the different reagents for sample conditioning. The pump in

this configuration was not as effective in pumping the sample in as it would have been when used to push the sample because the sucking pressure generated was not powerful although it was sufficient. However, this configuration was adopted because of lack of space in the standard metallic housing of the monitor. The sample was then directed into the optical cell. The set of valves controlled the direction of the reagent flow towards the mixing chamber when needed as is shown in Fig.6.11.

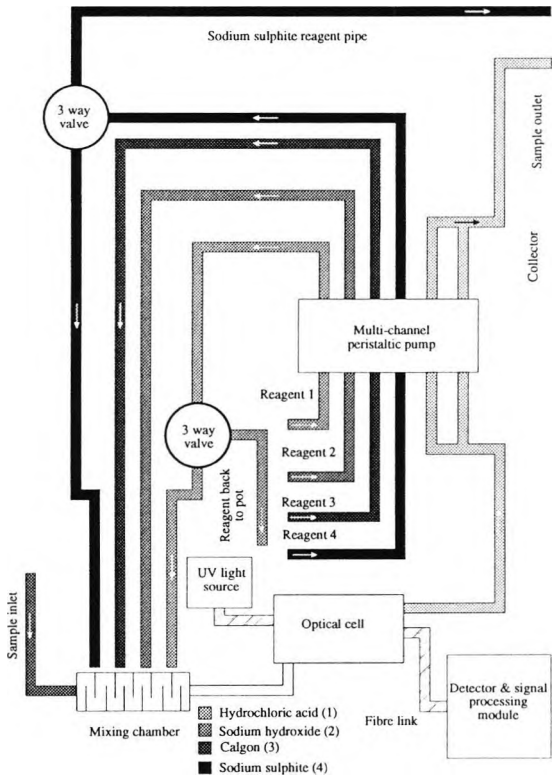

Fig. 6.11 Schematic diagram of the liquid handling section

The system operated in two cycles, the first cycle provided the background absorption information and the second, a measure of the chlorine present. During the first cycle, the sample was sucked into the mixing chamber where it was mixed with sodium sulphite solution to destroy the chlorine and was later fed to the optical cell for background measurement. During the second cycle the sodium sulphite solution was routed back to the reservoir, and the alkaline sample travelled through the optical cell for the measurement of the concentration of the OCl^- ion. During the whole process sodium hydroxide was continuously mixed with the sample to ensure that all the chlorine forms would be converted into the hypochlorite ion form.

It was found that waters containing a high concentration of cations such as calcium and

magnesium which define the hardness of the water, would precipitate when their solubility product was reached[121]. Increasing the pH of the solution, which is reflected in an increase in the OH^- ion concentration, usually tends to reduce the upper limit of calcium and magnesium before which the precipitation would occur.

Because of the different concentrations of ions such as calcium and magnesium present in water the effect of pH was found to vary from one type to another. The buffering ability of water was affected in the same way. This can be seen for example in different waters- for example hard water which is found in the south of England and soft water in the north of the country. The effect of increasing the pH of the tap water to a value higher than 9 resulted in the precipitation of some cations. As a consequence, the water became opaque and transmission of light through it was decreased.

Various reagents could be used in order to reduce the effect of the high pH values on hard waters. EDTA, a well known complexing agent, would maintain these cations soluble in water. However it was found that EDTA would react with chlorine and remove it from the sample. Calgon is widely used for the purpose of complexing the calcium and magnesium present in hard water samples so that they do not precipitate when the alkalinity is increased or when the temperature of the sample is increased to the boiling point. It is usually used in washing machines to hold the deposition of calcium on the metallic heaters of the machine or in electric kettles.

Sodium hexametaphosphate $(NaPO_3)_6$ (calgon) was therefore mixed with the sample prior to the addition of sodium hydroxide in order to prevent the precipitation of insoluble cations. Moreover it was found that calgon does not react with chlorine hence it was transparent to chlorine measurement.

6.3.2.1 Liquid Handling Section

A positive displacement peristaltic pump (Watson-Marlow 303FD/D) was used to suck the sample into a mixing chamber and then into the optical cell. This type of pump uses a 5 channel micro-cassette and can easily handle the relatively small volumes of sample as well as the smaller volumes of reagent. An added attraction of this pump was the complete isolation of the liquid from the mechanical parts.

A 130:1 ratio of reagent to sample concentration did not significantly alter the concentration

of chlorine present in the original sample. This dilution ratio and the high pH value present enabled the instrument to be used at its maximum sensitivity.

The flow rate depended upon the speed of rotation of the motor of the pump, the length of pipe in contact with the rollers and the internal diameter of the tubing. An inherent drawback with this type of pump was that it caused a pulsation effect on the flow. This would have introduced an error if the effect was not consistent when sampling was being carried out. However, this possible source of error was eliminated by stopping the pump whilst the measurement was made.

6.3.2.2 Mixing Ratio

The mixing ratio of the sample to the reagent was an important factor. It was important to keep the volume of the reagent small compared to the volume of the sample in order to minimise dilution errors, hence reducing the systematic error in the measurement. By adding a fixed volume of reagent to the sample the latter was diluted and the effect on the measurement was reflected in the decrease in the sensitivity of the measurement. For this reason, the volume added to the sample was kept to the minimum by using a more concentrated reagent. Since the same pump was used to pump the reagents and the sample, the volumes of these were controlled by the internal diameter (ID) of the tubing used. The ratio of the volumes i.e. sample to reagent, was proportional to the square of the ID of the tubing only as shown by Eq.6.4

$$Q=\left\{\frac{D_1}{D_2}\right\}^2 \qquad [6.4]$$

where D_1 and D_2 were the sample and the reagent tube diameters respectively. For an ID of reagent tubing of 0.25mm, and a sample tubing ID of 2.7mm, the ratio Q resulted in a value of 230 since two channels of the pump were used for the sample and only one channel for each reagent. Consequently, this induced a systematic error of less than 1% .

6.3.2.3 Mixing Chamber

The mixing chamber, used to mix the water sample and the conditioning reagents, was made from a hollow Perspex cylinder. Four reagent inlets were positioned at the entrance of the cell at right angles to the main sample inlet. Baffles attached to the side walls of the main cylinder disturbed the flow of the sample and hence created turbulence. As a result,

the reagents were mixed with the sample and the efficiency of the process was then increased. To maximise this process with a sample flow of 67ml/min, the dimensions of the mixing chamber were reduced to the minimum (20mm length and 3mm diameter). The diameter of the reagent inlets was smaller than 0.1mm and they were inserted inside the main cylinder so that their outlet was approximately in the centre of the main cylinder of the mixing chamber. The latter had the effect of forcing the reagent to flow in the centre of the main stream of the sample instead of flowing at the side as would have occurred if the reagent outlet was positioned on the side of the mixing chamber main cylinder. This effect can be illustrated in Fig.6.12.

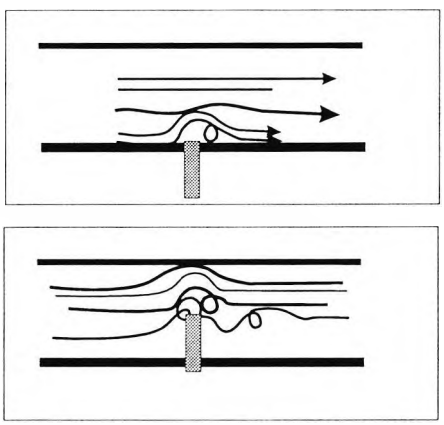

Fig. 6.12 Drawing showing the effect of the disturbance created by an obstruction when positioned on the border and in the centre of the main flow

The schematic diagram of the mixing chamber is shown in Fig.6.13. The inlet reagents, of which there were 4, were placed on opposite sides of the main body and hence cannot be seen in the side drawing.

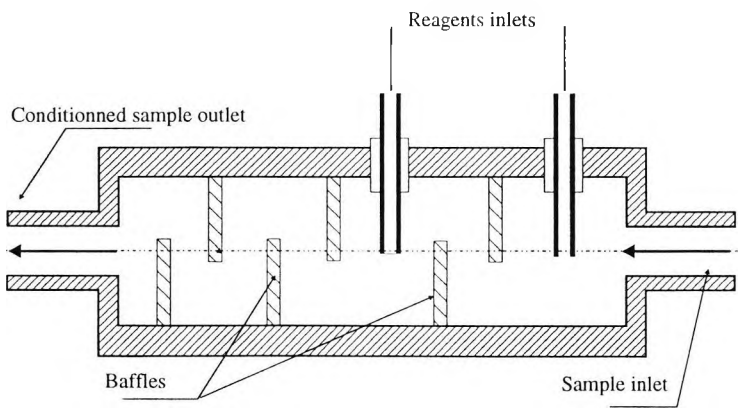

Fig. 6.13 Schematic drawing of the mixing chamber showing the position of the reagent inlets and the baffles.

To create powerful turbulences the baffles, whose size were roughly one third of the cross section of the mixing chamber, were glued inside the main chamber body and were positioned in such a way that the angles between their axes was 120° as is shown in Fig.6.14 which represents a front view drawing of the mixing chamber. The reagent inlets which were visible in Fig.6.13 are hidden in this drawing. With a sample flow rate of 67ml/min, a reagent concentration of 10g/l was efficiently mixed with the different samples.

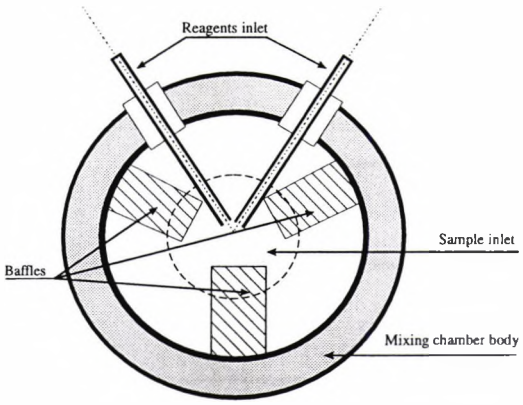

Fig. 6.14 Front view of the mixing chamber showing the disposition of the baffles and inlet reagents

6.3.3 Detection and Signal Processing Unit

The electrical system comprised a detector, a signal processing unit which enhanced the detected signal and reduced interference and noise, and a data manipulation unit which was included prior to the display. A sub-section of this system generated the appropriate signals for timing and control sequences to monitor the pump, valves, sample and hold devices etc.

The electronic circuit of the signal processing stage used in the RCM consisted of four main parts: the optical detector, the signal processing unit, the arithmetic unit and a timer and sequence generator unit. The block diagram of this unit is shown in Fig.6.15 and the control section in Fig.6.16

6.3.3.1 The Optical Detector

The optical signal was converted to an electrical signal using a photodiode (PIN silicon type, Hamamatsu S1722-02). Its characteristic was improved in the ultraviolet region over other such devices and a quartz window allowed the UV light to be transmitted through to

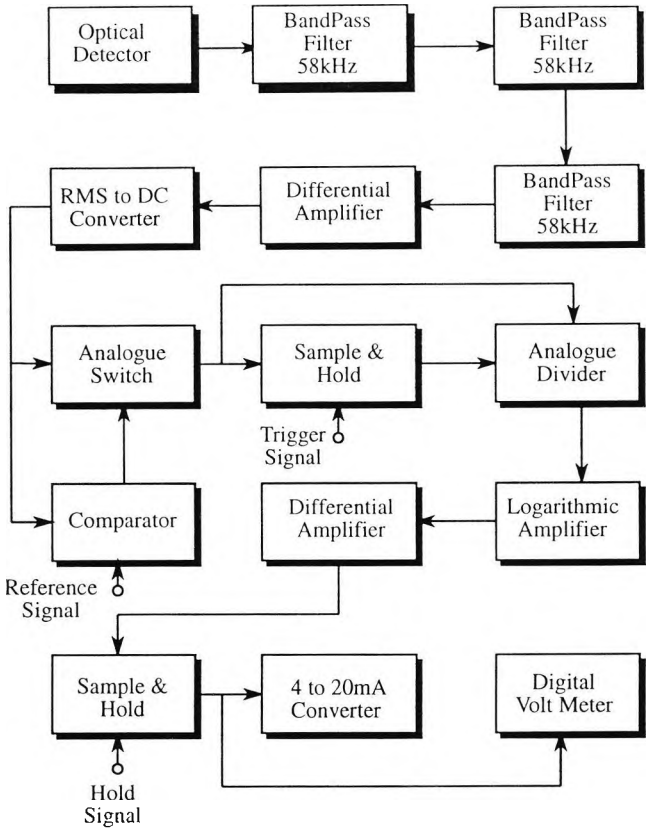

Fig. 6.15 Block diagram of the electronic signal processing section block

the semiconductor. The photocurrent generated was proportional to the light intensity and the detector 's wavelength response was shown in Fig.6.10. The ratio of sensitivity for the near infrared to UV was approximately 6. The sensitivity at the wavelength of interest (290nm) was 0.10A/W. The noise figure for this particular detector was of the order of 10^{-13}W(Hz)$^{-1/2}$ and a maximum dark current of 30nA. The frequency response of this detector was 300MHz which was more than adequate for this application.

A transimpedance circuit was used to convert the photo-current signal generated in the photodiode into a voltage signal. This circuit was reported to improve the input impedance and to reduce the loading effect on the diode [83]. The high input impedance of the operational amplifier was used to reduce the effect of biasing the amplifier by taking less current through its inverting input. Hence the totality of the photocurrent went through the feedback resistor thus producing an output voltage proportional to photocurrent as in Eq.6.7.

$$V_{out} = - i_s R_f \qquad [6.7]$$

Where R_f is the resistor and i_s is the photo current. The active component of this unit was

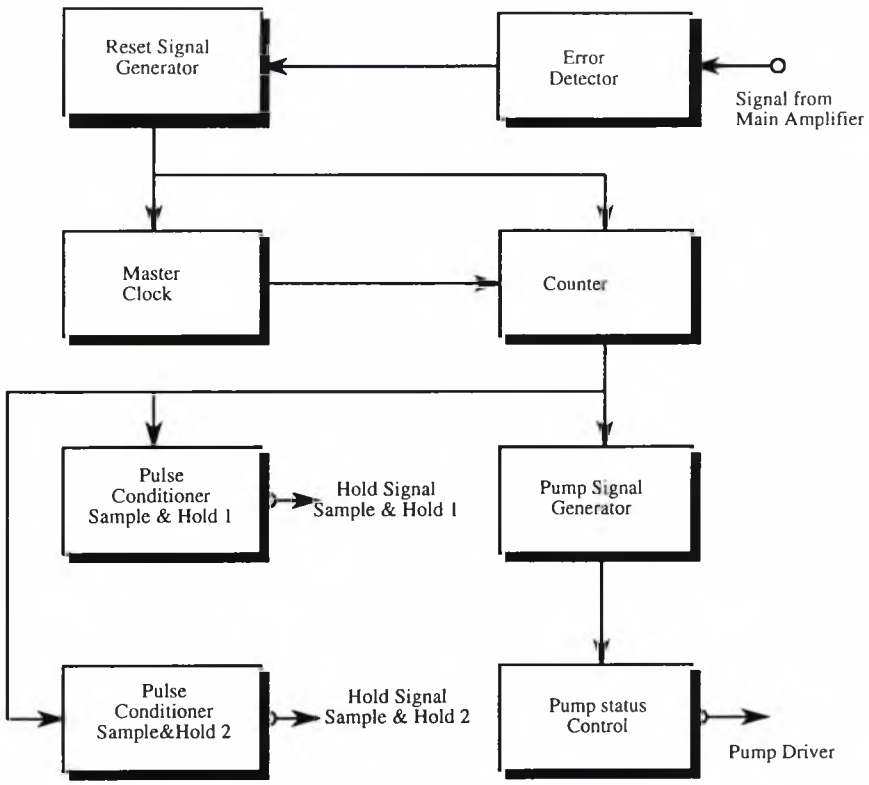

Fig. 6.16 Block diagram of the electronic control logic section.

a very low bias current, low noise, operational amplifier (Burr Brown OPA111). The choice of this component came as the result of comparing the rms value of the noise level at the output of the amplifier with that utilising alternative amplifiers. It was found that although the frequency bandwidth of the chosen operational amplifier was limited to 2MHz (gain bandwidth product GBP), the noise level was the smallest when compared with different operational amplifiers in the same circuit. It was also found that although FET input amplifiers gave a better response, however, this was limited by the gain bandwidth product and the central electrical frequency of the signal (58kHz). The feedback resistor value was then calculated to be 810kΩ using Eq.6.8 [124] . This also reduced the bandwidth of the circuit hence reducing the noise bandwidth at the same time.

$$f_{max} = \sqrt{\left(\frac{GBP}{2\pi\,(C_i + C_o)R_f}\right)} \qquad [6.8]$$

where C_i, C_o, R_f represent the capacitance of the diode, the feedback capacitance and the feedback resistance.

To further enhance the signal to noise ratio, the power supply to this unit has been reduced to operate at 5V [125]. This circuit, in addition to a bandpass filter which will be described

in the next section, was shielded in a metallic box to reduce the effect of noise and interference especially that due to the lamp power supply which was found to be emitting very strong electrical signals which were collected by a simple wire. However precautions had to be taken to suppress ground loops. This was achieved by connecting the ground of the circuit to the ground of the box. The latter was then connected to the common ground i.e. power supply, using a single connection to the common ground. This circuit is depicted in Fig.6.17

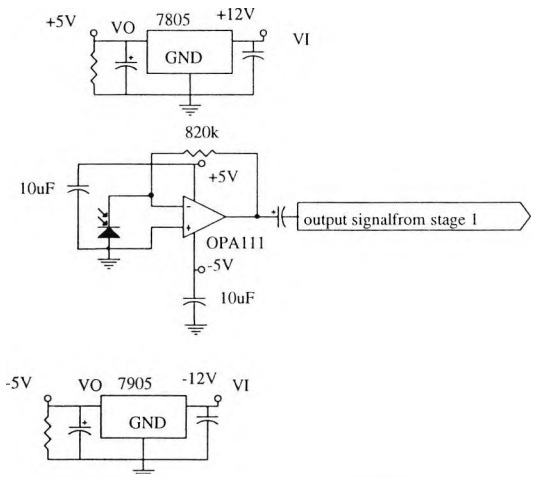

Fig. 6.17 Electronic circuit of the transimpedance amplifier

6.3.3.2 Bandpass Filter

The signal processing unit consisted of a combination of filters and amplifiers. Different noise sources, extrinsic and intrinsic to the system were superposed onto the main signal. The largest proportion of the noise signal (Shot) originated mainly in the photodiode[82]. The signal was fed to a biquad bandpass filter tuned at 58 kHz which eliminated undesirable frequencies such as the 50 Hz (electrical) and 100 Hz and dc (optical ambient light) as well as the 29 kHz emitted from the power supply of the lamp itself.

The biquad filter had been reported to be an effective and stable tunable active bandpass filter[126]. The analysis made by Thomas et al, showed that the effect of temperature can be reduced to the minimum[127]. This was achieved by choosing the resistors and the capacitors so that the temperature effect on them was minimised and hence the central frequency and the stability of the filter were not affected.

As a result of the limited bandwidth of the amplifiers (Burr Brown OPA404 four op-amps), the maximum Q factor achieved with this filter at a frequency of 58kHz was 14. This particular type of operational amplifier has a bandwidth gain product of 6.4MHz, a slew

rate value of 35 V/s, a bias current of 32 pA and a noise figure at 10kHz of 12 nV/Hz$^{1/2}$. The transfer function of such a filter is given by Eq.6.9

$$\frac{V_{out}}{V_{in}} = \frac{G}{1 + jR_1(C\omega^2 - \frac{1}{CR_2R_4\omega^2})} \qquad [6.9]$$

where $G = \frac{R_1}{R_3}$, the different values of resistors and capacitors are shown in the electronic circuit and ω is the operating frequency of the system. A schematic diagram of the electronic circuit is presented in Fig.6.18:

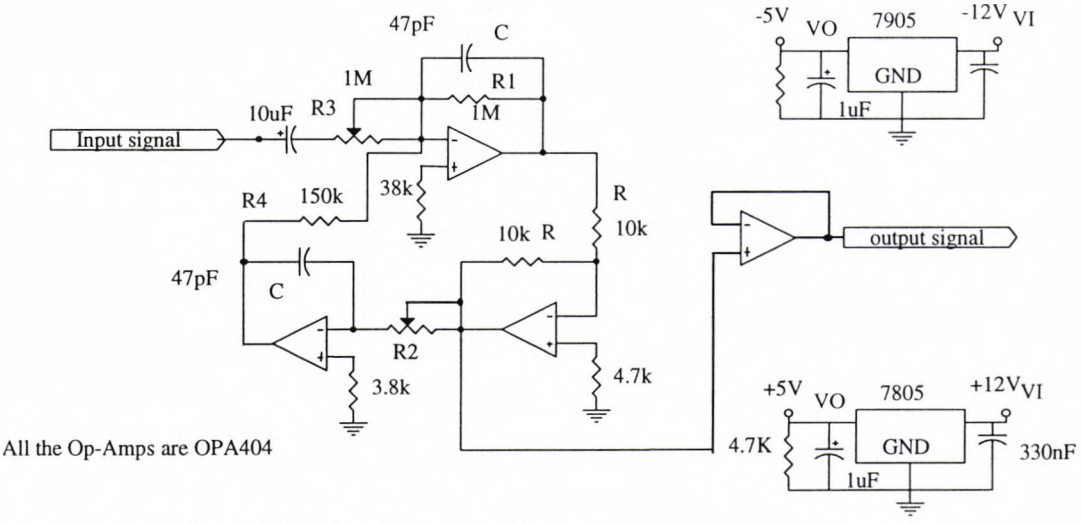

Fig. 6.18 Schematic diagram of the biquad filter

The system resonates at a frequency given by Eq.[6.11] for which the function is maximal:

$$D(\omega) = 1 + jR_1\,(C\omega^2 - \frac{1}{CR_2R_4\omega^2}) \qquad [6.10]$$

$$\omega_o^2 = \frac{1}{C^2R_1R_3} \qquad [6.11]$$

$$Q = (\frac{R_2}{2})\,(R_3R_4)^{-1/2} \qquad [6.12]$$

To enhance the Q factor, three similar filters were cascaded giving a total Q factor of 40 and the bandpass of this filter block was 1.45kHz. The gain of the three bandpass filters was 140.

6.3.3.3 Main Amplifier

The processed signal was ac coupled to an instrumentation amplifier (Burr Brown INA 110) for final amplification. The gain of this amplifier was set to approximately 19 by using an external variable resistor of 10k for optimum adjustment. The frequency response of this amplifier at -3dB and a gain of 200 covered a region up to 100kHz. This unit was of a low noise, low drift type. The overall gain of the combination filters amplifier was approximately 2700. The electronic diagram of the signal processing stage is shown in Fig.6.19.

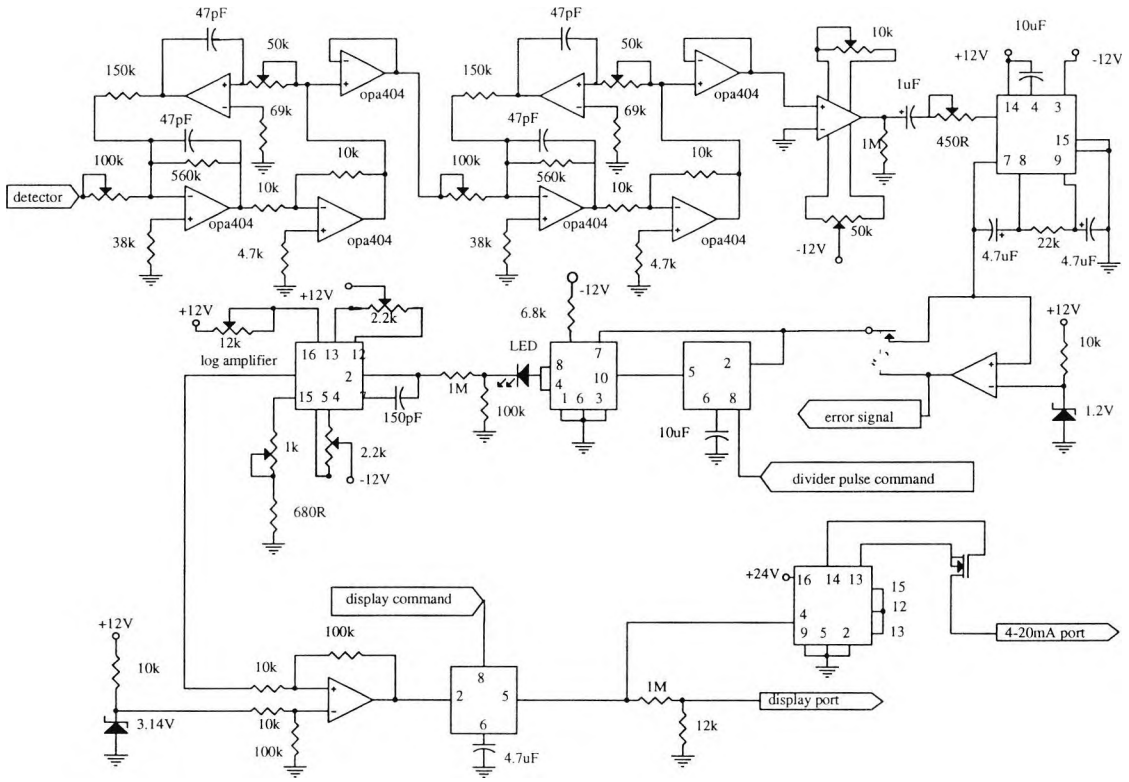

Fig. 6.19 Schematic diagram of the signal processing stage

6.3.3.4 RMS to DC Conversion

The division computation when using analogue devices requires the availability of the two signals at the same time. However the measurement of the reference and absorption signals were made sequentially and therefore the two signals were not present at the same moment. One measurement was performed and stored then a second measurement was made before a ratio of these two signal was computed. This procedure was more easily implemented with dc signals hence the need for converting the ac signal into dc. Moreover this conversion results in the lowering of the noise figure. This was achieved by using an rms

to dc converter. A second order filter was connected at the output of the rms to dc converter to reduce the ripple generated by the conversion. The device chosen for this unit was an Analogue Devices AD 635, with a stable response and low drift characteristic. An external capacitor (C_{AV}) was used to average the rectified ac signal, and its value determined the magnitude of the ripple, which was considered as an error superposed on the dc signal. There was a compromise to be made between the response time and the ripple rejection level, since the smaller the capacitor (smaller settling time) the larger the ripple[128]. The value of C_{AV} was set to 10μF. The ripple rejection was decreased by using a second order filter at the output of the device, hence increasing the response time while maintaining a good ripple rejection. This was found to be an advantage because the signal was then less prone to the effect of step changes caused by glitches generated from power motors and power switches.

6.3.4 Arithmetic Unit

The implementation of the arithmetic operation was the main function of the third unit. The output signal from the divider was then sent to a logarithmic amplifier. The resultant signal was then a linear function of the variable to be measured (mg/l OCl^-) which was displayed using a D.V.M. and a display unit.

The measurement of the reference and the absorption signal was carried out at two distinctive times during the full cycle. The reference signal was stored in a sample and hold device (LF309) during the first half cycle. The latter was triggered to store the value of the signal approximately one second after the pump was stopped. A large capacitor value (4.7μF) was used to average the sampled signal and retain it until the next triggering pulse. Polycarbonate capacitors were adequate for long hold time since their leakage current value was very small i.e. <1mV per minute. This signal was present at one input of the divider (denominator).

During the second half cycle the absorption signal was continuously fed to the numerator input of the divider. Hence during the second cycle, the output of the divider represented the value corresponding to the division of the absorption to the reference signals. The signal was then fed to the logarithmic amplifier. The output of the latter was sampled using a sample and hold device which stored the value until the complete cycle was restarted and the same output was sent to the DVM and current converter.

6.3.4.1 Divider

A four quadrant analogue multiplier (AD534) connected as a divider by feeding the output signal from the rms to dc converter through the analog switch to one of the input ports was used to divide the absorption signal by the reference signal which was stored in the sample and hold device. The gain of this device was controlled by setting the value of a resistor connected between the negative supply and the gain input of the device. This enabled the output signal to vary from 3 to 10V especially for signals that were numerically close to each other which was found to be the case for this operation. The gain was set to a value of 6 and was achieved by choosing the value of the resistor to be 9kΩ as given in Eq.6.13.

$$V_{out} = B\,(Z_2 - Z_1) / (X_1 - X_2) \qquad [6.13]$$

where $Z_2 - Z_1$ represents the differential numerator input, and $X_1 - X_2$ is the differential denominator input and B is the gain factor and is given by the following relation:

$$B = 10\,R / (5.4+R) \qquad [6.14]$$

where R is the resistor in kΩ. The divider performed linearly provided that its denominator input was larger than 1V. Consequently a circuit was incorporated to control the level of the input signal. Whenever the signal level went below 1.2V a comparator generated a signal which caused the switch connecting the output of the rms to dc converter and the denominator input of the divider to open. The same error signal was then used to trigger the pump to be continuously active until this error was cleared. This circuit is incorporated to control the level of the denominator signal and is described subsequently.

6.3.4.2 Logarithmic Amplifier

The logarithmic amplifier was an INTERSIL device ICL4048 (Farnell ICL4048). It was used to transform the input signal into a logarithmic output according to the Eq.6.15

$$Y = -1.57 Log\left(\frac{V_{sig}}{RI_{ref}}\right) + 4.66 \qquad [6.15]$$

where R = 1 MΩ and I_{ref} is the reference current and is set to be 1mA.

The actual measurement obtained through the detector is a measure of the attenuation of a transmitted signal which corresponds to a particular concentration of chlorine. However the Lambert-Beer law provides a logarithmic relation between light power and

concentration. In the previous circuit a ratio of the signal representing the absorption to reference was processed. The latter can only be associated with the Beer-Lambert law when the logarithm of each signal is taken. It was found that by taking the logarithm of the ratio of the transmitted signals and by writing the absorption at 290nm as the sum of the absorptions due to chlorine (C_{cl}) and the background (C_b), a linear relation between the detected signal and the concentration of chlorine can be expressed as in Eq.6.16.

$$Log\left(\frac{P_{abs}}{P_o}\right) = -l\left(\varepsilon_c C_c + \sum_i \varepsilon_{b_i} C_{b_i}\right) \text{ and } Log\left(\frac{P_{ref}}{P_o}\right) = -\sum_i \varepsilon_{b_i} l\, C_{b_i} \qquad [6.16]$$

where the index c represents the parameters associated with chlorine and the index b represents the background. By subtracting the two sub equations of Eq.6.15 the ratio of the absorption to reference light is obtained in Eq.6.16:

$$Log\frac{p_{abs}}{p_o} - Log\frac{p_{ref}}{p_o} = -l\left(\varepsilon_c C_c + \sum_i \varepsilon_{b_i} C_{b_i}\right) + l\sum_i \varepsilon_{b_i} C_{b_i}$$

$$Log\left(\frac{P_{abs}}{P_{ref}}\right) = -\varepsilon_c C_c l \qquad [6.17]$$

The last equation shows that the ratio method eliminates the effect of the background interference. It is justifiable to describe the absorption at the wavelength of 290nm as the independent sum of the different absorptions of the particular elements that absorb light in that region. This results from the fact that the weight of each particular element on the total absorption is governed by the extinction coefficient which is a function of the wavelength.

Because the logarithmic amplifier compresses the dynamic signal making the range of output small (1.5V per decade change), a differential amplifier was then used to extend the dynamic range by amplifying the difference between the signal provided by the logarithmic amplifier and a reference signal, taken from a zener diode (3.14V), with a gain of 4.2. The signal was then directed towards a sample and hold device for the sole purpose of memorising the signal until the complete cycle was completed and was triggered by a pulse generated in the logic circuitry when the absorption cycle was finished. The sampling and memorising of the signal was carried out in order to provide a stable reading for at least one complete cycle. The output of the sample and hold device was then present at the input port of both: the DVM and the current converter (4 to 20 mA).

6.3.4.3 Digital Volt Meter and Display

Since the Digital Volt Meter (D.V.M.) accepts a maximum dc signal of 199mV, a bridge divider was incorporated to reduce the signal amplitude. This was achieved using a set of two resistors joined in series between the signal input and ground. The output was taken from the bridge and provided a maximum signal amplitude of less than 199mV for a maximum input signal of 10V. The value of these resistors were 12kΩ and 1MΩ. The analogue to digital converter and the reference voltage were included in the D.V.M which also contained a 3 digits liquid crystal display (RS 258-041). The measured intensity of the signal was then displayed continuously. Although the value of the display was in mV, the output could have been a value in mg/l if the instrument was calibrated by choosing the right values of the resistors and also providing protection for the input port so that the maximum signal intensity remained smaller than 199mV.

6.3.4.4 Voltage to Current Converter

A 4 to 20mA port was provided as an output port from the instrument for the various interfacing to remote control instrumentation and data acquisition. This was achieved by using a ready made current converter Burr Brown XTR110 with a MOSFET transistor to drive a load of 267Ω. The unit was set to correspond to a lower current of 4mA for a zero volt output and 20mA for a maximum of 20V output for which the response of this circuit was linear.

The transfer function of this device is given by the following equation:

$$I_{out}=1.6V_{in}+4.03 \qquad [6.18]$$

Where I_{out} is in mA and V_{in} is in Volts for a load of 267Ω.

6.3.5 Control Unit

The control unit was set to trigger an alarm signalling a malfunction. The latter was caused either by a bubble in the optical cell which resulted in a complete loss of light at the detection stage or when the sample was too opaque due to high turbidity or fouling caused by deposition of particulates on the optical cell hence reducing the light transmission.

The lower limit of the processed signal at the output of the rms to dc converter unit was set to 1.2V. This corresponded to a reference diode output voltage and was found to be the

minimum acceptable level for the signal below which the signal to noise ratio was unity. This circuit was made of a comparator (LM339 RS 307-086) which was used to compare the signal level with a reference signal of 1.2V. The output of this unit was set to provide a TTL compatible signal when a malfunction occurred i.e. output low when the signal was smaller than the reference. This was used to open the analogue switch (DG308 RS303-551) connecting the signal to the divider input and also to reset the clock circuitry in the digital section to activate the pump so that in the case of an air bubble the latter is flushed out. When the signal level became larger than the reference signal the output of this unit was set to high and the cycle restarted. The output of this unit when set triggered an oscillator activating an error LED mounted in the front panel.

6.3.5.1 Digital Unit

The fourth unit whose schematic diagram is shown in Fig.6.20 consisted of a combination of logic gates which generated different types of control pulses to drive the sample and hold devices, the valves and the pump. The main clock signal was generated using a pulse generator (NE555) working in an astable mode producing a 50% mark to space ratio pulse at 0.5Hz. This signal was used to activate the valve via a transistor switch (BC183L). A current of 130mA was required to activate this valve (12 volts, 130mA, NResearch Incorporated model 225T) and maintaining it in its holding mode. This could be reduced by placing a capacitor in parallel with a resistor between the supply line (12V) and the valve so that the charging current of the capacitor triggered the valve and only a smaller

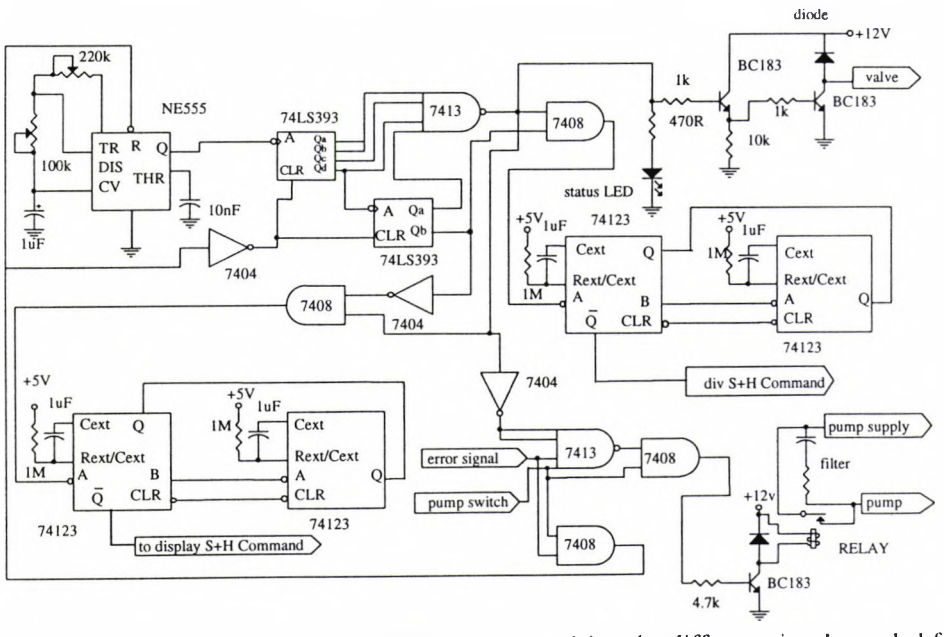

Fig. 6.20 Schematic diagram of the digital part comprising the different signals needed for the control and running of the RCM

current of 60 to 70mA was then required to maintain the valve in hold mode.

The same signal drove a dual binary counter from which all the sequences were generated using some combinational logic. The pump was activated through a relay. The latter needed 90mA through its coil in order to activate the mechanical switch. This current could not be provided by the logic gate hence a transistor switch (BC183L) circuit was used to provide the necessary current. A protecting diode was connected in parallel with the relay coil to guard against back emf current generated within the coil.

6.3.5.2 Command Pulses for Sample and Hold Devices

A set of two flip-flops (74LS123) connected in a multivibrator circuit as shown in Fig.6.21 were used to generate the appropriate command pulse used to trigger the sample and hold devices. The duration of the pulse and its occurrence time was controlled via two RC networks. Variable resistors were used to vary these parameters. The output signals of these devices were related to the pump driving signal and occurred after the pump was stopped. This delay was purposely introduced to permit the sampling of the signal once any external disturbances ceased (i.e. 0.5s). One of these signals was used to trigger the sample and hold device used to memorise the signal from the rms to dc converter before being sent to the denominator input of the divider while the second one was used to sample and then hold the signal from the second differential amplifier before the signal was sent to the DVM and display unit. This timing can be seen in Fig.6.22 as part of the timing sequences used in the residual chlorine monitor with all the necessary signals.

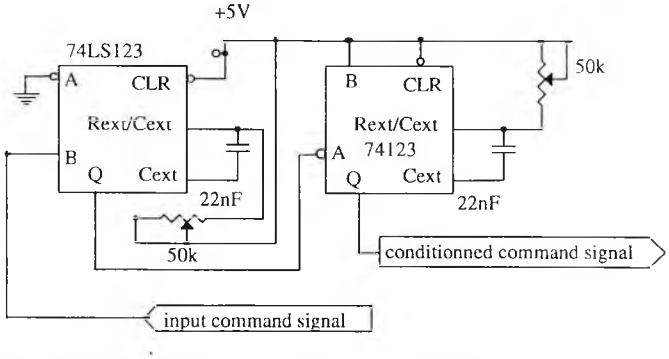

Fig. 6.21 Schematic diagram of the pulse conditioner circuit

6.3.6 Power Supply of the Instrument

The power supply of the monitor was provided so that the residual chlorine monitor was a self contained unit. Positive and negative power signals were needed to drive the different

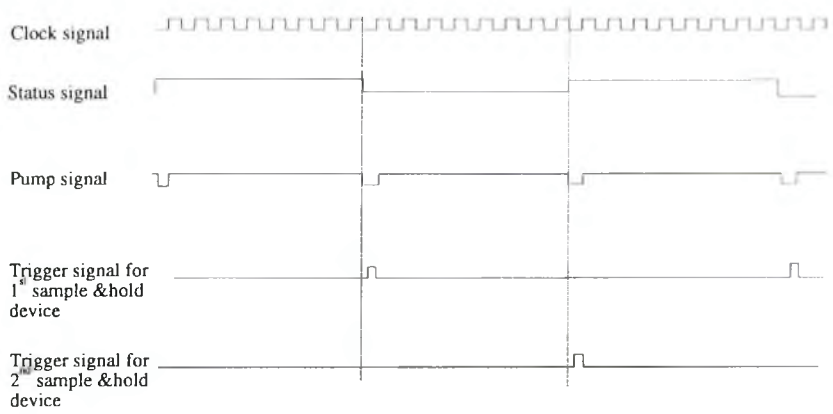

Fig. 6.22 Timing sequence used in the RCM

electro-mechanical devices and electronic circuits. The design of the power supply was based on a powerful 120VA mains transformer with two independent secondaries. The latter was useful in separating the supply of the two secondary coils from each other which was found to completely isolate the surge of current demanded by each circuit. The mains power was provided with a mechanical switch and a mains fuse. Each secondary was connected in parallel to two 3A 12V regulators. The output of each regulator supplied +12V with reference to common ground. The supply that originated from the first secondary was connected to the UV lamp power supply while the second one was powering the positive side of the electronic circuit. On the other hand the supply that originated from the second secondary and which provided +12V with respect to an isolated ground, was connected in such way that once the common ground was connected to the more positive output the isolated ground became -12V with respect to the common ground and hence was used to power the electronic circuit. The output of the second regulator connected to the second secondary was used to provide a floating +12V to drive the pump. This eliminated a problem which appeared when both secondaries of the transformer were connected to the common ground. In this case every time the pump started, the UV lamp went off for few seconds. This was detected by the control unit and an alarm signal was generated. As a result the error signal was high all the time. A second mains transformer was used to provide the supply to the current converter chip which needed +24V at its positive supply pin. Although supplying the chip with a floating +12V and -12V would have provided the necessary voltage, however since the device ground and the signal ground were the same, the negative supply -12V would have been shorted to ground. Fig.6.23 represents the schematic diagram of the power supply module.

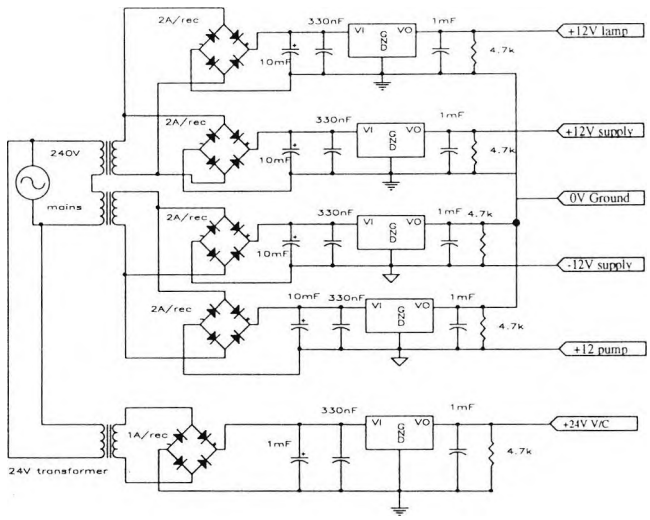

Fig. 6.23 Schematic diagram of the power supply module

6.4 Signal to Noise Ratio

The static signal to noise ratio was calculated from Eq.6.17:

$$S/N = 20\ Log_{10}\ (V_{signal}\ /V_{noise}) \qquad [6.17]$$

where V_{signal} is usually the average value of the signal and V_{noise} is the average value of noise. The static signal to noise ratio (S/N) is very important in order to assess the effect of noise on the measurement. It is a measure of the noise in the signal to the strength of the signal. On the other hand, the dynamic signal to noise ratio was used to give the actual ratio of the variation of the signal (between the two limits of transmission for the range of concentration of interest) and the noise level present. It also affected the ultimate sensitivity of the instrument since at this level the noise obscured the variation of the signal (i.e. the magnitude of the noise was larger than the variation of the signal itself). The static S/N was 42dB and the dynamic S/N was 26dB.

6.5 Experimental Procedure and Calibration of the RCM

Calibration of the Residual Chlorine Monitor was carried out utilising different types of water. Distilled water was used initially, followed by tap water from different origins which was found to yield a different behaviour from that obtained with distilled water.

Two important factors were identified; these were:

1) Depending on the type of water, a different absorption characteristic was obtained for

the same range in chlorine concentration. However this did not cause any error in the measurement, since the signals remained within the dynamic range of the instrument.

2) There was a link between the slope of the calibration curve (best fit) with different types of water and the corresponding background absorption.

The data, relative to the calibration curves, are given in appendix 3.

6.5.1 Sample Preparation

For each of the calibration experiments, a fresh sample of water containing chlorine was made available, shortly before the start of each experiment, from an aqueous solution of sodium hypochlorite (BDH 23039-3L) a concentration of 26g/l measured as Cl_2. A solution of low concentration, typically 130mg/l was prepared by diluting 1ml of the original hypochlorite solution in 100ml of distilled water. A volume of 1ml taken from this dilute solution (130mg/l) was mixed with appropriate volumes of either tap water or distilled water, depending on the type of experiment carried out. Using this procedure, the error in the preparation of the samples was reduced to a minimum.

The concentration of chlorine present in each sample was measured for calibration purposes using a DPD method which relied on the reaction of chlorine with a dye (N,N-diethyl-P-Phenylenediamine) to produce a red (Wurster's red) coloured solution. Light absorption at a wavelength of 560nm was related to the concentration of chlorine expressed in Cl_2 form. Cross-reference measurements of the chlorine in each sample were made using a water industry approved method (Dr Lange instrument LASA+ supplied by Robin Instruments Ltd.). The resolution of the instrument corresponded to ±50µg/l. This corresponded to ±25µg/l of chlorine when measured as OCl^-.

6.5.2 Stability of the Electronics

A sample of pure distilled water was used to investigate the response of the electronics over an extended length of time; this reduced the possibility of interference by any external element. The pump was disconnected, the optical cell was filled with water and the instrument functioned normally in all other respects. This experiment ran for 25 hours as shown in Fig.6.24. The readings were taken from the current output port. The stability of the instrument output was approximately 2%, for a signal of 8.15mA.

A series of experiments was then carried out in normal operating mode having first

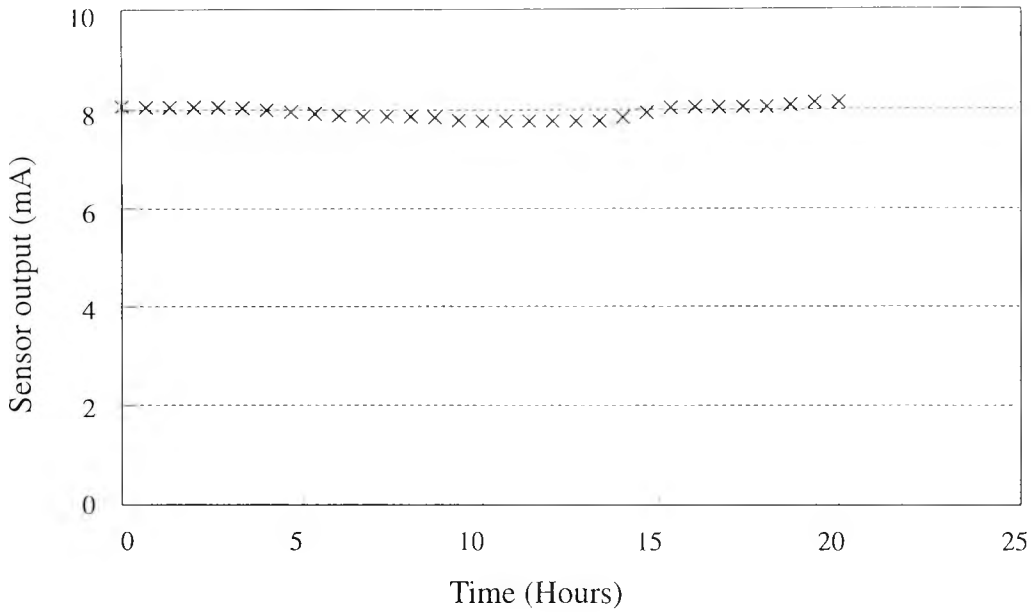

Fig. 6.24 Output signal from the RCM with distilled water maintained in the sample cell and the pump disconnected

established the stability of the equipment in the absence of sample interference. Results obtained with distilled water samples were reproduced within the stability error.

With tap water, however, the intensity of the transmitted signals decreased continuously with time although the ratio measurement remained constant. This effect was caused by the precipitation of particulates as the pH value of the sample was increased and when the instrument was left running for a long period.

6.6 Calibration Curves

The first calibration curve was established using a sample of distilled water to which different concentrations of chlorine were added in order to increase the concentration of chlorine present in the sample. The latter was then measured using the DPD test instrument. A polynomial least squares fit of the first order was computed resulting in the calculation of the first coefficient representing the intercept and the second coefficient representing the slope of the curve. This graph is shown in Fig.6.25 and is mathematically expressed in Eq.[6.19]

$$Y = 2.09 \ x + 2.94 \qquad [6.19]$$

where y represents the monitor output in arbitrary units and x is the concentration of chlorine expressed in mg/l. It was found that the standard deviation for this curve was

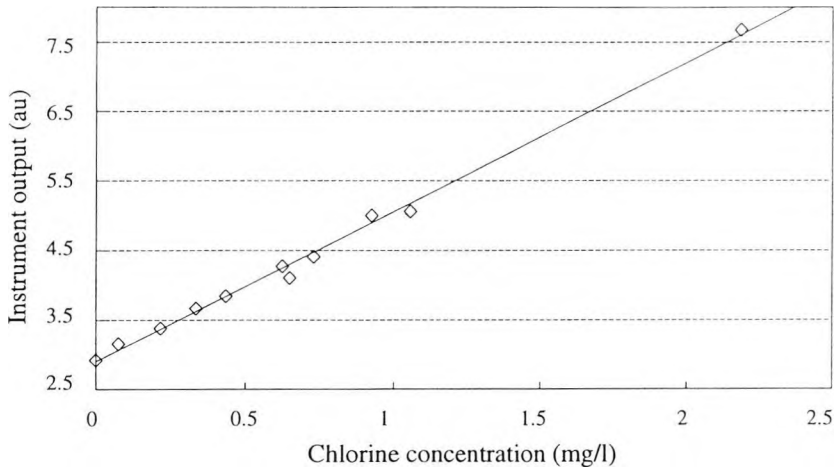

Fig. 6.25 Calibration curve of the RCM with a sample of distilled water for the range of 0 to 2.5mg/l.

0.07 u/mg/l with a relative error of 3% .

The above experiment was repeated in order to look at the consistency of the results. The curves obtained for the same range of concentration of chlorine was found to be within the error quoted, i.e. similar to the first one obtained (1.4% as the maximum error in the measurement).

Further experiments were carried out using tap water. The major difference between tap and distilled water is the presence of other elements that might in the short or long term affect the performance of the instrument.

When tap water was used the intensity of light reaching the detector was found to be half the intensity reaching the detector when distilled water was used. This was believed to be caused by high concentration of the nitrate ion present in the sample of tap water. The strong absorption peak centred in the vicinity of 200nm was seen to affect the transmission in the 290nm especially with a long optical path length of the optical cell.

A similar procedure was adopted in measuring the chlorine content of tap water and also in processing the acquired data. The mathematical expression which described the performance of the RCM for the calibration is given in Eq.[6.20]

$$y = 1.02\,x + 2.98 \qquad [6.20]$$

where x is the concentration of chlorine expressed in mg/l and y in arbitrary units. The

standard deviation for this experiment was found to be 0.03 u/mg/l. Even though, the intercept value was similar to the intercept value of the distilled water, the slope however was found to vary by a factor of half for the same range of concentration of chlorine. The calibration curve is shown in Fig.6.26

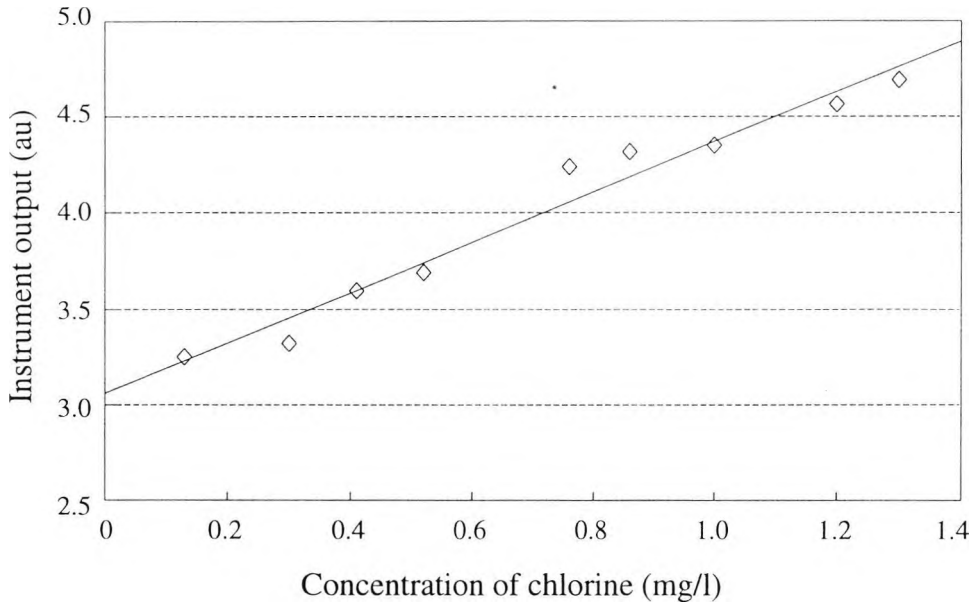

Fig. 6.26 Calibration curve on a sample of tap water for the range of 0 to1.4mg/l

A similar type of experiment was conducted in order to look at the slope value for a water sample which was made of different proportions of waters from different sources i.e. various mixtures of distilled water and tap water. As a consequence, the level of all the interfering elements' concentration were varied in the same proportion (mainly nitrate ion concentration).

In a first experiment a sample was made using a ratio of one (1) part of distilled water and two (2) parts of tap water. The same calibration procedure was carried out on the sample and a calibration curve was produced with the appropriate computation for the intercept and the slope. Similar experiments were carried out on mixtures of tap water and distilled water and the results were grouped in Table 6.1.

A graph relating the calibration curves of the residual chlorine monitor in the different types of water is drawn in Fig. 6.27. This emphasises the fact that all the curves pass through the same intercept within the expected error.

	Slope (U/mg/l)	intercept (U)	error
Distilled water	2.05	2.95	0.09
Mixture (3 vol D.W. to 1 vol tap water	1.63	2.95	0.06
Surrey area tap water	1.32	3.02	0.03
London tap water	1.02	2.98	0.03

Table 6.1 Table representing a summary of the different coefficients of the best fit calibration curves

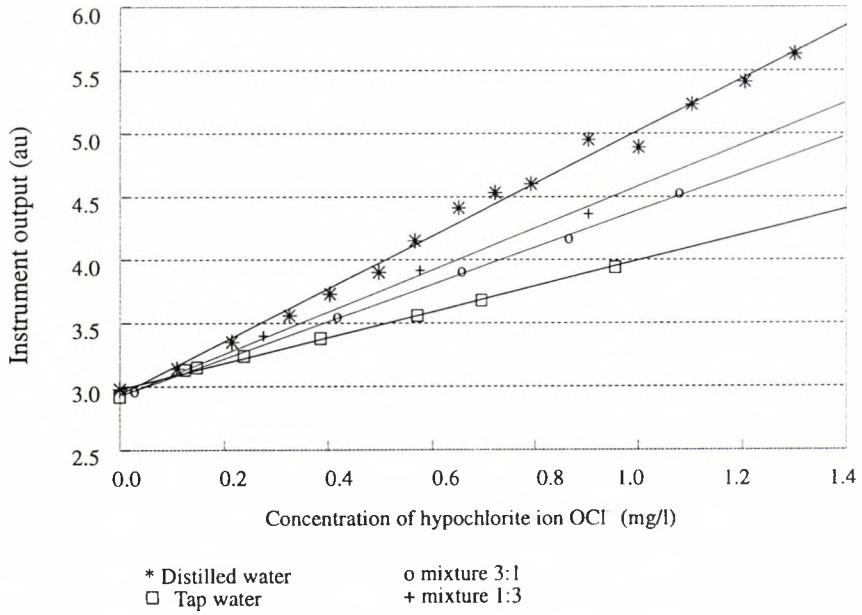

Fig. 6.27 Calibration curves of the RCM for different water samples

6.7 Effects of Various Types of Water

On the basis of the calibration curves determined using different samples of water, it was found that the slope of the best fit line varied with the type of water. The source of this problem resides in the fact that the dynamic range of the instrument for a fixed range of the concentration of chlorine is a function of the reference signal whose value is expressed in the Beer-Lambert law as P_o. This can be simulated by computing the graph of the instrument output as a function of the concentration of chlorine and varying the reference value for every set. The response of the instrument as a function of the concentration of chlorine can be expressed as follows:

$$\text{Log } P/P_o = - \varepsilon \, l \, C$$

Since the relation between the P_o and the reference light intensity e.g. P_{ref} is given as:

$$p_o = \psi p_{ref} \qquad [6.21]$$

where ψ represent the coefficient of proportionality between the initial light source intensity and the reference light intensity. Hence, ψ is a function of the background absorption. Consequently, when the background absorption varies, the dynamic range of the measurement varies, hence the variation of the slope. However, for a fixed type of water only one calibration curve applies.

$$\frac{p}{p_{ref}} = \psi \, 10^{-\varepsilon l C_{OCl^-}} \qquad [6.22]$$

The measurement of the value y can be used to determine which slope of the calibration curve to use to compute the value of the chlorine concentration. Hence, this determines the relationship between the background absorption and the slope of the correct calibration curve. For this, the background value was used to obtain an equation where the value of the slope is computed and determined. This is given in Eq.6.23

$$y = (2.45\, x + 5.82)\, x\, 10^{-4} \qquad [6.23]$$

Although the error on the slope of this curve is relatively high, (up to 8%), it can be used to obtain the right value for the concentration of chlorine. This equation can be utilised to determine which particular calibration curve is to be deployed on any particular type of water.

6.8 Long Term Operation

The residual chlorine monitor has been assessed for long term operation to look at the mechanical and optical problems that are usually generated by evaluating the prototype in situ rather than in the laboratory. These problems help in redesigning the proposed prototype so that it overcomes or minimises the effects of such problems when left to run in an unattended manner or monitored by non specialised personnel. This was necessary to achieve because most of the real life problems were not encountered during the design and the calibration of the prototype. These problems, which were not foreseen due to the lack of data, were mostly related to the functioning of the prototype in a harsh environment. Moreover, these problems were identified and solutions were then proposed for subsequent modifications to the prototype. Their implementation was not fully completed because a

further sponsorship was not available at that time. In Fig 6.28 and 6.29 continuous data are given, representing the variation of the RCM output as a function of time. This was cross-referenced to a potentiometric residual chlorine monitor equipped with digital hardware and software to ignore transient variations of the chlorine concentration.

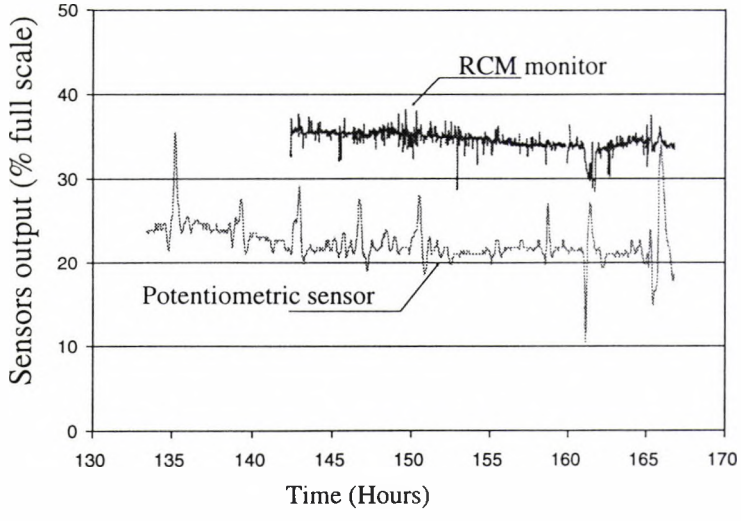

Fig. 6.28 Long term running data of the residual chlorine monitor whose output is compared to an electro-chemistry based chlorine monitor. (sample being tap water at the treatment plant)

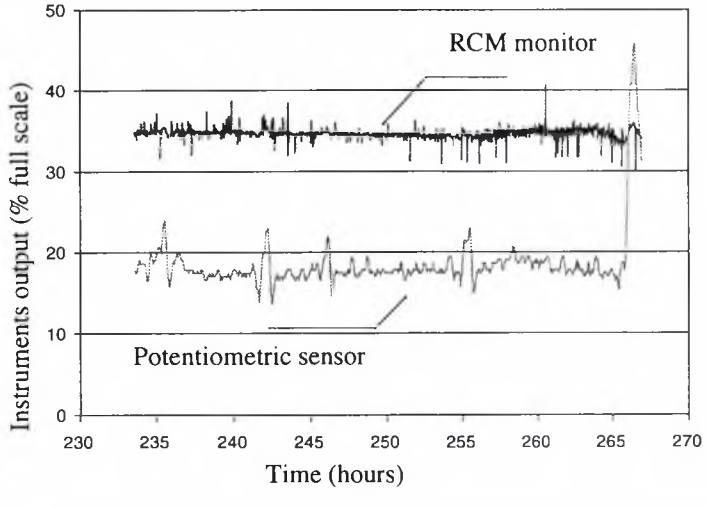

Fig. 6.29 Long term running of the residual chlorine monitor whose output is compared to an electro-chemistry based chlorine monitor. (acid wash data suppressed)

These problems are summarised as follows:

1) Due to the nature of the water at the distribution point of the water processing plant the mechanical section suffered most of the problems encountered. Deposition of particulates on the tubing wall and more important the optical cell wall, resulted in the

total loss of light transmission after a period of time of 10 to 12 hours. A cleaning procedure triggered by a timer was then implemented. It consisted of mixing a concentrated volume of hydrochloric acid with the sample which was allowed to flow through the mixing chamber, the optical cell and then through the sample tubing in the pump . This was found to be effective in cleaning the cell walls and extending the life of the sample tubing. It was also found that it reduced the deposition of any contaminant in the light path. However the measurements taken when the acid wash was activated were meaningless since the sample was not conditioned appropriately and appeared as spikes on the recorded data usually going downwards. An additional sample and hold device physically implemented at this location would be used to hold the signal during which period the acid wash is activated. This would remain in hold mode until the acid wash is deactivated e.g. between 1 and 2 minutes.

2) The silicone tubing used for the sample was not suitable for peristaltic pumps. The elasticity of the silicone rubber diminished after just a few working weeks. Moreover splitting of the tubing caused water leakage after an average of two working weeks. This was believed to be caused by microscopic crystallisation of calcium and magnesium occurring after precipitation and these punctured the tubing wall owing to the continuous pressure of the rollers of the pump. A new tubing material was chosen and consisted of Tygon. It was harder than silicone rubber and this loaded the pump slightly but its elasticity remained almost constant for a longer period of time.

3) The tubing used for the addition of reagents which were made of a different material namely Tygon, maintained their flexibility. However it was found that the effect of the rollers on the tubing not only compressed the tubing but pulled it out of the pump cassette. A hard plastic stopper glued on the external surface of the tubing was able to reduce this effect. However, sometimes it was responsible for blocking the tubing, especially because of the reduced internal dimensions of the tubing. Consequently, the flow of reagent was stopped.

Another source of problems was the small diameter of the reagent tubing (0.25mm). Although blockages only occurred a few times they resulted in starving the sample from the reagents necessary for the conditioning of the sample. This problem was observed to occur when reagents like sodium hydroxide were left in contact with air for a long time while the instrument was inactive. It also occurred when the pump rollers were left pressed on the tubing for long periods of time without the pump being activated.

Additionally, using a heat shrink material was found to be unsatisfactory when used to

join the different sections of a the reagent tubing. Heat shrink material became stiff once heated and was not as flexible as the tubing material and hence a difference in movement between the two material was at the origin of the problem of air bubbles being pumped into the mixing chamber.

4) Air bubbles which resulted from the high flow rate of the sample disturbed the measurement. Large air bubbles were cleared rapidly whilst the ones that were trapped in the mixing chamber or in the overflow broke into small air bubbles which were then guided through the sample cell by the flow of the sample. This resulted in a false measurement of light transmission. Hence the error detector did not trigger the alarm signal although the signal transmission decreased in intensity. The level of light intensity was not low enough i.e. below the threshold error level signal to activate a malfunction alarm signal.

5) When an error occurred during the absorption cycle, the output reading on the display was 10.07 and the output signal through the current port was 20mA. This was caused by the fact that when the error signal was triggered, the value of the detected signal was around zero. The output of the divider was zero and hence the logarithmic amplifier converted this value to -12V. This effect persisted for the whole measurement cycle. On a continuous measurement basis this looked like spikes.

6) A further problem occurred when one of the reagent pots was empty. The air was being pumped into the mixing chamber. This was not detected by the electronic circuit to stop the pump since it understood the error as being an air bubble in the system. In this case level detectors in each reagent pot would be sufficient to detect the low level of the reagent and trigger through a set of logic gates an alarm signal so that the instrument is stopped and the source of error is known.

Most of these problems were overcome by changing the set-up in a manner to reduce the effect of the described problems. The acid wash timer was incorporated as a separate module however no precaution was taken to stop the data varying when the acid wash was active. Hence removal of the data obtained during malfunctions was necessary for a proper evaluation.

6.9 Analysis of Results and Discussion

The calibration graph resulting from the data shown provides the "best fit" curve for these data. The slopes and intercepts of each graph have been calculated and represented as a

plot of instrument output versus concentration of chlorine, measured as OCl^-. The relative error for each data point and the standard deviation for the graphs showed that there was consistency in the relationship between the output of the instrument and the chlorine concentration. The instrument output varied linearly with chlorine concentration within the calculated errors. For distilled water the slope of the curve was 2.09 u/mg/l (u represents the output of the display and is an arbitrary unit) and the maximum relative error was 3%. Higher errors were found to occur with a relatively small probability. The errors in the slope of the calibration curve were used to calculate the error in the instrument output which in turn was utilised to calculate the error in the measurement of chlorine concentration occurring in practice. These were calculated and found to be ±0.1mg/l.

6.10 Cost Estimation

The residual chlorine monitor design and implementation was carried out over a period of 18 months. However, the time required for the research and development of the basic principles which were carried out prior to the imlementation was approximately 12 months. This included all aspects of design and testing. Hence the overall cost of the instrument does not take into account either the time taken to develop or to implement the instrument but rather the cost of components used. Although this does not give the right idea about the cost of the instrument since most of the components are more expensive when bought on a single unit basis, it however gives an approximate idea about the range of price at which the instrument would come to. For example a single optical filter, custom designed, costed approximately over £1,000 while five units of the same item would have costed ~£1,400. For this reason only a list of components that were used is given in Appendix 4, and a total cost is also appended.

6. 11 Conclusions

The set of experiments carried out in order to calibrate the Residual Chlorine Monitor was conducted with a variety a water samples. Multiple calibration graphs were then computed from data obtained in the different experiments. It was found that the measured optical properties of chlorine were slightly modified by different types of waters. A set of additional experiments led to the following conclusions:

Information about the type of water was needed in order to establish the appropriate calibration curve to use for a particular type of water. Although all the computed calibration

curves had a common point (at zero concentration), the slopes of these calibration graphs were different. The overall error for each particular type of water was found to be no more than 3%. A long term run (maximum of two weeks) was conducted to look at the different problems that might arise from such lengthy use and it was found that although distilled water did not create any problem, tap water, because of its composition, eventually modified the optical properties of the sample to the point where the signal was completely absorbed. Since it is known that precipitation of calcium and magnesium ions usually cause this problem, a complexing agent (calgon) was used to hold them in solution thus reducing the amount of precipitation that would occur. The stability of the Residual Chlorine Monitor which measures the concentration of chlorine as the OCl^- ion was found to be around 4% of scale at zero concentration.

Chapter 7

Conclusions

7.1 Summary of Work Carried Out and Significance of the Results

In order to fulfil a need in the water quality monitoring area, the work described in this thesis investigated the use of absorption of light in the visible and ultraviolet part of the spectrum for the monitoring of the concentration of chemical species dissolved in aqueous solutions. This formed the basis of the transducing principle on which the required fibre optic chemical sensors were designed. Fibre optics were used as an essential part of the sensor to provide flexibility in the design, possibility of monitoring various species remotely and a decrease in the health hazards and interferences that can affect either the user or the measurement. Additionally, the transducing effect is purely optical, hence no electrical connection to the sample is required. This is a major advantage especially in medical and potentially hazardous applications such as measurements in sewers.

Two different methods have been investigated both based on the Beer-Lambert law which is used to relate the concentration of the chemical species to its absorption of light at a convenient wavelength. The first approach was based on an indirect monitoring of the chemical species and was implemented using phenol red indicator dye to measure the concentration of the hydrogen ions, whereas the second approach comprised monitoring directly the concentration of the chemical parameter itself and was implemented by measuring the absorption of chlorine in its hypochlorite form, utilising the UV part of the electromagnetic spectrum. The advantage of the indirect method was shown to consist of the high sensitivity of the measurement as a result of the high value of the coefficient of extinction of the dye. Additionally, hydronium ion concentration cannot be be measured directly because it does not absorb in the visible part of the spectrum but it was still possible to use the same part of the spectrum in order to monitor it indirectly. However, when the indirect method was used to measure the pH of the sample, it showed a distinct disadvantage

namely a limited range of the measurement e.g. ±1 pH units. This is not attributed to the method used but rather to the logarithmic relationship between pH and absorption of light by the indicator. However, the measurement range can be extended by using a universal indicator dye combination, but multiple light sources would then be required. Another drawback of this particular application resides in the non-linearity of the measurement which made the use of a calibration curve difficult, although this could be overcome by memorising the calibration curve and relating the ratio measurement by comparing it with the curve in memory, but this would necessitate the use of digital design circuitry. The sensor becomes then complex which was not the aim of this work. The calibration curve was shown to be approximated to a linear curve when the measurement occurred around the inflexion point where the error due to the non-linearity of the response of the instrument was minimal.

The error analysis made in Chapter 3 showed that the resultant error in this type of measurement can be as low as 0.001pH units. This can be achieved with signal to noise ratios in the order of 40 to 50 dB. However, an additional error is introduced in the system because the measurement is affected by the ionic strength of the sample. Although, this error is negligible when the sample is dilute, it can be as large as 0.02 pH units in concentrated samples. Consequently, the absolute measurement of pH would not be as accurate as the relative measurement. Moreover it is the measurement of the variation of pH that is more important in practical situations.

From the implementation point of view, it was shown that a self referenced system based on the use of the fluorescence of ruby for referencing the measurement is an attractive approach. The advantage of this scheme consisted mainly of the fact that any external interference affects both the sensing and referencing wavelengths with the same factor. The resolution of the system i.e. ± 0.05 pH units, was found to be similar to the system using an external referencing scheme designed and implemented in the same body of work. However, the self referenced system needed an enhanced digital signal processing scheme in comparison to the simple analogue signal processing used in the first implementation. The major advantage of using the self referenced system resided in the fact that provision was made for minimising the effect of any ageing and (or) light intensity fluctuation occurring during the measurement.

In comparison, in the direct method there was no need to use dyes. For example, the

monitoring of chlorine in its hypochlorite form was based on the sensing of the variation of the intensity of a wavelength in the ultraviolet part of the spectrum. However, an inconvenience in the latter method resided in the fact that a far longer path length was needed in order to measure the concentration of the species at very low concentrations e.g. 0 to 1mg/l. This was necessary because the value of the coefficient of extinction of chlorine was small. However, the advantages of this method are the simple design of the on-line monitor as described in Chapter 6, and the use of economically cheap and less health hazardous reagents. However, the use of such reagents makes remote monitoring more difficult and costly.

It was shown in the spectral analysis that, independent of the form in which the chlorine occurred in the water sample, it was possible to measure its concentration by converting chlorine into a highly absorbing form e.g. hypochlorite ion, through a control of the pH value of the sample i.e. by increasing it to a value larger than 9. In doing so, the effect of temperature on the conversion process was minimised. Additionally, the reference signal was obtained by chemically removing the chlorine and measuring the background absorption at the same wavelength as the one used for sensing the chlorine concentration. This has the advantage of not introducing additional errors since no assumptions regarding the behaviour of the sample at other wavelengths need to be taken into account. In order to make the measurement possible in all types of water, further sample conditioning was necessary. Sodium hexametaphosphate ("calgon") was mixed with the sample prior to the addition of sodium hydroxide to reduce the effect of precipitation, and an acid wash was performed intermittently to clean the optical cell. The resolution of the measurement in this implementation was found to be a function of the average noise level in the detected signal and an SNR in the order of 30dB was achieved. This was not found to be the optimum SNR and it was shown that this could be improved by using different signal processing schemes i.e. lock-in amplifier techniques. However, with the original implementation, a resolution of ± 100 µg/l chlorine concentration was achieved and was found to be within the required specification.

The field trial results demonstrated that there are still engineering problems that need to be solved such as the clogging of the reagent lines and the fast ageing of the tube used in the peristaltic pump. However, even so, these results also show that the instrument was able to perform successfully for a limited period e.g. 14 days, and that a ±3% stability factor was obtained during this time. This highlights the fact that such sensors are reliable

for field as well as laboratory use.

The design and construction of chemical sensors using the absorption of light in either the visible or the ultraviolet part of the spectrum demonstrated that better performance resulted from combining fibre optic technology and spectral analytical methods. The fibre provided a large degree of flexibility in the design of the instrument and interference free automated sensors were produced at reasonable cost, but with performances comparable with those obtained with conventional methods.

The work also showed that the practicability of a method for the basic design of the sensor is largely dependent on the species and the value of their coefficient of extinction. Moreover, the use of dyes can enhance the sensitivity aspect but does introduce additional errors caused by interfering molecules. This effect was shown to be very small in the direct approach as a result of the referencing scheme as was implemented in the present work. One of the major conclusions of this work is that it highlights the existence of a large number of possibilities where remote sensing could become widespread and could be a major factor in increasing the safety and cost aspects, as well as increased convenience in the measurement.

7.2 Future Work

It has been shown that the use of optical fibres in the measurement field is as potentially interesting as in the communication field and has various application opportunities. However, sensors nowadays, as has been shown in this study, are lacking portability and can be costly when used for the measurement of a single parameter. Consequently, there is more work to be done in the field of multi-parameter monitoring. The latter provides a convenient means of measurement of various chemical species especially the ones that share, the same optical characteristics. Distinguishability between each chemical species could be obtained through the use of different reference schemes. Absorption of light represents the simplest approach to monitor the concentration of chemical species dissolved in water. However this does not exclude other methods or a combination of these such as the opto-acoustic methods. At the present time the absorption technique is being investigated in order to design a fibre optic multi-parameter chemical sensor to measure the concentration of ammonia, organic matter and nitrate ions with the same sensor.

The need for sample conditioning has been shown to be a necessity not only to remove the

interference effect of species present in a sample, but also to use the special characteristics of the chemical species under investigation in conjunction with absorption techniques. The present implementation of the sample conditioning is usually effective. However, the need to use less sample conditioning is an advantage since the water and water using industries require instrumentation which needs less attention. This is because of the high cost of running the instrument and the qualified personnel assigned to maintain it. Also, the large quantity of reagents required and their instability is a major drawback. For instance, the use of ion exchange techniques either to remove interfering molecules or for conditioning of the sample is becoming a practical answer to current problems. A future orientation of the work in this field would lie in the development of techniques where reagents would be generated from the sample itself such as in the case of monitoring ammonia where the only reagent is chlorine and this can be generating the chlorine on-site by electrolysis of saline water.

A significant improvement would result from the use of solid reagents that would dissolve in order to condition the sample for the appropriate measurement technique. Solid reagents were assessed but were found to be inadequate in the particular case of the chlorine monitor. They could be developed further to enhance their chemical and physical properties and would be valuable.

Electronic signal processing can also be enhanced by using techniques such as the lock-in amplifier which, by shifting the working frequency and reducing the bandwidth of the signal, a better SNR can be achieved. For example in the residual chlorine monitor, the output signal was used to compare the efficiency of improvement of SNR and it was found that a 12 dB enhancement was obtained. Consequently, by increasing the SNR value the sensitivity of the measurement was improved. However, this improvement in the SNR would not necessarily produce better sensitivity when the SNR was larger than 50dB. Furthermore, digital techniques for both signal processing and the building of intelligent sensor systems may be used to enhance the resolution of the measurement and to provide control of all the different parts of a sensor. Such devices could be self calibrated and self referenced to ensure that the data result from good working order of the sensor rather than intermittent faults.

In conclusion, overall the work described in this thesis demonstrates quite clearly the value of light absorption measurement utilising optical fibre based sensors in the field of monitoring molecular species in aqueous environments.

List of Publications

1 Grattan, K.T.V., Mouaziz, Z.and Palmer, A.W., (1987), "Dual Wavelength Optical Fibre Sensor for pH Measurement", Biosensors, Vol.3, No.1, p17-25.

2 Grattan, K.T.V., Mouaziz, Z.and Selli, R.K., (1987), "pH Sensor Using an LEDsource in a Fibre Optic Device", Paper presented at The Netherland Congress Centre, The Hague, The Netherland, 30 March- 3 April 1987.

3 Grattan, K.T.V., Mouaziz, Z., Palmer, A.W. and Selli, R.K., (1987), "Developement of Simple pH Sensors for Use in Acid-Base Titrations", J. Optical Sensors, Vol.2, N0.5, p-0-11

4 Briggs, R., Grattan, K.T.V., Mouaziz, Z. and Elvidge, T., (1990), "On-Line Monitoring of Residual Chlorine", In Advances in Pollution Control Instrumentation, Control and Automation of Water and Wastewater Treatment and Transport System, Ed. by Briggs, R., Pergamon Press, Oxford, U.K. p-39-49.

5 Briggs, R., Mouaziz, z. and Grattan, K.T.V., (1991), "Design and Implementation of a Prototype Optically Based On-Line Residual Chlorine Monitor", Internal Report To Severn Trent Plc.

6 Mouaziz, Z., Briggs, R., Hamilton, I and Grattan, K.T.V., (1993), "Design and Implementation of a Fibre-Optic based Residual Chlorine Monitor", Sensors & Actuators-B Chemical, Vol.11, p-431-440.

Appendix 1

Noise Performance of Detectors

A1.1 Limit of Detection

There are different types of detector-amplifier combinations which are used for the purpose of light detection namely low impedance and high impedance front end and the transimpedance amplifier. Each configuration has its advantages and limitations in terms of the noise and bandwidth performance. However, there is no single configuration that can be used for all purposes. For instance, in communication, large bandwidth and low noise performance of detectors are necessary. In this case, emphasis is put on the large bandwidth requirement to achieve signal transmission of the order of gigabit/sec.

In the field of sensing, the requirements are different and are case related. For instance, in the work described in this application, a maximum bandwidth of the order of 100kHz is required. The performance of the detector in terms of noise and sensitivity is more important. The latter factor is what defines the ultimate sensitivity of a particular implementation and is also related to the limit of detection of a measuring instrument. For this analysis, Signal to Noise Ratio (SNR) is a measure which is used to differentiate between the signal amplitude and the associated noise level. The value of the minimal detectable signal is a function of the SNR of the signal. This can be shown by plotting the minimal detectable concentration of the chemical species as a function of SNR computed by using the Beer-Lambert laws shown in Eq.A1.1:

$$Log\left(\frac{p_o - p_{noise}}{p_o}\right) = -\varepsilon\, l\, C_{\min} \qquad [A1.1]$$

The smallest variation that can be detected is (P_o - P_{noise}) and corresponds to the limit of detection of the detector C_{min} and ε and l are the coefficient of extinction and the path length respectively. The variation of the minimal detectable concentration which is logarithmic, decreases with decreasing SNR as shown in Fig.A1.1.

The variation of the minimal detectable concentration becomes relatively small when the SNR value reaches 40dB. However, as this is a function of the coefficient of extinction of

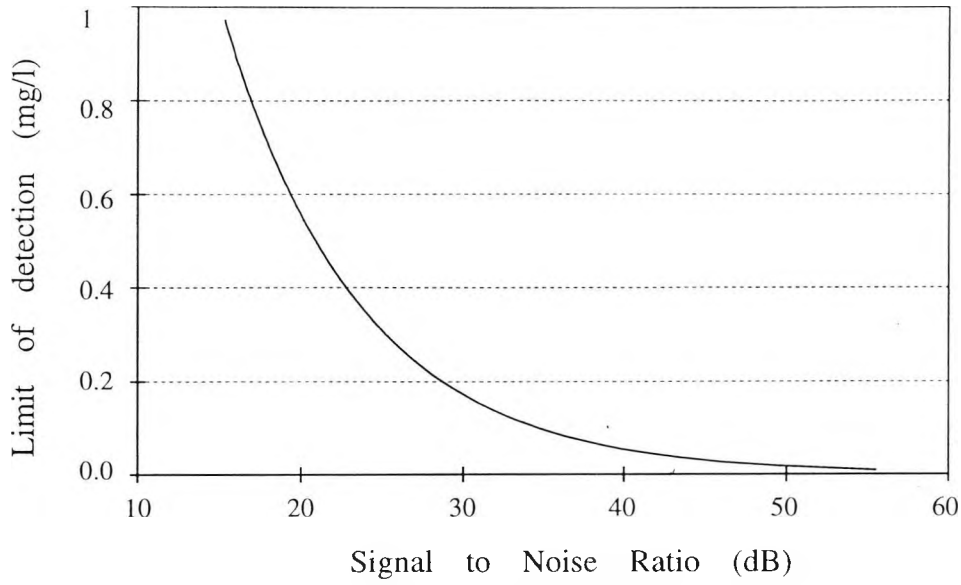

Fig. A1.1 Variation of the minimal detectable concentration as a function of the SNR

the chemical species the limit of the SNR value will depend on the factor (1/20εl).

A1.2 Detector-Amplifier Configurations

In the following detector configurations, the basic element used to convert the photocurrent generated in the photodiode into a voltage form consists of a resistor. Ideally, the circuit is drawn so that all the current which is proportional to the light intensity flows through the resistor. However, this is not the case since the amplifier front end requires biasing and hence a small portion of the photocurrent is used for this purpose. A second limiting factor is the inherent capacitance of both the diode and the amplifier which tends to degrade the frequency response of the detector.

A1.2.1 Low Impedance Front End

This circuit is shown in Fig.A1.2. The noise generated in this circuit is proportional to the value of the parallel impedance made from the load and the input impedance of the amplifier.

$$\langle i^2 \rangle = \frac{4kTB}{R_{comb}} \qquad [A1.2]$$

where R_{comb} is the parallel impedance of the load and the amplifier input impedances, k, B and T are Boltzman constant, bandwidth and the temperature respectively.

Because of the low value of the input impedance of the amplifier, the dominating noise is

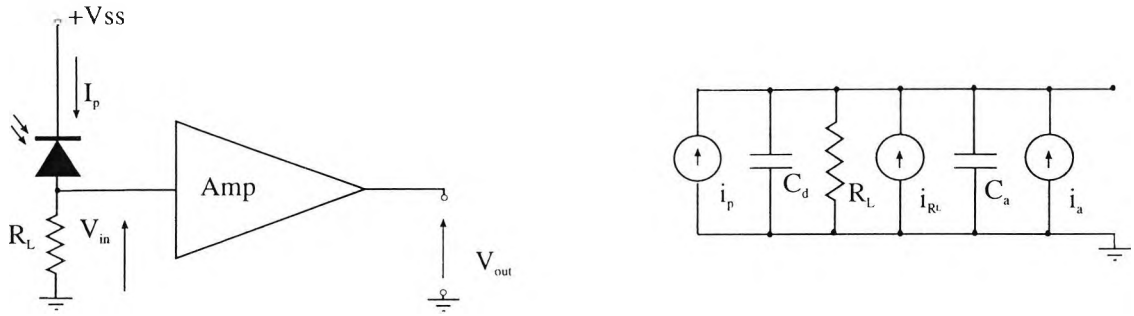

Fig. A1.2 Schematic diagram of the low and high impedance front end amplifier

the thermal noise compared with the noise of the diode which is given by Eq.A1.3

$$\langle i_d^2 \rangle = 2eB(I_p + I_d) \qquad [A1.3]$$

where I_p is the photocurrent, I_d is the dark current current (generated by current leakage in the photodiode), B is the bandwidth and e is the electrical charge of the electron.

A1.2.2 High Impedance Front End Amplifier

This circuit is similar to the previous circuit with a high input impedance of the amplifier. the input to the amplifier is taken from the bias resistor as shown in Fig.A1.2 as a voltage signal and is buffered and then amplified. Because of the high input impedance of the buffer, the thermal noise is reduced considerably. However, the bandwidth of the circuit is severely limited especially with higher values of photodiode capacitance.

A1.2.3 Transimpedance Amplifier

This circuit is used to convert the photocurrent signal into a voltage signal by using a resistor in the feedback loop of the amplifier. This configuration, which is shown in Fig.A1.3, has a number of advantages compared to the two other circuits described previously.

a) The bandwidth of the detector is increased for similar characteristics of the detector and is a function of the combination of factors such as the Gain Bandwidth Product of the amplifier (GBP) and the capacitance of the diode. However, the bandwidth of the detector is increased by decreasing the value of the feedback resistor which then increases the thermal noise as shown in Eq.A1.4

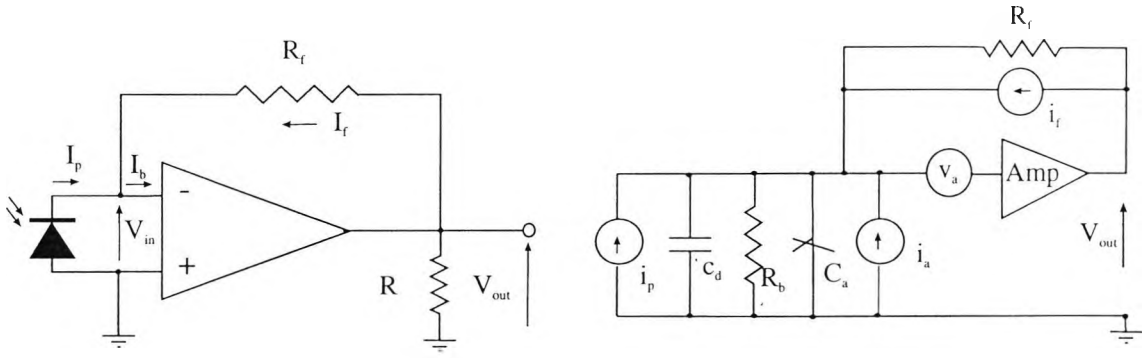

Fig. A1.3 Transimpedance configuration of the detector and its equivalent circuit

$$f = \sqrt{\left(\frac{GBP}{2\pi(C_d+C_a)R_f}\right)} \qquad [A1.4]$$

where C_d and C_a are the diode and amplifier capacitances and R_f denotes the feedback resistor.

b) The load effect on the diode is reduced and is inversely proportional to the open loop gain of the amplifier. R_f represents the feedback resistor in the transimpedance amplifier circuit and R_{fl} is the resistor in the low or high impedance front end. Ohms law is used to describe the input impedance of the transimpedance circuit :

$$R_{fl} = V_{out} / I_{in} \qquad [A1.5]$$

If A is the open loop gain of the amplifier then | Voutl = A |Vinl, thus for the transimpedance circuit the load impedance is obtained in Eq.A1.6 and can be written as follows:

$$R_f = V_{out} / I_{in} \text{ and } R_f = AV_{in} / I_{in} \qquad [A1.6]$$

$$\text{Hence } R_{fl} = R_f/A \qquad [A1.7]$$

Therefore the load on the photodiode is reduced in the case of the transimpedance amplifier.

c) The output voltage of this circuit is proportional to the photocurrent with the approximation that the bias current of the amplifier is so low that it is negligible and also the large value of the open loop gain A. The voltage of the cell made of the voltage across the amplifier's input, across the feedback resistor and the amplifier's output can be described as in Eq.A1.7

$V_{out} - I_f R_f = V_{in}$ with $V_{in} = -V_{out}/A$

Hence the relation between the output voltage and the photocurrent can be written as follows:

$$V_{out}(\frac{A+1}{A}) = (I_b - I_p) R_f \qquad \text{[A1.8]}$$

provided that A is large and the input impedance of the amplifier is large (e.g. FET input amplifier), equation A1.8 becomes as in Eq.A1.9

$$V_{out} = - I_p R_f \qquad \text{[A1.9]}$$

A1.3 Amplifier Characteristics

In the transimpedance configuration the amplifier bandwidth and input impedance can degrade the overall performance of the detector. An investigation into the effect of the amplifier's characteristics on the noise level of the signal was carried out. For this, the detector was shielded to remove external interference and a measure of the noise level at the output port of the amplifier was obtained for exactly the same conditions i.e. same circuit and component values apart from the operational amplifier. The characteristics of the amplifier were mainly concerned with input impedance, GBP and the open loop gain value. It was found that the worse result i.e. higher noise level, was obtained with amplifiers having higher values of bias current with large bandwidth amplifiers. The amplifier which gave minimum noise level for a frequency of 60kHz was the Burr-Brown OPA 111 with a bias current of 0.5pA and a GBP of 2MHz. These results are summarised in Table A1.1.

A1.4 Conclusion

No conclusive evidence shows that there is a general procedure for configuring a detector system. Personics did conclude that for analogue systems and in the case the high impedance amplifier front end, lower noise level was obtained although with limited

bandwidth due to the capacitance of the diode amplifier combination. However, provided that the characteristics of the detector and amplifier are known, it is possible, to a certain extent, to establish the best operating conditions which can only be determined for a particular application (e.g. bandwidth, noise, sensitivity etc.).

Operational Amplifier	Noise level (mV)	Signal level (mV)	Open Loop Gain dB	Amplifier Noise ($nV/Hz^{1/2}$)	GBP (MHz)	Bias Current (pA)	Ratio S/N
AD711JN	19.0	145.8	100	18	4	15	7.67
OPA606LM	6.6	69.5	118	11	13	5	10.53
AD37GN	4.8	43.9	125	3	63	15	9.14
071	14.3	79.0	83	18	3	30	5.52
741	2.3	14.8	106	>18	1	80 000	6.4
CA3140E	17.4	76.8	100	48	4.5	5	4.41
NE5534	7.6	46.4	100	4	10	500 000	6.10
OPA 111	0.09	14.4	125	7	2	0.5	14.4

Table A1.1 Table showingm major parameters in operational amplifiers used in the measurement of the signal to noise ratio.

Appendix 2

Calculation of the Inflexion Point

The calculation of the position of the inflexion point is carried out by taking the second derivative of the relationship between light transmission and the variation of pH values of the dye. Mathematically, the inflexion point denotes the point for which the derivative of the curve changes sign and the solution of the equation $\frac{d^2x}{d\delta^2}=0$ provides a value at which the most linear part of the calibration curve occurs. For this, a simplification of the initial relationship between the light intensity and the pH as described in the system response, (e.g. Eq.A2.1) is necessary for simplicity e.g. $x=p/p_o$.

$$\log(x) = -\frac{m}{10^{-\delta}+1} \qquad [A2\text{-}1]$$

$$x = 10^{-m/(10^{-\delta}+1)} \qquad [A2.2]$$

Initially the first derivative of Eq.A2.2 is obtained in the following manner (Eq.A2.4):

$$\frac{dx}{d\delta} = -m \ln 10 \; 10^{-m/(10^{-\delta}+1)} \frac{d}{d\delta}\left(\frac{1}{10^{-\delta}+1}\right) \qquad [A2.3]$$

$$\frac{dx}{d\delta} = -m(ln10)^2 \frac{10^{-\delta}}{(10^{-\delta}+1)^2} \; 10^{-m/(10^{-\delta}+1)} \qquad [A2.4]$$

The second derivative as a function of the same variable is computed and is presented in a simplified manner by splitting the numerator and denominator as follows:

$$\frac{d^2x}{d\delta^2} = \frac{A-B}{(10^{-\delta}+1)^4} \qquad [A2.5]$$

$$A = -m(ln10)^2 (10^{-\delta}+1)^2 \frac{d}{d\delta}(10^{(-m/10^{-\delta}+1)-\delta}) \qquad [A2.6]$$

$$B = (-mln10^2)\,(10^{-m/(10^{-\delta}+1)-\delta})\,(-2ln10)(10^{-\delta})\,(10^{-\delta}+1) \qquad [A2.7]$$

$$\frac{d}{d\delta}(10^{(-m/10^{-\delta}+1)-\delta} = (\frac{mln10\ 10^{-\delta}}{(10^{-\delta}+1)^2} - 1)\ .\ 10^{(-m/10^{-\delta}+1-\delta)}\ ln10 \qquad [A2.8]$$

$$\frac{d^2x}{d\delta^2} = (-m\ln 10^3)\,(\frac{10^{(-m/10^{-\delta}+1)-\delta}}{(10^{-\delta}+1)^3})\,[(10^{-\delta}+1)\,(\frac{mln10\ 10^{-\delta}}{(10^{-\delta}+1)^2} - 1) + 2\ .10^{-\delta}] \qquad [A2.9]$$

The value of δ, satisfying the inflexion point condition, is then calculated by solving $\frac{d^2x}{d\delta^2} = 0$ hence, only the part between brackets is used for the calculation of the solutions. since the first part cannot be nil

$$(10^{-\delta}+1)\,(\frac{mln10\ 10^{-\delta}}{(10^{-\delta}+1)^2} - 1) + 2\ .10^{-\delta} = 0 \qquad [A2.10]$$

This equation can be rewritten as the following:

$$10^{-2\delta} + mln1010^{-\delta} - 1 = 0 \qquad [A2.11]$$

The solutions to this equation are determined following a normal procedure. The specific determinant of Eq.A2.11 is $\Delta = (mln10)^2 + 4$ is always positive and hence two solutions exist.

$$10^{-\delta} = -\ mln10 \pm \sqrt{(mln10)^2 + 4} \qquad [A2.12]$$

Only the positive result will be taken since the part under the square root is always larger than the first factor. Hence the coordinate of the inflexion point are given below:

$$\delta = -\log(-\ mln10 + \sqrt{(mln10)^2 + 4}\ ) \qquad [A2.13]$$

As a result, the value of δ= pH- pK, is a function of the parameter m as was already shown graphically in chapter 3. The negative sign of the solution shows that the inflexion point occurs at a pH value smaller than the pK value of the dye.

Appendix 3

Calibration Data of the RCM

Calibration of the Residual Chlorine Monitor was carried out utilising different types of water. Distilled Water (DW), was used initially, followed by tap water from different origins which was found to yield different behaviour from that obtained from DW. The data, relative to the calibration curves are given in the following tables and an analysis of the data (best fit curve, errors, standard deviation) for each table is provided.

A3.1Sample Preparation

For each of the calibrations a fresh sample of water containing chlorine was made available, shortly before the start of the each experiment. A stock solution (BDH 23039-3L, 26g/l) was used to prepare a diluted stock sample typically 130mg/l chlorine concentration prepared from an aqueous solution of sodium hypochlorite. A volume of 1ml taken from this dilute solution (130mg/l) was mixed with appropriate volumes of either tap water or distilled water, depending on the type of experiment carried out.

A3.2 Calibration With Distilled Water

Calibration procedure carried out on distilled water. The pH of the solution was monitored and was maintained at a pH value of approximately 10. The following data were obtained:

X(mg/l)	Y(U)	Abs(V)	Ref(V)	LSF	Res (E-2)	Relative error
1.300	5.63	4.32	6.06	5.64	+ 2.0	0.4 %
1.204	5.41	4.99	6.11	5.45	+ 3.5	0.6 %
1.102	5.23	5.07	6.12	5.23	+ 0.7	0.1 %
1.000	4.89	5.17	6.07	5.02	+12.9	2.6 %
0.903	4.95	5.15	6.07	4.82	-13.1	2.7 %
0.792	4.60	5.30	6.05	4.59	- 1.5	0.3 %
0.722	4.53	5.32	6.03	4.44	- 8.6	1.9 %
0.650	4.41	5.38	6.04	4.29	-11.6	2.7 %
0.565	4.15	5.45	5.96	4.12	- 3.5	0.9 %
0.496	3.90	5.57	5.99	3.97	+ 7.1	1.8 %
0.403	3.73	5.70	6.06	3.78	+ 4.7	1.2 %
0.325	3.56	5.79	6.07	3.61	+ 5.7	1.6 %
0.214	3.35	5.88	6.02	3.38	+ 3.5	1.0 %
0.108	3.14	6.04	6.08	3.16	+ 2.2	0.7 %
0.000	2.98	6.18	6.16	2.94	- 4.1	1.4 %

(X) represents the concentration of chlorine as OCl^-, (Y) is the output of the instrument, Abs. is the absorption signal, Ref. is the reference signal, Res is the residual e.g difference between the fitted curve and the real data and LSF is the least squares fit.
A Polynomial Least Squares Fit of the first order was calculated and the two resultant coefficients for the least squares approximation were:

Coefficient 0: 2.937 and Coefficient 1: 2.085 and Standard Deviation : $\sigma = 0.07$ U/mg/l.
The above data fit a Linear equation of the following nature:

$$Y = 2.09\ X + 2.94 \qquad [A3.1]$$

where Y is the instrument output (u) and X is the concentration in mg/l

The calibration graph resulting from the data shown provides the "best fit" curve for these data. The slope and intercept of each graph were calculated and represented as a plot of instrument output versus concentration of chlorine, measured as OCl^-. The relative error for each data point and the standard deviation for the graphs show that there is consistency in the variation of the output of the instrument versus the chlorine concentration. The relation of instrument output varies linearly with concentration within the calculated errors. For distilled water the slope of the curve was 2.09×10^{-3} u/µg/l (u represents the output of the display and is an arbitrary unit) and the maximum error in this experiment was 3%. Larger errors (2.7% , 2.6% and 2.5%) occurred only a few times from a set of 15 samples. The average relative error was 1.3% with a standard deviation of 0.07.

A3.3 Calibration with Tap Water

In this calibration, the water sample was from tap water and the range of chlorine concentration used was in the range of 0 to 1mg/l. X is the concentration of chlorine (OCl^-) and Y is the output of the instrument in arbitrary units, Abs. is the absorption signal and Ref. is the reference signal. The following data points were obtained:

X(mg/l)	Y(V)	Abs(V)	Ref(V)	L S F	Res	Relative error
0.955	3.94	5.50	6.03	3.95	9.8E-03	0.3 %
0.695	3.68	5.57	5.94	3.68	4.5E-03	0.1 %
0.570	3.56	5.42	5.72	3.56	1.9E-03	0.1 %
0.385	3.38	5.46	5.65	3.37	-5.1E-03	0.2 %
0.237	3.24	5.37	5.49	3.22	-2.2E-02	0.7 %
0.147	3.15	5.12	5.18	3.13	-2.2E-02	0.7 %
0.123	3.13	4.87	4.90	3.10	-2.4E-02	0.8 %
0.000	2.92	4.93	4.45	2.98	5.8E-02	2.0 %

A Polynomial Least Squares Fit of the first order was calculated and the coefficients in the least squares approximation were obtained:

Coefficient 0: 2.977 and Coefficient 1 : 1.021 and Standard Deviation : $\sigma = 0.03$ u/mg/l

The above data fit a Linear equation of the following nature:

$$Y = 1.02\ X + 2.98 \qquad [A3.2]$$

Y is the output of the instrument in arbitrary units X is the concentration in mg/l

A3.4 Calibration with Various Water samples

(X) is the concentration of chlorine (OCl^-) and (Y) is the output of the instrument in arbitrary units, Abs. is the absorption signal and Ref. is the reference signal. The data are presented below:

X(mg/l)	Y(U)	Abs(V)	Ref(V)	LSF	Residual	Relative error
2.150	5.89	2.40	3.08	5.85	-3.8E-02	0.7 %
1.110	4.51	2.54	2.88	4.51	8.3E-03	0.2 %
1.050	4.42	2.57	2.88	4.43	2.1E-02	0.5 %
0.920	4.20	2.56	2.81	4.27	7.4E-02	1.7 %
0.710	3.98	2.64	2.85	4.00	2.5E-02	0.6 %
0.670	3.89	2.72	2.92	3.95	5.8E-02	1.5 %
0.473	3.75	2.66	2.82	3.69	-5.2E-02	1.4 %
0.378	3.69	2.65	2.81	3.57	-1.1E-01	3.1 %
0.266	3.45	2.78	2.86	3.43	-1.6E-02	0.5 %
0.088	3.24	2.79	2.81	3.20	-3.4E-02	1.1 %
0.000	3.03	3.00	3.02	3.09	6.5E-02	2.1 %

A Polynomial Least Squares Fit of the first order was calculated and the coefficients in the least squares approximation were obtained:

Coefficient 0: 3.0922 and Coefficient 1 : 1.283

Standard Deviation : $\sigma = 0.06$ u/mg/l

The above data fit a Linear equation of the following nature:

$$Y = 1.28\ X + 3.09 \qquad [A3.3]$$

Y is the output of the instrument in arbitrary units and X is the concentration in mg/l

From the results obtained, the absorption by the chlorine in tap water was found to be different from that in the distilled water, as the tap water background absorption is increased due to the presence of other absorbing material in the water, for example nitrate ions, traces

of organic matter and turbidity. The average error was found to be 1.2% whilst, the maximum error was found to be 3.1%. The standard deviation for these data was 0.06.

A3.5 Relationship Between the background absorption and the Slope

Data have been collected in order to examine the effect of background absorption. More data are required in order to explain this phenomenon and to define more precisely the degree of correlation between the sensitivity of the measurement and the background absorption. The reference data (X) are the average values for the reference signal during one experiment and the slope (Y) is the slope of the best fit curve for that experiment.

X(V)	Y (U/µg/l)E-4	L.S.F.	Residual	Relative error
2.886	13.060	0.001	-1.7E-05	1.3 %
3.239	13.240	0.001	5.1E-05	3.7 %
4.226	17.620	0.002	-1.4E-04	8.9 %
4.882	16.310	0.002	1.5E-04	8.3 %
6.059	20.850	0.002	-1.8E-05	0.9 %
6.147	21.520	0.002	-6.4E-05	3.1 %
6.159	20.460	0.002	4.5E-05	2.2 %

A Polynomial Least Squares Fit of the first order was calculated and the coefficients in the least squares approximation:

Coefficient 0: 5.817E-04 and Coefficient 1: 2.451E-04

Standard Deviation : σ = 1 E-4

The above data fit a Linear equation of the following nature:

$$Y = (2.45\ X + 5.82)E\text{-}04 \qquad [A3.4]$$

Although the error on the slope of this curve is relatively high, (up to 8%), it nevertheless contributes to finding a qualitative explanation to the problem of slope variation. This equation can be utilised to determine which particular calibration curve is to be deployed on any particular type of water.

Appendix 4

Cost Estimation of the RCM Implementation

List of components used in the implementation of the residual chlorine monitor and their price based on a single unit purchase.

Company	Item	Price	Address
BDH through Mercyl	Ammonia solution 10440-5Q Nitric acid 10168-4C Nitrate ion	£ 05.20 £ 04.40 £ 10.00	100 Boulevard Magnapark Lutherworth Leicester LE17 4XN
EG&G	EG&G UV-140B04 Photodiode	£ 60.00	IEC 3 Lilledale Units Colliers Green Cranbrook Kent TN17 2LS
Ebdon	ASF wall mounting series, Single door size 600x600x300mm with 19inch swing frame.	£ 60.00	
Farnell Electronic Components Ltd.	1 Weather Proof mains socket Aluminium Diecast Box 27969PSL Mains Plug. Transistor IRF96101R 10 PCB double sided	£ 03.00 £ 03.00 £ 02.00 £ 07.00 £ 56.30	Canal Road Leeds LS12 2TU
Jelight and Co	254nm Capillary lamp power supply 12Vdc	$225.00 $150.00	23052 Alcade #E, PO Box. 2632 Laguna Hills CA 92654-2632 U.S.A.
Jencons	Pyrex Glass Tube 6mm.OD 3mm Bore	£ 20.00	
Loctite UK	1 bottle Adhesive 648 1 bottle T (747) Activator	£ 05.00	Watchmead Welwyn Garden City Hertfordshire AL7 1JB

Ormantine International Ltd.	QD Connectors 8 LNS-2, 4 FTLL B230/9 4 FTLL B210/9, 4 MTLL 230/9 4MTLL 210/9 100 ft PTFE GT 13-H 1 mtr. Silicone Tubing GT0213	total £30.00 £ 05.00	St. Martins House 77 Wales Street Winchester Hampshire SO23 7RH
PD MARKETING	5 of 3 way valve 1003TMP12-62 Pellets (2312) Connectors (2210)	£ 350.00 £ 10.00 £ 10.00	Church Lane, Didlesham, Chichester West Sussex PO20 7RH
RS Components	19 in Sub Rack System 509-434 2 in Module 509-333 4 in Module 509-349 2in Screening Kit 509-355 Tapped Strips 509-462 OPA 606 OPA 404KP RS(655-408) TI 071CP RS(304-245) TI 072CP RS(304-239) RMS To Dc Converter AD536A RS(308-786) Comparator LM339 (302-429) Analogue Switch DG 308 (303-551) AD 734JH RS(263-611) LF 309H RS(307-086) Burr-Brown XTR 110KP RS(647-621) Stable Reference 1.2V RS() Transistors BC 183L Relay RS(348-526) 555 Timer 24 Volt Transformer 3VA Mains Transformer 12 Volts Regulator (3amp) 24 Volts Regulator Noise suppressor Inductor mains filter 100rev/min motor	 £ 40.00 £ 04.10 £ 11.64 £ 1.36 £ 1.61 £ 13.90 £ 01.50 £ 1.73 £ 20.60 £ 09.00 £ 12.00 £ 01.50 £ 00.50 £ 02.00 £ 0.70 £ 05.00 £ 20.00 £ 02.65 £ 01.10 £ 01.00 £ 04.60 £ 80.00	The Fairway Estate Green Lane Hounslow Middlesex TW4 6BU
TechOptics	Amphenol Connectors 2 x SMA 905-150-5005 10 m Quartz Optical Fibre	£ 20.00 £ 135.00	Unit 6 Cala Industrial Estate Tannery Road Tonbridge Kent TN9 1RF
TechOptics	Band pass optical filters (290nm)	£250.00	Isl of Man

Watson-Marlow	8 Rollers 5 Channels cassette (033.6855.000) Marprene tubing (0.5mm) Marprene tubing (2.5mm)	£ 130.00 £ 045.00 £ 045.00	Falmouth Cornwall TR11 4RU
TOTAL AMOUNT		£1543	

References

[1] EC Directives (80/778/EEC) obtainable from HMSO High Holborn London, U.K.

[2] Mouaziz, Z. Briggs, R. and Grattan, K.T.V., (1993) ,"Multi-parameter Fibre Optic Chemical Sensor for the Measurement of Nitrate Ion, Ammonia and Organic Matter", in Proceedings of the Symposium on Chemical SensorsII, Edited by Buttler, M., Ricco, A. and Yamazoe, N., The electrochemical Society Inc., New Jersey U.S.A., Vol. 93-7, p-303-316.

[3] Day, R. and Underwood, A.L., (1975), *Quantitative Analysis*, 4th Ed., Prentice-Hall, Chapter 12.

[4] Christiansen, T.F., (1986) "The Achilles Heel of Potentiometric Measurements, the Liquid Junction Potential", IEEE Trans. Biomed. Eng. Vol.33, No.2, p-79-82.

[5] Grattan, K.T.V., (1989), "New Development in Sensor Technology - Fibre and Electro-Optics", Meas. & Control. Vol. 22, July-August, p-l65-175.

[6] Saari, L.A., (1987), "Trends in Fibre Optic Sensor Development", Trends in Anal. Chem., Vol. 6, No. 4, p-85-90.

[7] Scheggi A.M., (1987), "Optical Fibre Sensors of Chemical Parameters for Industrial and Medical Applications", J. Optic. Sensors. Vol. 2, No. 1, p-3-9.

[8] Martin, M. J., Wicramasinghe, Y. A.B.D., Newson, T.P. and Crowe, J.A, (1987), "Fibre-Optics and Optical Sensors in Medicine", Medical& Bioengineering & Computing. Vol.25, p-597-604.

[9] Montgomery, J.D., (1978), "Fibre optic Applications and Markets", IEEE Trans. Comm. Vol.26, No. 7, p-lO99-1102.

[10] Maugh II, T.H., (1982), "Remote Spectrometry with Fiber Optics", Science. Vol.218, p-875-876.

[11] Boisde, G. Blanc, F. and Perez, J.J, (1988), "Chemical Measurements With Optical Fibres for Process Control", Talanta. Vol. 35, No.2, p-75-82.

[12] Tortoishell, G., (l991), "The Safety of Optical Systems in Hazardous Areas", Int.J. Optoelec.. Vol.6, No.6, p-545-52.

[13] Smith A.M., (1986), "Optical Fibre Sensors: New Opportunities for Chemical Sensing?", IEE Electronic & power. Nov/Dec, p-811-813.

[14] Willard, H.H., Merritt, L.L.Jr, Dean, J.A. and Settle, F.A.Jr, (1988), *Instrumental Methods of Analysis*, 7th Ed., Wandsorth Publishing Company, U.S.A., chapter 8.

[15] Briggs, R. and Grattan, K.T.V., (1990), "The Measurement and Sensing of Water

Quality: a review", Trans. Inst. MC. Vol.12, No.2, p-65-84.

[16] Aoki, T. and Munemori, (1983), "Continuous Flow Determination of Free Chlorine in Water", Anal. Chem. ,Vol. 55, p-209-212.

[17] Briggs, R. and Grattan, K. T. V., (1988), "On-Line Measurement of Residual Chlorine: Final Report", Internal Report to WRC.

[18] Willard, H.H., Merritt, L.L.Jr, Dean, J.A. and Settle, F.A.Jr,(1988), *Instrumental Methods of Analysis,* 7th Ed., Wandsorth Publishing Company, U.S.A, *chapter 15.*

[19] Ning, Y.N., Grattan, K.T.V., Wang, W.M. and Palmer, A.W., (1991), "A Systematic Classification and Identification of Optical Fibre Sensors", Sensors and Actuators A, Vol.29, p-21-36.

[20] Butler, M.A., (1984), "Optical Fiber Hydrogen Sensor", App. Phys. Lett. Vol. 45, No.10, p-1007-9.

[21] Konz, W., Brandenberg, A., Edelhauser, R. Ott, W. and Wolfelschneider, H., (1989), "A Refractometer with a Fully Packaged Integrated Optical Sensor Head", in Springer Proceedings in Physics Vol. 44, Ed. by Arditty, H.J., Dakin, J.P. and Kersten, R.Th., Springler-Verlag-Berlin, Heidelberg, p-443-447.

[22] Love, W.F., Walczak, I.M. and Slovacek, R.E. (1989), "High Sensitivity Fibre Optic Evanescent Wave for Fluoroimmunoassay", in Springer Proceedings in Physics Vol. 44, Ed. by Arditty, H.J., Dakin, J.P. and Kersten, R.Th., Springler-Verlag-Berlin, Heidelberg, p-431-435.

[23] Roger, A.J., (1986), "Principles for Optical-Fibre Applications in Electricity Supply", J.Optic. Sensors. Vol.1, No.1, p-5-25.

[24] Edmonds, T.E., Flatters, N.J., Jones, C.F. and Miller,J.N.,(1988), "Determination of pH with Acid-Base Indicators: Implications for Optical Fibre Probes", Talanta, Vol.35, No.2, p-103-107.

[25] Wolfbeis, O.S., (1985), "Acid-Base Titrations Using Fluorescent Indicators and Fibre Optic Light Guides", Fresenius Z. Anal. Chem., Vol. 320, p-271-273.

[26] Blum, L. J., Gautier, S. M. and Coulet, R., (1989), "Design of Luminescence Photobiosensor", J. Bioluminescence & Chemiluminescence, Vol.4, p-543-550.

[27] Briggs, R., Grattan, K.T.V., Mouaziz, Z. and Elvidge, T. (1990), "On-line Monitoring of Residual Chlorine", in Advances in Pollution Control instrumentation, Control and Automation of Water and Wastewater Treatment and Transport Systems", Ed. by Briggs, R., Pergamon Press, Oxford, U.K. p-39-49

[28] Aoki, T. (1989), "Continuous Flow Method for Simultaneous Determination of Monochloramine, Dichloramine and Free Chlorine: Application to a Water Purification Plant", Envi. Sci. Tech., Vol. 23, p-46-50.

[29] Liu, J., Shahriari, M.R.,Sigel, G.H.Jr.and Goldman, A.S., (1993), "Fibre-Optic pH Sensor Based on a Chemically Modified Porous Polymer Fibre Imrnobilized with Colorimetric Indicator", Inter. J. Optoelec.. Vol. 8, No.2, p-193-201.

[30] Wolfbeis, O.S., (1991), *Fibre Optic Sensor and Biosensors, Volume I* , Ed. by Wolfbeis, O.S, CRC Press, U.S.A., chapter 2.

[31] Yoshia, I., Himad Y. and Tanaka K., (1980), "Spectrophotometric Monitoring of Arterial Oxygen Saturation in the Fingertip", J. Med. & Bio. Eng. & Comput., Vol.18, p-27-32.

[32] Dakin, J.P. and Wade, C.A., (1987), "A Novel Optical Fibre Methane Sensor", J. Opti. Sensors, Vol. 2, No. 4, p-261-267.

[33] Stuart, A.D. and Grazier, P.E. (1988), "A Fibre Optic Relative Humidity Sensor", Inter. J. Optoelec., Vol. 3, No. 2, p-177-186.

[34] Giallorenzi,T.G., Bucaro, J.A., Dandrige, A. and Cole, J. H., (1986), "Optical-Fiber Sensors Challenge the Competition", IEEE Spectrum. Vol. 23, p-44-49.

[35] Scheggi, A.M. and Baldini, F., (1993), "Chemical Sensing with Optical Fibres", Int. J. Optoelec., Vol. 8, No.2, p-133-156.

[36] Kirkbright, G. F., Narayanaswamy, R. and Welti, N. A., (1980), "Fibre-Optic pH Probe Based on the Use of an Immobilised Colorimetric Indicator", Analyst. Vol. 109, p-1025-28.

[37] Bacci, M., Baldini, F., Cosi, F. Conforti, G. and Scheggi, A.M., (1989), "Probe Performance Optimization for pH continuous monitoring", in Springer Proceedings in Physics Vol.44, Ed. by Arditty, H.J., Dakin, J.P. and Kersten, R.Th., Springler-Verlag-Berlin, Heidelberg, p-425-430.

[38] Guthrie, A.J., Narayanaswamy, R. and Welti, N.A., (1988), "Solid-State Instrumentation for Use with Optical-Fibre Chemical Sensor", Talanta. Vol. 35, No.2, p-157-159.

[39] Munkholm, C., Walt, D.R. and Milanovich, F.P., (1988), "A Fiber-Optic Sensor for CO_2 Measurement", Talanta. Vol.35, No.2, p-109-112.

[40] Reichert, J., Czolk, R, Morales-Bahnik, A., Sellien, W and Ache, H.J., (1992), "Optical-Chemical Sensors for Environmental Analysis: Ammonium, Nitrate and Heavy Metal Ion Sensors", paper presented at the 1st European Conference on Optical Chemical Sensors and Biosensors, Graz, Austria, 12-15 April1992.

[41] Saari, L. A. and Seitz, W.R., (1982), "pH Sensor Based on Immobilized Fluoresceinamine", Anal. Chem.. Vol. 54, No. 4, p-821-823.

[42] Russell, D. A. and Narayanaswamy, R., (1989), "Fibre Optic Fluorimetric Determination of Fluoride Ions", Analyst. Vol. 114, p-381-385.

[43] Meadows, D. and Shultz, T. S., (1988), "Fiber-Optic Biosensors Based on Fluorescence Energy Transfer", Talanta, Vol. 35, No. 2, p-145-150.

[44] Optiz, N and Lubbers, D.W., (1988), "Electrochromic Dyes Enzyme Reactions and Hormone-Protein Interactions in Fluorescence Optic Sensors (Optode) Technology", Talanta, Vol. 35, No. 2, p-123-127.

[45] Li, P. Y. F. and Narayanaswamy, R., (1989), "Oxygen-Sensitive Optical Fibre Transducer", Analyst, Vol. 114, October, p-1191-1195.

[46] Carrabba, M.M., Edmonds, R.B., Spencer, K.M. and Rauh, R.D., (1993), "Fibre Optic Raman Chemical Sensors",in Proceedings of the Symposium on Chemical Sensors II, Ed. by Butler, M., Ricco, A. and Yamazoe, N., The electrochemical Society, Inc., New Jersey, U.S.A., Vol. 93-7, p-634-642.

[47] Kealy, D. (1972), "Quantitative Reflectometry - I Principles and Scope", Talanta, Vol.19, p- 1563-1571.

[48] Shah, Y. Valsler, R. A.and Palmer, A. W., (1985), "Optical Fibre Plethysmograph",.J. Biomed. Eng., Vol. 7, p-326-328.

[49] Attridge, J.W., Learer, K.D. and Cozens, J.R., (1987), "Design of a Fiber Optic pH Sensor with Rapide Response" J. Phys. E. Vol. 20, 1987, p-548.

[50] Smith, A. M., (1988), *Optical Fiber Sensors: Principles and Components,* Ed. by Dakin, J. and Culshaw, B.,Artech House Inc. p-189-207.

[51] Tran, C. D., (1992), "Acousto-Optic Devices; Optical Elements for Spectroscopy", Anal. Chem.. Vol. 64, No. 20, p-971A-981A

[52] Weir, K. Chitaree, R. Grattan, K. T. V. and Palmer, A. W., (1993), "High Speed Sensing Using an Ellipsometer for Investigation of Thin Films and Surfaces", in Proceedings of the Symposium on Chemical Sensors II, Ed. by Butler, M., Ricco, A. and Yamzoe, N., The electrochemical Society, Inc., New Jersey, U.S.A., Vol.93-7, p-236-243.

[53] Moulin,C., Rougeault, S., Dureault, B. and Mauchien, P., (1992), "Uranium Remote Sensing by Laser-Induced Fluorescence", in Procedings of the 1st conference presented in Graz, April 1992. p-81.

[54] Briggs, R., Meredith, W. D. and Solman, A. J., (1985), "Development in Sensor Technology", in New Technology in Water Services, Ed. by The Institution of Civil Engineers, p-29-58

[55] Falcial, R., Baldini, F. Bechi, P. and Cosi, F., (1991), "In Vivo Entero-Gastric Reflux Detection by Optical Fibres", Int. J. Optoelec.. Vol. 6, No. 5, p-443-450.

[56] Selli, R.K., (1987), *Fibre Optic Temperature Sensors Using Fluorescent Phenomena*, Ph.D. thesis, City University, chapter 1.

[57] Fry, S. M., (1988), "Market Analysis; The market For Surgical Infrared Fibres", Int. J. Optoelec., Vol. 3, No. 4, p-349-354.

[58] Calvert, J.G. and Pitts, Jr, J. N., (1967), *Photochemistry,* John Wiley & Sons Inc., U.S.A.,

[59] Atkins, P.W., (1978), *Physical Chemistry,* Oxford University Press, U.K.

[60] Laidler, K. J., (1978), *Physical Chemistry with Biological Applications*, The Benjamin/Cummings Publishing Company, Inc. U.S.A.

[61] Nassau, K., (1983), *The Physics and Chemistry of Color: The Fifteen Causes of Color*, John Wiley Sons Inc. U.S.A.

[62] Snook, R.D, (1989), "Electromagnetic Radiation for Compositional Analysis", in Instrumentation and Analytical Science, Ed. IEE series 6 (Peter Peregrinus Ltd.), London U.K., chapter 7 (p 183).

[63] Graybeal, J. D., (1988), *Molecular Spectroscopy,* Ed. McGraw Hill International Editions.

[64] Sharpe, M. R., (1984), "Stray Light in UV-VIS Spectrophotometers". Anal. Chem., Vol. 56, No.2, p-339A-356A.

[65] Kortum, G. and Seiler, M.T., (1939), Angew. Chem., Vol. 52, No48, p-687-694.

[66] Sommer, L., (1989), *Analytical Absorption Spectrophotometry in the Visible and Ultraviolet; The Principles,* Elsevier science publisher, The Netherlands, chapterl.

[67] Desurvivre, E., (1992), "Lightwave Communication: The fifth Generation", Sci. Ame., Vol.266, p-96-103.

[68] Pal, B. P., Thyagarajan, K. and Kumar, A., (1988), "Characterization of Optical Fibres for Telecommunication and Sensors; Part 1: Multimode Fibres", Inter. J. Optoelec., Vol.3, No.1, p-45-71.

[69] Thyagarajan, K., Pal, B. P. and Kumar, A., (1988), "Characterization of Optical Fibres for Telecommunication and Sensors; Part 2: Single Mode Fibres", Inter. J. Optoelec., Vol.3, No.2, p-153-176.

[70] Kimura, T., (1988), "Factors Affecting Fiber-Optic Transmission Quality", J. Light. Tech., Vol. 6, No. 5, p-611-619.

[71] Yupapin, P.V.P., (1993), *Optical pressure Sensors using Interferometric Techniques*, Ph.D. thesis, City University, Chapter 1.

[72] Weast, *R. C.* and Astle, . J. (1982), *Handbook of Chemistry and Physics*, Ed. 62. CRC Press, Inc. Boca Raton, Florida.

[73] Nagel, S. R., (march 1989), "Optical Fiber: The Expanding Medium", IEEE Circuit Design Magazine, p-36-49

[74] Nagel, S. R., (1992), "R&D Directions for Optical Fiber", IEEE LTS, Vol. 3, No.4, p-26-34.

[75] Gowar, J., (1984), *Optical Communication Systems*, PrenticeHall International, Inc., London, chapter 3.

[76] Iino, A., Kuwabara, M. and Kokura, K., (1990), "Mechanisms of Hydrogen-Induced Losses in Silica-Based Optical Fibers", J. Light. Tech., Vol. 8, No. 11, p-1675-79.

[77] Jones, K. A., (1987), *Introduction to Optical Electronics*, John Wiley & Sons, Inc., chapter 6.

[78] Phillips, R., (1983), *Sources and Applications of Ultraviolet Radiation*, Ed. Academic Press Inc., London, chapter 7.

[79] Forrest, S. R., (1986), "Optical Detectors: Three Contenders", IEEE Spectrum, Vol.23, No.5, p-76-83

[80] Hamamatsu, Technical Reference Manual.

[81] Hamstra, R. H.Jr and Wendland, P., (1972), "Noise and Frequency Response of Silicon Photodiode Operational Amplifier Combination", Applied Optics, Vol.11, No.7, p-1539-47.

[82] Senior, J. M., (1985), *Optical fibre Communications; Principles and Practice*, Ed. by Dean, P.J., PrenticHall International, London, U.K. Chapter 9.

[83] Malmstadt, H. ., Enke, C. G., Crouch, S.R. and Horlick, G., (1974), *Electronic Measurement for Scientists*, Benjamin, W. A., Inc. Publisher. Chapter 4

[84] Motchenbacher, C.D. and Fitchen, F.C ., (1973), Low-Noise Electronic Design,, *Ed. John Wiley & Sons, U.S.A., chapter 3.*

[85] Sienko, M. J. and Plane, R. A., (1979), *Chemistry: Principes and Applications*, McGraw-Hill Inc., Chapter 15.

[86] Briggs, R. and Melbourne, K.V., (1972), "Ion-Selective Electrodes in Water Quality Monitoring Techniques in Air and Water Solution", Institution of Mechanical Engineers, London, U.K., p-37-64.

[87] Janata, J., (1987), "Do Optical Sensors Really Measure pH", Anal. Chem., Vol. 59, p- 1351-56

[88] Koller, E. and Wolfbeis,O.S.(1992),"Sensor Chemistry", in *Fiber-OpticChemical Sensors and Biosensors Vol. 1*, Ed. by Wolfbeis, O. S., CRC Press, U.S.A.

Chapter 7.

[89] Peterson, J.I., Goldstein, S.R., Fitzgerald, R.V. and Buckhold, D. K., (1980), "Fiber Optic pH Probe for Physiological Use", Anal. Chem., Vol. 52, No.6, p-864-869.

[90] Kirkbright, G. F., Narayanaswamy, R. and Welti, N. A., (1984), "Studies with Immobilised Chemical Reagents Using Flow-Cell for the Development of Chemically Sensitive Fibre-Optic Devices", Analyst, vol. 109, p-15-17.

[91] Vogel, A. I., (1989), *Vogel 's Textbook of Quantitative Chemical Analysis,* 5th Ed., Longman Scientific & Technical, chapter 10.

[92] Collocott, T.C. and Dobson, A. B., (1976), *Chambers Dictionary of Science and Technology*, Ed. by Collocott T.C. and Dobson, A.B., W & R Chambers Ltd. U.K.

[93] Bates, G.R., (1964), *Determination of pH; Principles and Applications*, Wiley & Sons, Chapter 6.

[94] Skoog, D.A. and West, D.M., (1971), *Fundamentals of Analytical Chemistry,* A Holt London Edition, U.K.

[95] Bishops, E., (1972), *Indicators,* Chapter 3.

[96] Grattan K.T.V., Z. Mouaziz and Palmer, A.W, (1987), "Dual Wavelength Optical Fibre Sensor for pH Measurement", Biosensors, Vol.3, No.1, p-17-25.

[97] Kressel, H., Ettenberg, M., Wittke, J. P. and Ladany, I., (1982), "Laser Diodes and LEDs for Fiber Optical Communication", in *TopicS in Applied Physics,* Ed. by Kressel, H., Vol.39, Springer-Verlagb, p-9-60.

[98] Janata, J., (1992), "Ion Optodes", Anal. Chem., Vol. 64, No. 19, p-921A-927A.

[99] Wolfbeis, O.S., (1992), *Fibre Optic Sensor and Biosensors, Volume I*, Ed. by Wolfbeis, O.S, CRC Press, U.S.A., p-370.

[100] Hiskey, C. F. and Young, I. G., (Sep 1951), "Principle of Precision Colorimetry; Absorption Law Deviations in Measurements of Relative Transmittance", Anal.Chem., Vol.23, No.9, p-1196-1201.

[101] Bently, J. P., (1986), *Principles of Measurement System*, Longman Group Ltd., U.S.A.

[102] Wolf, H.F., (1979), *Handbook of Fiber Optics: Theory and Applications,* Garlam STPM Press, chapter 5.

[103] Keiser, G., (1983), *Optical Fiber Communications,* Intemational Student Edition, Chapter 5.

[104] Shumate P.W. and DiDomenico, Jr M., (1982), "Lightwave Transmitters", in

Topics in Applied Physics, Ed. by Kressel, H., Vol. 39, Springer-Verlag, p-161-200.

[105] Suematsu, Y and Iga, K.I., (1984), *Transmissions sur Fibres Optiques*, Masson Paris, Chapter 5

[106] Horowitz, P. and Hill, W., (1985), *Horowitz and Hill: The Art of Electronics,* Cambridge University Press, U.K.

[107] Radio Spares, Technical reference manual.

[108] Grattan, K.T.V., Mouaziz, Z., Palmer, A.W. and Selli, R.K., (1987), "Development of Simple Optical pH Sensor for Use in Acid-Base Titrations", J. Optic. Sensors. Vol.2, No.5, p-0-1.

[109] Fonger, W. H. and Struck, C.W, (1975), "Temperature Dependences of Cr^{+3} Radiative and Nonraditaive Transitions in Ruby and Emerald", Phy. Rev., Vol. l l, No.9, p-3251-60

[110] Nelson, D. F. and Sturge, M.D., (1965), "Relation Between Absorption and Emission in the Region of the R Lines of Ruby", Phys. Rev., Vol.137, No.4A, p-A1117-A1130.

[111] Maiman, T.H., 1960" ", Physics Review, Vol. 4., p-564.

[112] Burns, G. and Nathan, M.I., (1963), "Quantum Efficiency of Ruby", J. Applied Physics, Vol.34, No.3, p-703-705.

[113] Schawlow, A.L., (1961),"Fine Structure and Properties of Chromium Fluorescence in Alimunium and Magnesium Oxide", in *Advances in Quantum Electronics,* Ed. by Singer, J.R., Columbia University Press, p-50-62.

[114] Tektronix, Digital Oscilloscope Technical Literature Manual

[115] White, G.C., (1986), *The Handbook of Chlorination,* 2nd Ed., Van Nostrand Reinhold Company, New York, chapter 2 and 6.

[116] Rigdon, L.P., Moody, G.J., and Frazer, J.W., (1978), "Determination of residual chlorine in water with computer automation and a residual chlorine electrode", Anal. Chem., Vol.50, p-465-468.

[117] Johnson, J.D., Edwards, J.W. and Keeslar, F., (1978),"Chlorine Residual Measurement Cell: The HOCI Membrane Electrode", J. Am. Water Works Assoc., Vol.70, No.6, p-341-348.

[118] Marino, D.F. and Ingle, J.D., (1981), "Determination of Chlorine in Water by Luminol Chemiluminescence", Anal. Chem., 53, p-455-458.

[119] Balt, L., Stamhuis, E. J. and Joosten, E.H., (1981), "Continuous Flow

Determination of Molecular Chlorine in Nonpolar Media", Anal. Chem., 53, p-1799-1801.

[120] Montgomery, J.M., (1985), *Water Treatment Principles and Design*, John Wiley & Sons, Inc. U.S.A.

[121] Barns, D. and Wilson, F, (1983), *Chemistry and Unit Operations in WaterTreatment,* Ed. Applied Science Publishers Ltd, England, chapter 5, p-128.

[122] Mouaziz, Z. Briggs, R. Hamilton, I. and Grattan, K.T.V., (1993), "Design and Implementation of a Fibre-Optic-Based Residual Chlorine Monitor", Sensors & Actuators B- Chemicals, Vol.11, p-431-440.

[123] Hecht, E and Zajac, A., (1974), *Optics,* Addison-Wesley World Student Series, chapter 9.

[124] UDT, Detectors, technical reference manual, UDT Sensors, Inc.

[125] Jacob, J.M., (1982), *Applications and Design with Analog Integrated Circuits*, Reston Publishing Company.

[126] Thomas, L. C., (1972), "The Biquad: Part I,- Some Practical Design Considerations", IEEE Trans. Circuits Syst., CAS, 18, p-350-357 A

[127] Thomas, L. C., (1972), "The Biquad: Part II,- A Multipupose Active Filtering System", IEEE Trans. Circuits Syst., CAS p-358-361.

[128] Analog Devices, (1986), *RMS TO DC Conversion Application Guide*, Ed. by Kitchin, C. and Counts, L., 2nd Ed.